University of Oxford

Thesis submitted for the degree of Doctor of Philosophy

Department of Plant Sciences

Factors influencing the Dispersal of *Pseudomonas fluorescens* NZI7 by *Caenorhabditis elegans*

Author:
Annekathrin Wilkins
Lincoln College

Supervisors:
Dr. Gail Preston
Prof. Jonathan Hodgkin
Dr. Christian Yates

MT, 2016



Abstract

Caenorhabditis elegans is a natural predator of the mushroom pathogen *Pseudomonas fluorescens* NZI7. The bacterial mechanisms for reducing predation by the nematode through the secretion of secondary metabolites have been described, but not yet fully explored. The behaviour of nematodes is influenced by the different factors produced by the pseudomonads.

In this thesis we develop a range of assays to link the behaviour of *C. elegans* to these factors to identify their role in bacteria–nematode interactions. We show that these factors play two distinct roles: they may either repel nematodes, or harm them. This permits the classification of mutants of *P. fl.* NZI7 lacking these factors as either attractive, edible or both.

Many studies of *C. elegans* behaviour have demonstrated that the nematode can distinguish between different food sources. Our results show two distinct types of response: chemotaxis drives the response to attractive or repellent stimuli, and nematodes also show a choice behaviour that is independent of chemotaxis. This choice behaviour is determined by bacterial edibility and requires nematodes to come into contact with the bacteria. This contact is the foundation of the bacterial dispersal by nematodes. By making use of the luminescence property of the available bacterial mutants, we demonstrate an intimate link between the behaviour of *C. elegans* and the success with which bacteria are disseminated: if nematodes are induced to regularly leave a bacterial colony, whether through their genotype or the low edibility of the food, then they will spread bacteria effectively.

Throughout this thesis, we use computational simulations based on a hybrid cellular automaton model to represent the nematode–bacteria interactions. These simulations recreate the observed behaviour of the system, thus they help to confirm our hypotheses and establish the fundamental aspects of the interactions between the two species.

Acknowledgements

This work could not have been done without the help and support of a large number of people. Firstly I must thank my supervisors Gail and Jonathan, who have undertaken the painstaking task of teaching a Maths graduate how to work in a lab. They have encouraged me throughout this project, and were always happy to help me with any problem no matter how large or small. For support in the lab, I would also like to thank the members of the Hodgkin, Preston, van der Horn and Woollard labs, who were always happy to help me out as I blundered through the protocols. I also want to thank Kit, who has supervised the mathematical aspects of my work. I am very grateful to John Baker, for taking any photo I ever wanted to have taken and thus facilitating overnight studies. I would like to give special thanks to Mark Fricker, who let me use his photon counting camera. He very kindly helped me to establish the best setup for my experiments and has also advised me on the analysis of the resulting data. I am indebted to Kathryn Atwell for aiding me with some advice on MATLAB and Lim Zhi Bang for his help with Statistics. I must also thank Michele Ceriotti, who has accommodated me in his group, while I was writing up in Lausanne. I am particularly grateful to everyone who has proofread any part of my thesis and helped a poor German to navigate the minefield of English spelling. I also thank my examiners Andre Brown and Kayla King for their constructive feedback on my work.

So much for the academic support. Now for the even more important moral support which helped me to keep going and carry this project to the end without losing what is left of my sanity.

I would in particular like to thank Louise Hill and Delia O'Rourke, who have helped me to look after my health. I am grateful to Dominic Vella, who has guided me far more than any College advisor is expected to. I am very thankful for the friendship with such wonderful people like Johnny Brooks-Bartlet, John Baker, Louise Hill and Jo French, who have always been able to cheer me up when I needed it. Ich möchte mich bei meinen Eltern bedanken, die mir meine bisherige Laufbahn ermöglicht haben und mich jeden Schritt meines Lebens begleitet und unterstützt haben. Ich bedanke mich auch bei meinen Großeltern die mich immer ermutigt haben. I would also like to thank my inlaw family, into which I was welcomed as if I had always been there. In particular I would like to thank Nicholas, who has presumably only moved to Oxford in good time to support the last steps of my study and be at hand, while my husband was abroad. I dedicate this work to my dear husband, who has accompanied me every step of my DPhil, guided me through all the downs and enjoyed all the ups with me.

Contents

1 Introduction **1**

1.1 Introduction . . . 1
1.2 Mushroom Farming . . . 8
1.3 *Pseudomonas* . . . 12
1.3.1 Pseudomonads on a Mushroom Farm . . . 15
1.3.2 The Excretome of Fluorescent Pseudomonads . . . 16
1.3.3 The Mutant Library . . . 23
1.3.4 Bacterial Tagging Techniques . . . 33
1.4 *Caenorhabditis elegans*, a Bacterivorous Nematode . . . 34
1.4.1 Nematodes on the Mushroom Farm . . . 35
1.4.2 *C. elegans* as a Model for Pathogenicity . . . 36
1.4.3 Nematode Motion . . . 38
1.4.4 Chemosensation and Chemotaxis in *C. elegans* . . . 39
1.4.5 Learning . . . 45
1.4.6 Response to Presence or Absence of Food . . . 46
1.4.7 Pheromones . . . 48
1.4.8 Social Interactions . . . 50
1.4.9 Nematode Mutants used in this Study . . . 51
1.5 Interacting Species . . . 53
1.5.1 Predation . . . 53
1.5.2 Evading Predation . . . 54
1.5.3 Vectors of Disease . . . 56
1.5.4 Farming . . . 56
1.6 Modelling . . . 57
1.7 Summary . . . 59

2 Materials and Methods **63**

2.1 Experimental Procedures . . . 63
2.1.1 Strains and Media . . . 63
2.1.2 Bacterial Methods . . . 65
2.1.3 Nematode Methods . . . 71
2.1.4 Nematode–Bacteria Interaction Assays . . . 72
2.2 Data Analysis . . . 78
2.2.1 Bacterial Growth Assay . . . 78
2.2.2 Bioluminescence Assay . . . 79
2.2.3 Food Choice Assay . . . 80
2.2.4 Nematode Growth Support Assay . . . 80

2.2.5 Progeny Assay . . . 81
2.2.6 Linear Regression . . . 81

3 A Model of the Interactions 83
3.1 Introduction . . . 83
3.1.1 Model Outline . . . 87
3.2 Bacteria . . . 88
3.2.1 Background . . . 89
3.2.2 Modelling Assumptions . . . 89
3.2.3 Bacterial Parameters . . . 90
3.2.4 Initial Distribution . . . 91
3.2.5 During the Simulation . . . 91
3.3 Organic Chemicals . . . 92
3.3.1 Background . . . 92
3.3.2 Modelling Assumptions . . . 93
3.3.3 Initial Distribution . . . 94
3.3.4 Time Evolution . . . 96
3.3.5 Modelling Parameters . . . 96
3.4 Nematode Motion . . . 97
3.4.1 Background . . . 97
3.4.2 Modelling Assumptions . . . 99
3.4.3 Nematode Variables and Movement Parameters . . . 100
3.4.4 Realisation . . . 100
3.5 Interaction Between Nematodes and Bacteria . . . 103
3.5.1 Eating and Ageing . . . 104
3.5.2 Nematode reproduction . . . 106
3.5.3 Learning . . . 107
3.5.4 Dispersing Bacteria . . . 108
3.5.5 Modelling Parameters . . . 108
3.6 The Two Assays Modelled . . . 109
3.6.1 The Simulation Domain . . . 110
3.6.2 The Initial Conditions . . . 110
3.6.3 Output . . . 111
3.6.4 Parameter Calibration . . . 112
3.7 Discussion . . . 112

4 Growth Effects 117
4.1 Introduction . . . 117
4.2 Characterizing Bacterial Growth . . . 119
4.2.1 Logistic Model for Bacterial Growth . . . 120
4.2.2 Data Fitting and Analysis . . . 120
4.2.3 The Bacterial Growth Parameters . . . 121
4.3 Modelling Bacteria–Nematode Interactions with Different Bacterial Growth Parameters . . . 128
4.3.1 Effects of Stochasticity in the Model . . . 128
4.3.2 The Observed Effects are Non-linear . . . 129
4.3.3 The 54 h Time Point is Optimal for Further Analysis . . . 132

4.3.4 Classifying Strains According to Growth . . . 132
4.4 Solid Growth . . . 135
4.5 Conclusion . . . 141

5 Edibility of *Pseudomonas fluorescens* NZI7 143
5.1 Measures of Edibility . . . 146
5.1.1 Food Choice Assay . . . 146
5.1.2 Nematode Growth Support Assay . . . 148
5.1.3 Progeny Assay . . . 149
5.2 General observations . . . 155
5.2.1 Worm Clustering . . . 155
5.2.2 Edibility of *P. fl.* NZI7 WT . . . 156
5.2.3 Interassay Correlation . . . 159
5.3 Phenotypes of Selected Mutants . . . 160
5.3.1 Tagged Strains . . . 163
5.3.2 Known toxins: tolaasin, HCN and EDB . . . 166
5.3.3 GacS . . . 169
5.3.4 Edibility and Attraction are not always linked . . . 169
5.3.5 Stochastic Effects . . . 171
5.3.6 WT-like mutants . . . 172
5.4 Volatility Assays . . . 172
5.5 An Overall Edibility Score . . . 173
5.6 Nematode Variants . . . 174
5.7 Chemotaxis is Not Required for Food Choice . . . 183
5.7.1 Medium term Behaviour of *che-3* Mutants . . . 184
5.7.2 Model Without Chemotaxis . . . 185
5.8 Conclusion . . . 186

6 Nematodes Spread Bacteria 191
6.1 Measuring Spreading . . . 193
6.1.1 Visual Inspection . . . 193
6.1.2 Using fluorescence . . . 194
6.1.3 The Bioluminescence Assay . . . 194
6.2 Spreading Depends on Bacterial Phenotype . . . 198
6.2.1 Overview . . . 200
6.2.2 Spreading of *P. fl.* NZI7 WT . . . 202
6.2.3 Edibility Affects Spreading . . . 203
6.2.4 Attraction versus Edibility . . . 206
6.2.5 Bacterial Attachment . . . 208
6.2.6 Spreading in the Model . . . 211
6.3 Spreading Depends on Nematode Strain . . . 212
6.3.1 Pathogenicity . . . 213
6.3.2 Food-Leaving Probability . . . 214
6.3.3 Spreading in the Model . . . 217
6.4 Bacterial Clumping . . . 218
6.5 Conclusion . . . 219

7 Conclusion **223**
7.1 *P. fl.* NZI7 Reduces Predation by *C. elegans* 224
7.2 Attractive and Edible Bacteria 225
7.3 Edibility Determines how Bacteria are Spread by Nematodes 226
7.4 Food Leaving Probability is an Important Factor in Bacterial Dispersal 227
7.5 A Model of the Interaction 227
7.6 Future Work 229

Bibliography **230**

Appendix **254**

List of Figures

1.1 *Pseudomonas* phylogenetic tree 4
1.2 *C. elegans* life cycle 6
1.3 Modern mushroom farming 9
1.4 Pseudomonads in this report 13
1.5 Bacteria adhere to the surface of *C. elegans* 14
1.6 EDB locus 20
1.7 Chorismate pathway 21
1.8 GacS pathway 22
1.9 Bacterial screens 25
1.10 Tn7 chromosomal insertion in pseudomonads 34
1.11 *C. elegans* Dar phenotype 36
1.12 Ascarosides - nematode pheromone 49

2.1 Lux-plasmid 67
2.2 Internal reflection in petri dish 73
2.3 Choice assay template 74
2.4 Grid screen example 75
2.5 Scoring bacterial spreading 77

3.1 Interactions between the three agents modelled 85
3.2 The nematode behaviour modelled 98
3.3 Model versus Experiment 111

4.1 Bacterial carrying capacity 126
4.2 Bacterial growth rate 127
4.3 Stochasticity in the Model 129
4.4 Nonlinear effects in the model 130
4.5 Bacterial numbers depend linearly on carrying capacity 131
4.6 Total bacterial numbers during a simulation 133
4.7 Growth Levels 136
4.8 Lux Reporter 137
4.9 Diauxic Growth 139

5.1 Sick nematodes 145
5.2 Chemotaxis determines behaviour in the first hour 148
5.3 Nematode aggregation 157
5.4 Weak correlation between different assays of edibility 161
5.5 Temporal development of choice index 162
5.6 Att:Tn7 site in Pf5 164

5.7 Repellence Zone . . . 164
5.8 Attraction versus Edibility . . . 175
5.9 Grid screen Template . . . 175
5.10 Predation by nematode variants . . . 176
5.11 Food race scores for different nematode genotypes . . . 179
5.12 Food choice by different nematode genotypes . . . 180
5.13 Macrophotography . . . 184
5.14 Model without chemotaxis . . . 187

6.1 Estimating bacterial spreading using luminescence . . . 195
6.2 16 different methods for comparing histograms . . . 199
6.3 Spreading of WT-like mutants . . . 204
6.4 Edibility decreases spreading success . . . 205
6.5 Spreading versus Edibility . . . 207
6.6 Spreading of Edible and Attractive mutants . . . 209
6.7 Other factors important for spreading . . . 210
6.8 Edibility reduces spreading in the model . . . 212
6.9 Spreading by different nematodes . . . 215
6.10 Spreading by different nematodes . . . 216
6.11 Efficient spreading by Hawaiian nematodes in the model . . . 217
6.12 Development of phase change . . . 219
6.13 Bacteria change phase . . . 220

List of Abbreviations

Abbreviation	Explanation	Reference page
CLP	cyclic lipopeptide	24
EDB	edibility factor	20
FCA	Food choice assay	73
HCN	hydrogen cyanide	19
NGSA	Nematode growth support assay	75
tol	tolaasin	18
WLIP	white line inducing principle	24
WT	wild type	

Chapter 1

Introduction

1.1 Introduction

We all know how careful we have to be, when we are ill ourselves not to spread our disease to those around us. We use disinfectants to make doorknobs and taps safe to handle, and catch our sneezes with tissue. While these efforts might keep the common cold at bay, they are almost completely ineffective against vector borne diseases. Cholera, which is transmitted by water supplies, and the complex life cycle of plasmodium, which causes Malaria and is transmitted by mosquitoes, are well studied examples [1–4]. Control of these diseases is usually targeted at the vector [5]. The treatment of groundwater and the interruption of the mosquito lifecycle are effective strategies employed to save the lives of millions [6–8].

Plant diseases are understudied compared to human diseases. This is despite the fact that plants are the basis of all our food and that plant diseases have played an important role in history: the most well-known example is the Irish potato famine caused by the oomycete *Phytophythora infestans*, which affected millions of

people (reviewed in [9]) and is still a major concern today [10]. Such diseases are still threatening ecosystems [11] and many staple foods particularly of developing countries, like rice and cassava [12–14]. Understanding how such diseases spread between the non-mobile hosts is the first step towards limiting their impact [15]. While many plant pathogens can disperse without the aid of a biotic vector, there are also numerous diseases which benefit from a vector, or for which a vector is essential to success [5]. Controlled field studies exploring endemics of crop pathogens are costly and time-consuming at best. It is thus advantageous to find a small scale model system and develop a computational model.

Mushrooms are more closely related to Metazoa [16] but their diseases share many of the aspects of plant diseases and are even less well studied. In particular mushroom pathogens must also rely on biotic or abiotic vectors to infect fresh hosts. The study of mushroom diseases has the advantage that mushroom farms can be very small, and are usually a closed system, which reduces the cost of studies and facilitates controls. While studying mushroom diseases might be profitable for understanding plant diseases, they are also important in their own right. Over the past 40 years the mushroom industry has seen an increase greatly surpassing population growth: increasing from 0.25 kg of mushroom per capita in 1974 to 1.37 kg in 2013 [17]. Initially increased yields were achieved through improvements in culturing conditions (which are further detailed in the next section), in particular the compost soil properties [18], but over the past 30 years this increase in production has been met by an increase in cultivated area [17].

A considerable proportion of the mushroom crop falls victim to diseases. Reducing the loss to pathogens would provide a further increase in yields. *Agaricus*

bisporus, the mushroom farmed annually to a value exceeding 10 billion € can be infected by members from all areas of the phylogenetic tree such as green mould (*Trichoderma aggresivum*), Virus X, sciarid flies, *Burkholderia gladioli* and a large range of bacteria from the genus *Pseudomonas* [18,19]. Bacterial blotch has long been considered the most important bacterial disease of mushrooms [20]. There are two types of bacterial blotch distinguished: Brown Blotch and Ginger Blotch [21, 22]. The causative agents fall into the fluorescens cluster of *Pseudomonas* (see Figure 1.1). The very resilient pathogens can cause blotches on the sporocarps both pre and post harvest despite washing and refrigeration [22, 23]. Brown blotch alone is estimated to cause a loss of at least 5 % and up to 20 % of the yield in the UK [24, 25]. Many different strains of *Pseudomonas fluorescens* can cause brown blotch disease [26–29]. They are found globally [26,27,30,31] and do not only affect *Agaricus bisporous* but also other cultivated mushrooms like *Pleurotus ostreatus* [32] and *P. eryngii* [33] as well as *Lentinula edodes* [31] and *Flammulina velutipes* [30]. In this work we will study one of the causative agents of brown blotch disease: *Pseudomonas fluorescens* NZI7 [26].

A successful pathogen is well adapted to establish itself in the environment. It must ensure that rates of reproduction are higher than losses to predation, and it must develop strategies to facilitate spreading to new hosts. Many mushroom pathogenic bacteria are well adapted to avoid predation by *C. elegans* [34], and can exploit this predator as a vector, thus thwarting any attempt to use *C. elegans* as a biocontrol agent [35]. Pseudomonads commonly move at a speed of less than 100 μm h^{-1} on solid media [36], while they can reach speeds around 100 μm s^{-1} when riding a nematode [37,38]. The speed increase the bacteria achieve in this way

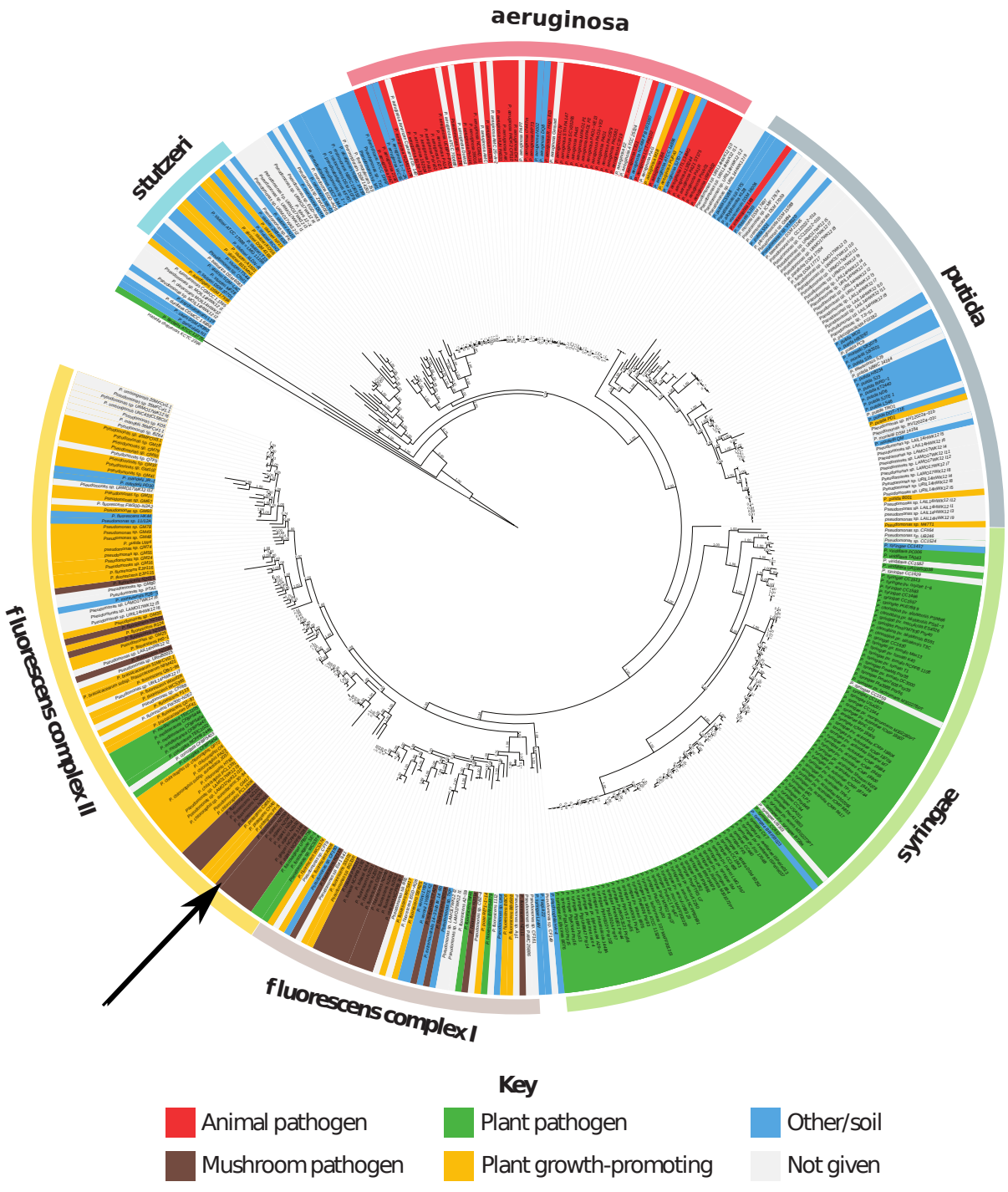

Figure 1.1: *Pseudomonas* form a functionally diverse group. The phylogenetic tree of *Pseudomonas* was constructed by Xuemei Shen (Preston group unpublished work). Mushroom pathogens (highlighted in brown) are found across the whole fluorescens complex. The arrow indicates the mushroom pathogen *P. fl.* NZI7, which is explored in this report. Its relationship to other pseudomonads can also be seen in the subtree shown in Figure 1.4 on page 13.

is the same order of magnitude as that achieved by a tortoise or a sloth catching a plane. In addition, much like the flea transmitting the bubonic plague uses rats as a secondary vector [39], nematodes have developed strategies to facilitate dispersal by larger organisms including flies, mites, mice and humans [40–44].

Bacterivorous nematodes have often been implicated in the dispersal of bacteria [45–48]. This can either happen by bacteria sticking to the nematode surface coat [46] or through ingestion by the nematode, if the bacteria manage to avoid being crushed by the grinder [49] and are excreted again [50]. Therefore, bacteria can potentially benefit from their predators or even form symbioses with them. The nematode *Heterorhabditis bacteriophora* regurgitates its symbiont *Photorhabdus luminescens* when infecting insect larvae. While colonising the larvae, the bacteria serve as food to their vector [51].

The 1.5 mm long soil dwelling nematode *Caenorhabditis elegans* is used extensively as a model organism to gain insight into embryogenesis, learning, innate immunity, ageing, asymmetric cell division and cancer [53–58]. Many of the signalling pathways involved are conserved through evolution so that knowledge derived from the study of the nematode can be applied to mammals and humans [53, 59]. The short life cycle (see Figure 1.2), easy maintenance, small genome and transparency of the worm make it an ideal system to study in the laboratory. The low maintenance costs make large numbers of experiments possible.

However, much less work is done on *C. elegans* interacting with bacteria from its natural environment [42]. *C. elegans* is most commonly found in bacteria rich environments like rotting fruits, compost or fresh soil [60]. The laboratory strain N2 used as a wild type reference strain for almost all of the *C. elegans* research

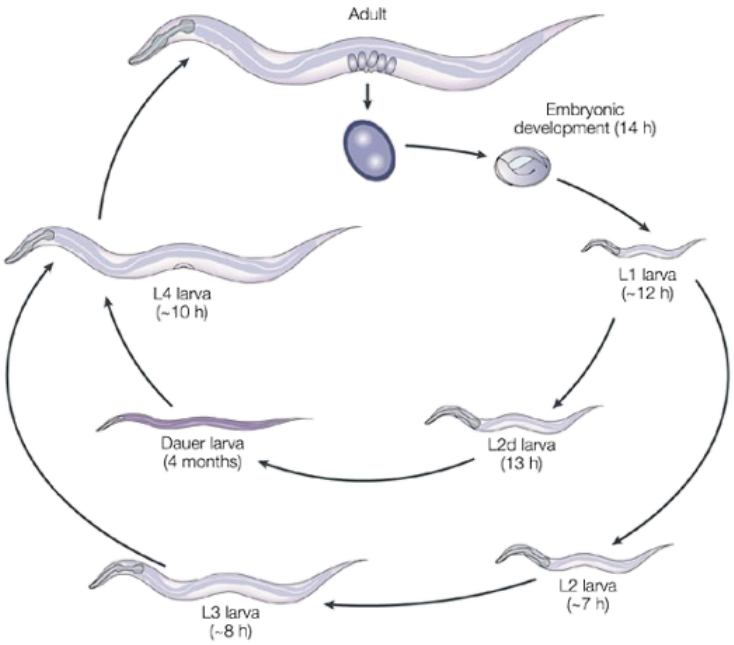

Figure 1.2: Life cycle of *C. elegans* indicating the four larval stages and the dauer pathway. Under favourable conditions (25 °C and abundant food) it takes approximately 42 h from egg to egg. Adult animals can live for another about 20 days after maturation. The length of the life cycle can be extended by incubating the worms at lower temperatures. In crowded conditions *C. elegans* enters into the dauer larval state. Figure reproduced with permission from Jorgensen *et al.* [52]

.

conducted was first isolated from a mushroom farm in the 1950s [60]. Since then *C. elegans* has always been associated with this man made environment, especially since Grewal found that *C. elegans* is the nematode most commonly found in UK mushroom farms [35].

C. elegans eats a variety of microorganisms including bacteria, yeast and small eukaryotes [44, 47, 61], and is thus a natural predator of *Pseudomonas fluorescens*, as they coincide on mushroom farms [35, 62]. The microorganisms encountered by *C. elegans* vary in their nutritional value and the harm they can do to nematodes. Some are pathogenic, some secrete lethal toxins, while others support very good

nematode growth [34, 42, 47, 63].

The interactions between *C. elegans* and *Pseudomonas fluorescens* depend on a variety of bacterial factors, including toxins such as cyanide and pathogenicity traits. Many of these factors are not well understood and will be explored further in this thesis. To do so we will investigate the role of a range of traits in the interaction with *C. elegans*. Knowledge of bacterial growth rates, gene regulation and secondary metabolites will be necessary. In Section 1.3 we will give a comprehensive review of fluorescent pseudomonads in general and the mushroom pathogen *P. fl.* NZI7 in particular. Investigating bacterial growth will be part of this study (see Chapter 4).

This project will investigate the role of *C. elegans* as a vector of pathogens in mushroom farms. To this end we are more concerned about nematode behaviour and health than about its molecular biology. Therefore we will briefly touch on aspects of nematode immunity in Section 1.4.2, which will help us to describe nematode health. The main focus of the introduction will be on chemosensation and decision making in *C. elegans*, which we discuss in Sections 1.4.4 – 1.4.8.

The mushroom farm represents a complex environment, where competing and predatory microorganisms coexist. We have selected one pair of predator and prey to help study the complex interactions in a simpler system, which is disconnected from other predators and other prey. Evolutionary pressure forces predators to distinguish between food with different edibility. We use our system to study how *C. elegans* learns to adapt to the different food sources presented to it (Chapter 5). Similarly prey will have evolved to defend against the large range of predators they encounter. We show how good defences against predation increase the bacteria's chances of survival. In addition this project aims to investigate how mushroom pathogenic *Pseu-*

domonas fluorescens can be spread by the small nematode *Caenorhabditis elegans* under consideration of the balance between reproduction and predation through its vector (Chapter 6). Although we will confine our attention to mushroom pathogens and nematodes found on a mushroom farm, the knowledge gained about this model system can be applied to a variety of similar systems [64, 65].

1.2 Mushroom Farming

Mushrooms have been gathered for many millennia: records of mushroom consumption date back to ancient Roman, Greek and Egyptian times [67]. It is not clear when the cultivation of edible mushrooms began, but it is certain that for over a thousand years mushrooms have been cultivated in China [68]. In Europe mushroom farming is often said to date back to King Louis XIV of France, who started the cultivation of *Agaricus bisporus* in unused limestone quarries [68, 69]. These first detailed records also cite the use of horse manure and stem from 1707 [24]. By the end of the 18th century the importance of composting to increase yields was recognized [24]. By the mid nineteenth century mushroom farming had became popular in the UK as it could be conducted in small or unusable spaces, required no specialised structures and little labour and was thus very cheap [70]. Many sources date industrial mushroom farming back to the end of the 19th century [66, 68, 69], when the introduction of the pure culture method allowed monoculture cultivation with reduced risks of disease and contamination. Around 1910, specialised greenhouses were developed for mushroom cultivation [24, 69].

Regardless of the farming method used, the steps involved make sterility difficult

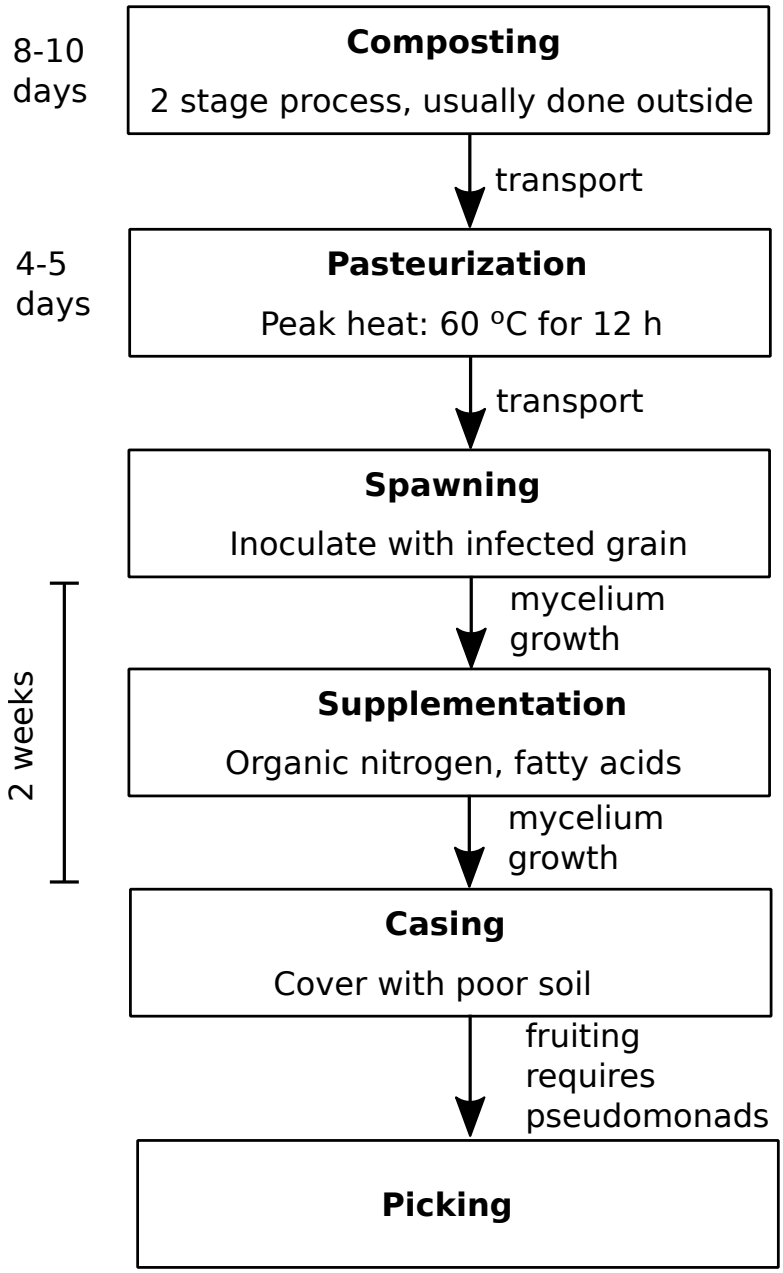

Figure 1.3: Mushroom Farming Modern day mushroom farming involves careful preparation of compost soil to ensure optimal growth conditions for mycelium. Sterility during the whole process is not feasible due to the transportation steps and the requirement for pseudomonads to initiate formation of fruiting bodies. Adapted from 'The biology and cultivation of edible mushrooms' [66].

during the initial phase and almost impossible during the last stages. In any method outdoor composting and transport of compost between different functionalised areas is necessary and the fruiting is promoted by the presence of pseudomonads [71]. For a detailed treatment of mushroom farming the reader is referred to Chang and Hayes Biology and Cultivation of Edible Mushrooms [66], but a brief outline will follow below and the process is summarized in Figure 1.3.

To prepare the growth compost the raw materials (horse manure, wheat straw, maize cobs, feather meal, chicken manure or similar) are composted usually in two phases while being turned regularly. During the first phase water, gypsum and/or calcium carbonate is added as well as any additives necessary to achieve a composition of 2 % nitrogen, 1 % phosphorous pentoxide and 2.5 % potassium oxide. The second stage is often carried out in a separate room, specialized for this purpose. Composting results in a selective medium, which is rich in nutrients that are easily accessible by *Agaricus bisporus* but do not cater well to pathogens and competing fungi [24]. The next step of preparation involves pasteurizing this resulting medium. During this stage the compost is heated to 60 °C and then slowly cooled in aerobic conditions. This results in a material which is rich in microorganisms, especially moulds and bacteria. The compost is now ready and is transported to the growth trays, beds or bags, which could either be in caves or houses. At this stage the compost is spawned with infected grains to inoculate the mycelium. The compost may be supplemented with organic nitrogen, fatty acids and other growth substances to optimize mycelium growth. After the mycelium has grown for some weeks, the beds are covered with a low nutrient casing soil, which encourages fruiting [18, 66, 71]. This soil needs to be permeable to carbon dioxide. At this stage the presence of

pseudomonads is key to the development of fruiting bodies as they absorb diffusible substances excreted by the mycelium, which would otherwise inhibit fruiting [71]. If completely sterile soil is used for farming, absorbers must be added at this stage [66]. Limestone may be added to the casing soil to adjust the pH to 7–7.5, and peat is often used to improve the physical properties of the casing soil [66].

For many diseases the casing soil is suspected to be the main source of contamination [72,73]. Wong and Preece (1987) identified peat and limestone (used for casing) as the most likely primary source for pseudomonads (those necessary for sporocarp initiation as well as those which cause disease) in mushroom farms. They also identified workers as the most prominent method for bacterial dispersal [62]. However this method of dispersal can be easily circumvented using disinfection methods. Thus dispersal methods relying on air, water, and small animals form the main threat to mushroom farmers today. In their study Wong and Preece identified air as a minor contributor towards spreading [62], but emphasized the potential for small mites and flies to spread bacteria. It is a natural extension to this suggestion to look at a natural predator of pseudomonads, *C. elegans*, which has been isolated from mushroom farms on multiple occasions. Microbivorous roundworms (e.g. *C. elegans*) have long been associated with mushroom farms [43, 60]. Even though they have been identified as carriers of bacteria and fungal spores, their role in dissemination has usually been neglected as it is small in comparison to other vectors like flies and mites [43]. However, the latter are much easier to control in a mushroom farm [43], so are less of a factor now than they were 40 years ago, when most of the research of pathogen dissemination on mushroom farms was carried out. *C. elegans* is a nictating worm, which means that it can stand on its tail in order to attach to other

passing animals [40,41,44]. In particular nictating worms attaching to the clothes of workers can spread large doses of bacteria across the farm [43]. Furthermore it will be much easier to explore dispersal in this accessible model system and then apply our findings to animals with different behaviour and movement patterns, than to try and study dispersal by flies directly.

1.3 *Pseudomonas*

Pseudomonads are gram-negative gammaproteobacteria. They form a diverse group of bacteria ranging from human pathogens [74] in the *aeruginosa* cluster (also referred to as intragenic cluster I) to those bacteria in the *fluorescens* cluster (also known as intragenic cluster II), which mainly interact with plants and fungi, either as pathogens [75], biocontrol agents [76–81] or symbionts [82] (see Figure 1.1 on page 4). The fluorescens cluster can be divided into two lineages, usually denoted A and B or complexes II and I (see Figure 1.4). The B lineage (complex I) includes the *tolaasii* strains normally associated with brown blotch disease on mushrooms [83]. However, mushroom pathogens can be found across the fluorescens cluster (see Figure 1.1) [84] and the *Pseudomonas fluorescens* (P. fl) strain NZI7 found in the A lineage was first misclassified as a *tolaasii*, as it can cause similar symptoms and also produces tolaasin. This strain was first isolated from a mushroom farm in New Zealand in 2001 [26].

On mushroom farms pseudomonads encounter *C. elegans* and other predators, which are naturally attracted to the bacterial food through the metabolites secreted. Any organism under threat from predation will develop strategies to defend

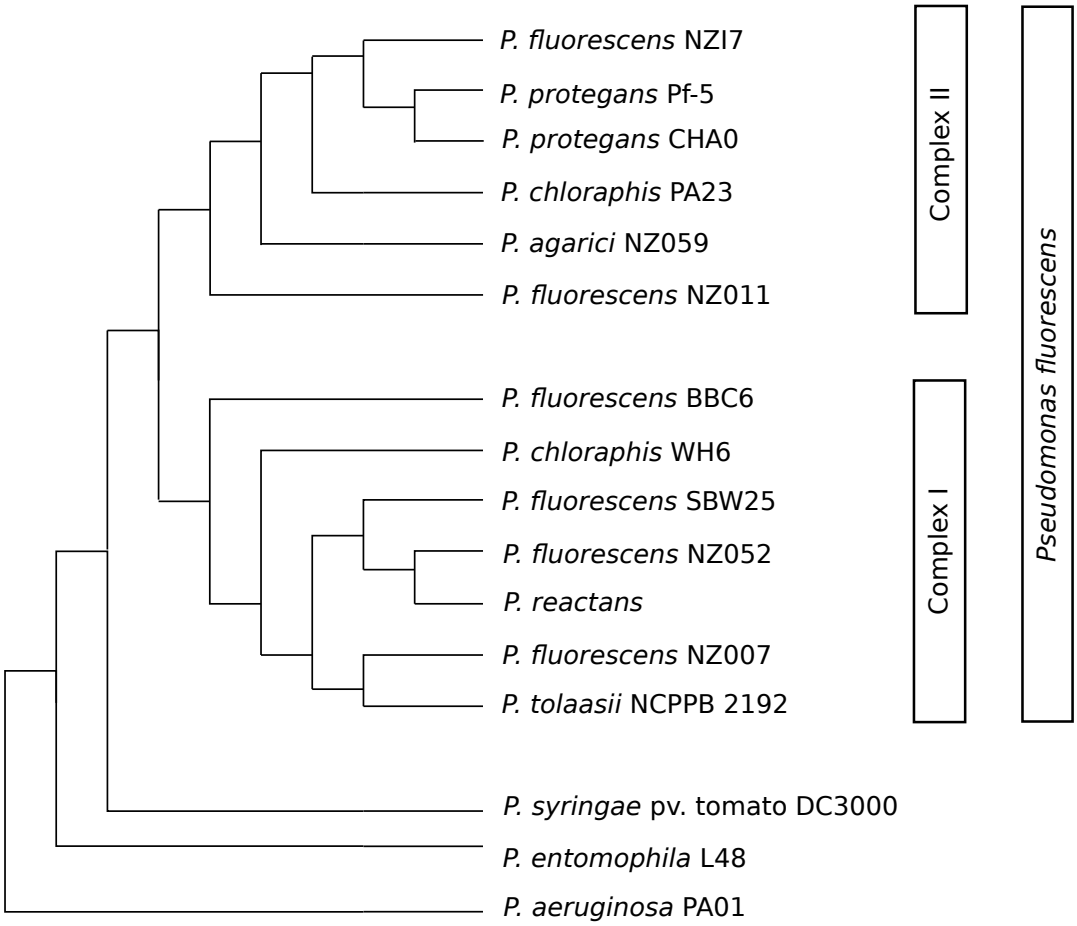

Figure 1.4: Pseudomonads in this report Unscaled phylogenetic tree of the *Pseudomonas* strains mentioned in this thesis for which we have phylogenetic information. Fluorescent pseudomonads are divided into two complexes, highlighting the large difference between the known mushroom pathogen *P. tolaasii* and the strain *P. fl.* NZI7 used in this work. The relations shown here are a subtree of the tree shown in Figure 1.1 on page 4.

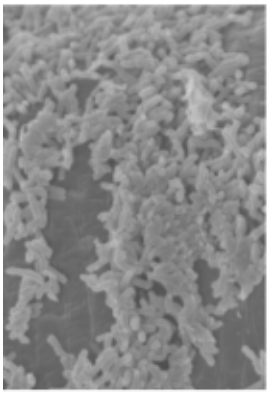

Figure 1.5: Bacteria adhere to the surface of *C. elegans*. Leucobacter Verde1 bacteria show particularly strong adherence to the *C. elegans* cuticle. Image is 50 μm wide. Image reproduced from Hodgkin *et al.* [86].

itself [85]. Among microbes these strategies include slow killing by infection [86], fast killing through the production of nematicidal cyanide [87] or secretion of repellent factors [34]. These strategies will be reviewed in more detail later on, and particularly in Section 1.5.2. Interactions with larger organisms also provides an opportunity to exploit the predator as a vector. Thus, as *C. elegans* explores a larger area, it may spread bacteria to new hosts. However, nematodes are unlikely to forage if they have good food available to them. Instead most of the local bacterial population will be eaten during the encounter [88]. Therefore bacteria must strike a delicate balance between avoiding predation, but also allowing predators to come into contact with them to facilitate dissemination.

Many studies have reported on the interactions between nematodes and bacteria. We will later discuss pathogenicity studies performed with *C. elegans* in Section 1.4.2. A small number of studies have also been carried out on the dispersal of bacteria by nematodes [47, 89]. It has been found on many occasions that bacteria can adhere to the nematode surface coat (see Figure 1.5) [56]. Anderson [90] showed

that *C. elegans* still sheds bacteria 5 hours after exposure and could thus transmit them on the cm to m scale. They also show that the shedding of bacteria is beneficial to nematodes, as it can act as bacterial farming. Transmission of bacteria can also happen when they are ingested but not destroyed by the grinder [48, 49]. In this case bacteria can pass through the gut and may be excreted again. While in the gut the bacteria are protected from a range of sterilisation methods, and thus *C. elegans* might be responsible for long term pathogen survival [43].

1.3.1 Pseudomonads on a Mushroom Farm

Many different pseudomonads are found on the mushroom farm. They mainly originate from the peat used in the casing [62]. Only a small portion of the pseudomonads which can be isolated from mushroom sporocarps are pathogenic. Other strains are necessary to initiate the formation of fruiting bodies [20]. Brown blotch disease in mushroom farms caused by pseudomonads has been the subject of investigation throughout the last century [20, 83]. Only recently have methods to identify strains become available. This has revealed that many closely related pseudomonads can cause brown blotch (see also Figure 1.1 on page 4) [26–29]. Traditionally the 'white line in agar' assay has been used to identify *Pseudomonas tolaasii* [62]. However, we now know that species across the *Pseudomonas* tree test positive in this assay [91].

Godfrey *et al.* [26] isolated more than 130 bacterial strains from mushroom farms in New Zealand. Phenotypically the isolate NZI7 proved very similar to the known mushroom pathogen *Pseudomonas tolaasii* (causing brown blotch and testing positive in the white line in agar assay), but genetic investigation identified it as a new strain closely related to the *P. syringae* strains [26]. However, the tolaasin gene clus-

ter bears close resemblance to that found in *P. tolaasii* and was probably acquired by horizontal gene transfer [26].

1.3.2 The Excretome of Fluorescent Pseudomonads

Except for type IV secretion all of the six secretion systems found in gram-negative bacteria have been identified in different strains of *Pseudomonads* to varying degrees [92–94]. Secretion has been particularly well studied in the human pathogen *Pseudomonas aeruginosa*, which features a particularly large arsenal of secreted compounds and employs all of the five different systems [94]. Less is known about the secretion systems in fluorescent pseudomonads. We do know that *P. fl.* NZI7 employs type II secretion and genes associated with type VI secretion are found in the genome (see also Section 5.3.1). Although type III secretion is common in *Pseudomonas fluorescens* and has been found in Pf-5 and SBW25 [95, 96], there is no evidence for a type III secretion system in *P. fl.* NZI7 [34].

Many secreted metabolites of *Pseudomonas fluorescens* have already been identified; these play important roles in interactions with other species like plants, fungi, other bacteria and predators [77, 80, 97–100]. They can act as growth stimulant for plants, eliminate competition from other bacteria or fight off predators. A large range of low molecular weight antifungal agents has been associated with *Pseudomonas fluorescens* [99]. They can either act as pathogenicity factors for those bacteria relying on fungi for their nutrition. Many secreted metabolites are known as biocontrol factors against a range of plant diseases like Take-all of wheat or flax wilt [78], this is most likely a side product of one of the other functions [101].

Secreted toxins used to deter predators act as public goods and thus cheaters are

likely to arise. Cheaters (usually mutants of the global regulator *gacS*, see below) have lost the ability to produce public good secondary metabolites and thus gain a growth advantage. They are still protected from predators by the toxins produced by non-cheating bacteria. The Yule-Simpson effect ensures that in natural populations these cheaters are kept at low levels through the selective action of predators [88].

Despite the presence of repellent we can observe nematodes close to bacterial colonies, which could be due to low concentrations or diffusion rates of repellents, nematode starvation or could be due to a delayed repellent action which might only become effective after ingestion.

Extracellular factors produced by *P. fl.* NZI7

P. fl. NZI7 is closely related to several other pseudomonads with antifungal properties, like the biocontrol agents in the *protegens* and *chlororaphis* families as indicated in Figure 1.4. However, so far there has been no evidence from the genome that *P. fl.* NZI7 produces factors like pyrrolnitrin and phenazine, which play very important antifungal and nematicidal roles in *P. chlororaphis* PA23, CMR12 or Pf5 [77]. On the other hand, several other aspects are conserved, including the global regulator GacS, which regulates all secretions, and the production of hydrogen cyanide (HCN), which is commonly produced by pseudomonads.

Previous work indicates that multiple factors are involved in nematode–bacteria interactions [91]. In the following paragraphs we will explore some of the factors which are known or thought to be important for this predator–prey interaction.

Proteases Extracellular proteases have been identified as nematicidal, and inhibitors of egg hatching in the biocontrol strain CHA0 [102, 103].

Chitinase Chitinases are usually secreted by bacteria as an antifungal agent, as chitin forms a fundamental part of the fungal cell wall. However chitinases might also have nematode activity, as chitin is part of the pharynx and the eggshell [104].

The Surfactant Tolaasin Estimates of surfactant producing strains among the fluorescent pseudomonads range from 2 to 40 % [76, 99]. These amphiphilic compounds often fall into the group of cyclic lipopeptides (CLP). CLPs contain a hydrophilic peptide moiety, which is cyclized and attached to a lipophilic fatty acid chain [105]. Large gene clusters are responsible for the non-ribosomal peptide synthesis of the peptide component. Lipopeptides are found in a large range of unrelated pseudomonads and include amphisin found in DSS73, massetolide found in SS101, viscosinamide, syringomycin, WLIP and tensin, as well as serrawettin, produced by *Serratia*, which we discussed in Section 1.4.2 [47, 99, 105–108]. The antifungal activity of cyclic lipopeptides secreted by pseudomonads have often been noted [91, 98, 99, 109]. Additionally they are also known for their surfactant properties, role in motility and biofilm formation [105–107]. Tolaasin was first described in the strain description of *Pseudomonas tolaasii* by Tolaas in 1915 [83].
It induces the formation of ion channels in lipid bilayers [110].
Both the surfactant and the pore-forming properties of tolaasin play a role in mushroom pathogenesis [98].

In CMR12a, a biocontrol strain and close relative of NZI7, the role of sessilin, a tolaasin like compound (differing in one amino acid) has been studied. It restricts the

motion of the bacteria, by localizing a mobility-promoting orfamide [106]. CMR12a produces phenazine antibiotics, the production of phenazine is enhanced in sessilin mutants. By analogy a mutant of the toxin tolaasin could be super-repellent or super-toxic.

Cyanide Cyanide is a cytotoxin commonly used by pseudomonads to kill predators and inhibit fungal growth, as observed in *Pseudomonas protegens* Pf-5 (formerly known as *Pseudomonas fluorescens* P.fl 5) and DSS73 [97, 109]. However cyanide production requires rich nutrient conditions, which are not often found in nature [111]. NZI7 retains its mushroom pathogenicity in low nutrient conditions with the non-ribosomal peptide tolaasin and can repel nematodes without killing them [34].

Cyanide production by bacteria and especially pseudomonads has been researched for over a century [112, 113]. It is found in about half of the members of both the fluorescent pseudomonads and *Pseudomonas aeruginosa* [114]. Hydrogen cyanide (HCN) is a secondary metabolite produced solely for the purpose of inhibiting other organisms [87, 113, 114]. It inhibits metaloenzymes, most notably cytochrome c oxidase [113]. Three genes (hcnABC) are necessary for the synthesis of cyanide [113] but producing bacteria must also ensure that they themselves are immune to its toxic effects [113]. Cyanide synthesis is under the control of the GacS regulator [113] and is induced in microaerophilic conditions [113] and mainly at entry into stationary phase [113, 114]. Cyanide poisoning is the main cause of death upon infection by *Pseudomonas aeruginosa* in humans [111, 115]. Cyanide is known to play a role as antifungal agent in biocontrol strains like CHA0 [113]. HCN production is particularly favoured in rich media [111], so is a less important factor in interactions with

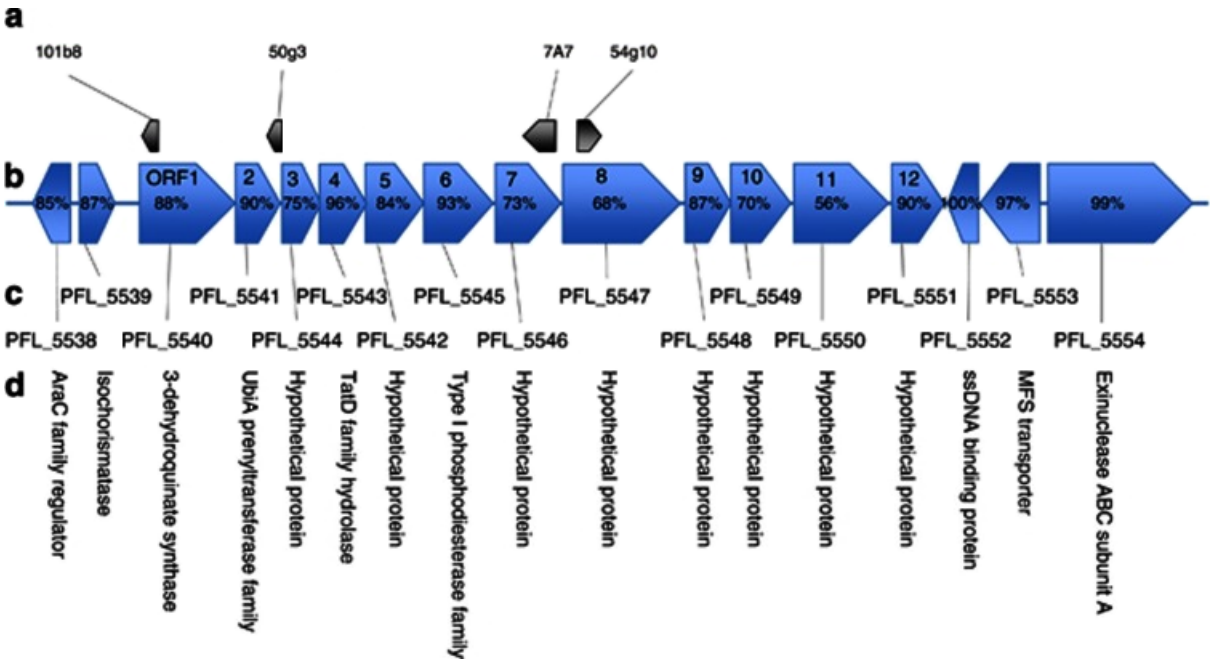

Figure 1.6: The EDB locus (a) Transposon insertions of the four EDB mutants used in this study. The arrows indicate the orientation of the promoterless gfp::lux reporter construct. (b) Predicted ORFs in the EDB region of NZI7. Those ORFs belonging to the cluster are numbered, and the sequence identity to *Pseudomonas protegens* Pf5 is given for each. (c) Locus tags for corresponding ORFs in *Pseudomonas protegens* Pf5 (see Table 1.2). (d) Predicted functions of ORFs in the EDB region. Image reproduced from Burlinson *et al.* [34].

nematodes on the nutrient poor nematode growth medium (see Section 2.1.1). We will nonetheless include a cyanide mutant in our analysis.

EDB The EDB locus in *P. fl.* NZI7 (Figure 1.6) was first described by Burlinson [34] as a gene cluster involved in nematode interaction. No homologous cluster is found in the close relative Pf5, but in other pseudomonads including WH6, *P.tolaasii* NCPPB2192 and *P. entomophila* L48. The gene product of this cluster is – to date – unknown, though it is believed that it is derived from chorismate (see Figure 1.7) (Gail Preston, personal communication).

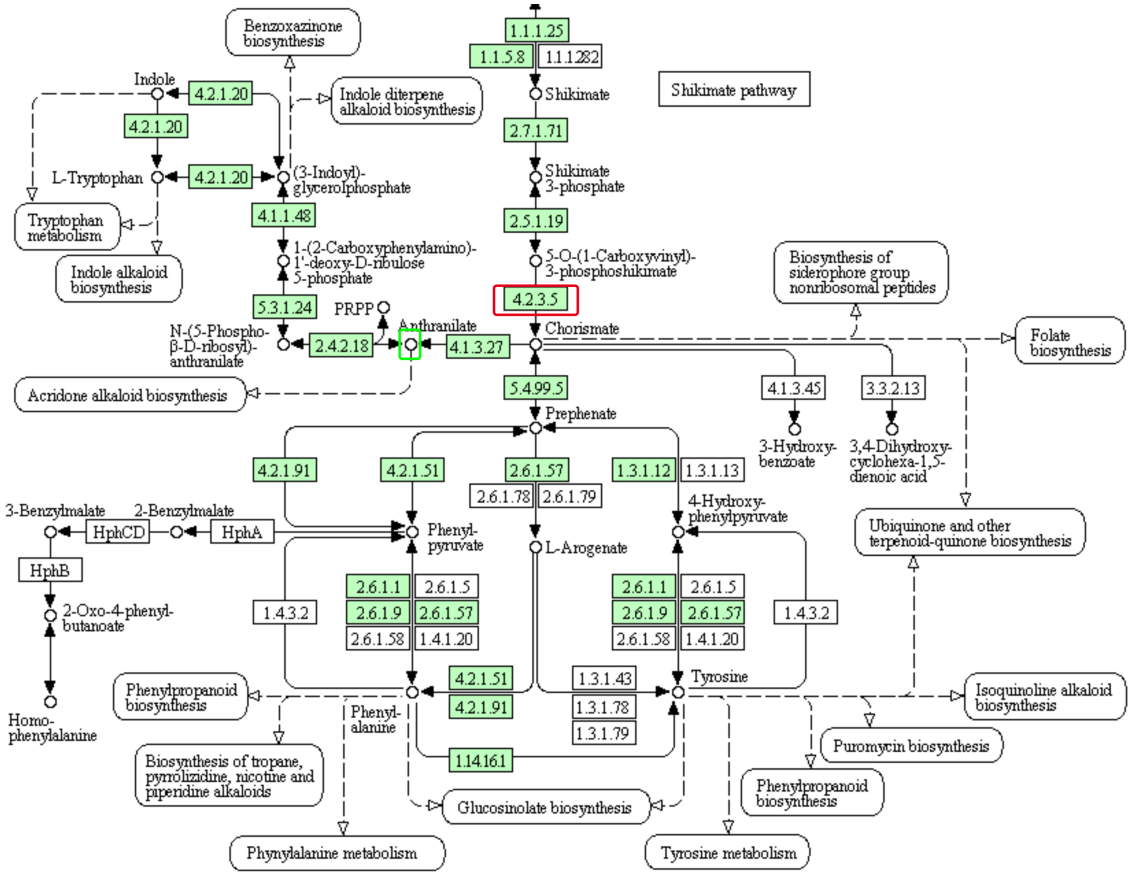

Figure 1.7: Chorismate is central to many synthetic pathways Chorismate synthase (4.2.3.5 highlighted in a red box) is disrupted in three of the edible mutants identified by Burlinson (see Table 1.2). Chorismate is a precursor for a large variety of biomolecules, including some amino acids, and non-ribosomal peptides. The product of the EDB locus is speculated to require precursors from the anthranilate pathway (green). Pathway reproduced from KEGG [116]

Chorismate Chorismate is the precursor for a range of primary metabolites including amino acids. Compounds dependent on chorismate synthesis are highlighted in Figure 1.7. Furthermore anthranilate, which can be derived from chorismate is believed to be a precursor of the extracellular factor EDB (Gail Preston, personal communication).

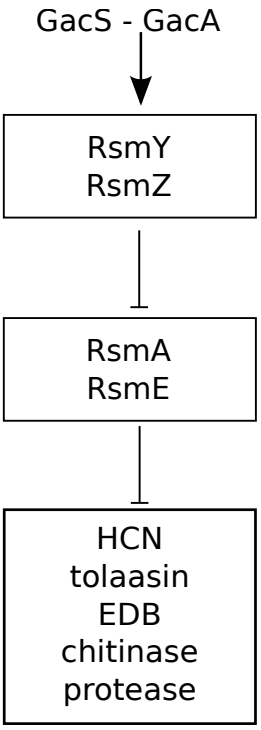

Figure 1.8: GacS pathway The GacS pathway has been investigated in CHA0 [117]. The small regulatory RNAs RsmY and RsmZ sequester the RNA-binding proteins RsmA and RsmE, and thus facilitate the transcription of RNA. Burlinson identified several factors in *P. fl.* NZI7 which are regulated by this pathway [91]. Table 1.2 also highlights genes regulated by the Gac pathway.

GacA/GacS GacS is a global regulator that influences most of the secreted factors, including the pathogenic tolaasin-like-toxin (TOL) and cyanide [118,119]. The unknown nematode repellent factors usually secreted by NZI7 are also under the control of GacS [34]. The disruption of this global regulator makes the bacteria highly attractive, even when compared to the standard laboratory food, *E. coli* OP50 [34,47]. Most extracellular factors are controlled by the GacA/GacS pathway. The pathway has been studied in a close relative of NZI7, *Pseudomonas fluorescens* CHA0 [117,118] (see Figure 1.8). As this pathway is well conserved across the *Pseudomonas fluorescens* species, it is likely that it functions the same in NZI7 as in

CHA0. The GacS mutant of DSS73 is known to be a superfood for *C. elegans*, accelerating nematode growth and increasing fertility when compared to the standard food *E. coli* OP50 [47].

1.3.3 The Mutant Library

In this project we use different mutants of *P. fl.* NZI7 to gain insight into the behaviour of the wild type (WT) strain. Studying a range of existing NZI7 mutants which have lost some or all of their ability to repel nematodes will facilitate an understanding of the mechanism of repellence. The mutants were created by Burlinson [34] through the random insertion of a mini-Tn5 derived transposon into the bacterial chromosome. Mutants thus created were screened for palatability and secretion of exofactors, and those with a non-wild-type phenotype were sequenced. Of the 84 edible mutants, 11 were mutants of the edibility (EDB) cluster (Figure 1.6) [34].
Of the mutants identified by Burlinson we selected those for which we had genotypic information for further study. Additionally we selected mutants of the known toxins tolaasin and HCN. As we wish to study bacterial dissemination, we have also included a flagella mutant in our investigation. To study the cost of the transposon insertion we include 5 mutants with no phenotype as control. Finally during this study we have constructed strains with fluorescent and luminescent markers, which are included here.
All of these selected mutants are summarized in the Tables 1.2 and 1.3 with the results from the initial screens.

The results from chitinase and blood lysis (indicating pore formation [120]) assays can serve as a proxy for mushroom pathogenicity [120], although mutants of

P. tolaasii have been generated which were mushroom pathogenic but negative in the blood lysis assay [98]. The chitinase activity might also be relevant to nematode interactions, as chitin is present in nematode eggs and pharynx [104]. Lecithinase activity was assayed using egg yolk agar and tributyrin agar was used to screen for lipase activity. Lecithinase and lipase activity might point to pathogenicity factors.

The White line assay has often been used in the past to test for tolaasin. Historically all bacteria testing positive against *P. reactans* in this assay have been classified as *P. tolaasii* [23]. The assay is based on the interaction of two Cyclic LipoPeptides (CLP): WLIP (White Line Inducing Principle secreted by *P. reactans*) and many toxins which are closely related to tolaasin, the pathogenic metabolite employed by *P. tolaasii* to cause brown blotch disease. A white line is formed between the two bacterial colonies if one produces and releases WLIP and the other a tolaasin-like substance. The white line is the result of the interaction and precipitation of the two Cyclic LipoPeptides (CLP). However, it has been observed that the presence of one of the CLP can restrict the diffusion of the other. Sesselin in CMR12a also acts as a tolaasin-like substance in that it produces a white line, and, like tolaasin, it restricts the secretion and diffusion of a WLIP [106]. Due to the interaction of WLIP with tolaasin, WLIP has been investigated as a mean to prevent mushroom browning [23].

All screens conducted by Burlinson [91] are summarized in Table 1.1 and the results are indicated in Table 1.3. Furthermore we can identify those genes, which we believe to be under the regulation of the global regulator GacS. This information is based on microarray transcriptomic data with which Hassan *et al.* identified many of the differentially expressed genes in mutants of the GacA/GacS regulatory system

[121] in the close relative Pf-5.

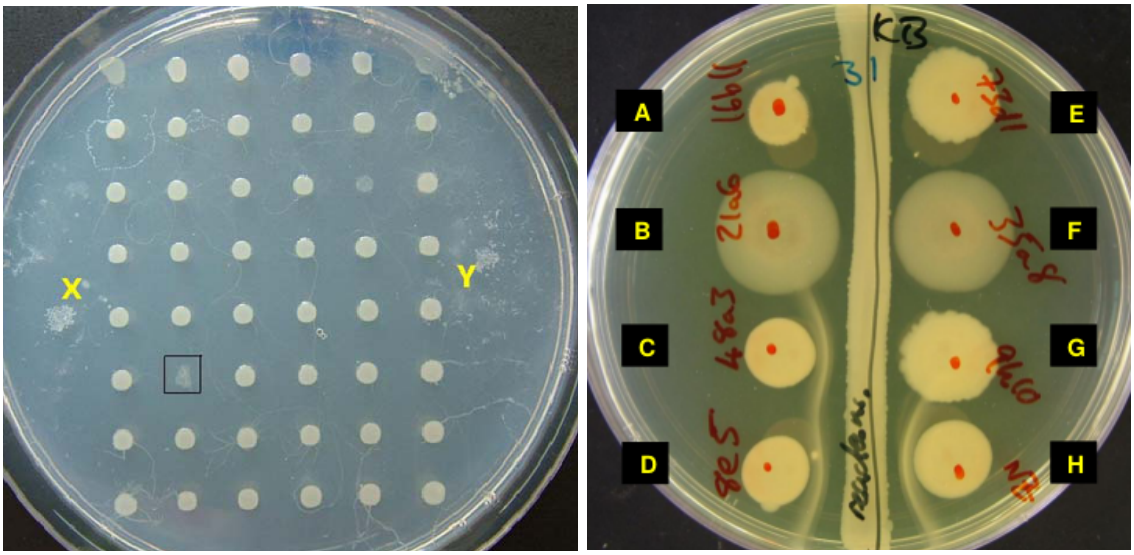

Figure 1.9: Screening bacterial mutants Top: Initial screen for edibility. Nematodes were placed into the areas marked X and Y. Bacterial colonies were scored during the first three days for loss through predation. One of the more edible mutants is highlighted by a box. Numerous trails of bacteria between colonies, created as nematodes move, are also visible. Bottom: The white line in agar assay has been traditionally used to identify *Pseudomonas tolaasii*. It is still used to screen for tolaasin deficient mutants of producing strains. Eight different transposon mutants are tested either side of a central streak of *Pseudomonas reactans*. The GacS mutants (B, F) are negative in this assay. Mutants C, D and H test positive. Images reproduced from Burlinson [91].

Table 1.1: Screens on bacterial mutants Screens conducted by Burlinson on mutants of *P. fl.* NZI7.

screen	**notes**	**relevance**
edibility	see Figure 1.9	selection criterion
chitinase	LB - colloidal chitin agar	proxy for mushroom pathogenicity
blood lysis	Columbia horse blood agar	proxy for mushroom pathogenicity
lipase	tributyrin agar	lipases are virulence factors
lecithinase	egg yolk emulsion agar	a specific lipase
HCN	picrate solution	known nematicidal compound
WLA	against *P. reactans*	tolaasin production

Table 1.2: Mutants of the mushroom pathogen NZI7. Some mutants will be referred to by an abbreviation of the genotype or phenotype later in the report. This is highlighted in bold.

Identifier	Blast Hit [1]	Predicted function	Lux promotor
Insertion mutants in genes with homologues in Pf5			
904	PFL_0085 +	thiol:disulfide interchange protein DsbA family	cryptic
956	PFL_0116	CoA dehydrogenase	reporter
955	PFL_0117	glutaryl-CoA dehydrogenase	reporter
908	PFL_0836 -	ATP-dependent metalloprotease FtsH	cryptic
912	PFL_0836 -	glutamate–cycteine ligase	cryptic
961	PFL_0928; PFl_0929 -	ATP phosphoribosyltransferase histidinol dehydrogenase	reporter
920	PFL_1449	mucA sigma factor algU (negative regulator) **mucoid**	cryptic
906	PFL_1595 -	YCII-related domain protein/ intracellular septation protein A	reporter
905	PFL_1638	M ring component **FliF**	reporter
1638	PFL_1685	cytochrome c-type biogenesis protein CycL	cryptic
959	PFL_2066	3-isopopylmalate dehydrogenase	reporter
1015	PFL_2578 +++	hydrogen cyanide synthase HcnB **HCN**	cryptic
970	PFL_2761	haemagglutinin repeat protein	reporter
1642	PFL_2816	COG 5499: predicted transcription regulator containing HTH domain	cryptic
954	PFL_3902	NADH-quinone oxidoreductase G subunit	reporter
910	PFL_3930; PFL_3931	OmpA/MotB, and acyl-CoA dehydrogenase family protein	reporter
957	PFL_3987; PSPPH_1698	ATP-dependent CLP protease	reporter
964	PFL_4192	Periplasmic binding Protein	reporter
1046	PFL_4347	chorismate synthase	reporter
967	PFL_4348	chorismate synthase	reporter

Continued on next page

[1] + or - indicate whether this gene is positively or negatively regulated by GacA in Pf5 [121].

[1] +++ indicates an 8-fold change in expression in a GacA mutant [121].

Table 1.2 – continued from previous page			
Identifier	**Blast Hit**	**Predicted function**	**Lux promotor**
921	PFL_4348	**chorismate** synthase	reporter
1644	PFL_4448	cysteine synthase B	cryptic
913	PFL_4451	**GacS**	reporter
963	PFL_4788	Acetolactate synthase	reporter
1663	PFL_4870	glycerol-3-phosphate dehydrogenase	reporter
1646	PFL_5273 -	sensory box histidine kinase	cryptic
1654	PFL_5277	3-methyl-2-oxobutanone hydroxymethyltransferease	reporter
1659	PFL_5326 -	Glutamate 5-kinase	cryptic
1643	PFL_5388	major facilitator family protein	cryptic
969	PFL_5425	fadE8	reporter
923	PFL_5540	3-dehydroquinate synthase domain protein **EDB2**	cryptic
1009	PFL_5541	UbiA prenyltransferase family superfamily **EDB3**	cryptic
1648	PFL_5546	conserved hypothetical protein **EDB4**	cryptic
917	PFL_5547	hypothetical protein in pf5 **EDB1**	reporter
916	PFL_5629 +	anthranilate synthase component I	cryptic
985	PFL_5629, PFL_5630 +	anthranilate synthase component I/ phosphoglycolate phosphatase	cryptic
1639	PFL_5650	Bis(5'-nucleosyl)-tetraphosphatase	cryptic
1657	PFL_5742; PFL_5743	Zn-dependent dipeptidase	cryptic
958	PFL_5850 -	thiazolebiosynthesis protein ThiG	cryptic
1655	PFL_5877 +	dihydroxy-acid dehydratase	reporter
1660	PFL_5899; PFL_5900	PTSINtr with GAF domain, PtsP NUDIX hydrolase	reporter
1653	PFL_5899; PFL_5900	phosphoenolpyruvate-protein phosphotransferase (PtsP)	cryptic
918	PFL_5919	penicillin amidase family protein	cryptic

Continued on next page

[1] + or - indicate whether this gene is positively or negatively regulated by GacA in Pf5 [121].

[1] +++ indicates an 8-fold change in expression in a GacA mutant [121].

Table 1.2 – continued from previous page			
Identifier	**Blast Hit**	**Predicted function**	**Lux promotor**
965	PFL_6125	phosphoribosylaminoidazole	reporter
1048	PFL_6125; PFL_6126	phosphoribosylaminoimidazole carboxylase ATPase and catalytic subunits	cryptic
971	PFL_6158	acetyl-CoA carboxylase	reporter
1734	PFL_6226	gidA	reporter
1652	PFL_6229	trmE tRNA modification GTPase	reporter
1664	PFL_6230	inner membrane protein, 60kDa	cryptic
Other transposon insertion mutants			
903	Psyr_2616	non-ribosomal peptide synthetase **tol**	reporter
2073	unknown	unknown	unknown
2074	unknown	unknown	unknown
2075	unknown	unknown	unknown
2076	unknown	unknown	unknown
2077	unknwon	unknown	unknown
Mutants constructed by Burlinson			
978		ΔGacS in tol mutant	reporter
989		Δ GacS in WT	n.a.
1003		ΔGacS in EDB1	reporter
1004		ΔGacS in EDB1	reporter
1086		ΔEDB in HCN	cryptic
1712		Δtolaasin in HCN **double**	cryptic
1713		Δtolaasin and ΔEDB in HCN **triple**	cryptic
1900		ΔEDB in WT	n.a.
Mutants constructed in this study			

Continued on next page

[1] + or - indicate whether this gene is positively or negatively regulated by GacA in Pf5 [121].

[1] +++ indicates an 8-fold change in expression in a GacA mutant [121].

Table 1.2 – continued from previous page			
Identifier	**Blast Hit**	**Predicted function**	**Lux promotor**
2079		WT with mini-Tn7 insertion of GFP	n.a.
2080	PFL_5541	EDB3 with mini-Tn7 insertion of RFP	cryptic
2081	PFL_4451	GacS with mini-Tn7 insertion of GFP	reporter
2082		WT with mini-Tn7 insertion of RFP	n.a.
2083		*lux* cassette plasmid in WT	pNEO
2084		mCherry plasmid in WT	n.a.
2085		GFP plasmid in WT	n.a.
2086		*lux* cassette plasmid in ΔGacS	pNEO

[1] + or - indicate whether this gene is positively or negatively regulated by GacA in Pf5 [121].

[1] +++ indicates an 8-fold change in expression in a GacA mutant [121].

Table 1.3: Phenotypic characterisation of miniTn5 insertion mutants created by Burlinson [91].

Identifier	**Edibility**	**Chitinase**	**Blood lysis**	**Protease**	**Lipase**	**Notes**
904	edible	-	+	+	+	spread out morphology
956	edible	+	+	+	+	stronger orange pigment in chitinase assay
955	weakly edible	+	+	+	+	
908	weak	+	+	+	-	negative in WLA
912	edible	+	+	+	+	negative in WLA, small colony
961	edible	+	+	+	+	
920	edible	+	+	+	-	mucoid colony morphology
906	edible	+	-	+	+	negative in WLA
905	none noted	+	+	+	weak	no flagellum, less smooth colony morphology

Continued on next page

Table 1.3 – continued from previous page						
Identifier	**Edibility**	**Chitinase**	**Blood lysis**	**Protease**	**Lipase**	**Notes**
1638	edible	weak	+	+	+	weak cyanide production
959	edible	+	+	+	+	
1015	not edible	+	+	+	+	no cyanide production
970	edible	+	+	+	+	
1642	very edible	n.t.	-	weak	+	growth impaired
954	edible	+	+	+	+	
910	strongly edible	+	+	+	+	precipitate in cyanide assay
957	edible	+	+	+	+	
964	edible	+	+	+	+	
1046	edible	+	-	+	+	negative in WLA
967	weakly edible	-	+	+	+	
921	strong edibility	+	+	+	-	
1644	very edible	+	+	+	+	
913	strongly edible	-	-	-	-	HCN and WLA negative, spread colony morphology
963	weak	+	+	+	+	
1663	edible	weak	-	+	+	
1646	edible	+	+	+	weak	weak cyanide production
1654	edible	+	+	+	+	
1659	edible	+	+	+	+	
1643	edible	+	-	-	weak	negative in WLA
969	weak	+	+	+	+	
923	edible	+	+	+	+	
1009	edible	+	+	+	+	
1648	edible	+	+	+	+	
917	edible	+	+	+	+	
Continued on next page						

Table 1.3 – continued from previous page						
Identifier	**Edibility**	**Chitinase**	**Blood lysis**	**Protease**	**Lipase**	**Notes**
916	edible	+	+	+	+	
985	edible	+	+	+	+	
1639	edible	weak	-	+	+	negative in WLA
1657	edible	weak	-	very weak	+	
958	edible	+	+	+	+	weak growth
1655	edible	+	+	+	+	
1660	edible	+	weak	+	+	
1653	edible	+	+	+	+	
918	strongly edible	-	-	-	-	not complemented, possibly GacA mutation
965	weak	+	+	+	+	
1048	edible	+	+	+	+	
971	weak	+	+	+	+	
1734	weak	+	-	-	+	weak cyanide production, negative in WLA
1652	edible	+	-	weak	+	
1664	edible	+	-	weak	-	-ve in WLA
903	none noted	+	-	+	+	negative in WLA, tolaasin deficient
2073	not edible	+	+	+	+	
2074	not edible	+	+	+	+	
2075	not edible	+	+	+	+	
2076	not edible	+	+	+	+	
2077	not edible	+	+	+	+	

1.3.4 Bacterial Tagging Techniques

Bacteria can be tagged in a range of ways to aid determining their location, number and identity. Most commonly this is done using the lux system [122, 123] or fluorescent proteins [124, 125]. These reporters can be either inserted as a plasmid or chromosomally.

Plasmid insertions Plasmids are small strands of circular DNA which can be transferred horizontally between different strains. They are commonly used as an easy method for insertion of foreign genes into a microorganism [126]. This requires a selective marker, and bacteria will need to be cultured in the presence of the antibiotic at all times to avoid loss of the plasmid.

Chromosomal insertion Unlike the random miniTn5 insertion used to generate the mutants described in Tables 1.2 and 1.3, the Tn7 system can be used to chromosomally insert a vector at a specific site. This site (attTn7) [127] is found downstream of the GlmS gene (see Figure 1.10) [124]. The mini-Tn7 tagging mechanism decouples the proteins necessary for the movement of the transposable element from the element itself, thus, once insertion into the chromosome has been achieved the vector will remain there stably [128] without the need for selection by an antibiotic. This system has been used multiple times without ever any side-effects of the tagging having been reported [129, 130]. To date, the insertion site has been described as neutral [124], in Chapter 5 we will see that insertion at this site might not be neutral.

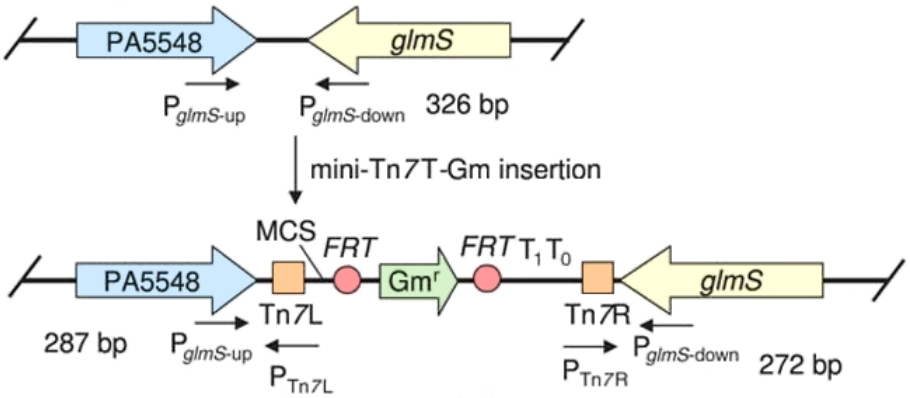

Figure 1.10: Tn7 insertion site in *Pseudomonas aeruginosa* The att:Tn7 site in *P. aeruginosa* is located downstream of *glmS*. Terminators (T) prevent read-through in either direction. Primers $P_{glmS\text{-down}}$ and P_{Tn7R} are used to confirm insertion at the correct site. Image reproduced from Choi *et al.* [131]

1.4 *Caenorhabditis elegans*, a Bacterivorous Nematode

Due to the length of time *C. elegans* has been the focus of research, its development and behaviour are well understood. The cell lineage has been completely traced [53], and the neuronal network with its 302 neurons is mapped [53, 132]. The whole genome of this model organism is known [133], and more than 21 000 mutants are described and available [134]. This model organism is used to investigate a range of human diseases like cancer, diphtheria or *Staphylococcus aureus* and *Enterococcus faecalis* infection [57, 59, 135, 136], infection studies with these or with natural pathogens allow insights into the human immune system. The compact nervous system allows robust behavioural studies, where behaviours can be linked to individual genes and neurons through gene knock out and laser ablation [137–139].

Our understanding of how *C. elegans* perceives bacteria is limited by our incomplete knowledge of the bacterial excretome. Chemosensation allows *C. elegans*

to sense bacterial food over long distances, as submillimolar concentrations can be perceived [132, 140]. Chemosensation will be reviewed in more detail in Section 1.4.4. The behaviour of *C. elegans* is not only directed by the chemical environment, but also influenced by satiation, health and past experience. Many experiments have proven that nematodes can learn to associate certain compounds or concentrations with favourable or adverse conditions like quality, abundance and pathogenicity of food [54, 132, 141–143]. This mechanism can also turn previously neutral compounds into chemoattractants or repellents and facilitates the recognition of previously encountered food. This process, known as associative learning, could be facilitated by pheromones (reviewed in Section 1.4.7), although there is also evidence for sensory adaptation (known as olfactory plasticity) being involved in the learning processes [144]. In Section 1.4.5 we will further examine the learning behaviours observed in this nematode. The combination of a large range of chemosensors with the ability to learn, leads us to expect complex behaviour in the presence of diverse chemical stimuli such as the metabolites secreted by bacteria. Taxis is achieved through a swim and pirouette mechanism (similar to the well-known run and tumble of *Escherichia coli*) [145], combined with a weathervane strategy, by which the nematode curves towards the attractant [37].

1.4.1 Nematodes on the Mushroom Farm

Nematodes have long been tightly associated with mushroom farms [43]. They have been studied very little as a disease vector, since many other microorganisms found in this environment have greater effect on mushroom yields. However, while the killing of flies is a long standing practise, nematodes are much harder to get rid

of [43].

Since *C. elegans* was first isolated from a mushroom farm near Bristol [60] it has mainly been studied outside this context, although there have been some studies of the impact of nematodes on mushroom yields. Within three months Grewal found that *C. elegans* can act as a biocontrol agent agains *P. tolaasii*, but also causee lower mushroom yields through spreading the pathogenic bacteria [35, 89]. With this study we aim to return attention to the mushroom farm, by investigating *C. elegans* interactions with a bacterium commonly found on mushroom farms.

It has been noted that the bacteria isolated from *C. elegans* can have a range of effects on mycelial growth, ranging from enhancers (e.g. *P. reactans*) to strong inhibitors (e.g. *Bacillus cereus*) [146]. It is thus only natural to ask, what effects *C. elegans* has on its natural environment.

1.4.2 *C. elegans* as a Model for Pathogenicity

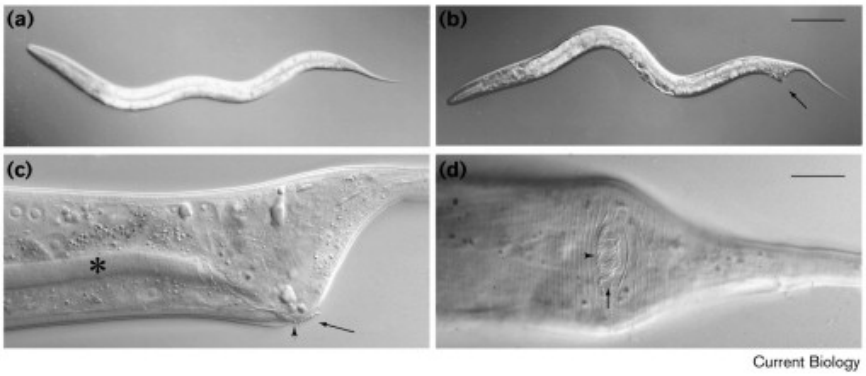

Figure 1.11: Dar – Deformed anal region The Dar Phenotype in *C. elegans* is caused by infection with *Microbacterium nematophilum*. a) uninfected WT nematode, b) nematode infected with *M. nematophilum*, c) lateral and d) vertical close up of the swollen post anal region. The rectal swelling is indicated with an arrow. The * highlights the extended gut lumen characteristic of constipation. Scale bars: a,b) 100 μm and c,d) 20 μm. reproduced from Hodgkin *et al.* [147].

C. elegans is a popular model for bacterial infection with human pathogens like *Corynebacterium diphtheriae* (causing diphtheria), *Pseudomonas aeruginosa* (an opportunistic pathogen causing a range of diseases including pneumonia and gastritis) and *Yersinia pestis* (the causal agent of bubonic plague) [55, 135, 148–151]. The biofilm generated by *Yersinia* spp. that blocks the digestive tract of the flea, also inhibits food intake by *C. elegans*, *P. aeruginosa* and *Serratia marcescens* can colonize the *C. elegans* gut, triggering an immune response in an analogous fashion to the human response [152,153], and the different virulence factors of *Corynebacterium spp.* are reflected in the rate at which they kill their nematode host [154].

In challenges of *C. elegans* with human pathogens death is usually the main symptom considered [55, 150, 155] and often expression of marker genes is monitored at the same time [103, 153]. However, studies have also been carried out with natural pathogens of *C. elegans* [56, 147]. In 2000 the pathogenic *Microbacterium nematophilum* was described to cause a Dar (deformed anal region) phenotype [147] (see Figure 1.11). The swelling of the near rectal region is caused by an innate immune response of *C. elegans* to the constipation caused by the bacterium and is necessary to "prevent developmental arrest and sterility" [156]. The constipation, also noticeable by an extended, very visible, gut lumen is a common symptom of infection and is likely to restrict nutrient uptake [44].

Leucobacter strains Verde1 and Verde2 were coisolated with *C. tropicalis* in Cabo Verde. They cause infection through adherence to the nematode surface coat [86]. Another common symptom is increased transparency of the worm caused by osmotic stress. This is partly due to arrested ovulation [157], and partly due to the formation of fluid vesicles [158]. Osmotic stress can also cause worms to shrink [159]. Combined

with the extended gut lumen caused by the constipation [44, 47, 136] this causes the gut to be visible as a zigzag-line through the body. Worm shrinking could also be due to an overlap in signalling between size determination and chemosensation. The exact link between these two is not yet understood [160].

In monitoring nematode health when investigating bacteria nematode interactions in this study, we will make use of these commonly found symptoms.

1.4.3 Nematode Motion

The most striking feature of nematode motion are the sinusoidal waves which gave *C. elegans* its name. On their own these result in a net forward movement without any turning. Looking at the larger scale trajectories of *C. elegans* we can observe various methods for altering the direction of movement. It has been postulated that this is sufficiently described though a mechanism which resembles the well studied run and tumble observed in chemotactic bacteria [161]. Bacteria display sections of straight forward motion (run) interrupted by random reorientation events (tumble). Adapting the frequency of those reorientation events allows bacteria to move according to chemical gradients. A similar mechanism determines the locomotion of *C. elegans*, except that the nematode does not reorient (pirouette) randomly [145], and can control the length of its forward movements (swim) to a higher degree [162]. Gradual turns are a further strategy by which nematodes can respond to stimuli. Sensing the difference between stimuli as the head moves along the sinusoidal trajectory, the nematode bends its path through breaking the symmetry of its periodic swim [37].

1.4.4 Chemosensation and Chemotaxis in *C. elegans*

C. elegans does not navigate by sight (though they show some phototaxis [163]) and there is no evidence that sound has any effect on its behaviour, thus reducing the number of variables which must be controlled in laboratory experiments. *C. elegans* does exhibit responses to mechanical stimuli: the tap reversal response is often used to check whether an individual is alive and mechanosenstation plays an important role in feeding and the food leaving response (see Section 1.4.6) [132, 164, 165]. The nematode mainly navigates using chemical and thermal gradients [139, 142, 143, 160, 166, 167] which can be easily controlled and modelled. Chemosensation is the most important mechanism by which *C. elegans* senses its environment [160]. Other mechanisms include mechano-, magneto- and thermosensation [160, 168–170]. More than 5 % of the nematode's genes are involved in chemosensation and the processing of chemical cues [160]. Over half of the cells in the head region of *C. elegans* are neurons or are related to them, and most of these are sensory neurons [171]. The largest assembly of sensory neurons is the amphid in the head region, which consists of 12 neurons. The names of amphid neurons begin with the letter A (see Table 1.4). A large range of organic and inorganic compounds can be distinguished by the receptors in the 32 chemosensory neurons [139, 160]. It is known that nematodes are attracted by a wide range of organic or inorganic compounds such as cAMP, short chain ketones and NaCl [139, 167], while other compounds like surfactants can act as repellents [172] (see Table 1.5 for more details).

Many studies are concerned with the behaviour triggered by different chemical environments in different conditions [132]. These studies are usually concerned with

isolated compounds, but even so can give a glimpse of the complexity of chemosensation and associated behaviour in *C. elegans* [139,160]. Type as well as concentration are important in determining the behaviour towards a perceived stimulus [139,173].

For studies of chemotaxis, the *tax-2* and *tax-4* mutants are commonly used [160, 174–177]. These mutants have a defect in one of the subunits of a cyclic nucleotide gated channel expressed in some of the neurons and affect thermo-, chemo-, and gustatory sensation. However, it is unlikely that all chemotaxis is disabled by the alleles commonly in use [165]: in addition to residual functionality in the encoded channel, some other channels make other paths of chemosensation available (see Table 1.4). Nonetheless, we have been able to confirm a significant increase in the time taken to locate food in *tax-2* and *tax-4* mutants (data not shown).
For a more complete knockout of chemosensation various *che* strains are commonly used [178, 179], particularly *che-2, che-3* or *che-13*. The cilia dysfunction in these strains is known to affect almost all sensory neurons [180] (see Table 1.4), but this approach is very crude and it is not known which other neurons are affected by the mutation.

All severe chemosensation mutants (*che* or *tax*) are known to have lower food leaving probabilities [165]. It has also been noted that they dwell more when on food [160, 179]. While an N2 WT worm intersperses its dwelling behaviour with roaming behaviour 20 % of the time when on food, this is not observed in *che* mutants. This alteration of behaviour might be benefitial due to the inability of the afflicted animal to find back to a food patch, once it has been left.

An altered response to chemical stimuli is also observed in another natural strain of *C. elegans* isolated from Hawaii which provides an alternative genetic

background. *Serratia* is a common bacterial pathogen to investigate nematode behaviour. In response to *Serratia*, altered chemotaxis has been reported for the Hawaiian strain [181]. This could be due to altered olfaction, though there is some evidence against this [38], or could also be caused by a different behavioural response to the pathogenic bacteria [182]. The Hawaiian strain also responds differently to gradients of oxygen, which we will discuss further in Section 1.4.8.

Chemosensation mutants provide a powerful tool to study how *C. elegans* senses bacteria. However, the effects of mutations are often very complex, including reduced food leaving probability and increased time taken to locate food, as well as the desired inability to discriminate between bacterial odours, meaning that it will be difficult to interpret the results.

Table 1.4: Some neurons found in *C. elegans* which are involved in behavioural regulation.

neuron [1]	**ref**	**description**
ADE *	[185]	basal slowing response to bacteria through mechanosensation
ADF *	[142]	responsible for associative learning
	[167]	contributes partially to the chemotaxis towards Cl^-, Na^+ and cAMP
	[186]	responsible for repressing dauer formation under normal conditions
ADL *	[187]	nociceptive neuron necessary for social interactions
	[167]	chemical avoidance
AFD * ˆ	[165]	promotes food leaving
	[160]	thermosensation
AIA	[188]	required for aversive but not appetitive learning
	[189]	required for chemotaxis to indole ascerosides
AIY *	[160]	interneuron downstream of ASE
	[160]	suppresses pirouettes
	[190]	sufficient to control chemotaxis
AQR *	[160]	sensory neuron for aerotaxis, and implicated in regulating social feeding
ASE * ˆ	[167]	most important amphid neuron in chemosensation
	[167]	necessary and sufficient for chemotaxis
	[160]	senses water soluble attractants like Cl^-, Na^+, cAMP, biotin, lysine and seratonin
	[165]	promotes food leaving
ASG *	[167]	minor role in chemotaxis towards Cl^-, Na^+ and cAMP, as well as leucine
	[186]	represses dauer formation under normal conditions
ASH *	[187]	necessary for social interactions
	[160]	nociceptive neuron ensuring avoidance of metals, alkaloids and some organic odours

Continued on next page

[1] Neurons indicated with * have cilia and are dysfunctional in the *che-3* mutant [183, 184].

[1] Neurons indicated with ˆ are dysfunctional in *tax-2/4* mutants.

Table 1.4 – continued from previous page		
neuron [1]	**ref**	**description**
	[160]	responsible for avoidance reaction to nose touch and osmotic imbalance
ASI * ˆ	[167]	minor role in chemotaxis towards Cl^-, Na^+ and cAMP as well as leucine
	[186]	represses dauer formation under normal conditions
	[160]	repressor of social feeding
ASJ * ˆ	[186]	activating dauer formation and regulating its recovery
	[160]	implicated in lifespan regulation
ASK* ˆ	[160]	implicated in lifespan regulation
	[132]	minor role in avoidance of alkaloids, protons and detergents
	[167]	minor role in chemotaxis towards Leucine
	[140]	minor role in male attraction towards hermaphrodites
AVA	[160]	forward/backward command interneuron
AVB	[160]	forward/backward command interneuron
AVD	[160]	forward/backward command interneuron
AWA *	[140]	attraction to hermaphrodites in males
	[160]	responsible for attraction to volatile odors like diacetyl, pyrazine and 2,4,5-trimethylthiazole
AWB * ˆ	[160]	responsible for repulsion from volatiles like 2-nonanone
AWC * ˆ	[140]	attraction to hermaphrodites in males
	[160]	responsible for attraction to volatiles like benzaldehyde, butanone, isoamyl alcohol and 2,3-pentanedione
	[160]	implicated in lifespan regulation
CEM *	[140]	Male-specific amphid neuron responsible for the attraction to hermaphrodites
CEP *	[185]	basal slowing response to bacteria through mechanosensation
OLL *	[191]	mechanosensation
	[182]	negatively regulates pathogen avoidance

Continued on next page

[1] Neurons indicated with * have cilia and are dysfunctional in the *che-3* mutant [183, 184].

[1] Neurons indicated with ˆ are dysfunctional in *tax-2/4* mutants.

Table 1.4 – continued from previous page		
neuron [1]	**ref**	**description**
OLQ *	[192]	mechanosensation
PDE *	[185]	basal slowing response to bacteria through mechanosensation
PHA *	[166]	antagonist in avoidance behaviour
PHB *	[166]	antagonist in avoidance behaviour
PQR *	[160]	sensory neuron required for aerotaxis, and implicated in regulating social feeding
RMG	[189]	inter/motor neuron stimulating social behaviour. inhibited by *npr-1*
URX ^	[160]	sensory neuron used in aerotaxis, and implicated in regulating social feeding
[1] Neurons indicated with * have cilia and are dysfunctional in the *che-3* mutant [183,184].		
[1] Neurons indicated with ^ are dysfunctional in *tax-2/4* mutants.		

Integrating the information gathered through chemosensation, *C. elegans* can chemotax towards bacteria, which naturally produce a range of attractive metabolites (see Table 1.5).

Chemotactic bacteria are too small to sense spatial gradients across their body length, and thus use a temporal gradient to guide their motion. *C. elegans* only uses the amphid for navigation towards attractive stimuli and thus must rely on the same principles which are so well understood in bacteria. Aversive stimuli are mainly sensed by ASH and AWB in the amphid as well as PHA and PHB in the phasmid which is located in the tail. This allows *C. elegans* to sense aversive gradients across its body length and favours more rapid and exact reaction in an emergency [166]. The many sensors and neurons involved in distinguishing between the large spectrum of odours lead us to expect complex behaviour when nematodes are confronted with the chemically complex environment of bacterial excretomes.

1.4.5 Learning

Olfactory adaptation describes the altered response to chemical stimuli after prolonged exposure [194]. The type of the adaptation can vary between stimuli and different environmental situations. This phenomenon is known as olfactory plasticity [194]. Many experiments have demonstrated olfactory plasticity in *C. elegans* [54, 144, 194]. Several factors influence the development of such olfactory plasticity, including pH, osmotic pressure, starvation, population density (via ascarosides, which will be introduced in Section 1.4.7) and other chemical or mechanical stimuli [54, 140, 144].

Nematodes also show associative learning. This allows the nematode to adapt the

Table 1.5: Some known nematode attractants and repellents

Attractant	Repellent
volatile compounds [1]	
short-chain alcohols, ketones and esters pyrazine some thiazoles, aromatic compounds and aldehydes diethyl ether	long-chain alcohols and ketones serrawettin
water soluble compounds [2]	
Na^+ K^+, Mg^{++}, Ca^{++} Cl^-, SO_4^{--}, NO_3^-, CH_3COO^- cAMP OH^- biotin lysine serotonin	

[1] Volatile compounds can be sensed at nM concentrations, they are described in Bargman *et al.* [139]
[2] Water soluble compounds are sensed at μM to mM concentrations, they are described in Dusenbery [193] and Bargman *et al.* [167].

strength of attraction based on past experience (e.g. presence of food or pathogens), changing the preference for chemical stimuli, osmotic pressure, temperature or oxygen tension [54,141–143]. This ability to learn will be important in interactions with bacteria which use slow acting toxins or pathogenesis to deter their predator, as we expect in *P. fl.* NZI7 [34].

1.4.6 Response to Presence or Absence of Food

Dwelling describes a behaviour of nematodes associated with feeding. During dwelling *C. elegans* increases its turning frequency and decreases its motion speed [38, 132, 162, 179, 195]. Usually the dwelling behaviour is interspersed with short instances of roaming behaviour, during which larger distances are covered. This type of behaviour facilitates optimal exploitation of available food patches [165, 179]. These

short intervals of roaming are not found in chemosensation mutants [165, 179], and dwelling is largely absent in the Hawaiian strain [38, 165].

Several studies have investigated food leaving probabilities, that is, the probability of leaving the food, given that the edge is encountered [165]. Close observation of nematodes encountering the edge reveals that they usually reverse back into the bacterial colony when either head or tail exit the food patch, leaving only a small residual probability of exiting the bacterial colony [165].

C. elegans animals are considered as starved, if they have not encountered food for 30 minutes. After this period the behaviour of the worm changes dramatically [132]. A starved individual will start searching the wider area and migrating into new territory [196, 197]. During this process known as travelling or dispersal, *C. elegans* is found to maintain a directional memory which facilitates traversing long distances in one direction, even when interrupted by reorientation events [160, 198]. During starvation olfactory responses alter to increase sensitivity to food [160]. This can override other learned aversions and thus also increases the chances of eating pathogenic bacteria [196].

Insufficient nutrition has a range of effects on *C. elegans*. Shortage of food can cause L1 arrest [199], but also triggers the dauer larvae developmental pathway (see Figure 1.2 on page 6). The dauer larva is an alternative L3 larva which can persist for months in adverse conditions (no food, dry) and is the state in which *C. elegans* is commonly isolated from the wild [42, 44]. We will not work with dauer larvae in this project, but the increased attraction nematodes display for food when starved will be relevant in the context of repellent bacteria.

1.4.7 Pheromones

In addition to relying on its own chemosensation of bacteria, *C. elegans* is also guided by pheromones. The pheromones employed by *C. elegans* are ascarosides: that is, glycosides of the dideoxysugar ascarylose. More than 140 ascarosides have been identified so far [201] (some are shown in Figure 1.12), though the function of many of them is not yet determined. Pheromones are used to attract males [202] and as an indicator of population density and food availability to guide dauer larvae formation [203]. In addition pheromones are employed to repel nematodes, which causes an even spread of feeding worms across bacterial colonies [140], thus optimising foraging strategies and nematode health [204]. However this is only noticeable in so-called solitary feeders like the laboratory strain N2. Social feeders like the isolate CB4856 of the nematode (more commonly referred to as Hawaiian; see Section 1.4.8), which was first isolated in 1972 from a pineapple field [60] are found to clump together [187]. This may be due to an additional class of ascarosides, containing and indole moiety, which act as attractants. There is great overlap in the neurons involved in pheromone sensing, and the same ascaroside can have different roles depending on its concentration [140, 205].

To study the importance of pheromones in food choice we can study the *daf-22* mutant. This mutation affects the final gene in the pheromone biosynthesis pathway [186] (see Figure 1.12). Daf stands for dauer larvae defective, as the absence of pheromones was originally noticed through the lack of dauer larvae. Later it has been reported that *daf-22* mutants have a defect in olfactory plasticity [144], suggesting that pheromones are important for food choice behaviour. There is a known

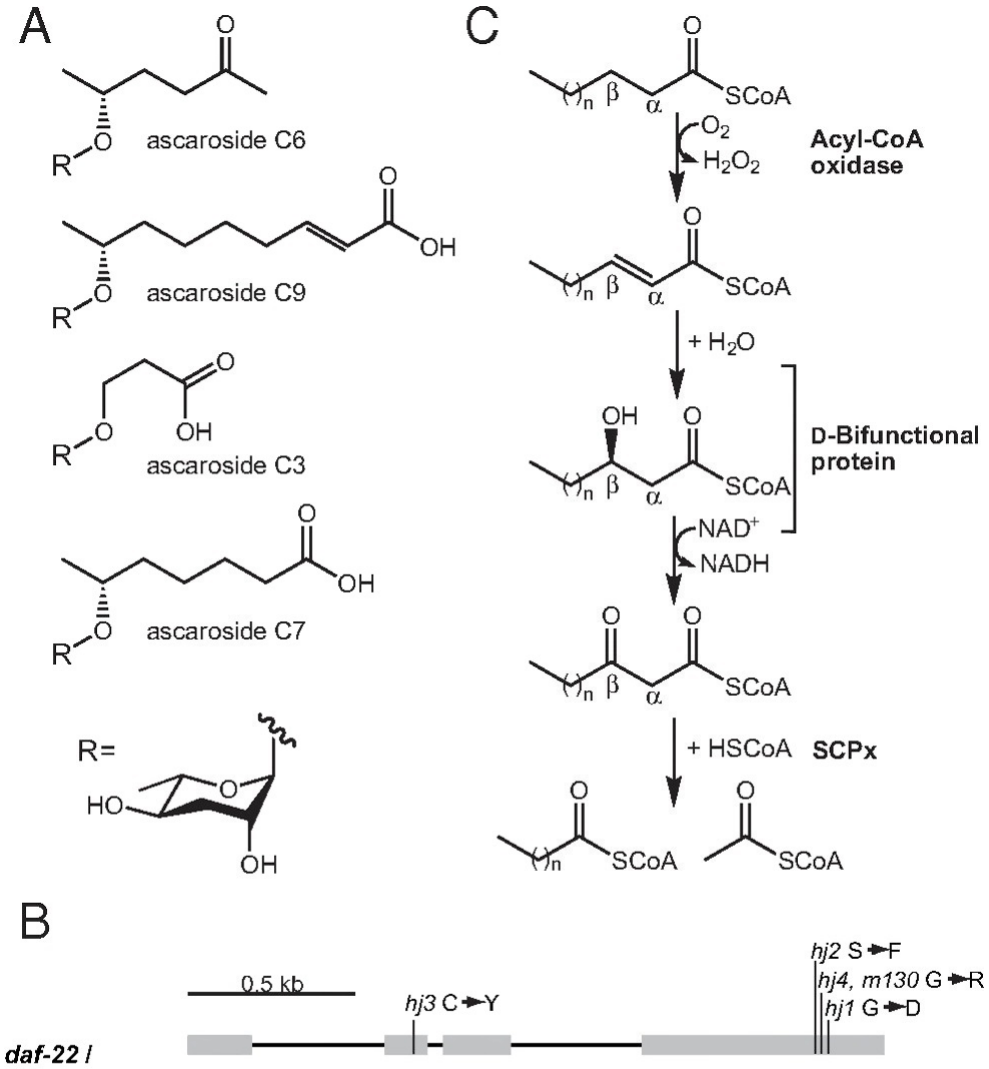

Figure 1.12: Ascarosides - nematode pheromone A: some examples of ascarosides; B: the gene map of *daf-22* showing the location of some mutants of this gene including allele m130 a substitution causing loss of function in the strain DR476; C: the biosynthesis pathway of the fatty acid side chain highlighting the importance of *daf-22* here labelled as SCPx (the mammalian homologue is called sterol carrier protein). Reproduced with permission from Butcher *et al.* [200].

link between the ability to produce pheromones and the ability to show olfactory plasticity [203], but whether *C. elegans* uses pheromones as an external memory requires further investigation. It has recently been found that mutations in *daf-22* do not prevent aggregation [187] which might originate from the few ascarosides that can be produced by *daf-22* mutants [201] or implicate other mechanisms for aggregation (see below) [206].

1.4.8 Social Interactions

The laboratory adapted strain N2 is known as a solitary feeder. This means that nematodes will aim to maintain a large distance between individuals to maximize exploitation of the food patch [140]. The Hawaiian strain on the other hand is known for its social feeding, bordering and burrowing. All of these are believed to be a consequence of avoiding high ambient O_2 levels [165, 206]. The differences between this strain and the laboratory strain N2 can be accounted for by a single gain of function mutation in N2 in *npr-1* encoding a neuropeptide transmitter receptor [38, 176]. The mutation was probably caused by laboratory domestication (as reviewed in [44, 60]). As far as is known, all solitary feeders carry NPR-1 215V, while a less functional version like NPR-1 215F or even complete missense lead to the social phenotype [38].

NPR-1 is expressed in many sensory and interneurons, including the body cavity neurons AQR, PQR and URX, which regulate the response to aggregation stimuli [207]. One confirmed action of *npr-1* is integrating the information gathered from the amphid neurons [140], by repressing the action of RMG (see Table 1.4).

C. elegans prefers oxygen levels of 12 % [176]. In the laboratory where ambient

oxygen is about 21 % social feeders prefer the lower oxygen environments found in the bacteria rich border of the bacterial lawn [176] and in groups of nematodes [206]. At lower ambient oxygen both of these phenotypes are abandoned indicating that it is only the discomfort due to high oxygen tension which causes nematode clustering. While clusters of nematodes have measurably lower oxygen levels [206], this is not enough to explain formation of clusters. The behaviour observed when two individuals encounter each other suggests that other driving forces act, these could be mechanosensation or surface tension forces [208].

In addition to its social behaviour the Hawaiian strain has been found to be more explorative, which is a consequence of its higher on food speed [165]. All genetics of the nematode are based on the N2 strain, but the Hawaiian strain behaves more like a nematode recently isolated from the wild. In this work we will investigate the Hawaiian strain to gauge the influence of behaviour in our system, and appreciate the modifications we must make in our assumptions when transferring knowledge to the mushroom farm.

1.4.9 Nematode Mutants used in this Study

The ciliary dynein heavy chain encoded by *che-3* is required for cilia formation. It is usually expressed during early development to aid the transport of material from the developing ciliary structures. Lack of *che-3* results in shorter, rounded cilia [184]. The neurons affected by this mutation are indicated in Table 1.4. This strain will be useful in investigating the effects of chemotaxis on the behaviour of nematodes and on the subsequent dispersal of bacteria.

Daf-16 encodes a FOXO homologue which acts as a transcription factor in the

insulin pathway, and thus regulates innate immunity, metabolism and longevity in *C. elegans* [209,210]. The *daf-16* mutant was originally described as dauer defective. In later studies it has emerged that *daf-16* is an important regulator of longevity and stress response [210, 211]. However, the mutant also has a phenotype in food exploitation as it constantly experiences satiation (and thus does not enter the dauer pathway) and therefore has a higher food leaving probability than N2 wild type [212]. *Daf-16* nuclear translocation is often observed in challenges of *C. elegans* with pathogens [103, 211]. The defect in the insulin pathway may result in altered susceptibility of the *daf-16* mutant to pathogens. In addition we expect to see an increased spreading by this mutant due to its higher food leaving probability.

Daf-22 encodes the final enzyme in the ascaroside biosynthesis pathway [200] (see Figure 1.12). Mutants of this gene were first described as dauer defective [203], and it was established this was due to the inability to produce the dauer pheromone. Further analysis revealed that most pheromones cannot be synthesised by this strain [201]. Analysis of this strain will reveal the importance of pheromones in the interactions with bacteria. We are particularly interested to find out whether pheromone deposition could accelerate decision making.

Sek-1 encodes a MAPK kinase and is thus an important regulator of innate immunity [213]. Mutants of sek-1 have been isolated in screens for *C. elegans* with enhanced sensitivity to bacterial pathogens [213, 214]. This strain will help us to probe the sensitivity of the nematodes to *P. fl.* NZI7 and explore the effect of pathogenic traits on spreading.

1.5 Interacting Species

The main focus of our investigation is the interaction between two different species. Species can interact in a variety of different ways. In our example of bacteria–nematode interactions we can have the following interactions:

- Predation of bacteria by nematodes
- Evading predation through pathogenicity and toxicity
- Spreading of bacteria by nematodes
- Farming of bacteria by nematodes

1.5.1 Predation

The most basic interaction between the two species is the predation. Nematodes consume a large variety of microorganisms and are thus often found in microbe rich environments like mushroom farms and composts [42,44]. Predator prey interactions between two species are very well understood and follow simple rules: If prey is abundant predators flourish and reproduce [44, 85, 215]. As predators deplete their food source, they too decline, this decline allows the prey to recover, and the cycle starts again. This oscillatory pattern, familiar to everyone who has opened a biology textbook and looked at the development of lynx and hare, is found in many simple systems [215,216]. This relationship is also easily represented mathematically [216–219]. In our laboratory system we will usually only consider one predator and one prey, however we will not observe the same cyclic behaviour, as the prey (bacteria) itself is depleting a limited resource of nutrients.

Systems with multiple predators or prey are much more complex, as the survival of the predator does not depend on just one prey [85,220]. Each of the different prey available will have different nutritional value and thus the hunting cost to energy benefit ratio will not only depend on the density, but also on the type of prey.

Predator prey interactions often force an evolutionary arms race between the defence mechanisms of the prey and the ability of the predator to overcome them [219]. For the prey it is enough to be simply less attractive than other prey that is available, for example through toxins (see below), or a high consumption cost [220]. Therefore there will usually be one preferred prey in an environment [220]. This will be the prey with the lowest cost/benefit ratio for the predator, and / or the lowest toxicity and pathogenicity. However, only rarely is a prey eradicated by its predator, instead a switch in diet is usually observed in the predator when prey densities are low [85]. Completely eradicating its prey would reduce the fitness of the predator in the long term and is thus selected against by evolution, but is also difficult to achieve by the predator, as the prey will take refuge, either physically or by changing state, and at low prey densities the rate of encounter between predator and prey might be lower than the prey's reproduction rate [85, 218, 221]. As a rule predator and prey manage to coexist in a long term steady state in natural settings [85]. In artificial settings short term fluctuations are frequent and complete eradication is often observed [85].

1.5.2 Evading Predation

In the laboratory *C. elegans* is commonly raised on the non-pathogenic *E. coli* strain OP50 [53] which was mainly chosen on the basis of availability and edibility [44],

but in its natural environment the nematode generally encounters different strains of *Pseudomonas*, which can range from harmless for nematodes to pathogenic [222].

Being able to avoid predation is one of the most important traits of any living organism. Defensive behaviours include great strength or speed in the animal kingdom while spikes and symbiotic relationships are often found in the plant kingdom. Microorganisms exploit a variety of different shapes and communities to make it more difficult to be swallowed and they also employ a wide arsenal of toxins. Most predators are specialized on a particular size and shape of prey, and will find it difficult to swallow prey outside their preferred range [223, 224]. Communities of microorganisms can be formed through the fomation of microcolonies or biofilms [225, 226]. Although these communities are less mobile and thus easier to catch for predators, the agglomeration has a net protective effect. Either the sheer size of the community or the coordinated chemical defence can check predators [226].

Extracellular metabolites can have a range of effects on predators, they can be repellent, kill predators instantly or through slow killing and sterilisation can reduce predation pressure in the future [227]. All of these principles are employed by bacteria against the nematode *C. elegans*. *P. fl.* NZI7 has been found to repel nematodes without killing them [34]. The cyanide secreted by many of the pseudomonads is responsible for fast killing of *C. elegans* by inhibiting mitochondrial chytochrome oxidase [87, 228]. However, in low nutrient conditions cyanide is too costly to produce, and a slow killing through intestinal colonisation is observed instead [228]. Killing and sterilisation effects can be observed on a population level through reduced number of nematode [88].

1.5.3 Vectors of Disease

Animal pathogens are usually highly vector specific. This means that it is easy to control animal pathogens at the vector level [6–8]. The same approach has worked against some plant pathogens, for which the principal vector was known [5]. However many plant diseases have a broad range of vectors, and this we also find for mushrooms [5]. Plant diseases are mainly spread by insects, in particular pollinating insects and herbivores [5, 229]. Dominant vectors of diseases on a mushroom farm include mites, sciarid flies and humans as well as *C. elegans* [43]. Sciarid flies are considered a major pest on mushroom farms, as they do not only damage mushroom mycelium as larvae, but can also transmit a variety of diseases. The control of sciarid flies accounts for 0.5 % of the value of the mushroom crop and is common practise [230]. Nematodes on the other hand cannot be efficiently eliminated from a mushroom farm. We have long known that *P. fl.* NZI7 can attach to the nematode cuticle and disperse by these means [35, 56]. In this thesis we wish to characterize the dispersal of pseudomonads by *C. elegans* further.

1.5.4 Farming

Saveral animals practice farming, where they facilitate the growth of microorganisms which are beneficial to them. This is particularly prominent with ant colonies, which culture fungi and microbes capable of controlling diseases in their crop [231]. But farming has also been discovered in much more primitive organisms like *Dictyostelium* [232]. Farming is also observed in the nematode *Heterorhabditis bacteriophora*, which regurgitates *Photorhabdus luminescens* when infecting insect larvae.

The bacteria colonize and degrade the larvae and serve as food to their vector [51]. It is quite likely that *C. elegans* has evolved the ability to disperse bacteria so that more food is available to the nematode at a later stage. It is beyond the scope of this work to discuss this possibility any further.

1.6 Modelling

To enhance our understanding of nematode–bacteria interactions and to make our findings applicable in a more general setting, we will construct a model of the system. Such a model could be applied to more natural domains and conditions than those found in the petri dish, and it could also be adapted to other systems with similar dynamics, such as predators with different movement patterns. The model will help us to identify critical parameters and mechanisms.

A model of the interaction will need to describe nematodes and bacteria. In order to represent the chemotaxis behaviour of *C. elegans* it must also include the chemical fields generated by bacteria. The model will combine aspects of two common mathematical models: predator-prey models and disease dissemination models. For an introduction to mathematical modelling as well as the basic versions of the models mentioned below, the reader is referred to Murray's Mathematical Biology [217].

Predator-prey models, even in their simplest form are an example of the complex patterns that can arise from interacting species. SIR (Susceptible, Infected, Removed) models are common methods to represent disease dynamics in a population. Xia *et al.* [233] as well as Ruan and Xiao [234] extended this model to include vectors that aid in pathogen dispersal. The spatially averaged approach

used in models like the predator-prey model and SIR models, which are described by ordinary differential equations, will not allow us to generate the spatial patterns we wish to observe, although extensions of these models to include spatial variation have been attempted [234]. Yoshimura *et al.* also use a spatially averaged approach to model the spread of pine wilt by a vector [235]. This approach can be used, if enough field data is present to estimate the relevant parameters, which will represent an average of the vector's behaviour.

Geotemporal modelling of epidemics (be they diseases, information or fashion) are at the same time very useful and very difficult [217]. This is partly due to the problems in estimating the parameters of models, especially when complex spatial structures are to be accounted for [217]. Balcan *et al.* [236] investigated the spread of an infectious disease across the globe taking commuting and air traffic into account. Even though parameters could be well characterized for this model, this is an immense task, involving several layers of information for each location and individual.

In this light we must set modest goals for our own model. Cellular automata are grid-based models, in which each site has variables associated with it. They are often used as a first step towards developing a more complex model, as they can sometimes be taken to a continuous limit to generate a grid free model [237]. The simple spatial arrangement of the model is well suited to accommodate interacting species models such as predator-prey, host-parasite and infection models [238–240]. There is no limit to the complexity that can be introduced into such a model, thus making an age structured model possible and facilitating any number of motion rules. A hybrid cellular automaton allows for the interaction of continuous species

with individuals [241]. Continuous species are governed deterministically by partial differential equations, like the mean field models described above. Individuals are governed by stochastic rules to describe their motion.

Many of the necessary parameters and mechanisms of *C. elegans* motion are very well characterized, making this aspect of the model straightforward. Other aspects of the model and their associated parameters will be investigated as part of this study. We will be unable to investigate every unknown aspect of nematode–bacteria interactions in this thesis, therefore some parts of the model will have to rely on our intuition rather than our knowledge.

1.7 Summary

Mushroom farming is an important branch of agriculture. The crop falls victim to many different diseases, of which bacterial blotch is the most important. Being able to control the disease starts with an understanding of how it is spread. The pathogen *P. fl.* NZI7 and the bacterivorous nematode *C. elegans* coincide and interact in mushroom farms. While *C. elegans* preys on the bacteria, *P. fl.* NZI7 uses toxins and repellents to deter the predator. *C. elegans* uses its complex chemosensation system to distinguish between bacterial colonies with differential toxin levels.

In this project we study *C. elegans* interacting with its natural food. We will further investigate the inedibility of the *Pseudomonas fluorescens* strain NZI7, which was first described in Burlinson *et al.* [34], and explore how it links to the ability of NZI7 to be spread by nematodes. To distinguish between toxic and pathogenic effects we will use the immunodeficient *sek-1* mutant. To investigate the mechanisms

by which *C. elegans* forages we will use the Hawaiian strain and the *daf-16* mutant as more explorative strains, a *daf-22* mutant as a communication deficient example and the chemotaxis deficient *che-3* mutant. Understanding more about worm learning behaviour will aid in gauging the robustness of the bacteria's dispersal strategy and how dependent it is on encountering the right 'type' of nematode or predator in general. To aid the understanding of the interactions from these experiments, we will also perform *in silico* simulations.

In Chapter 3 we will construct a model of the bacteria–nematode interactions based on the knowledge derived from literature. Where necessary we will use our experimental work to guide parameter estimation. It is plausible that bacterial growth dynamics play a role in bacteria–nematode interactions and in bacterial spreading. We will therefore characterize the growth of all selected mutants in Chapter 4 before investigating them further. In Chapter 5 we will investigate the edibility of *P. fl.* NZI7 using a range of different assays. The aim of this part of the project is to establish a rank in terms of edibility which can be used to link edibility and spreading. In addition, we will explore the impact of nematode behaviour and pathogen susceptibility through studying nematode variants. In the final chapter we will explore how efficiently *P. fl.* NZI7 are spread by *C. elegans* and what kind of influence nematode foraging strategies have on the spreading success.

Developing a relationship between edibility and spreadability will be useful in assessing the optimisation undergone by *P. fl* NZI7 to facilitate spreading. It will also serve to predict how much other bacteria will spread through the action of nematodes, and compare this to NZI7's spreading speed. Some bacteria are antagonists of mushroom pathogens, and knowing their relative spreading speeds will be

important in assessing their value as biocontrol agents.

Chapter 2

Materials and Methods

2.1 Experimental Procedures

2.1.1 Strains and Media

Media

Nematode Growth Medium - NGM [53]

NGM agar: 0.3 % NaCl, 1.7 % agar, 0.25 % bacto-Peptone, 1ml/l 5mg/ml Cholesterol in Ethanol,after autoclaving add, using sterile technique, filter sterilised 1 mM $CaCl_2$, 1 mM $MgSO_4$ and 25 mM $HKPO_4$ buffer pH6

For phytagel agar use 0.425 % of phytagel gelling agent instead of agar.

NGM liquid medium: 0.3 % NaCl, 0.25 % bacto-Peptone, 1 mM $CaCl_2$, 1 mM $MgSO_4$ and 25 mM $HKPO_4$ buffer pH6

M9 [53]

3 g KH_2PO_4, 6 g Na_2HPO_4, 5 g NaCl, in 1 l MilliQ water, after autoclaving add 1 ml of 1 M $MgSO_4$. M9 buffer was prepared by the Biochemistry Department Media Kitchen

Antibiotics

Ampicillin is used at 100 μg/ml to culture *E.coli* SM10 for four-parental mating.

Chloramphenicol is used to select against *E. coli*. Food choice assay plates are supplemented with 35 μg/ml to prevent *E. coli* OP50 transferred with the nematodes from growing.

Gentamycin at 25 μg/ml is used to select for transformed pseudomonads carrying the mini-Tn7 chromosomal insertion.

Kanamycin is used at 25 μg/ml to culture *E. coli* HB101 for four-parental mating.

Tetracycline at 30 μg/ml is used select for and culture pseudomonads carrying a plasmid with tetracycline marker. Tetracycline at 15 μg/ml is used to culture *E. coli* bearing the same plasmid.

Strains

All strains and mutants of *C. elegans* used are listed in Table 2.1. *Pseudomonas* strains used in this study are found in Table 2.2 in addition those mutants of the strain *P. fl.* NZI7 which are listed in Tables 1.2 and 1.3 were used. *E. coli* strains

Table 2.1: ***C. elegans*** strains and mutants used in this study.

C. elegans	**Background**	**Reference**	**Brief description**
N2	WT strain	[60]	laboratory domesticated reference strain
CB4856	WT strain	[60]	social strain isolated in Hawaii
CB7308	N2	[243]	*daf-22* (m130), outcross of DR476 (see Figure 1.12)
CF1038	N2	[244]	*daf-16* (mu86), deletion, null
CB1124	N2	[245]	*che-3* (e1124), substitution, null
AU1	N2	[213]	*sek-1* (ag1) G212R
CX11839	N2	[246]	*tyra-3* (ok325)
DA1774	N2	[247]	*ser-3* (ad1774) deletion

Table 2.2: *Pseudomonas* strains used in this study

Pseudomonad	**Source**	**Taxonomy**	**Phenotype**
P.fl NZI7	[26]	P.fl complex II	mushroom pathogen
P.fl PF5	[95]	P.fl complex II	biocontrol strain
P.fl NZ052	[84]	P.fl complex I	mushroom pathogen
P.fl NZ011	[84]	P.fl complex II	mushroom pathogen
P.fl NZ007	[84]	P.fl complex I	mushroom pathogen
P.fl NZ111	[84]	P.fl complex I	mushroom pathogen
P.fl NZ017	[84]	P.fl complex II	mushroom pathogen
P.st DC3000	[248]	*P. syringae*	plant pathogen
P.fl BBC6	[249]	P.fl complex I	plant growth promoting
PAO1	[250]	*P. aeruginosa*	animal pathogen
P. tolaasii NCPPB 2192	[84]	P.fl complex I	mushroom pathogen
P. gingeri NCPPB 3146	[21]	P.fl complex II	mushroom pathogen
P. fl WH6	[251]	P.fl complex I	plant pathogen

used for four-parental mating are listed in Table 2.3. In addition *E. coli* λpir was used for plasmid cultivation and *E. coli* OP50 was used to culture nematodes [242].

2.1.2 Bacterial Methods

Unless otherwise stated bacterial strains were cultured from 20 % Glycerol -80 °C stock in LB broth to stationary phase and stored at 4 °C for at most 2 weeks.

Plasmid cultivation

The plasmid pIJ11282 (see Figure 2.1) [122] is carried and multiplied in *E. coli λ pir*, which is stored as 20 % Glycerol stock at -80 °C. The Qiagen kit 'QIAprep Spin Miniprep Kit' is used for plasmid extraction.

Electroporation

Plasmid with tetracycline markers were inserted into *P. fl.* NZI7 using electroporation. A solid overnight culture was grown on LB medium. One cubic millimetre of bacteria were scraped off and suspended in ice cold 10 % glycerol 1 mM HEPES pH8. The suspension was centrifuged for 4 min at 4 °C at 8 500 rpm. The supernatant was discarded and the cells were resuspended in 1 ml fresh ice cold Glycerol buffer. This process was repeated three times. After the final wash the bacteria were resuspended in 200 μl of the Glycerol solution. Approximately 100 ng plasmid DNA was added and the mixture transferred to an ice cold electroporation cuvette. The bacteria were incubated with the plasmid for at least five minutes before electroporating at 200 Ω, 25 μF and 2.5 kV. One millilitre prewarmed SOC was immediately added to the shocked cells and they were transferred to a 15 ml tube in which they grew for 2.5–3 hours at 28 °C in a shaking incubator before plating on selective media.

Four-parental mating

Insertion of genes into the genome of *Pseudomonas fluorescens* was conducted using four-parental mating at the Tn7 site. The protocol was adapted from [252] as follows. All strains (see Table 2.3) were grown in 5 ml liquid LB (supplemented with the

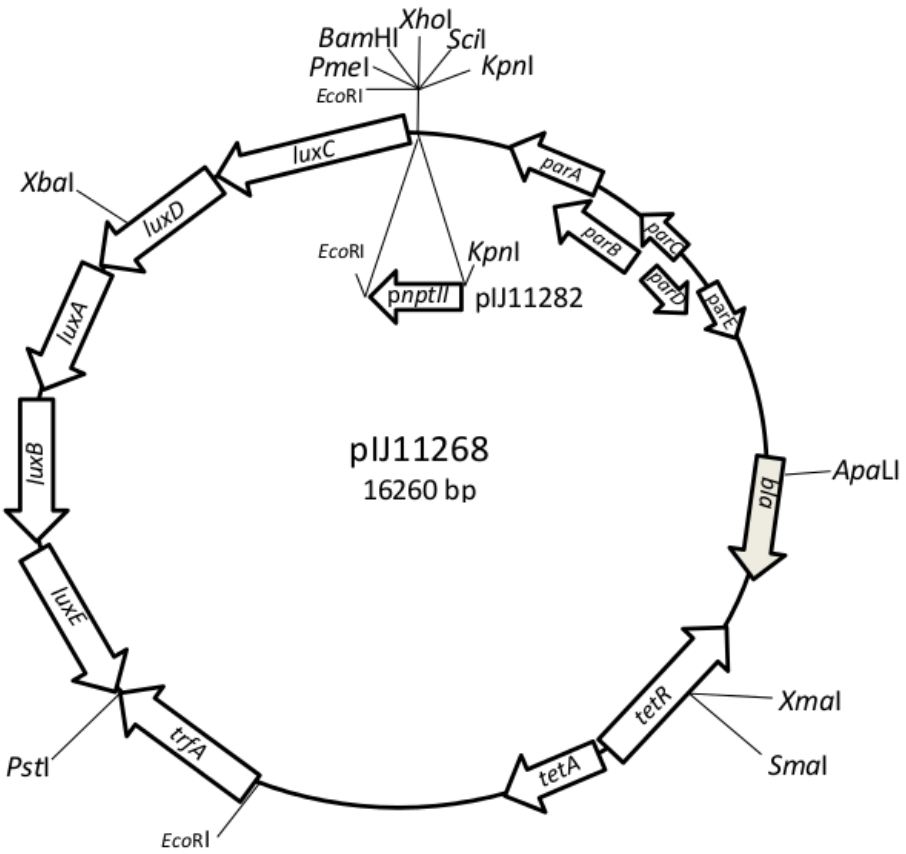

Figure 2.1: The plasmid pIJ11282 contains a *lux* cassette driven by a pNeo promoter. Image reproduced from [122].

Table 2.3: Bacterial strains used in four-parental mating, with their culture conditions as described in Choi *et al.* [252].

Strain	Function	Plasmid	Antibiotic	Temperature
P. fl. NZI7	recipient	none	none	28 °C
E.coli	donor	pUC18T-mini-Tn7T-Gm	Gentamycin	37 °C
E.coli HB101	helper	pRK2013	Kanamycin	37 °C
E.coli SM10 *λpir*	mobiliser	pTNS1	Ampicillin	37 °C

respective antibiotic) overnight. The liquid culture was concentrated into 1 ml and washed three times by spinning for 5 min at 8000 rpm and resuspending in fresh liquid LB. *P. fl.* NZI7 was heatshocked for 15 minutes at 42 °C, meanwhile all *E. coli* strains were kept at 37 °C. Seven hundred microlitres of *Pseudomonas fluorescens* were mixed with 300 μl of each of the *E. coli* strains. The mixture was spun at 8000 rpm for 5 min and resuspended in 40 μl of fresh LB. The suspension was spotted as a single spot onto an NGM plate, left to dry and incubated for 16 hours. The bacterial colony was scraped from the plate and suspended in 1 ml isotonic salt solution. This suspension was spun at 13000 rpm for 2 min, the supernatant discarded and the pellet resuspended in 100 μl isotonic salt solution. These were plated onto a VBMM plates containing Gentamycin.

Bacterial growth assay

Bacterial overnight culture was spun, the supernatant discarded and the pellet re-suspended in milliQ water. A bacterial suspension of $OD_{600} = 0.9 - 1.1$ in MilliQ water was generated. The growth was assayed in a black, clear bottomed 96-well plate using 75 μl of 2× NGM and 75 μl of the bacterial suspension per well.
Each plate contained 8–12 replicates of each strain tested, at least 8 blank wells with 1× NGM and 8 wells with WT NZI7. The growth of each strain was investigated in two independent assays.
Plates were shaken and read every 30 minutes using a TECAN plate reader 'infinite 200'. The device was controlled using the i-control 1.5.14.0 software supplied by TECAN.

Checking Tn7 insertion site

The accurate insertion of the mini-Tn7 vector into the *P. fl.* NZI7 genome was checked using the protocol described by Schweizer [252], with a modification of the primer $P_{GlmS\text{-}down}$ to $P_{GlmSdownNZI7}$. The latter was designed to match conserved nucleotides in the analogous region in GlmS in *Pseudomonas fluorescens* using the sequences of Pf5 (*Pseudomonas protegens* Pf5, GenBank WP_011064377.1) and CHA0 (*Pseudomonas protegens* CHA0, GenBank WP_015637571.1) and SBW25 (*Pseudomonas fluorescens* SBW25, GenBank WP_015886641.1), as the sequence of the relevant section in *P. fl.* NZI7 was not available in the draft genome sequence.

$P_{GlmSdownNZI7}$: CACAGCATAACTGGACTGATTTC

The PCR reaction was carried out by Caroline Stone (Preston group-unpublished work).

Determine miniTn5 Transposon Insertion Site

Bacterial cultures were grown on LB plates overnight. Colony PCR was performed using the following ingredients for each reaction:

- 19.3 μl MilliQ water
- 0.2 μl Taq-polymerase
- 2.5 μl 10 $\times$ Taq buffer
- 1.25 μl primer gfpmut3.1p1 at 10 μM (sequence: ATCACCTTCACCCTCTCCAC)
- 1.25 μl primer mix CEKG2ABC at 40 μM
- 0.5 μl dNTP mix at 10 mM each

CEKG2ABC is a 1:1:1 mixture of three primers with sequences:

GGCCACGCGTCGACTAGTACNNNNNNNNNNAGAG,

GGCCACGCGTCGACTAGTACNNNNNNNNNNACGCC,

GGCCACGCGTCGACTAGTACNNNNNNNNNNATAT.

Bacteria were scraped from the plate using a pipet tip and the reactions inoculated. A touchdown PCR program was run as described in Table 2.4.

Table 2.4: Reaction conditions for first step of tail PCR reaction.

step	name	temperature	length	cycle
1	denaturation	95 °C	3 min	1
2	3-step	95 °C	30 s	5
3	high stringency	62 °C	1 min	5
4	cyle	72 °C	2.5 min	5
6	3-step	95 °C	30 s	1
7	low stringency	25 °C	3 min	1
8	cycle	72 °C	2.5 min	1
9		95 °C	15 s	15
10	super cycles	67 °C	1 min	15
11	with two	72 °C	2.5 min	15
12	nested	95 °C	15 s	15
13	high and	67 °C	1 min	15
14	one low	72 °C	2.5 min	15
15	stringency	95 °C	15 s	15
16	cycles	44 °C	1 min	15
17		72 °C	2.5min	15
19	final extension	72 °C	5 min	1
20	store	4 °C	forever	1

This was followed by a second PCR reaction using

- 18.3 μl MilliQ water
- 2.5 μl 10 $\times$ Taq buffer
- 0.2 μl Taq polymerase
- 1.25 μl primer gfptnS2 at 10 μM
- 1.25 μl primer CEK4G at 10μM

- 0.5 μl dNTP mix at 10mM each
- 1 μl DNA template (1/50 dilution of product from first reaction)

and the conditions described in Table 2.5.

Table 2.5: Reaction conditions for second step of tail PCR reaction.

step	name	temperature	length	cycle
1	denaturation	94 °C	3 min	1
2	extension	94 °C	30 s	30
3	cycles	56 °C	30 s	30
4		72 °C	3 min	30
5	final extension	72 °C	5min	1
6	store	4 °C	forever	1

PCR clean-up was performed using ExoProStar. The mixture was incubated for 20 min at 37 °C and 15 min at 80 °C. Sequencing was performed using the Eurofins sequencing service and primer gfptnS2 designed by Burlinson [91] (CCAGTGAAAAGTTCTTCACC).

2.1.3 Nematode Methods

All strains and mutants of *C. elegans* were cultured on 55 mm Nematode Growth Medium (NGM) plates seeded with *E. coli* OP50 and stored at 15 °C. All nematode methods are in accordance with standard handling methods [53]. Nematode picking was done using a flame sterilised worm pick manufactured from a 0.3 mm platinum wire.

Bleaching

Worms were bleached using alkaline hypochlorite solution (200 μl sodium hyperchloride 175 μl sodium hydroxide 125 μl MilliQ water) 5 days before an experiments to

synchronise them and kill any possible contaminants. Some bleach was spotted onto a seeded small NGM plate. Gravid adult hermaphrodites were picked from culture plates and suspended in the spot.

Washing

Two millilitres M9 buffer were added to a culture plate of *C. elegans*. The nematode suspension was transferred to a 1.5 ml Eppendorf tube using a pipette. Worms were allowed to settle for 3 min before removing the supernatant. Worms were resuspended in fresh M9 buffer and the process was repeated 5 times. After the supernatant was removed the last time, the dense worm suspension was spotted onto a fresh NGM plate and worms are picked from this plate.

2.1.4 Nematode–Bacteria Interaction Assays

Bioluminescence assay

This assay uses blackened plates to reduce edge effects (see Figure 2.2). These were generated by applying black electric tape to the outside of the edge of the plastic petri dishes. Ten microlitres of a 1 in 10 dilution of liquid overnight bacterial culture were spotted onto a small (55 mm), blackened NGM plate. Three types of plates were generated for each strain analysed: a control without nematodes, a fully spread plate, using 60 μl of the diluted culture, and sample plates onto which 5 washed nematodes were placed into a small droplet of M9 medium about 5 mm away from the bacterial culture. The plates were left to adjust to the temperature of the room in which the photon counting camera is situated for at least 30 min before taking any measurements. Measurements were taken using the photek IFS32 system and

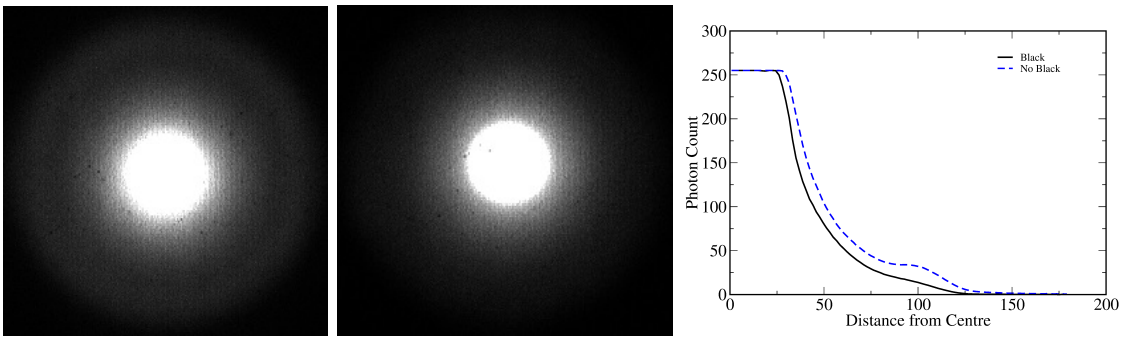

Figure 2.2: Internal reflection in bioluminescence assays. Left: Using a clear plate we observe internal reflection. Middle: applying black electric tape to the edge of the same plate and placing it on a black cloth reduces internal reflection and also gives a better definition of the colony edge. We used the flagella mutant to generate these examples. The plate was exposed for 10 minutes for each of the images. Right: The average photon count on the two images.

software. Photons were collected for one hour per image.

Food choice assay

Forty microlitres of liquid bacterial culture were spotted onto each inoculation site of a large (90 mm) NGM plate according to the template illustrated in Figure 2.3 and incubated overnight at 29 °C. Diagonally opposite spots were inoculated with the same strain of bacteria. Approximately 45 washed adult hermaphrodite nematodes were transferred to a droplet of M9 buffer in the centre of the assay plate. Plates were only used if the bacterial spots were circular and had not run due to plate defects, as we could show that the larger bacterial colonies were more attractive to nematodes (data not shown).

Grid - edibility screen

Two hundred microlitres of bacterial overnight culture were pipetted into each well of half a 96-well plate. A 48-pin replicator was cleaned in ethanol, flamed and cooled,

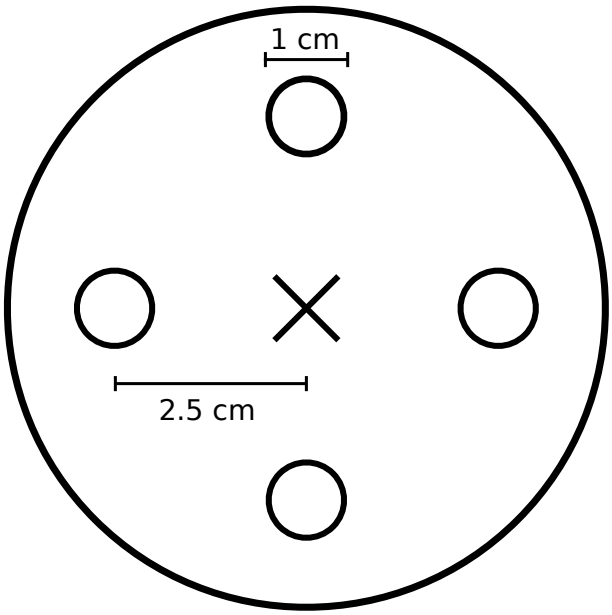

Figure 2.3: Food choice assay template Template of a 90 mm assay plate marking the bacterial colonies (small circles) and the nematode set down area (cross). Opposite sites are innoculated with the same strain.

before being dipped into the bacterial cultures and then gently touched onto a 90 mm NGM agar plate. The sites marked with an X (see Figure 2.4) were inoculated with 5 μl of liquid culture *E. coli* OP50. The plate was incubated overnight. Nematodes were suspended from their culture plate using M9 buffer. Nematodes were allowed to settle before removing the supernatant and spotting the dense suspension onto the spots marked X in Figure 2.4. The number of nematodes placed was estimated before incubating the plates at room temperature. This screen was conducted with the help of students enrolled on the University of Oxford DTC experimental techniques course, who inoculated the plates with nematodes and scored colonies for occupancy by nematodes.

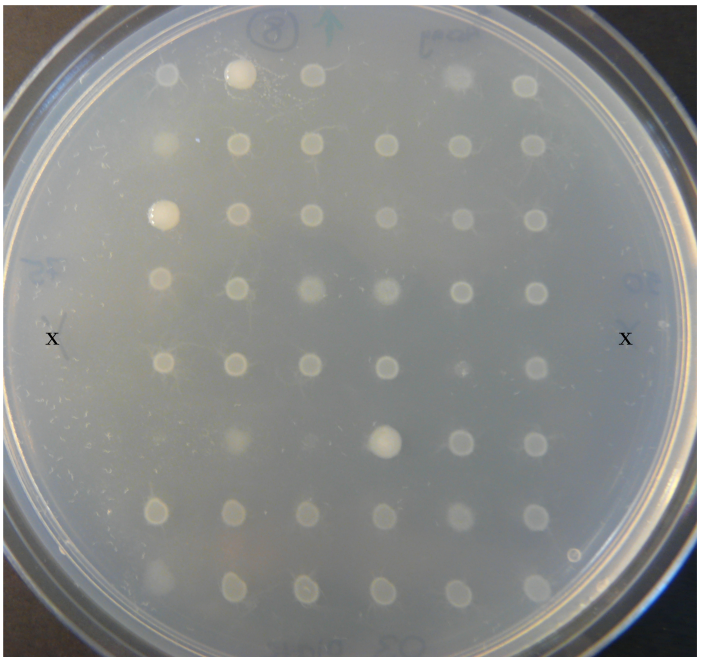

Figure 2.4: Grid edibility example 48 bacterial strains are inoculated onto a 90 mm NGM plate using a pin replicator. Five microlitres of *E. coli* OP50 suspension were inoculated onto the sites marked X. After overnight incubation nematodes are placed onto the *E. coli* spots.

Nematode Growth Support assay

Forty microlitres of overnight bacterial culture were spotted into the centre of a small NGM plate. The plates were incubated overnight at 29 °C. Ten washed young adult nematodes were placed into a drop of M9 buffer approximately 5 mm away from the bacterial colony. Plates were incubated at room temperature ($\sim$ 22 °C) throughout the experiment. Worm health was monitored throughout by assessing mobility and transparency. The endpoint was defined as the time when either of the two following cases has happened: the bacteria have been completely depleted as described in [147] or no more nematodes are present.

Phase change screen

Forty microliters of overnight bacterial culture were spotted into the centre of a small NGM plate. The plates were incubated overnight at 29 °C. Ten microliters of *E. coli* OP50 were spotted 1 cm away from the *Pseudomonas fluorescens* culture. 10 adult nematodes were placed into a drop of M9 spotted onto the *E. coli* culture. Plates are incubated at room temperature throughout the experiment. This experiment was conducted in collaboration with Caroline Stone and the Experimental techniques course of the DTC.

Progeny assay

Fifty microliters of overnight culture were spread across a small NGM plate. Plates were incubated at 29 °C overnight to achieve a stationary culture. Ten synchronised adult nematodes were placed onto these plates and left to lay eggs for 6 hours of which they were incubated at 25 °C for 5 hours. After that time they were removed from the plates and the plates were incubated at 15 °C for 3 days. After the 3 days plates were inspected daily and incubated at room temperature. The progeny were counted with the aid of a vacuum pump to avoid double counting. The experiment was conducted in triplicate and two independent experiments were conducted for each bacterial strain. During each experiment three plates of *E. coli* OP50 were included. The number of offspring as well as the date they were grown to adulthood was recorded.

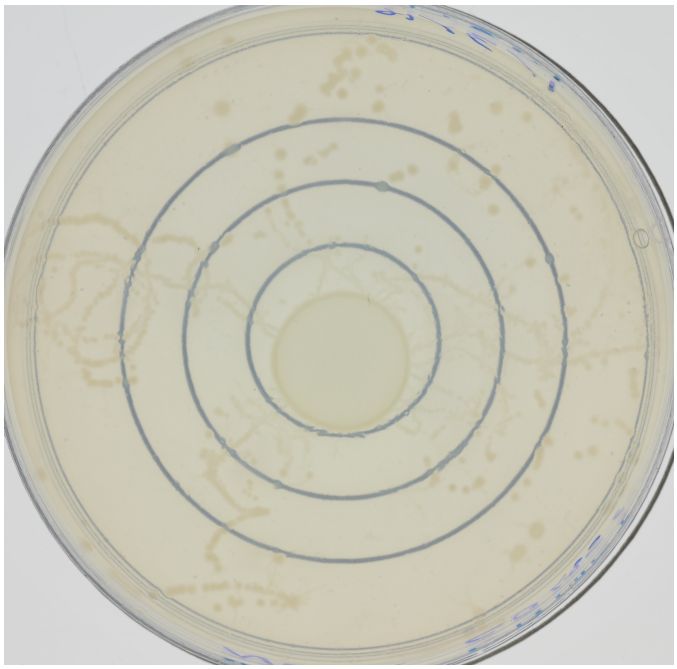

Figure 2.5: Visual estimation of bacterial spread Bacterial spread is estimated using the template shown. The circles represent 10, 25 and 50 % plate coverage. This example shows *P. fl.* NZI7 spread by N2 nematodes after 2 days.

Spreading screen

Forty microliters of overnight culture were spotted onto small (55 mm) NGM plates. These were incubated overnight at 29 °C. Ten washed adult nematodes were placed near the bacterial colony. The area occupied by bacteria was estimated daily for 3 days using a template as seen in Figure 2.5. The full extent of the lawn cannot be photographed well. Although some of the first tracks left by nematodes are very thick and easily visible, the thinner bacterial lawn cannot be distinguished (see Figure 2.5).

Volatility assay

To test the reaction of *C. elegans* to volatile compounds secreted by bacteria two different assays were conducted. The first was developed by Caroline Stone (unpub-

lished work) and the second was adapted from Nandi *et al.* [77].

Stone assay: Fifty microlitres of liquid overnight culture of the bacteria to be tested are spread onto a 55 mm NGM plate and incubated overnight. A 1 cm cork borer is used to cut a section from the plates and transfer two plugs to the opposite ends of the lid of a 90 mm NGM plate. There are two versions of this assay, which differ in whether *E. coli* OP50 has been spread evenly on the assay plate beforehand and incubated overnight. A suspension of washed nematodes was transferred to the assay plate. The plates are sealed with Para film. Every half an hour we record the number of nematodes found on each half of the plate.

Nandi assay: Plates were prepared as described in the food choice assay. The lid was kept on one set of the plates, while the other was placed without lid into a flow hood (to prevent contamination). A dish of water was placed into the flowhood at the same time to help prevent dehydration of the plates, but this also reduced the temperature of the assay plates. Plates are scored every half an hour exactly like in the food choice assay.

2.2 Data Analysis

2.2.1 Bacterial Growth Assay

The growth is assumed to follow a logistic model, which is described by the differential equation [217]

$$\frac{dB}{dt} = rB\left(1 - \frac{B}{K}\right), \tag{2.1}$$

which has the solution

$$B(t) = \frac{B_0 K e^{rt}}{K + B_0(e^{rt} - 1)}, \tag{2.2}$$

where B is a measure of bacterial numbers and B_0 is the initial bacterial population. The parameters r (growth rate) and K (carrying capacity) are obtained by fitting the data to the solution of the above equation using a least squares fitting method. We divide the growth parameters r and K thus obtained by the corresponding growth parameters for the WT strain, to account for experiment specific effects like inconsistency in media and growth temperatures. This will result in the normalized growth parameters r_N and K_N respectively.

2.2.2 Bioluminescence Assay

The equipment used for this assay is not very reliable. On many occasions it interrupted a run of image taking prematurely. All runs of less than 50 hours were discarded as providing insufficient information. A video of the individual images with one frame per hour was created using the IFS32 software provided by Photek. The software records the image in bit depth 16, i.e. the brightness of each pixel is recorded as a 16 digit binary number. For further analysis this bit depth has to be reduced to 8. If the image exceeded a brightness of 256, then the first 8 bits such that at least some pixels were non-zero in the first digit were chosen to retain maximum information. The same bit depth was chosen for the entire time series.
Image analysis was primarily conducted using MATLAB. For each plate the function bwlable was used to find the centre of the bacterial colony spotted onto the plate during the experiment setup. A normalized histogram with 100 bins giving the av-

erage light intensity as a function of distance from the centre was constructed using C++ code. This was chosen for the benefit of speed, but the same results were obtained using MATLAB (data not shown). Thus for each experiment one histogram was generated for each hour, each strain and each of the control and sample plates. Matlab is used to compare these histograms. There are several methods for comparing histograms, which have cross-bin relations, like those we have generated here, where each bin represents a certain distance from the centre. Traditionally these methods have been the Quadratic Form, the Earth Mover's Distance or χ^2 distances. The first two allow cross bin relationships, which are essential for our purposes, the latter reduces the effects of large bins, which have often caused skewed analysis. The Quadratic Chi Distance combines both of these advantages [253]. All methods were tried on the data to establish the most robust measure for our purposes.

2.2.3 Food Choice Assay

The choice index CI:

$$\mathrm{CI} = \frac{\text{worms in mutant colonies} - \text{worms in WT colonies}}{\text{worms on plate}}. \tag{2.3}$$

was computed after 30 minutes and after 6 hours.

2.2.4 Nematode Growth Support Assay

The food race score is defined as

$$\frac{sig}{\text{number of weeks}} \tag{2.4}$$

where *sig* is -1 if nematodes were eradicated, and +1 if the nematodes consumed all visible bacteria and number of weeks is the endpoint as explained above (see Section 2.1.4).

2.2.5 Progeny Assay

The ratio of progeny obtained on the assay plate to the progeny obtained on the *E. coli* plate was determined. The rate of egg laying per worm per hour was computed by dividing the number of offspring counted by the average number of adults originally on the plate. (The number of adults removed from the plate was recorded, as it is possible for adults to leave the plate.)

2.2.6 Linear Regression

Linear regression analysis was performed in MATLAB using the polyfit function, to find a fit of y to the expression $mx + c$.

In accordance with the description in [254] the suitability of the linear fit was estimated by computing a value of R^2 as follows:

$$R^2 = 1 - \frac{\text{SSR}}{\text{SSE}}, \tag{2.5}$$

where SSR is the residual variation after the fit and SSE measures the variation in the original y data.

$$SSR = \Sigma_{i=1}^{N}(mx_i + c - y_i)^2 \tag{2.6}$$

$$SSE = (N-1) \times \text{var}(y), \tag{2.7}$$

where var(y) is the variance of y.

Where necessary the resulting product moment correlation coefficient ($r = \sqrt{R^2}$) is transformed using Fisher's z-transformation to yield a normally distributed random variable.

$$Z = \frac{1}{2} \ln \left(\frac{1+r}{1-r} \right) \tag{2.8}$$

Chapter 3

A Model of the Interactions

3.1 Introduction

In order to make predictions about the outcome of the bacteria–nematode interactions, we must first discover which aspects of the complex system are most fundamental. For this purpose we will develop a model based on a small set of simple rules and parameters, which we can verify against experiments. Once established, we can use the model to vary parameters and mechanisms that are not easily modified in the lab. We are particularly interested in using the model to investigate bacterial spreading and the balance between the advantages bacteria gain from the presence of their predator versus the loss they suffer from predation. As we will see in Chapter 6, there are no straightforward and robust ways to gauge this phenomenon experimentally, making a computational approach particularly desirable. The model will also allow us to identify key parameters of the interactions, which will be useful when trying to transfer knowledge gained from this system to other systems of vector borne disease transmission.

In the following section we will develop a computational model, with which we can simulate the different aspects of the nematode–bacteria interactions. We are particularly interested in representing the aspects of nematode behaviour linked to bacterial edibility and how bacteria are spread by the actions of their predator. As well as representing nematodes and different types of bacteria this model includes hypothesised chemicals secreted by the bacteria, which will influence nematode behaviour. The large number of chemical stimuli is coarse grained into just one chemical. While this implies a loss of information, it reduces the chemical cues to a level which can be understood and parameterized experimentally. The fundamental interactions between the three agents are shown in Figure 3.1.

A cellular automaton, in the widest sense, is a completely discrete model [239]. Space is divided into discrete cells (for clarity we will call these sites, in order to avoid confusion with bacterial cells). Each site can take any of a finite set of states, and is updated at discrete time steps using deterministic or stochastic rules. This makes them computationally fast and efficient and allows a complete (though coarse-grained) description of what is happening at every site modelled, thus facilitating intuitive graphical representation.

Cellular automaton models have often been used to represent interacting species in a spatially dependent manner, e.g. for predator-prey models, host-parasite models or infection [238–240]. Here we will further develop the age-structured predator prey model, which allows for age dependent reproduction, but usually does not include movement of either species [239].

Nematode motion will be the most complex part of the model. There are nu-

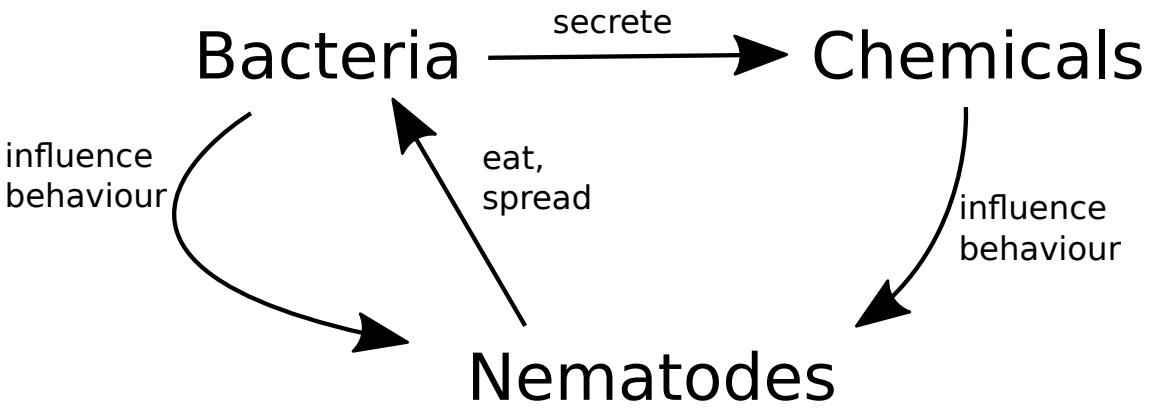

Figure 3.1: Fundamental interactions between the three agents in the model.

merous models describing nematode motion with various levels of complexity from purely shape based models [255] to models linking motion to the underlying neuronal network and biochemical state [256]. Xu and Deng [257] have identified the different neuronal wiring diagrams required to model attraction to food and aversion from toxins. Roberts *et al.* [258] also identify appropriate levels of coarse graining when describing the state of the nematode. Most models of *C. elegans* motion are grid-free, however, in order to construct a cellular automaton we will have to restrict the motion of *C. elegans* to a grid. This approach is used for vascular tip cells by Anderson and Chaplain [241], who model the motion of cells in response to chemical stimuli generated by growing tumors.

We will be using a square lattice cellular automaton, which is straightforward computationally as it allows the representation of the domain as a matrix. This is particularly advantageous when programming in MATLAB (MATrix LABoratory). The range of agents modelled makes a hybrid cellular automaton desirable, in which we will model nematodes as individuals and all other agents as continuous on a discretised grid. The continuous quantities are treated entirely deterministically,

governed by differential equations describing growth (bacteria), diffusion and decay (chemicals). The movement of nematodes is stochastic, where the probabilities of moving in each direction are influenced by the state of the nematodes and the surrounding environment of chemicals and bacteria. Like Anderson's tip cells [241] the movement of nematodes is governed by the states of the nearest neighbour sites, and thus dependent on the discretisation of the continuous bacterial and chemical environment. To investigate grid effects, one could alter the grid to a hexagonal one, which is superior to a square one [259], or to prevent grid effects altogether, one could use an off lattice model using a velocity jump algorithm, which has been used for bacterial run and tumble [260] and could describe nematode movement more accurately. However these models are a lot more complex and computationally intensive and thus more suitable for further investigation, so they will not be explored in this study.

Because the spreading of bacteria is the main focus of the model, we will need to incorporate attachment and detachment to and from the nematode. Edibility influences worm behaviour in different ways, only some of which are linked to chemotaxis. This is evident in the reduced - but not entirely absent - ability of chemosensation defective nematodes to make a choice (see Chapter 5 for details of the experimental observations and Burlinson *et al.* [34]). In order to link spreading to edibility, we will need to represent both of these aspects of nematode behaviour. The following sections will explain how these basic ingredients are implemented in a cellular automaton, and how they can be combined with each other.

Table 3.1: The agents represented in the model.

Agent	Initial	At each time step
Bacteria	stationary phase	grow, get eaten, are spread
Chemicals	steady state	diffuse, secreted by bacteria
Nematodes	naive	move, age, spread bacteria, learn

3.1.1 Model Outline

There are three types of agents represented in this model, as described in Table 3.1. The variables associated with each of these are evolved at each time step. Bacteria will be in stationary phase at the beginning of the experiment we are trying to represent, which results in a steady state distribution of chemicals. Initially nematodes have no experience with the bacteria present in the assay (they are naive).

At each time step:

- nematodes move,
- bacteria reproduce,
- nematodes eat and age,
- bacteria attach to and detach from the surface coat of nematodes,
- nematodes learn about bacterial edibility,
- new chemicals are deposited and diffuse,
- nematodes reproduce.

As the agents influence each other in all of these actions (see Figure 3.1) the order in which these happen is important. We have listed them here in the order in which we have implemented them in our model, though more details are provided

later. The following sections are ordered based on information flow.

We will first describe the initial distribution and subsequent growth of bacteria (Section 3.2), which influence chemical fields and nematode behaviour. Then (Section 3.3) we will develop the description of the chemical fields, which only depends on bacterial distribution (see Figure 3.1). Once we have described both bacteria and chemicals we can construct nematode movement (Section 3.4), which determines the location of nematodes and finally (Section 3.5) lets us define the interactions between nematodes and bacteria, which will occur at every site which is inhabited by both agents. This final section includes information on the consumption of bacteria by nematodes and subsequent aging of nematodes and nematode reproduction, which depends on age. Nematodes update their perception of bacteria based on their surrounding. Finally the attachment and detachment of bacteria from the nematode cuticle, which is necessary for bacterial spreading, is described.

3.2 Bacteria

The distribution of bacteria influences chemical fields and nematode behaviour (see Figure 3.1). Here we describe how we model bacterial reproduction, which is completely independent of the other two agents. In later sections we will explain how bacteria secrete chemicals (see Section 3.3) and their interactions with nematodes (see Section 3.5).

3.2.1 Background

Bacteria divide at a constant rate as long as nutrients are available. This rate decreases as nutrients become limiting until bacteria enter stationary phase. Under normal culture conditions (18-28 °C, standard medium like LB or NGM) *Pseudomonas fluorescens* reaches stationary phase after 10 to 16 hours if grown from an initial liquid culture. In a shaking liquid culture, the bacterial density is almost constant throughout the medium. On an agar plate or in any other solid culture the situation is more subtle: bacteria deplete the nutrients from their surrounding, thus influencing the growth in neighbouring sites. When growing a stationary solid culture from a liquid inoculation, one can observe that the edge of the colony is thicker. The reasons for this are twofold: when spotting the liquid, more bacteria are deposited at the edge of the colony due to the coffee stain effect (more liquid evaporates from the edge, thus more particles are deposited). Additionally, due to the effect explained earlier, the bacteria at the edge can reproduce faster, as they gain additional nutrients from uncolonised agar, thus forming a thicker edge and making the area around the colony less nutritious for bacteria colonising this area at a later point in time.

3.2.2 Modelling Assumptions

Despite the effects noted above we will assume that bacterial growth at each site of the cellular automaton is independent of growth in the neighbouring sites. The only way to realistically represent the nutrient effects described above would be to model the nutrient field, thus adding at least one more variable and several unknown

parameters to the system, as the quantity and diffusion of the nutrients must be described.

Instead we assume that bacteria grow according to a logistic model, which is well established for the kind of population growth described above (see Murray's Mathematical Biology [217] for a more in-depth explanation). Logistic models form the basis for many attempts to represent bacterial growth mathematically in liquid or solid medium [261–263]. Here we will restrict our attempts to a very simple model in order to reduce the number of parameters. The rate of change of bacterial number at a location (B) is given by:

$$\frac{dB}{dt} = rB\left(1 - \frac{B}{K}\right), \tag{3.1}$$

where K is the maximum number of bacteria that can be sustained, r is the growth rate and t measures time. In Chapter 4 we will see that this description fits the liquid growth very well and also applies to some extent to growth on solid medium (see Section 4.4).

3.2.3 Bacterial Parameters

Bacterial numbers are measured on an arbitrary scale such that parameters from liquid culture growth assays can be used without rescaling. Thus we need to define a new 'unit' for B and K. We will call this unit bac. It is a number that relates the numbers used in the model to the number of bacterial cells. It is defined such that $K_{WT} = 0.2423$ bac, as WT bacteria achieve an optical density (OD_{600}) of 0.2423 at stationary state in liquid phase. Thus the units of K are: OD_{600} these bacteria

would have if they were grown in liquid culture. The variable B can take any value between 0 and K on this scale.

Table 3.2: Modelling parameters used to characterize bacterial growth.

Parameter	Range	Units	Justification
carrying capacity (K)	0.15–0.315	bac	see Section 4.2.3
growth rate (r)	4.5–10 $\times 10^{-5}$	s^{-1}	see Section 4.2.3

3.2.4 Initial Distribution

Bacteria are initially distributed as illustrated in Figure 3.3 on page 111. The spots are generated by the following difference of two Gaussian functions, to achieve the thicker edge characteristic of bacterial colonies grown from liquid culture:

$$K\left(e^{-\frac{r^2}{10}} - 0.9e^{-\frac{r^2}{5}}\right), \tag{3.2}$$

where r is the distance of the center of the site from the centre of the bacterial spot. The spot is centred on the centre of the plate in nematode growth support assays (NGSA), and a distance of 2.5 cm away from the centre in food choice assays (FCA). The sharp edge is achieved by thresholding such that all sites with less than half the carrying capacity are set to zero.

3.2.5 During the Simulation

Equation (3.1) is numerically solved for every site as

$$B_i^m = B_i^{m-1} \times \left(1 + \Delta t \times r_i \times \left(1 - \frac{B_1^m + B_2^m}{K_i}\right)\right), \tag{3.3}$$

where B_i is the bacterial density of strain i (for $i = 1$ or 2), m indexes time, Δt is the same time step used for nematode motion, and r_i and K_i are the bacterial growth rate and carrying capacity specific to each strain.

We include both B_1 and B_2 in the equation to capture competition by the two bacterial strains. B_2 is 0 if only one strain is used. As equation (3.3) is a numerical approximation to equation (3.1), it is also necessary to enforce K as the upper limit by setting any values of B greater than K to K.

3.3 Organic Chemicals

This section will describe the initial distribution of chemicals and their subsequent evolution as they are secreted by bacteria and diffuse through the agar.

3.3.1 Background

Bacteria secrete organic metabolites which are attractive to nematodes (see Table 1.5) as they signal the presence of food. To reduce predation, bacteria also secrete toxins and repellents. The nature of these is largely unknown. Many of these compounds are volatile and diffuse quickly [139]. However, volatility assays (see Chapter 5) suggest that volatile compounds do not play a major role in determining nematode behaviour in our experimental system. This may be because the rapid diffusion does not allow for the establishment of gradients.

As *C. elegans* chemotaxes using gradients of chemicals rather than absolute concentrations [145, 160], the exact concentration of attractants and repellents is not important, only their relative spread, so concentrations can be measured on an

arbitrary scale.

3.3.2 Modelling Assumptions

For each type of bacteria we summarize all chemicals as a single gradient. The chemicals can be either attractive or repellent depending on learned attraction. Nematodes can alter their response to chemical gradients and we can thus capture olfactory plasticity and learning without representing the full range of hundreds of organic molecules sensed by *C. elegans*. To test the hypothesis of short ranged repellents as formulated previously [34] we have also tested an additional short ranged repellent gradient, but lacking further information on its strength and diffusion relative to other bacterial metabolites we cannot represent it accurately enough to be valuable in our model. However as we will see in later realisations of the model where we do not make use of such a repellent, we have found that such a repellent gradient is not necessary to describe the behaviour of nematodes.

Diffusible chemicals, whose concentration is denoted by c, evolve according to the reaction diffusion equation.

$$\frac{\partial c}{\partial t} = D\nabla^2 c - \lambda c + \sigma B, \tag{3.4}$$

where D is the diffusion constant, λ is the degradation rate and σ is the rate at which the chemical is deposited by the bacteria (whose concentration is B). This equation holds across the plate D, which is large compared to the length scales of the gradients. We will assume no-flux boundary conditions.

3.3.3 Initial Distribution

To obtain the initial distribution of chemicals we note that nematodes are placed on the assay plate after it has been incubated for 16 hours with the bacterial colonies. We assume that bacteria have reached stationary phase at this point, so that the gradients of any chemicals secreted during these 16 hours have reached steady state. The steady state form of equation (3.4) is:

$$0 = D\nabla^2 c - \lambda c + \sigma B, \tag{3.5}$$

where the term σB is a known function of space, depending only on the initial distribution of bacteria at the start of the simulation. We will solve this linear equation treating each site containing bacteria separately and superimposing the resulting solutions. Thus the point source term σB becomes a delta function, which can be considered as part of the boundary conditions. The radial symmetry of the problem favours polar coordinates. The boundary conditions ensuring decay from the source are thus: c is finite at $r = 0$ and $c = 0$ as $r \to \infty$, where r is the distance from the spot occupied by the bacteria.

We can formulate

$$D\nabla^2 c = \lambda c, \tag{3.6}$$

in plane polar coordinates as

$$\lambda c = \frac{D}{r}\frac{d}{dr}\left(r\frac{dc}{dr}\right) = \frac{d^2c}{dr^2} + \frac{1}{r}\frac{dc}{dr}, \tag{3.7}$$

and rearrange to yield.

$$r^2\frac{d^2c}{dr^2} + r\frac{dc}{dr} - \beta^2 r^2 c = 0, \tag{3.8}$$

where $\beta^2 = \frac{\lambda}{D}$. This is the modified Bessel's equation of order 0. The solutions, called the modified Bessel functions, are denoted by $I(\beta r)$ and $K(\beta r)$. For $r>0$ we can use the analytical approximations [264] given as:

$$I(\beta r) \approx \alpha\frac{2}{\sqrt{2\pi\beta r}}e^{\beta r}, \tag{3.9}$$

$$K(\beta r) \approx C\frac{\pi}{\sqrt{2\pi\beta r}}e^{-\beta r}, \tag{3.10}$$

of which only the latter satisfies the boundary conditions (i.e. $\alpha = 0$).

The initial distribution of chemicals will be given as

$$c(x, y, 0) = \sum_j \frac{\gamma B_j}{\sqrt{\beta}\sqrt[4]{(x - x_j)^2 + (y - y_j)^2}} e^{-\beta\sqrt{(x-x_j)^2+(y-y_j)^2}}, \tag{3.11}$$

where j indexes the sites (with coordinates x_j and y_j) occupied by bacteria, and γ is a scaling factor. This definition is only valid for sites not occupied by bacteria, those which are will be given a chemical concentration of γB_j.

The initial distribution of chemicals is related to σ by noting that integration of equation (3.5) over all space, D yields the relationship:

$$\sigma \int_D B \; dxdy = \lambda \int_D c \; dxdy \tag{3.12}$$

using the no-flux boundary condition of c around the edge of the plate, where D is the entire plate. This allows a definition of the γ in terms of σ or vice versa.

3.3.4 Time Evolution

As the bacterial distribution changes, the chemicals will no longer be in a steady state. At each time step more chemicals are deposited (at a rate σ) and the reaction diffusion equation (3.4) is solved using a forward Euler Method. In our model we will use the same grid and time step as the cellular automaton for this, but we will extend the domain to a square covering the whole circular domain.

No-flux boundary conditions are implemented by forcing the boundary sites to take the same value as those one layer further in. These outer sites are not used as part of the allowable domain for nematodes or bacteria.

3.3.5 Modelling Parameters

We do not have accurate parameters for the diffusion of chemicals in this model. This is partially due to the large number of chemicals involved, which will all have slightly different properties. Furthermore we do not know all of the chemicals involved, and even if we did the relevant parameters in agar are not easy to obtain. Table 3.3 shows the estimates we can make and our justification for these estimates.

Table 3.3: Modelling parameters used to characterize chemicals.

Parameter	Value	Units	Justification
diffusion constant (D)	0.01	mm^2s^{-1}	medium sized organic molecules in agar. [265]
degradation rate (λ)	0.1	s^{-1}	empirically determined to generate gradients
concentration scale (γ)	1	bac^{-1}	nondimensional
deposition rate of diffusibles (σ_d)	0.0118	$\text{s}^{-1}\text{bac}^{-1}$	determined by eqn. (3.12)

3.4 Nematode Motion

3.4.1 Background

Like many microorganisms *C. elegans* exhibits chemotaxis. Nematodes can recognize and respond to gradients of attractants, even when these are at nM concentrations [160]. The chemotaxis mechanism employed by *C. elegans* is facilitated by a range of strategies. The major strategy resembles the run and tumble mechanism observed in chemotactic bacteria [160]. In *C. elegans* motion, long stretches of forward movement (known as runs in bacteria) are called swims and in addition to being shortened when moving away from attractive stimuli (as seen for example in *Rhodobacter sphaeroides* [266]), they are also prolonged when moving up gradients of attractant [162]. The stop phase (known as tumble in bacteria) is called a pirouette in nematodes. However, rather than reorienting randomly during the stop period as bacteria do, the pirouette a nematode performs has a higher probability of turning the worm towards the attractant [37,145]. It has been postulated that all fundamental motion patterns of *C. elegans* can be explained using just the swim and pirouette mechanism [161]. A pirouette usually consists of a pause, short reversal and another pause [258]. A nematode will spend about one quarter of its time in one of these three parts of the pirouette [258].

C. elegans alters its behaviour in response to its environment and internal state. We know that food abundance and quality, the risk of predation and desiccation, nutritional state, concentration of oxygen and carbon dioxide as well as the presence of mating partners all influence nematode behaviour [162, 212]. We can eliminate mating behaviour by concentrating on hermaphrodite-only populations. Similarly

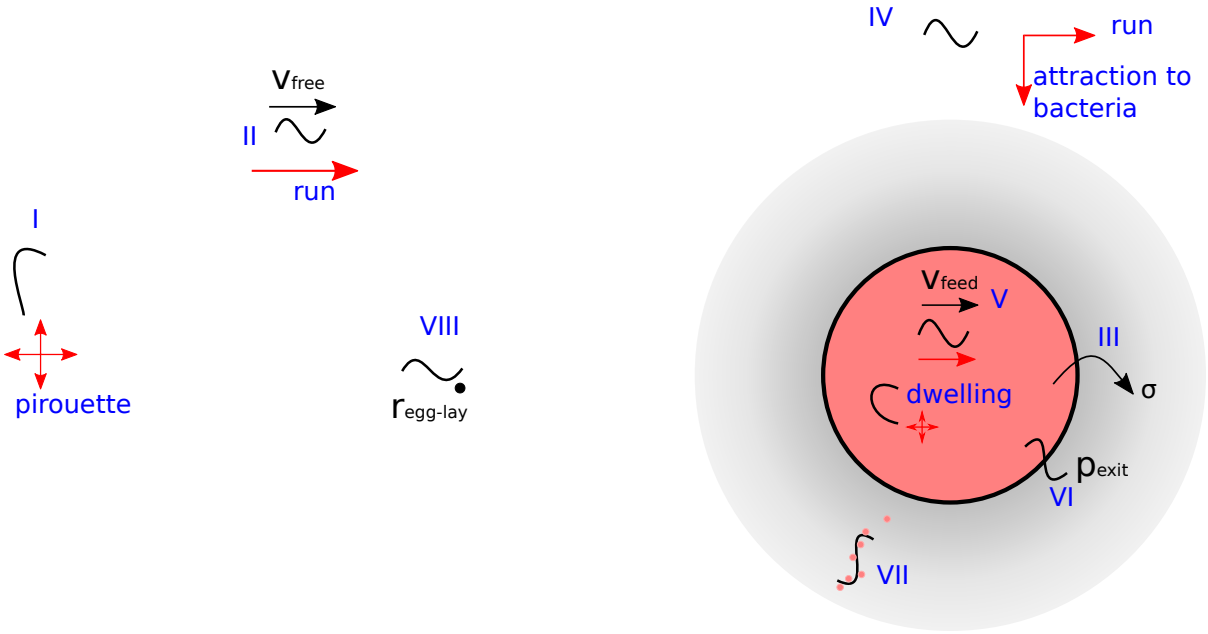

Figure 3.2: Fundamental aspects of nematode behaviour captured in the model. I and II: swim and pirouette mechanism, III: bacteria (pink) secrete chemicals (grey), which could attract nematodes (IV), V: dwelling in food slows down movement. VI: behaviour at the edge of the bacterial colony is captured in the exit probability, VII: bacteria attached to nematode surface coat can drop off, VIII: nematode reproduction.

desiccation and predation are less prominent in a laboratory environment, however, as associated behaviour is linked to oxygen sensation some of it will still be observed [176]. We do not model oxygen linked behaviour directly, as it is less pronounced in *npr-1* gain of function variants (i.e. N2) but some indirect characteristics will have to be preserved when modelling the Hawaiian variants. The impact of nutritional state is realised through the starvation response, which increases attraction to all bacteria, it will be further described in Section 3.5. The response to abundance and quality of food and the associated chemical fields forms the core of the nematode movement behaviour modelled here.

3.4.2 Modelling Assumptions

In this model we restrict the motion of *C. elegans* to a square grid, where it can travel to a neighbouring site during each time step. Figure 3.2 captures the aspects of nematode behaviour described in the model. A stationary worm in the absence of a chemical field has an equal probability of turning in any of the four directions (I). A moving worm has a high probability of continuing movement in the given direction and a small probability of entering a pirouette during which it is stationary [258] (II). Here we summarize all of the known reorientation mechanisms (Ω-turns, pirouettes and weathervane strategies) under the heading 'pirouette', and assume that combined they allow a reorientation in any direction.

Bacteria secrete metabolites (III) which influence the nematode behaviour. In the presence of an attractive gradient *C. elegans* has a higher probability of moving towards the attractant and decreased probability of moving away from it (IV). Repellent gradients have the opposite effect.

Nematodes slow down as they enter an area of high bacterial density and also show an increased probability of turning (V). This is known as dwelling [185]. Dwelling facilitates remaining on the bacterial colony, but is only observed in *npr-1* gain of function variants (like N2) and not in the Hawaiian strain.

Nematodes have a low probability of exiting a bacterial lawn (VI). This probability is influenced by their feeding state and the quality of the food they are currently on. We do not model this probability directly but as a result of a balance between food re-entry and repulsion due to repellents. The additional mechanism of reversing back into a bacterial colony when either head or tail exit the colony is observed

in both WT strains.

3.4.3 Nematode Variables and Movement Parameters

Nematodes are the most complex agents in the model. This is reflected in the large number of variables required to represent them (see Table 3.4). The first two of these variables (location and inertia) are required to represent locomotion. The other variables will become important in the later sections (see Section 3.5).

Table 3.4: Variables associated with each nematode

Variable	Description	Necessary for
location	x and y variables of location on plate	interaction with other agents
inertia	direction the nematode last travelled in	swim and pirouette
age	internal clock	reproduction counter
bacteria carried	bacteria attached to cuticle	spreading
attraction	attraction to each type of bacteria	learning

Table 3.5: Modelling parameters used to characterize nematode motion.

Parameter	Value	Unit	Justification
off food speed	200	μm s^{-1}	[38]
on food speed	100	μm s^{-1}	[38]
pirouette probability	0.05	s^{-1}	[258]

3.4.4 Realisation

In this model a nematode can be in one of two states, reflecting the movement observed in real life: moving and stationary. Movement can be in any of the four possible grid directions, thus allowing for a total of 5 states, which are monitored using the inertia variable.

The motion speed is realised through the relationship between time step and grid spacing. At each time step the nematode can move one space. Using a grid

Table 3.6: Notation used in Section 3.4.4

symbol	meaning
A	learned attraction (see Section 3.5.3)
B	bacterial density
B_f, C_f	Bacterial or chemical density at future spot
B_c, C_c	Bacterial or chemical density at current spot
R	concentration of repellents
K	Bacterial carrying capacity
p	overall motion probability $p = \Sigma p_i$
p_i	motion probability in direction i

Table 3.7: Factors influencing the motion of *C. elegans*.

factor	**effect**
presence of food	reduces total motion probability
repellents	increase total motion probability
learned attraction	modify overall probability and directional probability
chemical gradients	modify probability of moving in certain directions

spacing of 1 mm (the length of one worm) and a time step of 5 s this will equate to a speed of 200 μm/s. At each time step, nematodes can move one space into any of the four grid directions or remain stationary. Thus there are four probabilities (p_i) associated with movement which take into account the factors in Table 3.7.

At each time step a probability of moving into each of the four directions (as well as remaining stationary) is computed for each nematode based on its environment and state. The state (moving or stationary) provides the base probabilities: Without bacteria the nematode has a 75 % probability of continuing in the direction last travelled in, otherwise it will become stationary. A stationary worm has a probability of 18.75 % of moving into each of the four directions and a probability of 25 % of remaining stationary, thus resulting in an overall basic motion probability of 75 %. The following paragraphs describe how these probabilities are modified by bacteria. Table 3.6 provides details of the notation used. Bacteria directly influence nematode

motion probabilities as follows:

- Dwelling (V) is induced when the bacterial number exceeds 0.025 bac at the site occupied by the nematode, which is a tenth of the WT maximum (K). Dwelling will halve the motion probability. This produces a reduction in average speed as well as increased pirouetting, both of which are observed [162]. This mechanism is switched off when modelling the Hawaiian strain. By preserving the high speed even on food, the higher food leaving probability characteristic of this strain is adequately represented [212].

- We model food preference by modulating the overall motion probability using the learned attraction and the bacterial density at the current site as $p = p + A \times B$. This uniformly increases or decreases the probability of movement, and provides an aversion mechanism which is independent of chemotaxis.

- The probability of going into an area of lower bacterial density is reduced proportional to the difference in bacterial density between the two sites. $p_i = p_i/d$ where $d = \max(1, 10 * (B_c - B_f)/K)$. This allows modelling of food re-entry (VI), and reflects adaptive food leaving as observed in diminishing resources [165]

Bacteria will also indirectly influence nematode motion through the deposited chemicals:

- During chemotaxis nematodes will use the chemical gradients to guide their motion (IV). The probabilities are adjusted as $p_i = p_i + A(C_f - C_c)/\gamma$.

Furthermore bacteria influence the attraction nematodes experience towards them through their edibility and through the starvation response (see Section 3.5.3 for further details).

Very rarely (less than 0.01 % of the time) these modifications of the base probabilities lead to a total movement probability greater than 1. In these cases the probabilities are rescaled by dividing by p to achieve a total motion probability of 1.

We have assumed that nematodes obey a zero-flux boundary condition, therefore, if the motion of a nematode would cause it to leave the simulation domain, its motion is aborted and the worms remain stationary. This induces a small bias for nematodes to be found at the edge of the plate. In experiments where a bacterial lawn is evenly spread across the plate (e.g. the progeny assay) we do observe that nematodes favour the plate edge, thus the bias introduced in the model should not make the model less applicable, if anything the bias is probably not strong enough.

3.5 Interaction Between Nematodes and Bacteria

Table 3.8: Interactions between nematodes and bacteria.

Nematode action	Reason for inclusion	Depends on
eat bacteria	predation	presence of bacteria
age	developmental arrest	presence of bacteria
starvation response	long term behaviour	presence of bacteria
learning	medium term behaviour	bacterial edibility
pick up bacteria	spreading	presence of bacteria, bacterial stickiness
shed bacteria	spreading	bacteria attached to coat

Nematodes and bacteria interact in multiple ways beyond the nematode behaviour described above (see Table 3.8). Bacteria can stick to the surface of the nematode cuticle. As nematodes forage for food, the bacteria attached to the surface will fall off and form new bacterial colonies (VII in Figure 3.2). Nematodes will eat bacteria upon encountering them, which in turn influences ageing (and thus egg laying (VIII)) and learning.

The order of these interactions is important in the model, for example if ne-

matodes would eat at a site just after having shed some of their bacterial load, the bacteria could not establish themselves in the new environment. In reality this would not happen, as both processes are continuous in time and more importantly there is a spatial separation between the tail of the worm (where bacteria are attached) and the pharynx. Consequently the interactions are implemented after nematode movement and bacterial growth and in the following order:

1. nematodes age,
2. nematodes eat,
3. nematodes learn, pick up bacteria and deposit them,
4. nematodes reproduce.

Each of the actions is performed for all nematodes on the plate, before the next listed action is started.

3.5.1 Eating and Ageing

As *P. fl.* NZI7 is not known to restrict food uptake in the nematode, unlike, for example, *Yersinia spp.*, which form a biofilm on the nematode head [148], we assume that nematodes will eat bacteria whenever they encounter them, independent of edibility (which will only be important for movement and learning). Thus whenever the two coincide each worm will decrease the bacterial density at their location by a number equal to the eating rate (r_{eat}) or to zero if there are not enough bacteria left.

The eating rate is chosen such that it balances the rate of bacterial reproduction. Observations from experiments using very edible bacteria show that small numbers

of nematodes do not noticeably deplete the bacterial lawn, but a few hundreds of *C. elegans* can consume all of the bacteria present before any spreading occurs. In our simulations a bacterial colony initially consists of about 75 nodes on the grid. If we assume that about 300 nematodes, spending about half of their time feeding would consume all the available bacteria, then we can describe the bacterial dynamics at each site as a combination of logistic growth and predation.

$$\frac{\mathrm{d}B}{\mathrm{d}t} = rB(1 - \frac{B}{K}) - 2 \times r_{eat}, \tag{3.13}$$

where B is the bacterial number at the site, r and K are the growth parameters described before (Section 3.2) and r_{eat} is the bacterial consumption rate of one worm. This model does not predict extinction of bacteria, but that for effects to be noticeable the eating rate must be of the order of $0.1 \times r$. A similar estimate for r_{eat} but with extinction can also be made by considering a predation term which is proportional to the bacterial density. Using these estimates we can conduct a parameter sweep for the eating rate by monitoring the bacterial population over a period of 24 hours in a NGSA (see Section 3.6) setting with between 100 and 300 nematodes.

Nematodes arrest development when they cannot find food, thus delaying egg laying [137]. Therefore the age of the nematode is modelled as increasing only if they are eating at the maximum rate. Thus each nematode carries its own clock according to which it will lay eggs. We will use nematode age only to guide reproduction, a more advanced model will incorporate the effects of age on motion and pathogen susceptibility.

3.5.2 Nematode reproduction

Nematode reproduction is an essential part of modelling the longer term behaviour of the system (1–2 days). Nematodes start laying eggs approximately at 65 hours (measured from the moment the egg was laid) [267]. Here we model reproduction as an increase in nematode numbers. In this simplified picture of nematode reproduction, newly hatched nematodes instantly acquire adult properties like motion speed and rate of bacterial consumption. As eggs are completely inert in the system, we will not include them in our model and instead assume that reproduction occurs 11 hours later, when the new eggs have hatched (see Figure 1.2 on page 6), thus increasing reproductive age to 76 hours, and birth to 11 hours relative to biological age. It is therefore most convenient to represent the age of a worm since hatching rather than since the start of embryogenesis, as is usual in an experimental setting. An alternative method would be to average nematode behaviour between L1 (when nematodes eat less and move less) and adult, and thus define birth at the biological age of an L2 larvae.

From experiments we know that after reaching reproductive age the rate of egg laying increases initially up to a peak rate of approximately 9 eggs an hour, from where it will decrease again [267]. For simplicity we will model the rate as constant, based on the observation that around 275 eggs are laid during 60 hours. We use an average of one egg every 1000 seconds.

These are the parameters determined for N2 nematodes feeding on *E. coli* OP50, but as we will see in Chapter 5 the rate of egg laying when nematodes are fed on less palatable bacteria can be considerably reduced. This factor can be implemented in

the model by simply altering the egg laying rate parameter.

3.5.3 Learning

Upon encountering bacteria the nematodes update their attraction (A) to the metabolites secreted by these bacteria, which are encoded in the long range chemicals. This alteration depends on the toxins present, and thus on the rate of bacterial toxin production (as parameterised by edibility) as well as on bacterial density (B) and is implemented as: $A_i = \text{forget} \times A_i + \text{edibility}_i \times B_i$ for each bacterial strain i during each time step.

This slow stepwise adaptation of attraction is consistent with the observation that nematodes explore bacteria for several hours before leaving them on account of toxicity or pathogenicity. It has been demonstrated that associative learning is significant after 4 hours of exposure to pathogenic bacteria [142].

The starvation response is triggered by the absence of bacteria and causes nematodes to be increasingly attracted to bacteria [196]. This is implemented during every time step as $A = \text{forget} \times A + \text{starvation_attraction}$.

In the above equations variables A and B are as described in Table 3.6 and the parameters edibility and starvation_attraction are listed in Table 3.9.

Memory loss through the forget parameter ensures that the attraction is limited, and will be set such that is correspond to 50% retention after 2 hours [268]. The way we have chosen to implement memory decay is based on an exponential decay with a half life (T) of 2 hours, i.e. $\text{forget} = exp\left(-\frac{\Delta t}{T}\right) = 0.9995$. An alternative mechanism of memory loss would involve the modelling of a longterm memory, such that information is lost on a first in first out basis. While this model of memory

and learning would be more computationally intensive, it could also form the basis of modelling gradual turns more accurately.

3.5.4 Dispersing Bacteria

A proportion (attachment_rate - see Table 3.9) of bacteria present on a given spot will attach to the nematode currently occupying the same location. From that moment on, those bacteria are considered to be associated with the nematode, they are no longer part of the bacterial field as described in Section 3.2. We assume for simplicity that they are no longer eaten and can no longer reproduce, although both happen to some extend. A proportion (deposition_rate - see Table 3.9) of the bacteria carried by a nematode will be shed at each time step, and thus they are added back to the bacterial field.

3.5.5 Modelling Parameters

We can sumarize all the factors influencing bacterial numbers at a particular site as follows:

$$B^{m+1} = B^m + B^m \times \left(1 + \Delta t \times r \times \left(1 - \frac{B^m}{K}\right)\right) - N \times r_{eat}$$
$$- N \times \text{attachment_rate} \times B^m + \Sigma_{\text{all nematodes } i} \text{ deposition_rate } b_i, \quad (3.14)$$

where the first term represents growth as described in Section 3.2. The second term represents predation by nematodes, where N is the number of nematodes at the site. The third term represents bacterial attachment to the nematodes at the site. The final term shows deposition of bacteria from the nematode cuticle, where b_i is

the number of bacteria attached to nematode i.

Table 3.9: Parameters used to model nematode–bacteria interactions.

Parameter	Value	units	Justification
initial_attraction	-2–2	bac^{-1}	empirically determined (Section 5.1.1)
r_{eat}	0.000007	s^{-1}	balance bacterial growth
attachment_rate	0.0007	s^{-1} bac^{-1}	empirically determined (Section 6.2.1)
deposition_rate	0.07	s^{-1} bac^{-1}	empirically determined (Section 6.2.1)
edibility	-0.5–0.5	bac^{-2}	empirically determined (Section 5.1.1)
starvation_attraction	0.0001	bac^{-1}	empirically determined (Section 6.2.6)
forget	0.9995	nondimensional	[268]
rate of egg laying	0.001	s^{-1}	[267]

The initial_attraction is the starting value for the adaptable attraction. It reflects the instant chemotactic response and influences only the short term behaviour. It is the balance between edibility and increased attraction due to starvation that mainly determines the medium and long term attraction to bacteria and thus the probability of a nematode visiting a bacterial spot. Simulations of this model show that the attraction after 24 hours is independent of the initial_attraction. While it is difficult to corroborate this observation with experiments, we do have some evidence confirming the phenomenon (Section 5.3.4).

3.6 The Two Assays Modelled

The model can be run to simulate each of the two nematode–bacteria interaction assays conducted experimentally (see Chapter 2), the Food Choice Assay (FCA) and the food race assay (Nematode Growth Support Assay - NGSA). Each requires slightly different initial conditions and simulation domain, but the rules established

Table 3.10: Two different model settings

	Food Choice Assay	**Food Race Assay**
abbreviation	FCA	NGSA
domain diameter	90 mm	55 mm
number of nematodes	40	10
initial location of nematodes	centre	22 mm off centre
run time	6–24 hours	up to 3 days

so far hold in both cases.

3.6.1 The Simulation Domain

The length of one site of the computational domain is taken to represent one worm length, which is 1 mm. The domain is circular. Food choice assays are simulated on domains with 90 mm diameter and growth support assays on domains with 55 mm diameter. The realisation of the domain is depicted in Figure 3.3.

3.6.2 The Initial Conditions

Initially, nematodes are placed in an area of 3×3 pixels in the centre (FCA) or halfway between the centre and the top edge of the plate (NGSA). The exact position within this area follows a uniform distribution for each nematode. Forty nematodes are placed in the FCA and 10 in the NGSA. All nematodes are initially at the age of 43 hours, this is 11 hours before they reach maturity. Nematodes are initially naive, i.e. they all have the same attraction to the bacteria, which results from attractive metabolites secreted by them.

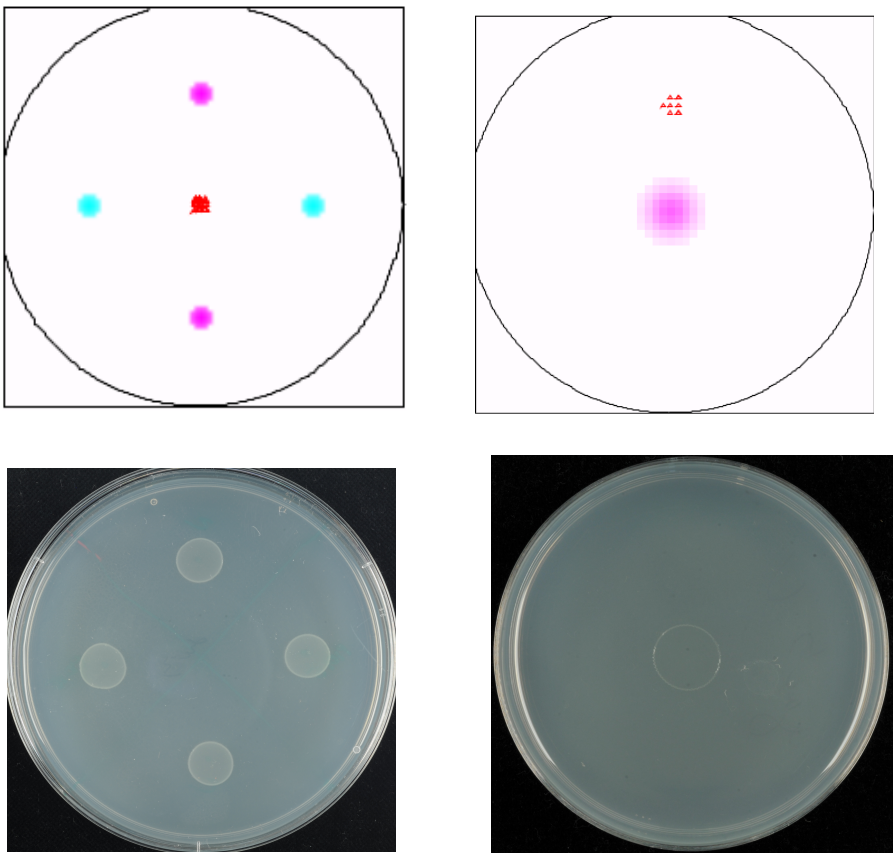

Figure 3.3: Nematode–bacteria interaction assays in the model and in the lab Top: The simulation domain for the food choice assay (left) and the food race assay (right). The domain permitted for nematode movement is indicated by the black outline. The two different colours used for the bacteria indicate the two different types of bacteria used and the red triangles indicate the initial distribution of nematodes. Bottom: The corresponding assays as conducted in the lab.

3.6.3 Output

All variables (chemical and bacterial fields and all variables associated with nematodes) are recorded at regular, user-defined intervals. This happens in two ways:

- **Visual** – One of the main attractions of cellular automatons is an easy and intuitive visual representation. Bacteria and chemical densities as well as the locations of all nematodes are output to an image.
- **Analysis** – Several quantities can be calculated for comparison with those found in experiments. These depend on the specific simulation conducted and

reflect bacterial growth and nematode choice.

3.6.4 Parameter Calibration

The output described above is used to compare the model to experimental observations in order to determine those parameters, which we cannot extract from the literature or measure directly. In Table 3.9 these parameters are indicated as 'empirically determined'. To find appropriate values for the empirical parameters we run the model with one set of parameters for both of the experiments and use the observed differences between model and experiment to decide which parameters need to be adjusted. For example if we find that bacteria are not spread far enough, it is likely that the parameters attachment_rate and deposition_rate need to be altered in order to achieve the desired outcome. This process is repeated until we have determined one complete set of parameters, which accounts for all the observed phenomena. This set of parameters has been detailed in the previous sections and will be used for all the representations of the model in later chapters. In the following chapters we will describe further, which phenomena these parameters influence, and thus how we could arrive at the values given. Some of the parameters like edibility remain variable, as we are looking at bacteria with a range of different edibilities.

3.7 Discussion

In this chapter we have developed a model of the nematode–bacteria interactions which includes chemical stimuli and takes nematode chemotaxis and learning into account. The model can be used to make predictions about other systems of vector-

borne pathogens by evaluating conserved patterns. We will use the model to allows us to track agents in more detail than we can do in an experimental setting. Any measures for bacterial numbers we will make in later chapters to analyse the efficiency of spreading are made by indirect proxies. There is no reliable way to get accurate bacterial numbers, nor can we tell the two different strains of bacteria apart which will merge in the food choice assay.

In the following chapters we will use and test the model developed above and will thus be able to appraise how well it accounts for the fundamental aspects of nematode–bacteria interactions in the assays conducted in this study. The following chapters will also aid in finding suitable parameter ranges for all of the unknown parameters.

In Chapter 4 we will make use of the model to investigate the effects of the bacterial growth parameters on the interactions. Observing nematode behaviour in Chapter 5 will help us to find a suitable range for parameters concerned with the attraction of nematodes by bacteria and we will be able to evaluate our description of learning. Furthermore, we will test the hypothesis that chemotaxis is not required to find or choose food, but that it does accelerate the process. Finally we will vary the edibility parameters in Chapter 6 to test whether we can reproduce the effect of edibility on spreading success. We will also be able to use observations from the spreading assays to determine ranges for bacterial attachment and detachment rates.

In constructing the model we have necessarily made many assumptions and simplifications. Assumptions are necessary whenever we do not know the exact underlying mechanisms or parameters. For a complete description in a model, much more

detail is usually required than is known. In our case this is particularly evident when attempting to describe nematode learning. Although much is known about the neurons, genes and stimuli that can be associated with nematode learning, we do not have enough detail to give a complete description of the process. Until more is discovered about the underlying mechanisms, it will be difficult to estimate what effect wrong assumptions might have on the outcome of a simulation.

We have also made many simplifications, which will limit the applicability of the model. We have made our simplifications such that we expect the model to perform well in reproducing the assays described in Table 3.10. In trying to extend the model to situations beyond these limits, the model will necessarily become more complex and computationally expensive. Representing large numbers of nematodes would require a description of nematode clustering, especially in the Hawaiian strain. This could be achieved through a phenomenological approach, which increases the chances of nematodes staying together, or through encoding one of the proposed mechanisms for clustering, i.e. pheromones, or an oxygen field. Extending the time for which the interactions are modelled will require the addition of a nematode health variable to adequately capture slow killing of nematodes and the associated reduction in reproduction and motion and eventual death of the nematode. This will be particularly important when representing those bacteria (WT) or nematodes (*sek-1* mutant), where slow killing plays an important role. A variable egg-laying rate will also be necessary if modelling more complex environments with multiple food sources for more than a day. This could be linked to the health variable, although further investigations will be necessary to establish the connection. Our simplified model of bacterial growth will probably be sufficient as long as we are

interested in qualitative investigations.

Although some parameters can be measured directly, others (like bacterial attachment and detachment rates) must be determined by fitting the results of the model to those of experiments, which is a more indirect form of measurement and usually only establishes ratios of some parameters to others, rather than their absolute values. In order to go beyond this fitting, and thus to make better quantitative statements with this model, a significant amount of further work is required. For example, the nature of the chemicals involved in nematode–bacteria interactions must be known before their diffusion rate can be determined; in turn, the diffusion rate influences the range over which bacteria interact with nematodes. Bacterial attachment and detachment rates to and from the nematode cuticle need to be measured to describe spreading more accurately, especially over longer distances. We will discuss these parameters further in Chapter 6.

The large parameter space makes parameter sweeps impractical, meaning that the parameters used are most likely sub-optimal. However, the following chapters provide reasonable bounds for these parameters. The agreement between model and experiment indicates that the choice of parameters in relation to each other is good. While using the model in later chapters we will also be able to discover, which parameters it is very sensitive to and thus for which parameters accurate measurements are particularly necessary. This will also help to highlight the most critical aspects of the interaction. During simulations we note that, as in experiments, the model is very sensitive to nematode numbers which depend on reproductive rates and thus on eating rates, the latter of which is not a very well characterized parameter.

More extensive alterations to the model would be necessary to represent nema-

todes as one- or even two-dimensional. The resulting separation of head and tail would allow us to improve the representation of spreading and incorporate a more accurate description of nematode motion.

After the nematode–bacteria interactions have been exhaustively studied using this setup a more complex model should be considered, for example using a grid-free model with a velocity-jump model for nematode motion.

Chapter 4

Growth Effects

4.1 Introduction

The aim of this thesis is to look at the relationship between the edibility of bacteria and their dispersal by the predator *C. elegans*. However, other factors may play a role in nematode–bacteria interactions. These factors include bacterial motility, their attachment to the nematode cuticle and their growth. Very little variation in motility has been observed within the mutants of *P. fl.* NZI7 on solid agar plates (though differences are observed on swarm agar, but this is not relevant here). The study of attachment to the nematode cuticle is beyond the scope of this work, and we have little reason to suspect that many of the mutants we investigate in this study have altered attachment properties, except for the mucoid mutant (mucA), which we will further investigate in Chapter 6. However, many mutants have been identified as growth deficient [91] and we have observed some strains like those bearing plasmids and the mutant 1654 (PFL_5277) which appear to have reduced growth on NGM agar plates, therefore characterizing bacterial growth parameters will be essential

when trying to understand bacteria–nematode interactions. Altered growth could affect the ability of the bacteria to establish themselves in a new environment once they have been spread by the nematodes, as it would change the balance between bacterial reproduction and consumption by nematodes. Furthermore the levels of bacterial toxins and repellents will also depend on bacterial growth dynamics. It is likely that in monocultures, all other aspects remaining equal, pathogenicity and toxicity traits are proportional to the bacterial numbers [98], so that growth defects might be the cause of increased edibility. We know that the effects of toxins are dose dependent, from experiments conducted with the close relative of *P. fl.* NZI7 CHA0. Nematodes were fed a mixed diet of WT bacteria and GacS mutant. The nematodes thrived better on a diet in which the ratio of WT bacteria (and thus toxins) was low [88]. Additionally we also know that GacS regulated traits are especially expressed during stationary phase [117]. Many, perhaps all of the factors involved in bacteria–nematode interactions are regulated by the GacS/GacA pathway [121]. Bacterial toxicity will therefore depend not just on bacterial density, but also on the phase the bacteria are in.

We will study the two main aspects of bacterial growth dynamics [269]: the growth rate and carrying capacity. Growth rate will be an important aspect of how fast bacteria can colonize new territory and is often used as the main indicator of bacterial fitness [270, 271]. The carrying capacity represents the maximum number of bacteria which can be sustained by the resources available, this will influence the bacterial density nematodes will encounter and thus the levels of toxins they will face. The interplay of both parameters will determine the time at which stationary phase is reached and thus GacS regulated traits are expressed.

After determining the relevant bacterial growth parameters we will use the model to estimate the impact of alterations in these parameters in order to group strains with altered growth based on the predicted effect on nematode–bacteria interactions. Most of our investigations into bacterial growth will be done using bacteria growing in liquid culture, but in the last section of this chapter we will study bacterial growth on solid agar in order to justify the model of bacterial growth we are using in Chapter 3 and to evaluate the transferability of our findings to the remaining investigations.

4.2 Characterizing Bacterial Growth

It is well known that bacterial growth follows a sigmoidal curve, with saturation occurring due to exhaustion of nutrients [217, 269]. The bacteria are said to enter stationary phase during this later stage [272]. Many different models can be used to describe such a curve including Verhulst (Logistic), Gompertz, Richards, Schnute and Stannard models [269]. We have chosen a three parameter model, as it is perceived to describe bacterial growth better, is more stable, and less liable to overfitting than any of the four parameter models in existence [269]. There is little difference between the individual models, as all produce a good fit to bacterial growth [269]. As in Section 3.2 we will assume a logistic model for bacterial growth and in this Chapter we will estimate the associated parameters. Logistic models are common for bacterial growth [263, 269, 273]. For a detailed derivation of the model the reader is referred to Murray's Mathematical Biology [217]. Many extensions of the basic model have been proposed [261, 262] introducing more parameters to the system. Here we will use it in its most basic form.

4.2.1 Logistic Model for Bacterial Growth

The logistic model is commonly used in mathematics to represent growth of a population in an environment where resources are limited. It is known to perform well in low nutrient conditions [274], like those found in our system. Growth is assumed to be proportional to the current population, but also to the amount of limiting nutrient remaining. Thus growth is assumed to be governed by the differential equation:

$$\frac{\mathrm{d}N}{\mathrm{d}t} = rN\left(1 - \frac{N}{K}\right), \tag{4.1}$$

where N is the population number, the carrying capacity K is the maximum N which the environment can support and r is the rate at which each individual reproduces. This equation can be solved to yield:

$$N = \frac{N_0 K e^{rt}}{K + N_0\left(e^{rt} - 1\right)}, \tag{4.2}$$

where N_0 is the initial population.

For a more in-depth treatment of this and similar models the reader is referred to Murray's Mathematical Biology [217] and Zwietering *et al.* [269].

4.2.2 Data Fitting and Analysis

To determine bacterial growth parameters for each bacterial strain at least two independent experiments were conducted with at least 8 technical replicates per experiment. The growth curve representing the average of the 8 replicates in one experiment was fitted to Equation 4.2 using Mathematica's nonlinear least squares

method. This resulted in a mean and standard deviation for the two parameters r and K for each strain measured during a particular experiment.

To obtain normalized values, the growth parameters of a mutant strain were divided by those obtained for WT growth during the same experiment. This will reduce the effect of variations between experiments generated by differences in growth medium and room temperature. The resulting statistics were analysed using ANOVA theory [254], which is described in the Appendix.

4.2.3 The Bacterial Growth Parameters

In order to determine the possible effect of bacterial growth dynamics on bacteria–nematode interactions, we obtained growth parameters for all of the mutants which will be used in this study (see Table 1.2). We will determine growth parameters for a minimal medium, NGM, which is used in all of our bacteria–nematode interaction assays. The growth parameters were obtained from growth in liquid culture in a 96 well plate. The optical density reading OD_{600} is used as a proxy for bacterial density. While this method will not give exact growth parameters, it will serve to compare the growth between different mutants and determine those which are growth deficient. In Table 4.1 the growth parameters are given as measured (i.e. without normalization). The following analysis will always refer to the normalized growth parameters and their standard deviations, which are represented in Figures 4.1 and 4.2.

Table 4.1: Bacterial Growth Parameters For each strain growth parameters were measured in two independent experiments, with 8 replicates in each experiment. Those mutants which are further studied in later chapters are highlighted in bold, more details about the genotypes and phenotypes can be found in Tables 1.2 and 1.3. Errors given are standard deviation.

Identifier	**r** $(\times 10^{-5})$ [1]	K [2]	**Rating** [3]
904 (PFL_0085)	5.1 ± 1.6	0.22 ± 0.4	***
956 (PFL_0116)	10.2 ± 0.3	0.23 ± 0.02	
955 (PFL_0117)	9.1 ± 0.4	0.22 ± 0.02	
908 (PFL_0836)	6.5 ± 0.2	0.28 ± 0.004	**
912 (PFL_0836)	7.5 ± 0.9	0.23 ± 0.03	**
961 (PFL_0928/9)	6.5 ± 2.0	0.22 ± 0.03	**
920 mucoid (**mucA**)	9.7 ± 1	0.27 ± 0.02	*
906 (PFL_1595)	7.8 ± 1.2	0.23 ± 0.02	*
905 **FliF**	3.3 ± 0.05	0.28 ± 0.006	*
1638 (PFL_1685)	8.1 ± 0.2	0.27 ± 0.005	*
959 (PFL_2066)	7.8 ± 0.8	0.22 ± 0.02	*
1015 **HCN**	10.4 ± 2.2	0.23 ± 0.04	*
970 (PFL_2761)	7.1 ± 0.4	0.24 ± 0.04	
1642 (PFL_2816)	9.0 ± 0.7	0.27 ± 0.03	
954 (PFL_3902)	6.7 ± 0.2	0.21 ± 0.006	**
910 (PFL_3930/1)	10.6 ± 0.8	0.22 ± 0.02	*
957 (PFL_3987)	12.0 ± 0.2	0.23 ± 0.01	
964 (PFL_4192)	12.4 ± 0.3	0.23 ± 0.03	*
1046 (PFL_4347 chorismate)	6.4 ± 1.9	0.22 ± 0.03	**
967 (PFL_4348 chorismate)	10.6 ± 0.3	0.24 ± 0.002	
921 (PFL_4348 **chorismate**)	8.7 ± 0.9	0.21 ± 0.01	*
1644 (PFL_4448)	8.6 ± 0.7	0.22 ± 0.01	*
913 (**GacS**)	11.3 ± 1.8	0.25 ± 0.02	**
963 (PFL_4788)	9.9 ± 0.8	0.22 ± 0.02	
1663 (PFL_4870)	4.5 ± 0.5	0.21 ± 0.01	*****
1646 (PFL_5273)	2.9 ± 0.9	0.27 ± 0.03	****
1654 (PFL_5277)	3.0 ± 1.1	0.27 ± 0.002	*****
1659 (PFL_5326)	4.2 ± 2.8	0.14 ± 0.03	**
1643 (PFL_5388)	6.8 ± 0.7	0.20 ± 0.003	
969 (PFL_5425)	8.4 ± 2	0.23 ± 0.03	
923 (EDB2)	7.8 ± 1.1	0.24 ± 0.03	
1009 (EDB3)	8.9 ± 1.4	0.24 ± 0.04	

Continued on next page

[1] r is the growth rate in s^{-1} of the bacterial population.

[2] K represents the maximum optical density the bacterial culture can reach

[3] Growth levels are determined as described in Section 4.3.4. It is indicated in five levels indicated by asterisks, where red denotes deficiency and cyan enhancement.

Table 4.1 – continued from previous page			
Identifier	**r** $(\times 10^{-5})$[1]	K [2]	**Rating** [3]
1648 (EDB4)	8.3 ± 0.4	0.28 ± 0.005	
917 (**EDB1**)	8 ± 1	0.24 ± 0.03	
916 (PFL_5629)	7.4 ± 1	0.26 ± 0.02	*
985 (PFL_5629/30)	7.1 ± 0.2	0.22 ± 0.04	**
1639 (PFL_5650)	5.3 ± 0.2	0.25 ± 0.01	***
1657 (PFL_5742/3)	7.2 ± 0.1	0.22 ± 0.01	
958 (PFL_5850)	7.3 ± 0.8	0.26 ± 0.03	*
1655 (PFL_5877)	7.7 ± 0.6	0.24 ± 0.03	*
1660 (PFL_5899/900)	13.1 ± 1	0.22 ± 0.02	*
1653 (**PtsP**)	13.6 ± 0.7	0.22 ± 0.004	**
918 (PFL_5919 (*GacA?*))	13.3 ± 1.5	0.27 ± 0.008	***
965 (PFL_6125)	11.5 ± 2.5	0.17 ± 0.008	
1048 (PFL_6125/6)	7.9 ± 0.2	0.16 ± 0.001	**
971 (PFL_6158)	9.0 ± 1.4	0.22 ± 0.04	
1734 (PFL_6226)	5.6 ± 0.06	0.23 ± 0.001	*
1652 (PFL_6229)	5.9 ± 0.8	0.18 ± 0.002	*
1664 (PFL_6230)	6.2 ± 1.6	0.20 ± 0.003	*
903 (**tol**)	9.2 ± 4.0	0.25 ± 0.02	
2072 (WT-like)	9.1 ± 1.4	0.27 ± 0.02	
2073 (WT-like)	7.3 ± 1.7	0.24 ± 0.04	
2074 (WT-like)	8.6 ± 0.9	0.26 ± 0.05	
2075 (WT-like)	8.8 ± 0.3	0.28 ± 0.01	
2076 (WT-like)	7.8 ± 0.3	0.23 ± 0.05	
2077 (WT-like)	8.7 ± 1.0	0.25 ± 0.03	
2078 (WT-like)	9.4 ± 0.6	0.28 ± 0.04	
WT	9.1 ± 1.3	0.24 ± 0.03	
978 (ΔGacS tol)	11.8 ± 2.8	0.25 ± 0.02	***
989 (ΔGacS)	11.8 ± 3	0.23 ± 0.02	***
1003 (ΔGacS EDB1)	13.3 ± 2.7	0.26 ± 0.01	***
1004 (ΔGacS EDB1)	11.6 ± 2	0.25 ± 0.02	**
1086 (ΔEDB HCN)	6.5 ± 0.8	0.21 ± 0.01	
1712 (**double**, HCN, tol)	7.2 ± 1.6	0.20 ± 0.01	*
1713 (**triple**, HCN, tol, EDB)	6.5 ± 1.2	0.23 ± 0.01	*
1900 (ΔEDB)	7.9 ± 1.7	0.25 ± 0.04	*
2079 (**WT with mini-Tn7:GFP**)	8.1 ± 0.5	0.25 ± 0.03	*
2080 (**EDB1 with mini-Tn7:RFP**)	8.1 ± 0.8	0.23 ± 0.03	
2081 (WT with mini-Tn7:RFP)	12.3 ± 0.2	0.26 ± 0.001	*
2082 (**WT with mini-Tn7:RFP**)	7.6 ± 0.7	0.22 ± 0.003	

Continued on next page

[1] r is the growth rate in s^{-1} of the bacterial population.

[2] K represents the maximum optical density the bacterial culture can reach

[3] Growth levels are determined as described in Section 4.3.4. It is indicated in five levels indicated by asterisks, where red denotes deficiency and cyan enhancement.

Table 4.1 – continued from previous page			
Identifier	**r** $(\times 10^{-5})^1$	K [2]	**Rating** [3]
2083 (**WT with pIJ11282**)	4.9 ± 0.7	0.21 ± 0.04	***
2084 (mCherry plasmid in WT)	5.2 ± 0.1	0.22 ± 0.002	*****
2085 (GFP plasmid in WT)	6.1 ± 1.8	0.22 ± 0.03	**

[1] r is the growth rate in s^{-1} of the bacterial population.
[2] K represents the maximum optical density the bacterial culture can reach
[3] Growth levels are determined as described in Section 4.3.4. It is indicated in five levels indicated by asterisks, where red denotes deficiency and cyan enhancement.

Many of the values shown here display great variation, where the bulk of the variance comes from the differences between experiments, rather than the variation within one experiment. The coefficient of variance of unnormalized values can exceed 20 %. After normalization as described above, the variation in the data is approximately halved resulting in much smaller error bars in Figures 4.1 and 4.2. This finding confirms our hypothesis that variation was partly caused by inconsistencies in growth conditions.

It is immediately obvious that the strains containing plasmids are growth deficient. While they reach approximately the same maximum as the WT, their growth rate is diminished. The same is also true for some of the transposon insertion mutants like 1654 (PFL_5277) for which we have also observed diminished growth on NGM agar plates. We will be able to confirm these observations more rigorously in our later analysis in Section 4.3.4.

All strains with a GacS mutation and the strain with a suspected GacA mutation (PFL_5919) showed enhanced growth as previously demonstrated [91]. This is expected, as approximately 10 % of their genes are not expressed [275]. Furthermore the cyanide mutant appears to be growth enhanced, which could be due to self-inhibition in cyanide producing strains, and could also further explain the

enhancement of mutants of the Gac regulatory system.

The flagella mutant (FliF) reaches a much higher bacterial density, which could be because it does not need to make a flagellum, and thus more resources are available for bacterial reproduction. This mutant also shows a significantly reduced growth rate, which might be due to the inability of individuals to disperse in the mostly stationary liquid culture and thus use the nutrients efficiently. This could be a factor that is only important in liquid growth, which is consistent with the fact that we have not observed any growth deficiency on plates.

There are several other strains which could be growth deficient or growth enhanced. We will further classify their severity in the next section using the model constructed in Chapter 3.

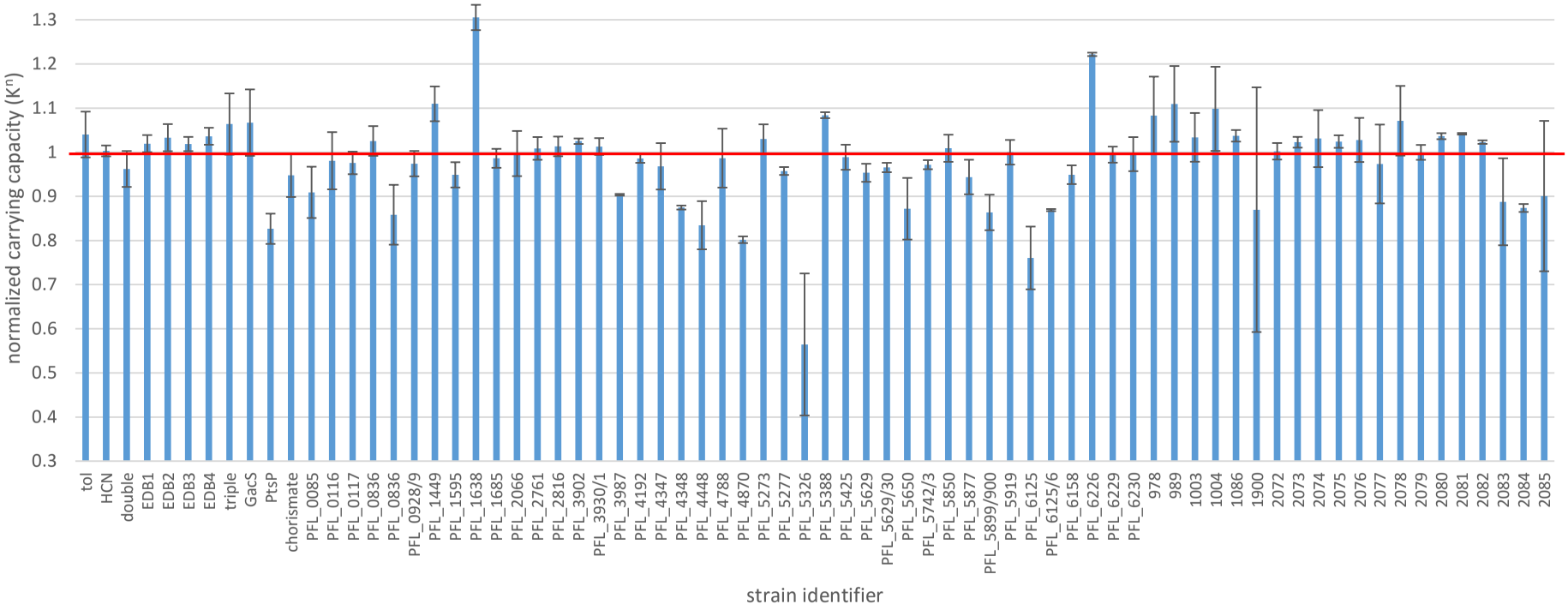

Figure 4.1: Normalized carrying capacity (K^n). For each experiment the average carrying capacity is divided by the WT carrying capacity determined during the same experiment to normalize for environmental inconsistencies. The red line indicates WT growth. Error bars represent standard deviation, which was calculated using ANOVA theory. For each strain at least two independent experiments with 8 technical replicates were conducted.

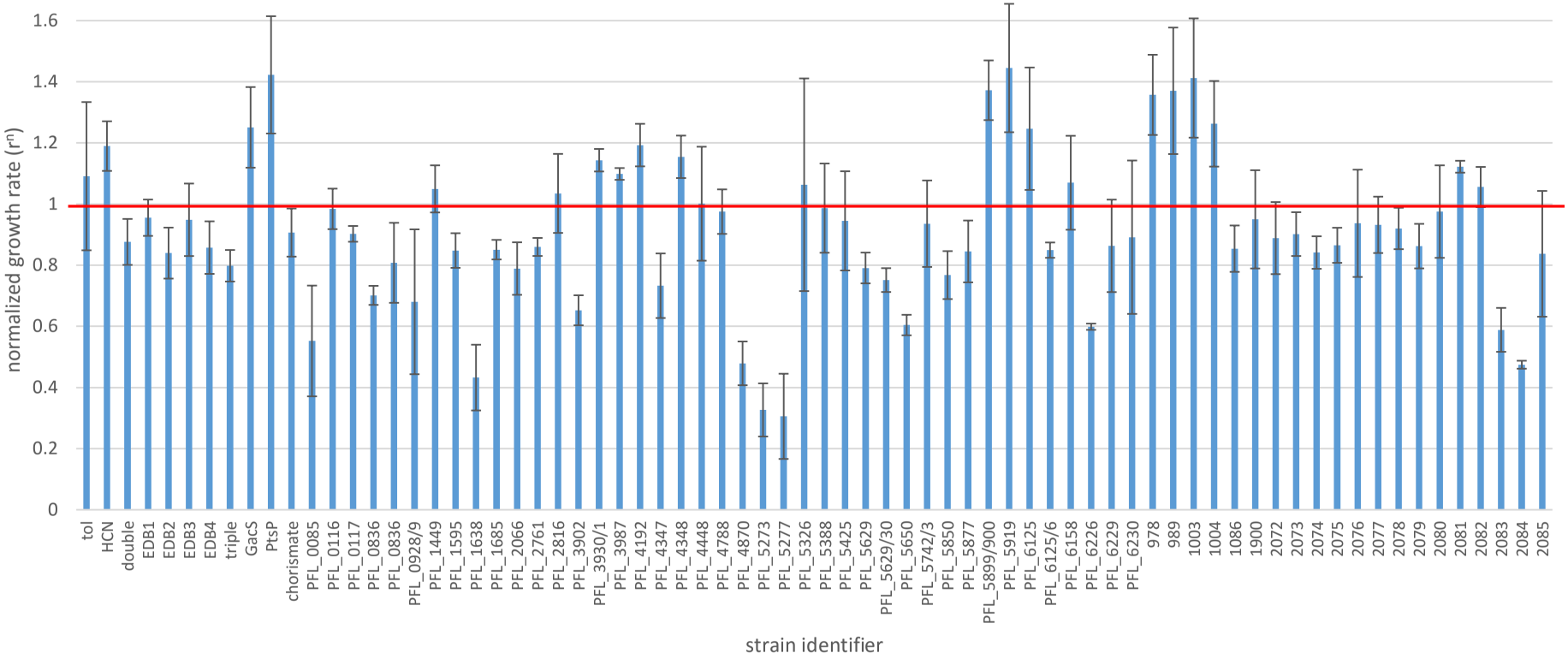

Figure 4.2: Normalized growth rate (r^n). For each experiment the growth rate is divided by the corresponding WT growth rate to normalize for environmental inconsistencies. The red line indicates WT growth. The Appendix provides the details of how the mean and standard deviation (indicated by error bars) were computed. For each strain at least two independent experiments with 8 technical replicates were conducted.

4.3 Modelling Bacteria–Nematode Interactions with Different Bacterial Growth Parameters

To estimate the impact of the two growth parameters r and K on nematode–bacteria interactions, we can run the model constructed in Chapter 3 using the NGSA simulation (see Section 3.6) with different growth parameters. The total number of bacteria on the plate during the simulation can be used as a measure of the effect variation in growth parameters has on the bacteria–nematode interactions.

In this section we describe the observations made during such simulations. The model was run at least three times for each set of parameters, where the only difference between runs is the random number seed which underlies nematode motion. The parameters we used in this simulation span the full range of parameters observed in experiments. We sampled bacterial numbers and nematode numbers every 6 hours.

4.3.1 Effects of Stochasticity in the Model

Unlike all other agents in the model, nematode motion is not deterministic. The uncertainty behind the behaviour of *C. elegans* accounts for all stochastic effects in the model. One example of the variation observed in bacterial numbers can be seen in Figure 4.3, which shows the errors associated with each simulation. For clarity error bars are omitted in all further figures.

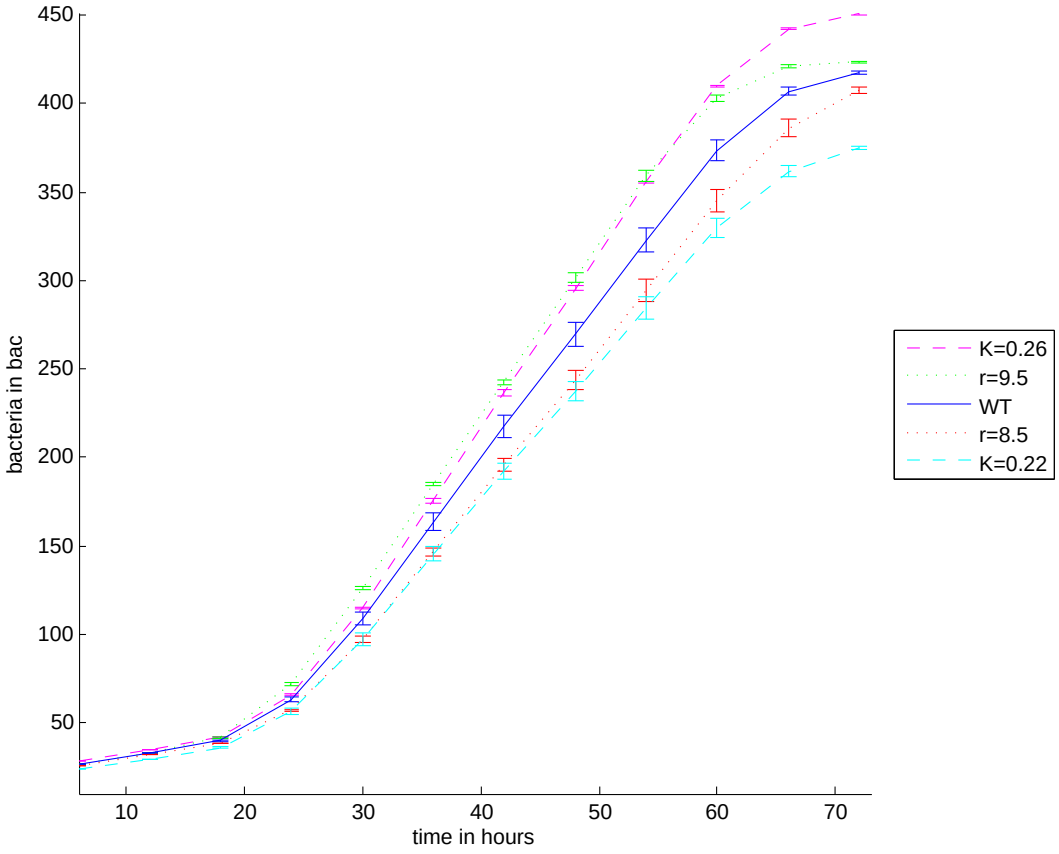

Figure 4.3: Stochasticity in the model Different random number seeds lead to variation in the model for the same set of parameters. However, variation is small enough that we can distinguish runs with different parameters. Bac is the arbitrary scale we defined for bacteria in Chapter 3. Fixed parameters are as detailed in Chapter 3, WT parameters: $K = 0.2423$, initial_attraction= 0.001, edibility= -0.0015, $r = 0.00009$, deviations from these are indicated in the figure legend. Each line represents the mean of three runs and error bars indicate standard deviation.

4.3.2 The Observed Effects are Non-linear

Total bacterial numbers are a strictly increasing function of both growth parameters, but this increase is not linear in all cases. At fixed carrying capacity (K), altering r has nonlinear effects on total bacterial numbers (see Figure 4.4). This means there are areas of the r–K plane in which altering r has less effect than in other areas. The response curve appears to be sinusoidal, with its linear part being around the

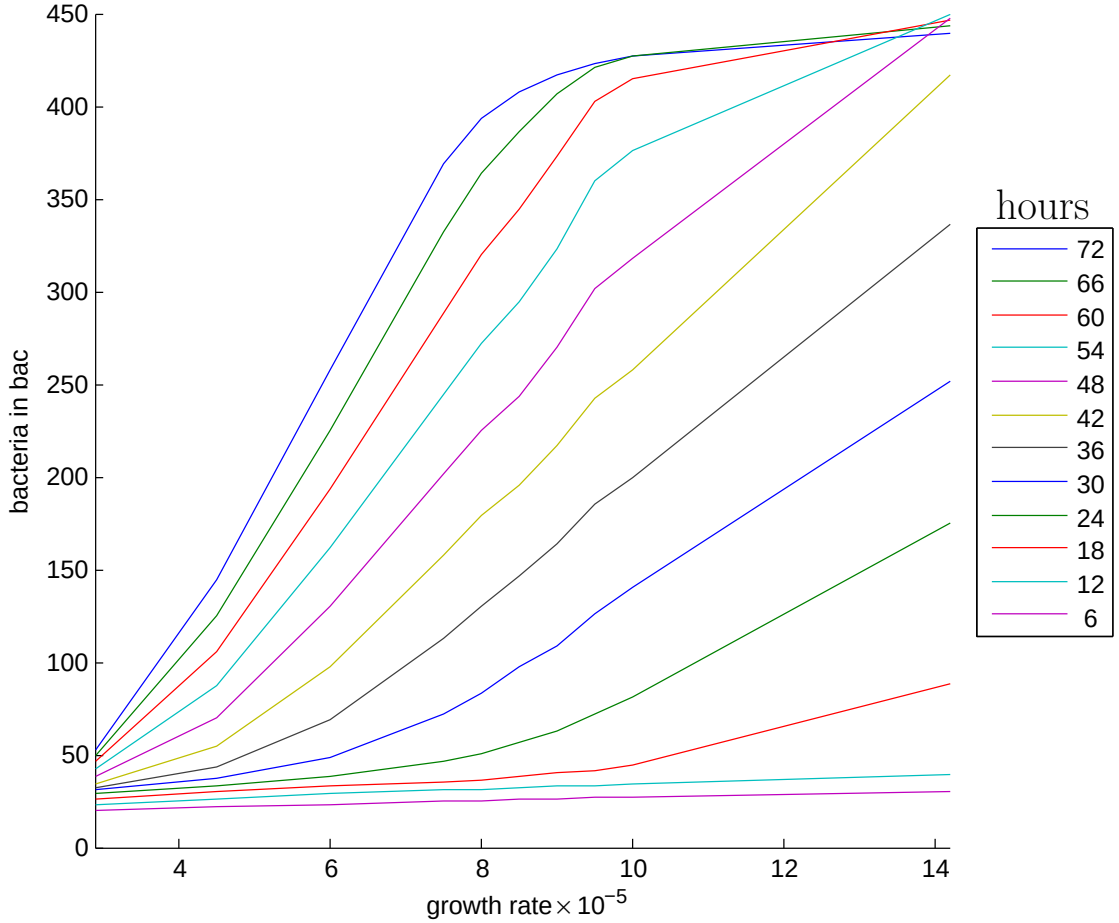

Figure 4.4: Nonlinear effects Mean of three simulations with different random number seeds. Varying the bacterial growth rate r has unexpected effects on the bacterial numbers observed in a simulation of the bacteria–nematode dynamics. Bacterial numbers are measured in bac, the arbitrary scale we defined in Chapter 3. Fixed model parameters are as described in Chapter 3. Variable parameters are: $K = 0.2423$, initial_attraction= 0.001, edibility= -0.0015.

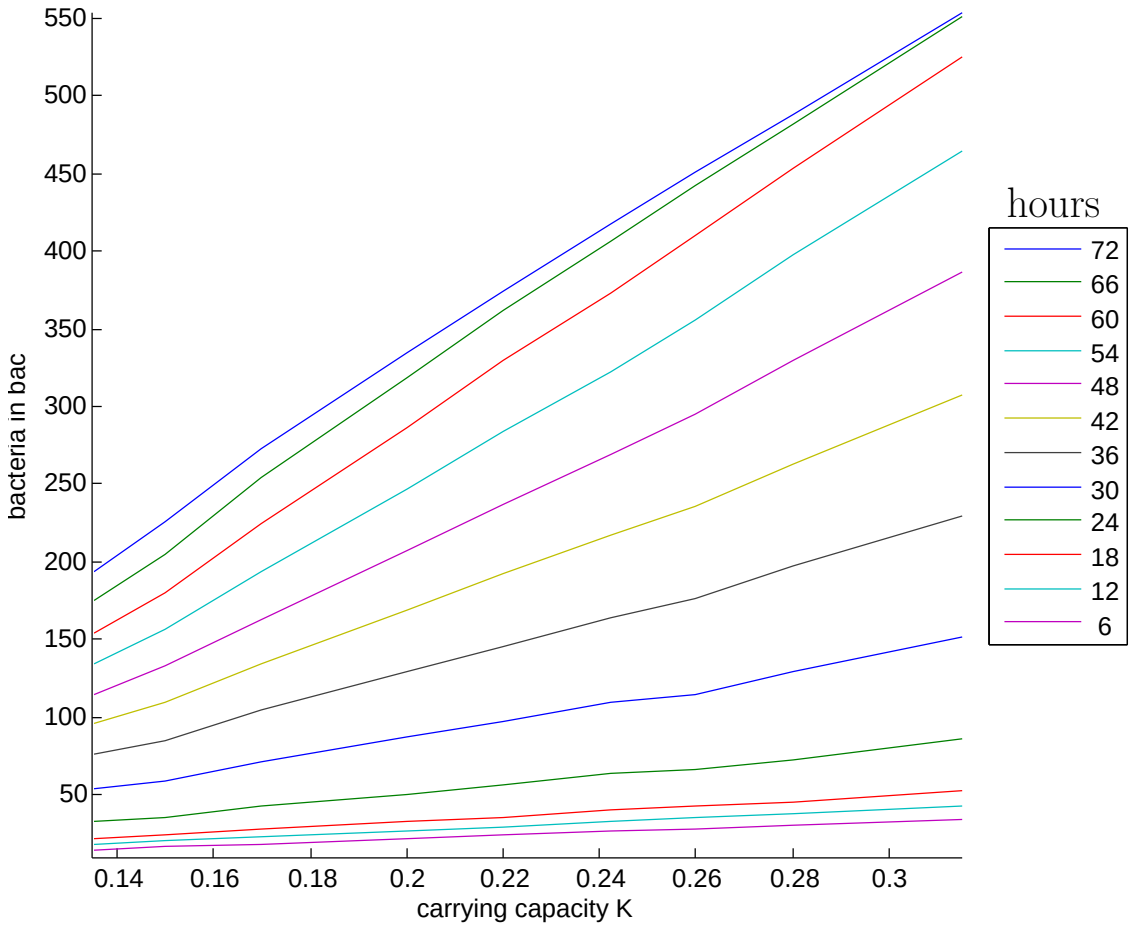

Figure 4.5: Linear effects In the parameter space relevant for our experiments the effects on bacterial numbers of altering the carrying capacity K is linear. The fixed model parameters are as described in Chapter 3. Variable parameters are: $r = 0.00009$, initial_attraction$= 0.001$, edibility$= -0.0015$. Lines represent the mean of three runs with different random number seeds. Error bars have been omitted for clarity but are as seen in Figure 4.3

WT parameters at early time points. Just as in classical predator–prey models, the complex interactions between two species can mean that the predicted outcome is very sensitive to the parameters.

On the other hand, altering K and fixing r generates a linear response (see Figure 4.5).

4.3.3 The 54 h Time Point is Optimal for Further Analysis

During experiments severe growth deficiency results in noticeably altered patterns after around 2 days. The nonlinear effects we observed in our simulations above are particularly strong before 30 hours and after 60 hours in our parameter range. Thus we will be looking for a time in this interval for our further analysis. The 54 hour time point gives the best separation between parameters (see Figure 4.3), e.g. comparing the WT run to one where r is increased to 9.5×10^{-5} we obtain $p = 0.004$ at 54 hours but $p = 0.006$ at 48 and 60 hours. Therefore we will focus on the data obtained at the 54 hour time point, to guide our classification of growth deficient or growth enhanced strains.

4.3.4 Classifying Strains According to Growth

All of the mutants tested have growth which is significantly different from WT. For the purposes of evaluating bacterial growth patterns in the context of bacteria–nematode interaction, which we are interested in in later chapters, we will therefore look at strains, which are so altered in growth that their interaction with nematodes changes. For this purpose we shall look at the effect of altered growth on the outcome

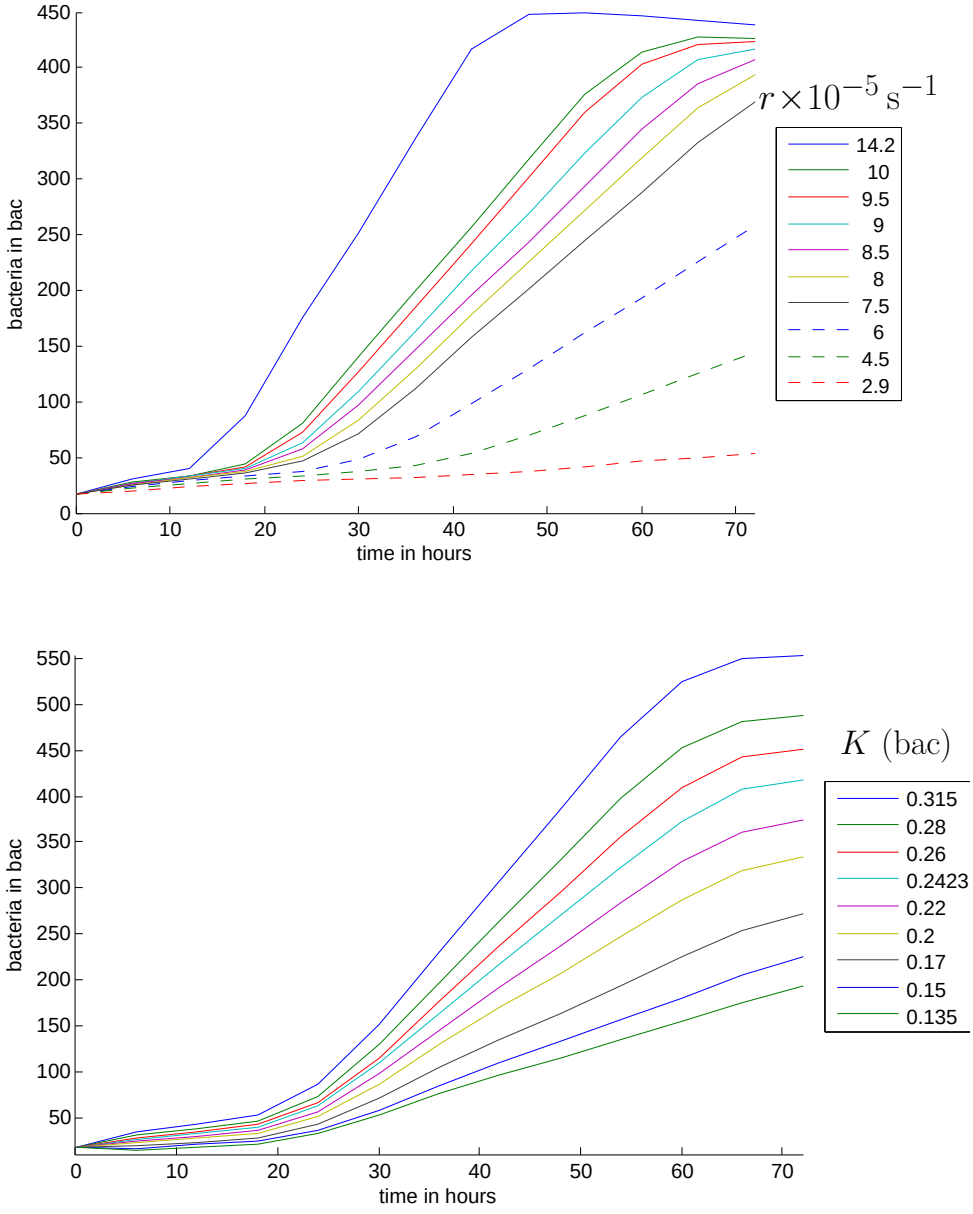

Figure 4.6: Total bacterial numbers during a food race assay simulation at WT carrying capacity (top) or growth rate (bottom). Bac is the arbitrary scale for bacterial numbers we defined in Section 3.2. The fixed parameters used for this simulation are as described in Chapter 3, and variable parameters are as follows: $K = 0.2423$ (top) or $r = 0.00009$ (bottom), initial_attraction= 0.001, edibility= -0.0015. Initially there are 16.8 bac on the whole plate. Growth rate (top) and carrying capacity (bottom) are varied within the ranges observed experimentally. Each line represents the mean of 3 runs.

of our model. Fitting of the response to a linear equation results in the equation

$$B(t = 54) = 4930000r + 1840K - 564 \tag{4.3}$$

with very small errors for each of the parameters, and an R^2 of over 0.99. This equation allows us to define a weighted distance D for the two parameters and thus assign levels of growth deficiency to the mutants tested. As we will be working in the normalized parameter space this distance is defined as:

$$D = |(1 - r^n) + 1.004(1 - K^n)| = |2.004 - r^n - 1.004K^n|, \tag{4.4}$$

where r^n and K^n are the normalized growth parameters as described in Appendix A1. This suggests, that the two parameters are almost equally important in determining the outcome of the interaction.

It remains to find a suitable cut-off threshold. For this purpose we will look at the WT-like mutants, i.e. mini-Tn5 insertion mutants which show no phenotype in any experiment. These mutants might represent the cost of the mini-Tn5 insertion, and they do not show any signs of growth deficiency in experiments, so we will define a normal growth region such that these mutants are classified as normal growing mutants.

The average distance of a strain with no phenotype is 0.078 with a standard deviation of 0.041 (see Table 4.2). We will acordingly define the first thresholds at 0.135 corresponding to the 99 % confidence limit of this distance. All further thresholds will be defined by taking multiples of this first threshold. In Figure 4.7

Table 4.2: The distance of WT like mutants from WT. For all WT-like mutants the distance of the growth parameters is computed according to the formula in Equation (4.4).

WT like	r^n	K^n	D
2072	0.902	1.005	0.093
2073	0.911	1.024	0.065
2074	0.834	1.041	0.125
2075	0.87	1.026	0.104
2076	0.923	1.033	0.044
2077	0.928	0.966	0.106
2078	0.914	1.084	0.008

we highlight these thresholds and in Table 4.1 each strain is annotated with its growth level.

4.4 Solid Growth

In mutants of *P. fl.* NZI7 in which the mini-Tn5::gfplux transposon is inserted in such a way that the promoter of the interrupted gene does not drive the expression of *lux*, *lux* expression is driven cryptically. To date, when using these strains, *lux* expression has always been observed to mirror metabolic activity and thus growth rate (Gail Preston, personal communication). During exponential phase, when bacteria grow at their maximum rate, each cell will luminesce at a maximum intensity. Therefore, during this phase, luminescence is proportional to bacterial cell number. During any other phase, especially during the stationary phase, luminescence is proportional to metabolic activity of the bacterial culture and thus can be an indicator of the rate of reproduction. In liquid culture we can observe this trend very well (see Figure 4.8), as luminescence mirrors bacterial numbers during the exponential phase (i.e. up to about 6 hours) and then drops as bacteria enter stationary phase. The reporter

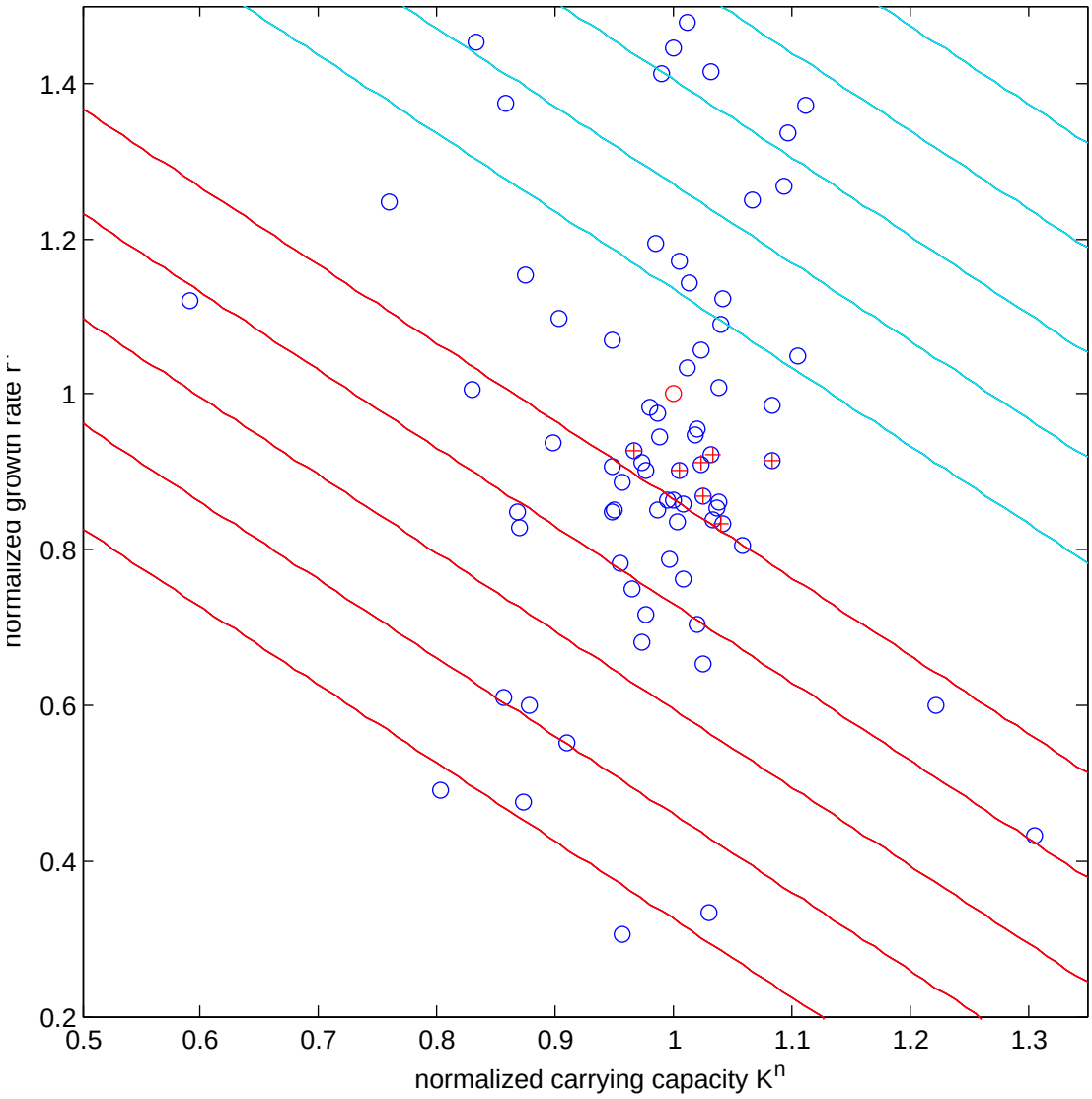

Figure 4.7: Growth Parameters and Levels of Growth Each blue circle represents the mean normalized growth parameters of one bacterial mutant. The red circle indicates the WT and WT-like mutants are highlighted with a red cross. Lines of constant D (see Equation 4.4) indicate the thresholds for our definition of growth levels. Strains underneath the red lines are growth deficient, while strains above the cyan lines are growth enhanced.

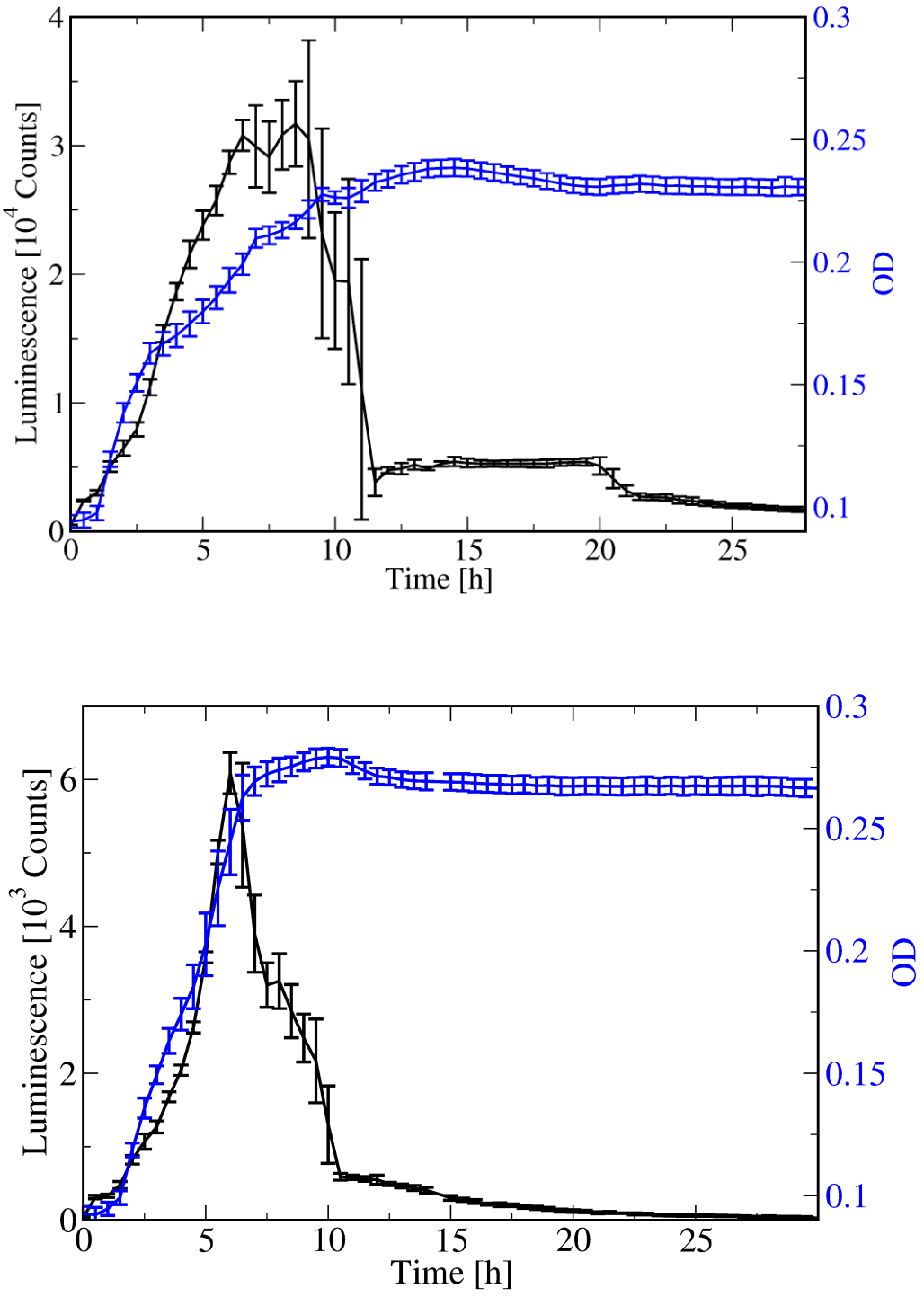

Figure 4.8: Luminescence as a proxy for bacterial numbers Luminescence (black) and OD (blue) measurements in NGM liquid culture at 28 °C. Top: the GacS mutant where luminescence is driven by the GacS promoter. Bottom: the penicillin amidase mutant (918 PFL_5919), where luminescence expression is driven cryptically. Average of 8 technical replicates, with error bars representing standard deviation.

insertion of the *lux* cassette into the GacS gene shows an increased expression of GacS after the bacteria have entered stationary phase, where the GacS/A system is known to be switched on [117, 119], indicating that this could be unsuitable for investigating growth using luminescence as a proxy. We suspect that our penicillin amidase (PFL_5919) mutant has a GacA mutation [91] and thus is phenotypically similar to the GacS mutant. In this mutant however, luminescence expression is driven cryptically and we observe an expression pattern which reflects growth (see Figure 4.8 bottom panel). All other strains with cryptically driven luminescence genes showed the same trends in luminescence dynamics (data not shown).

Using luminescence as a proxy for bacterial numbers, we can investigate the growth dynamics on solid media. We take a small NGM plate and spread a suspension of those mutants with cryptically driven *lux* expression evenly across it. The luminescence can be monitored using the same photon counting setup as will be used in Chapter 6 to investigate spreading dynamics.

When looking at the time course of luminescence over 90 hours (i.e. the length over which we observe bacteria in spreading assays in Chapter 6) we observe a bimodal growth (see Figure 4.9). Comparing different such luminescence curves (data not shown), it is evident that this is not an error in the machinery as the time scale of the oscillation is different in each strain. This diauxic growth pattern is observed in all strains tested, and can also be seen, though less overtly, in the liquid growth data (see Figure 4.9). It most likely originates from a shift in catabolism, as one resource becomes limiting. The time taken to modify expression patterns and adapt to the changing environment (called the diauxic lag [276]) might account for the dip we see in the pattern. This kind of explanation has been offered before,

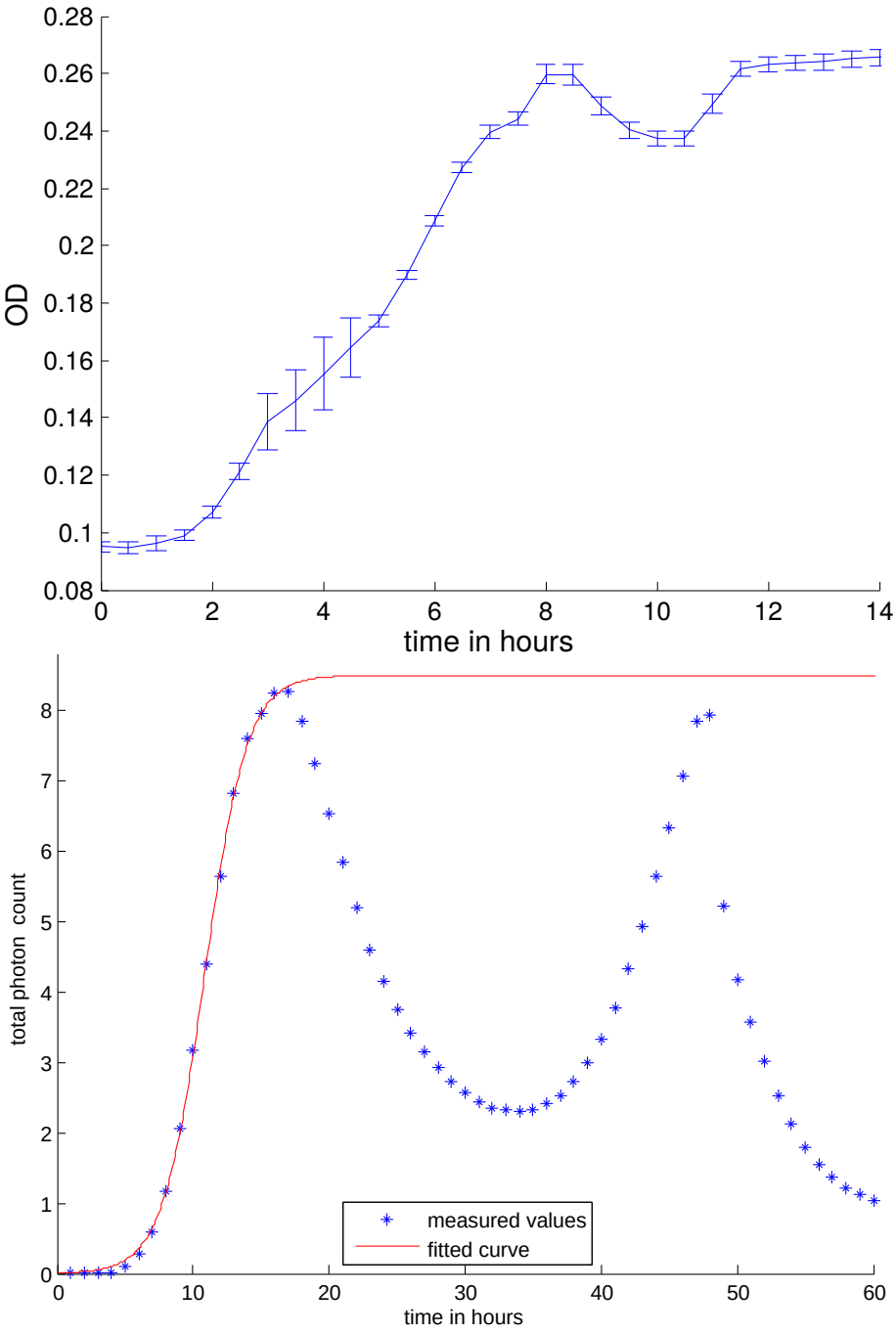

Figure 4.9: Diauxic Growth can be observed in optical density reading in liquid culture (top) or through the luminescence expression of solid cultures (bottom). The EDB3 mutant is used in both cases. Top: Optical density of the strain grown in NGm liquid culture. The data represents the mean of 8 technical replicates and error bars represent standar deviation. Bottom: Total light emitted by a representative plate per hour, which has EDB3 mutant spread across the whole NGM plate (blue stars). The logistic function is fitted using a least squares method to the first 17 hours of the luminescence readings (red line) with parameters: N_0=757.3, K=850663, r=0.647s^{-1}.

when multiple carbon sources were provided to bacteria [277]. Many previous studies focused on diauxic growth in liquid culture [277, 278]. As luminescence is a reporter of growth rate rather than numbers (at least during limiting conditions) the diauxic effect is much more evident in this setting.

The biphasic growth we observe could result from a shift from free amino acids to peptides, which requires proteolysis. The peptone used in the growth medium consists of less than 15 % of free amino acids. It is mainly composed of oligopeptides between 5 and 100 amino acids [279]. This makes the assumption unlikely, as that would indicate that most of the growth happens after the diauxic lag, which is not what we are observing.

Alternatively, it could be a shift of energy sources from one preferred amino acid to another, e.g. it has been observed that *P. syringae* strains prefer glutamate over other amino acids, when provided with a choice [280]. It could also be that critical trace elements like magnesium become limiting, and bacteria need to adapt [281]. Further investigations will be necessary to determine which of these possibilities is the case. The final decline is most likely due to a complete exhaustion of nutrients and thus stationary phase bacteria which are less metabolically active, as well as bacterial death. This shows that luminescence data gathered after around 50 hours of bacterial growth must be treated with caution.

If we take the initial rise (i.e. until the first maximum), we can fit the data to the same logistic model (see Equation (4.2)), which we used for growth in liquid medium. We have done this for 21 different experiments with wrong orientation insertion mutants, and have observed a very good fit in all of them. One randomly selected representative is shown in the bottom panel of Figure 4.9. The good fit

obtained is encouraging, as it justifies the use of the logistic model in our cellular automaton.

4.5 Conclusion

Bacterial growth dynamics might play an essential role in bacteria–nematode interactions. Bacterial growth rate can influence the bacteria's ability to establish themselves in a new environment, while bacterial density and growth phase will determine the level of toxins that nematodes are likely to encounter. Our model supports the hypothesis that bacterial growth is an important factor in bacteria–nematode interactions.

In this chapter we have measured bacterial growth rate and carrying capacity for all the bacterial mutants we wish to use in our study of nematode–bacteria interactions. All measurements were done in liquid culture, but studies of bacteria grown on agar plates confirm that the logistic model can be used to describe initial growth in solid culture as well. The strains cover a large range of each parameter on either side of the WT parameters. The model predicts that the interplay between bacterial numbers and nematode numbers is complex, mirroring the delayed oscillatory patterns we know from predator–prey models. However, we have found that near our WT parameter regime, there are some times when a linear model is appropriate and thus can simplify the classification of growth parameters. The method we have employed has identified a few strains, which we have already noticed to be growth deficient when grown on agar plates. However, we have not been able to pick up all of those strains very well, like for example the strain 2085, which bears GFP on a

plasmid, appears to be just as growth deficient as the other two WT strains bearing plasmids when grown on NGM agar plates, but according to this analysis is less so.

Our model does not take bacterial phase dependent traits into account and thus we have not been able to differentiate between strains with significantly different entry into stationary phase. Strain 905 will have particularly delayed entry into stationary phase, as it has a higher carrying capacity and a reduced growth rate, however, in our analysis it is classified as only level 1 growth deficient. On the other end of the spectrum the strain 965 will have a particularly early entry into stationary phase, and could thus be more toxic purely on this account.

Among a few other growth deficient strains, we have found that plasmid tagged strains are growth deficient. Therefore we will probably not be able to use them to investigate bacterial spreading caused by interaction with nematodes. On the other hand, strains with a chromosomal insertion of fluorescent protein do not show growth deficiency, and thus might be used instead. When evaluating the importance of certain genes in the interactions, we must also check their impact on growth parameters, as this might account for the observed phenotypes.

Chapter 5

Edibility of *Pseudomonas fluorescens* NZI7

Disgust commonly prevents us from eating anything unwholesome, but past experience and hunger will modify our perception of what is acceptable food. These fundamental rules of behaviour can also be observed in *C. elegans*. In addition to an innate perception of attractive and repulsive stimuli, it can adapt its behaviour based on past encounters and satiation. *C. elegans* mainly perceives its environment through chemosensation, which allows it to distinguish between the large range of waste products and secondary metabolites secreted by bacteria [160, 167, 195]. This facilitates recognition of good food patches and pathogenic bacteria.

C. elegans can develop symptoms of sickness (see Figure 5.1) because of pathogenic bacteria [86, 147], or when they are poisoned by toxins [87]. In many cases, it is unclear whether bacteria act as pathogens or secrete toxins simply to decrease predation. *Pseudomonas fluorescens* is not usually considered an animal pathogen (see Figure 1.1 on page 4). The majority of interactions of *Pseudomonas fluorescens*

with nematodes described to date has involved toxins [77, 103, 113], rather than effects of pathogenicity. We will assume *a priori* that any symptoms observed on *C. elegans* are due to toxins secreted for the purpose of deterring predators, rather than pathogenicity [103]. This will have no effect on the analysis of the results, and will only simplify the terminology used in the next few sections. We will overarchingly use the term edibility to describe bacteria which do not have adverse effects on nematode health. *Pseudomonas fluorescens* NZI7 had previously been described as non-pathogenic to *C. elegans* [34], with any growth defects resulting from food avoidance and thus underfeeding, rather than being caused by *P. fl.* NZI7 directly. However, this seems unlikely as *C. elegans* is known to overcome avoidance when starving [196]. In addition recent work suggests that *P. fl.* NZI7 can colonize the nematode gut (Maria Ordovas-Montanes, personal communication). We will investigate pathogenic interactions by exploring the immunocompromised *sek-1* mutant nematode in Section 5.6. The effects of pathogenicity and toxicity operate on different timescales. Toxic effects depend only on the current colocalization of bacteria and nematodes and will take effect as soon as the two meet. Pathogenic effects on the other hand would last longer, possibly even forever (leading to morbidity and possibly mortality), but only after bacteria have been able to establish in the host. Our model at the moment does not monitor nematode health, however, if this variable were introduced, it might be possible to distinguish between the two effects in the model.

It is known that bacteria secrete a range of toxins like HCN and pyrrolnitrin which can repel predators and/or poison them [77, 88, 97]. To investigate toxicity of the different bacterial mutants we will develop different nematode survival assays

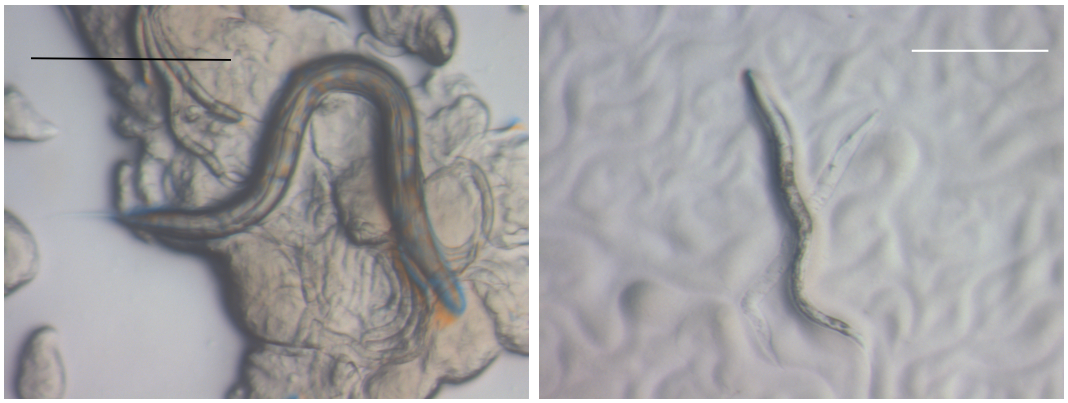

Figure 5.1: Bacteria influence nematode health Healthy (left) and sick (right) Nematode. Both nematodes shown are adults, which have been raised on non-toxic (left) or toxic (right) bacteria. The smaller size and increased transparency are clearly visible. Scale bars are 0.5 mm.

(Sections 5.1.2 and 5.1.3). It has previously been reported that *C. elegans* can learn to avoid pathogenic or toxic bacteria, this process is partially guided by chemotaxis [103, 195]. We will investigate this choice behaviour in the context of *P. fl.* NZI7 and its mutants, and will be able to link it to the toxicity of the bacteria in Section 5.2.3. The importance of chemotaxis will be studied in Section 5.7 both experimentally by using a chemosensation deficient nematode mutant (*che-3*) and *in silico*, using the model constructed in Chapter 3.

Impaired bacterial growth might be beneficial for sustaining nematode populations, as the smaller bacterial numbers will secrete fewer toxins. From the previous chapter we know that the plasmid carrying strains are growth deficient, so we can investigate the effects of bacterial growth on nematode fitness in Section 5.3.1.

As the *C. elegans* strain N2 used in our studies is a lab adapted strain, we will also include a study of the Hawaiian WT strain in Section 5.6, which closely resembles most nematodes isolated from the wild recently in its behaviour [38].

5.1 Measures of Edibility

The edibility of bacteria by nematodes can be characterized in a range of ways, either through measuring nematode health and survival or by looking at the behaviour of the nematodes. In the following we will develop several different measures to characterize bacteria.

5.1.1 Food Choice Assay

Burlinson [91] used a grid assay to screen for more edible *Pseudomonas fluorescens* mutants in a high throughput assay (see Figure 1.9 on page 25). As with most high throughput assays this did not allow for a very quantitative investigation. The nematodes in this assay are placed into such a complex environment that their behaviour is difficult to interpret beyond a qualitative statement. In a much simpler, but less high throughput manner we can use the same idea to give nematodes the choice between two different types of bacteria (see Figure 2.3 on page 74). Using this behavioural assay we can score mutants quantitatively. We observed nematode behaviour for at least 6 hours, and scored bacterial colonies for their occupancy. The chemotaxis index (CI) has previously been proposed as a measure of attraction [139]. It is given by

$$\mathrm{CI} = \frac{\text{worms in mutant colonies} - \text{worms in WT colonies}}{\text{worms on plate}}. \tag{5.1}$$

Chemotaxis vs. Learning

To establish the importance of chemotaxis in the behaviour observed in the food choice assays, we investigate the behaviour of the *che-3* mutant, which is defective in all chemosensation. Full details of the outcome of this investigation will be given in Section 5.7. Here we will use one of the results to help us in our interpretation of food choice assays. During the first hour of the experiment the nematode distribution appears to be entirely random in the *che-3* mutants, while the N2 strain already shows a clear preference for the more edible bacteria (see Figure 5.2). We can thus attribute behaviour during this period to chemotaxis. After 2–3 hours the *che-3* mutant significantly prefers the more edible bacteria. Thus the long term effects are driven by a choice that is independent of chemotaxis. The longer term behaviour is a result of choice and learning, and thus for any observations after more than 1 hour the term choice index is more appropriate. Chemotaxis index and choice index are calculated using the same formula (see Equation (5.1)) and abbreviated to CI on graphs for simplicity.

Investigating the initial attraction behaviour and the time scale over which nematodes learn to prefer more edible bacteria will let us parameterize edibility and initial_attraction for our model through a parameter sweep. We will use the experimental results displayed in Figure 5.2 to estimate these two parameters by using one inedible and one edible strain in our model in the FCA setting. To distinguish between initial_attraction and edibility we need to disable chemotaxis in some of our simulations.

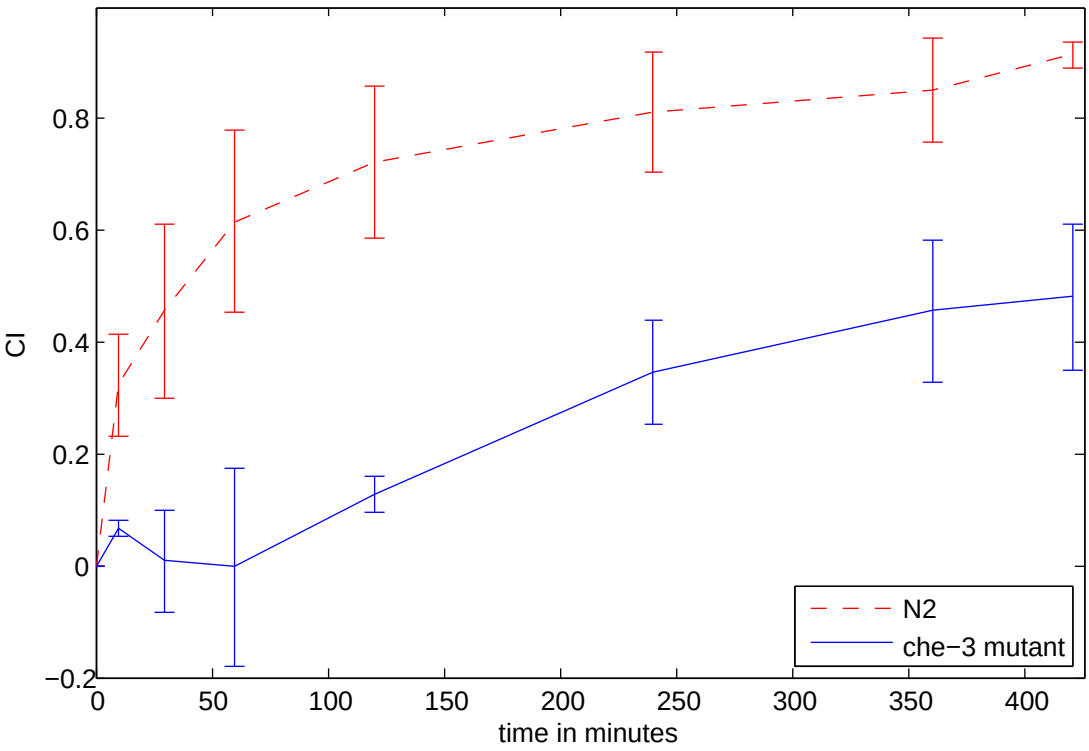

Figure 5.2: Initial response to bacteria is governed by chemotaxis When given the choice between *P. fl.* NZI7 WT and a GacS mutant of *P. fl.* NZI7, nematodes prefer the mutant (positive choice index (CI)). The nematode chemosensation mutant *che-3* (blue) shows a delayed and reduced preference compared to N2 WT (red). Error bars show standard deviation. More than three assays were conducted for each of the two strains.

5.1.2 Nematode Growth Support Assay

Edibility can be measured using a setup similar to the food race experiment described by Hodgkin *et al.* [147]. In this assay we determine how long it takes the founder nematodes and their progeny to consume all of the bacteria on the plate, or alternatively how long the nematodes can resist the toxins produced by the bacteria.

The outcome of this assay is influenced by a range of effects including bacterial growth rate, spreading and the effect the bacteria have on fertility and development. The first we have already determined separately in Chapter 4. The latter two will be investigated separately in a progeny assay.

The score is obtained using the number of weeks taken until the co-culture reaches one of two ends: either the bacteria have efficiently killed all the nematodes, or the nematodes have eaten all of the bacteria available. To convert this observation into a continuous scale, we assign 0 if after two months both species coexist. In any other case the score is obtained from the inverse of the number of weeks taken until only one of the two species can be found on the assay plates, and negative numbers are assigned to all cases where nematodes are killed (see also Chapter 2).

5.1.3 Progeny Assay

In this assay we will count the number of offspring that grow to adulthood as well as the time taken to reach adulthood. This allows us to look at delayed development, as well as effects on fertility. The number of offspring is normalized by the number produced on *E. coli* OP50 during the same interval, to account for fluctuations due to temperature and length of incubation period.

Table 5.1: Edibility scores obtained for the different NZI7 mutants created by Burlinson [91].

Identifier [1]	**CI$_{30\ min}$** [2]	**CI$_{6\ h}$** [3]	**race score** [4]	**progeny score** [5]	**maturation time** [6]
WT	-0.03 ± 0.06	-0.05 ± 0.08	-0.50	0.04 ± 0.06	11
904	-0.02 ± 0.26	0.49 ± 0.08	0.40	0.57 ± 0.06	5
956	0.39 ± 0.27	0.43 ± 0.32	0.57	0.54 ± 0.23	3–5
955	0.26 ± 0.27	0.41 ± 0.40	0.88	0.72 ± 0.02	4
908	-0.06 ± 0.10	-0.02 ± 0.14	0.10	0.46 ± 0.09	7
912	0.23 ± 0.35	0.61 ± 0.13	0.35	0.67 ± 0.01	6
961	-0.03 ± 0.12	0.04 ± 0.23	-0.11	0.02 ± 0.01	10–17
mucoid (mucA)	0.30 ± 0.12	0.59 ± 0.13	1.0	0.70 ± 0.08	4–5
906	0.50 ± 0.12	0.18 ± 0.14	-0.42	0 ± 0	n.a.
FliF	0.10 ± 0.14	0.05 ± 0.09	-0.34	0 ± 0	n.a.
1638	0.20 ± 0.13	0.46 ± 0.40	-0.22	0.13 ± 0.13	11
959	0.12 ± 0.18	0.22 ± 0.20	0.45	0.57 ± 0.05	4–6
HCN	-0.03 ± 0.15	-0.06 ± 0.07	-0.50	0.01 ± 0.02	11
970	0.16 ± 0.13	0.05 ± 0.06	-0.55	0.30 ± 0.25	6
1642	0.15 ± 0.26	0.19 ±0.13	0.93	0.82 ± 0.08	4
954	0.21 ± 0.24	0.34 ± 0.23	-0.45	0.44 ± 0	10

Continued on next page

[1] Numerical identifiers correspond to those given in Table 1.2. Mutants discussed in the text are indicated in bold.

[2] The chemotaxis index describes initial preference (positive score) for the mutant compared to WT. It ranges from -1 to 1

[3] The choice index describes long term (6 hours) preference (positive score) or aversion (negative score) for the mutant, when faced with a choice between it and WT. It is measured on a range from -1 to 1

[4] The race score is the inverse of the time taken for nematodes to consume all the bacteria available (positive score) or be killed by the bacterial toxins (negative score).

[5] The progeny score indicates brood size compared to those obtained on *E. coli* OP50 under the same conditions.

[6] Maturation measures the days taken from egg to adult on the given food source.

Table 5.1 – continued from previous page					
Identifier [1]	**$CI_{30\ min}$** [2]	**$CI_{6\ h}$** [3]	**race score** [4]	**progeny score** [5]	**maturation time** [6]
910	0.54 ± 0.15	0.73 ± 0.04	1.04	0.76 ± 0.15	4
957	0.45 ± 0.10	0.19 ± 0.22	0.54	0.56 ± 0.21	8
964	-0.18 ± 0.45	0.38 ± 0.18	-0.50	0.18 ± 0.18	10
1046	0.39 ± 0.16	0.67 ± 0.07	1.40	0.93 ± 0.18	3
967	0.34 ± 0.26	0.63 ± 0.26	0.52	0.39 ± 0.07	6
chorismate	0.42 ± 0.09	0.43 ± 0.22	0.50	0.21 ± 0.16	6–9
1644	0.41 ± 0.16	0.58 ± 0.20	-0.28	0.30 ± 0.38	6
GacS	0.56 ± 0.16	0.82 ± 0.09	1.75	1.01 ± 0.24	3
963	-0.10 ± 0.10	0.09 ± 0.11	-0.30	0.01 ± 0.02	10
1663	0.14 ± 0.17	0.46 ± 0.41	0.81	0.58 ± 0.05	4
1646	0.13 ± 0.06	0.47 ± 0.12	-0.35	0.41 ± 0.39	6–13
1654	0.20 ± 0.19	0.88 ± 0.10	0.85	0.86 ± 0.11	4
1659	-0.03 ± 0.09	0.34 ± 0.24	-0.54	0.001 ± 0.001	13
1643	0.34 ± 0.34	0.49 ± 0.14	0.74	0.66 ± 0.03	5
969	0.16 ± 0.14	0.15 ± 0.06	0.74	0.49 ± 0.05	5
EDB2	0.07 ± 0.20	0.18 ± 0.24	1.67	0.74 ± 0.05	4
EDB3	0.04 ± 0.09	0.14 ± 0.12	1.17	1.27 ± 0.29	4

Continued on next page

[1] Numerical identifiers correspond to those given in Table 1.2. Mutants discussed in the text are indicated in bold.

[2] The chemotaxis index describes initial preference (positive score) for the mutant compared to WT. It ranges from -1 to 1

[3] The choice index describes long term (6 hours) preference (positive score) or aversion (negative score) for the mutant, when faced with a choice between it and WT. It is measured on a range from -1 to 1

[4] The race score is the inverse of the time taken for nematodes to consume all the bacteria available (positive score) or be killed by the bacterial toxins (negative score).

[5] The progeny score indicates brood size compared to those obtained on *E. coli* OP50 under the same conditions.

[6] Maturation measures the days taken from egg to adult on the given food source.

Table 5.1 – continued from previous page					
Identifier [1]	**$CI_{30\ min}$** [2]	**$CI_{6\ h}$** [3]	**race score** [4]	**progeny score** [5]	**maturation time** [6]
EDB4	0.08 ± 0.13	-0.08 ± 0.29	1.04	0.79 ± 0.03	4
EDB1	0.02 ± 0.21	0.23 ± 0.27	1.00	0.82 ± 0.06	4
916	-0.08 ± 0.14	-0.07 ± 0.14	0.56	0.31 ± 0.23	7
985	-0.07 ± 0.10	-0.10 ± 0.25	0.65	0.63 ± 0.06	7
1639	0.14 ± 0.04	0.28 ± 0.17	-0.45	0.005 ± 0.005	14
1657	-0.01 ± 0.11	-0.01 ± 0.09	-0.54	0.07 ± 0.005	9–11
958	-0.30 ± 0.22	-0.05 ± 0.13	0.081	0.18 ± 0.002	7–10
1655	0.25 ± 0.18	0.51 ± 0.21	-0.30	0.23 ± 0.03	7
1660	0.31 ± 0.23	0.49 ± 0.20	-0.50	0.62 ± 0.12	5–6
PtsP	0.28 ± 0.12	0.71 ± 0.12	-0.44	0.32 ± 0.15	7
918 (GacA?)	0.40 ± 0.10	0.89 ± 0.03	2.33	1.14 ± 0.2	3
965	0.44 ± 0.33	0.55 ± 0.23	1.17	0.79 ± 0.04	4
1048	0.49 ± 0.11	0.56 ± 0.41	1.00	0.94 ± 0.4	4
971	0.58 ± 0.27	0.90 ± 0.10	0.46	0.78 ± 0.06	4
1734	0.35 ± 0.12	0.72 ± 0.12	0.44	0.99 ± 0.07	4
1652	0.42 ± 0.20	0.41 ± 0.25	-0.50	0.25 ± 0.25	7
1664	0.21 ± 0.09	0.29 ± 0.09	-0.37	0.10 ± 0.10	11

Continued on next page

[1] Numerical identifiers correspond to those given in Table 1.2. Mutants discussed in the text are indicated in bold.

[2] The chemotaxis index describes initial preference (positive score) for the mutant compared to WT. It ranges from -1 to 1

[3] The choice index describes long term (6 hours) preference (positive score) or aversion (negative score) for the mutant, when faced with a choice between it and WT. It is measured on a range from -1 to 1

[4] The race score is the inverse of the time taken for nematodes to consume all the bacteria available (positive score) or be killed by the bacterial toxins (negative score).

[5] The progeny score indicates brood size compared to those obtained on *E. coli* OP50 under the same conditions.

[6] Maturation measures the days taken from egg to adult on the given food source.

Table 5.1 – continued from previous page					
Identifier [1]	**$CI_{30\ min}$** [2]	**$CI_{6\ h}$** [3]	**race score** [4]	**progeny score** [5]	**maturation time** [6]
tol	0.45 ± 0.15	0.23 ± 0.10	-0.45	0 ± 0	n.a.
2073	0.00 ± 0.06	0.04 ± 0.06	-0.54	n.t.	n.t.
2074	0.14 ± 0.10	0.20 ± 0.15	-0.33	0.28 ± 0.1	9
2075	-0.05 ± 0.06	0.00 ± 0.06	-0.50	0.30 ± 0.1	6
2076	0.04 ± 0.06	0.05 ± 0.06	-0.41	n.t.	n.t.
2077	0.25 ± 0.14	0.08 ± 0.13	-0.50	0.06 ± 0.06	9
978 (GacS, tol)	0.52 ± 0.19	0.87 ± 0.06	1.75	1.49 ± 0.36	3
989 (GacS)	0.48 ± 0.20	0.88 ± 0.04	1.75	1.16 ± 0.21	3
1003 (GacS, EDB)	0.58 ± 0.18	0.87 ± 0.09	1.75	1.34 ± 0.07	3
1004 (GacS, EDB)	0.66 ± 0.05	0.78 ± 0.29	1.75	1.47 ± 0.11	3
1086 (EDB, HCN)	-0.08 ± 0.09	0.10 ± 0.05	1.00	0.92 ± 0.02	4
double	0.33 ± 0.21	0.63 ± 0.23	-0.16	0.66 ± 0.09	5–6
triple	0.56 ± 0.21	0.84 ± 0.16	1.17	0.89 ± 0.05	4–6
ΔEDB	-0.09 ± 0.13	0.07 ± 0.20	0.86	0.65 ± 0.12	4
2079	-0.19 ± 0.205	-0.25 ± 0.16	-0.50	0.003 ± 0.003	13
2080	-0.13 ± 0.023	-0.15 ± 0.02	0.87	0.25 ± 0.10	5
2083	0.39 ± 0.103	0.87 ± 0.07	1.46	1.05 ± 0.004	4

Continued on next page

[1] Numerical identifiers correspond to those given in Table 1.2. Mutants discussed in the text are indicated in bold.

[2] The chemotaxis index describes initial preference (positive score) for the mutant compared to WT. It ranges from -1 to 1

[3] The choice index describes long term (6 hours) preference (positive score) or aversion (negative score) for the mutant, when faced with a choice between it and WT. It is measured on a range from -1 to 1

[4] The race score is the inverse of the time taken for nematodes to consume all the bacteria available (positive score) or be killed by the bacterial toxins (negative score).

[5] The progeny score indicates brood size compared to those obtained on *E. coli* OP50 under the same conditions.

[6] Maturation measures the days taken from egg to adult on the given food source.

Table 5.1 – continued from previous page					
Identifier [1]	**$CI_{30\ min}$** [2]	**$CI_{6\ h}$** [3]	**race score** [4]	**progeny score** [5]	**maturation time** [6]
2085	0.41	0.45 ± 0.35	1.75	n.t.	n.t.

[1] Numerical identifiers correspond to those given in Table 1.2. Mutants discussed in the text are indicated in bold.

[2] The chemotaxis index describes initial preference (positive score) for the mutant compared to WT. It ranges from -1 to 1

[3] The choice index describes long term (6 hours) preference (positive score) or aversion (negative score) for the mutant, when faced with a choice between it and WT. It is measured on a range from -1 to 1

[4] The race score is the inverse of the time taken for nematodes to consume all the bacteria available (positive score) or be killed by the bacterial toxins (negative score).

[5] The progeny score indicates brood size compared to those obtained on *E. coli* OP50 under the same conditions.

[6] Maturation measures the days taken from egg to adult on the given food source.

5.2 General observations

Before we begin describing the bacterial mutants in detail, we will focus on some general observations, and also describe the *P. fl.* NZI7 WT phenotype.

5.2.1 Worm Clustering

The Hawaiian strain CB4856 is known to cluster when observed under normal conditions. Research suggests that this is due to a measure of stress, which upregulates hyperoxic avoidance [176, 187]. *P. fl.* NZI7 stimulates worm aggregation in the usually solitary N2 as well as in a range of mutants tested (see Figure 5.3). This is consistent with previous observations that aggregation is stimulated in aversive conditions [187]. The most probable driving force is aversion from toxic bacteria, which makes worms favour areas with low bacterial density (usually found at the edge of the assay plate). An uneven distribution of nematodes is also predicted by the model, where we find nematodes favour areas of low bacterial density (see Figure 5.3). This uneven distribution might be enough to drive cluster formation. If nematodes were completely randomly distributed across our model plate, we would expect most sites to be occupied by at most 1 nematode and would expect less than one occurence of more than 6 worms at a single site (see Appendix). However, we find that the average site occupancy is 6 nematodes. In experiments we often observe the formation of small cluster, which may grow over time or dissociate again. Once a cluster has reached a more substantial size (around 25 nematodes) it is usually stable and will grow and migrate. The formation of such larger clusters is always observed in the model, if the plate is at least 90 % covered with bacteria

and at least 300 nematodes are on the plate. In the model as well as in experiments clusters often originate from the edge of the plate. To test whether the formation of aggregates is a result of the edge effect described on page 103, we set the outer ring of the plate to be always free of bacteria. Even in this artificial case we can observe the formation of clusters in the model (see Figure 5.3), though they are now started at interior spots.

We have observed that clusters of nematodes are better able to resist bacterial toxins. This is particularly noticeable on food choice assay plates after several days, where clusters of nematodes have penetrated the less edible bacteria. This strength in larger numbers could originate in a number of different ways: It has been suggested before that the secretion of enzymes could provide a protective mechanism [187]. Alternatively the hyperoxic conditions in the cluster favour the formation of reactive oxygen species (ROS) and could thus have a protective role [282].

Clusters also form in the *daf-22* mutant, indicating that cluster formation probably does not rely on pheromones. Clusters rarely form in the chemosensation mutant *che-3*. This, however, is not surprising as all neurons implicated in social interactions are impaired in this mutant (see Table 1.4 on page 42).

5.2.2 Edibility of *P. fl.* NZI7 WT

All choice assays are conducted relative to WT. When offering only WT bacteria, we observe that nematodes are mainly on areas of the assay plate which are free of bacteria. They might even attempt to leave the assay plate, in which case we can find them on the edge of the petri dish. Those nematodes on bacterial colonies are evenly distributed across the four colonies available. This indicates that there is no

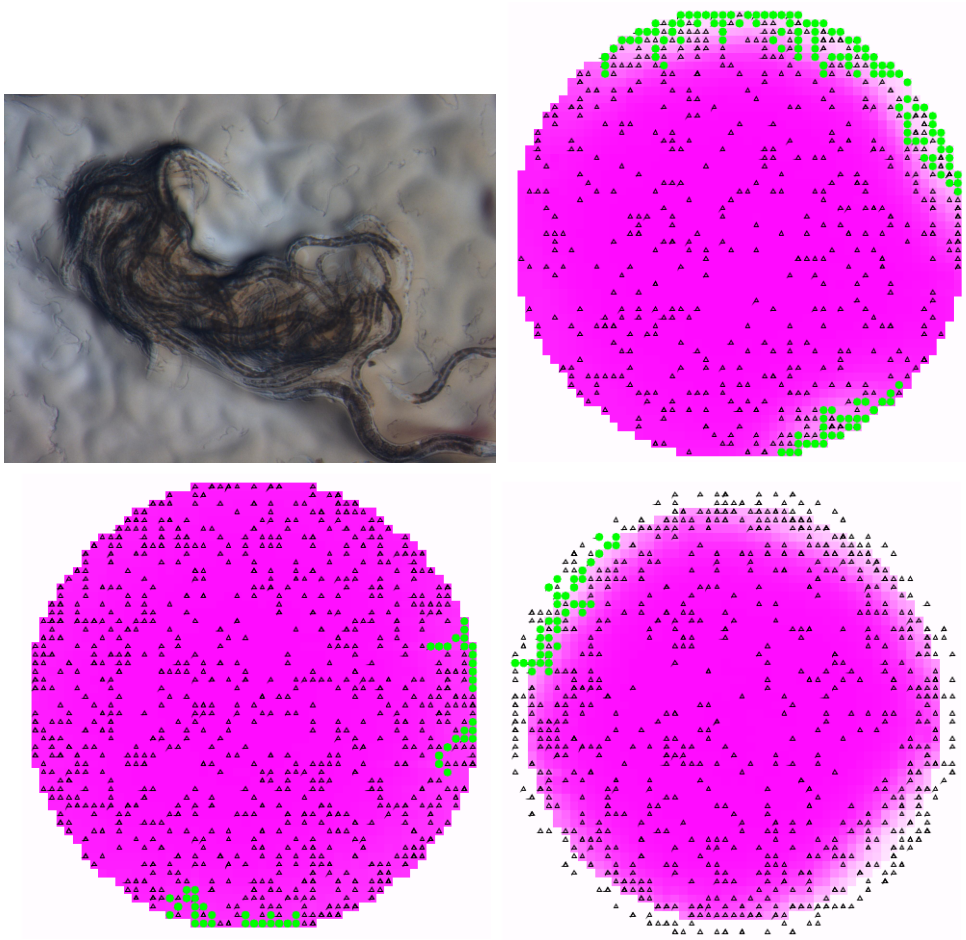

Figure 5.3: Nematode aggregation from left to right and top to bottom: Nematode cluster observed in experiments. An uneven distribution of nematodes is predicted by the model with cluster formation usually starting at the edge of the plate. The model predicts the same behaviour in the Hawaiian nematode. Clusters are still formed, even if the edge effect is reduced (see text). Pink: repellent bacteria. Black triangles: Sites occupied by nematodes. Green star: sites which are part of a cluster with more than 25 nematodes. All model images age taken after 42 simulated hours of the nematode growth support assay setting (see Table 3.10 on page 110). Parameters: attachment_rate: 0.001, 0.0007, 0.0007, deposition_rate: 0.07 (all), edibility: -0.0015, -0.0015, -0.001, initial_attraction: -0.0001 (all). All other parameters are detailed in Chapter 3

inherent bias in our assays. After several days nematodes form clusters at the edge of the bacterial lawn. These clusters slowly move through the bacterial lawn and consume all the bacteria available. Over time, as nematode numbers increase, all bacteria on the plate are consumed.

The long term edibility assays (nematode growth support and progeny assays) paint a completely different picture of the interaction. Nematodes show many symptoms of sickness (see Figure 5.1) including:

- delayed development,
- increased transparency due to osmotic stress,
- short,
- extended gut lumen,
- sterility,
- slowed movement,
- Dar phenotype (Figure 1.11).

Premature death, low fertility and attempts to leave the petri dish cause nematodes to become extinct usually within 2 weeks.

To explore the cause of the large difference in the two assays we inoculated nematode growth support assays with larger numbers of nematodes, but this did not change the outcome. Therefore we hypothesise that this difference is due to bacteria-free areas. Plates used for progeny assays are fully covered with bacteria before inoculation with nematodes. The small (55 mm) plates used for nematode growth support assays are fully covered with bacteria after two days through the dispersal action of the nematodes. The larger plates used for choice assays (90 mm) do not get completely covered for many days, leaving bacteria free areas on which

nematodes can escape from the toxins. We observed that nematodes on the larger plates show fewer symptoms of sickness and remain fertile. This means that nematode numbers can increase enough to initiate cluster formation. Clusters are usually formed on the boundary between bacteria free areas and the bacterial lawn. The dose effect responsible for this phenomenon could be captured in a model that includes a nematode health variable.

To prevent starvation, nematodes will return to toxic bacteria if there is no other food available [196]. Observing the behaviour of nematodes on *P. fl.* NZI7 WT bacteria helps us to define the model parameter starvation_attraction.

5.2.3 Interassay Correlation

Using the edible mutants identified by Burlinson [91] as well as some other selected mutants, we determined edibility using the assays described above (see Table 5.1). Figure 5.4 displays the relationships of the different scores with each other. We can see that all the long term assays (measuring edibility) correlate well with each other, highlighting that the bacteria affect the health of the nematode in multiple ways, as also indicated by the large range of symptoms observed. The two short term assays (measuring choice) also correlate with each other indicating a strong importance of initial attraction. However the two groups of assays do not correlate very well (as indicated by the red frames). We know that choice is not always linked to bacterial edibility from experiments performed on *Serratia* [172]. While this is initially surprising, as we would expect very strong selective pressure on nematodes to quickly choose the correct food, it is difficult to extrapolate to more complex settings, where there are many different types of bacteria to distinguish between.

It appears that a slow learning does take place, as nematode choice (measured after 6 hours) correlates better with bacterial edibility than chemotaxis (measured after 30 minutes), which indicates that nematodes learn about bacterial edibility and adapt their choice within less than 6 hours. However the observed differences are not statistically significant (one tailed test after Fisher's z-transformation yields p between 0.2 and 0.25 for the three different comparisons). To obtain statistically significant results the mutant screen would have to be extended to nearly 200 bacterial mutants, assuming that the relationships remain the same. It also possible that more time is required for nematodes to learn enough to choose the most edible food, however, dispersal of bacteria makes it difficult to quantify choice after 24 hours or more.

The small correlation between short and long term assays makes it clear that it is necessary to distinguish between attraction and edibility of bacteria. Attraction may be desirable for the bacteria, as nematodes will come in contact with the colony and thus allow bacteria to attach to the cuticle and be dispersed. On the other hand, edibility will not be a desirable property, as it allows nematodes to reproduce, thus increasing predation.

5.3 Phenotypes of Selected Mutants

In this section we will further examine some of the bacterial mutants. Firstly we shall explore whether bacteria tagged with fluorescent or luminescent markers have a phenotype in these assays. Next we shall investigate the relationship between the known toxins HCN, tolaasin and EDB. We will also look at mutants which have

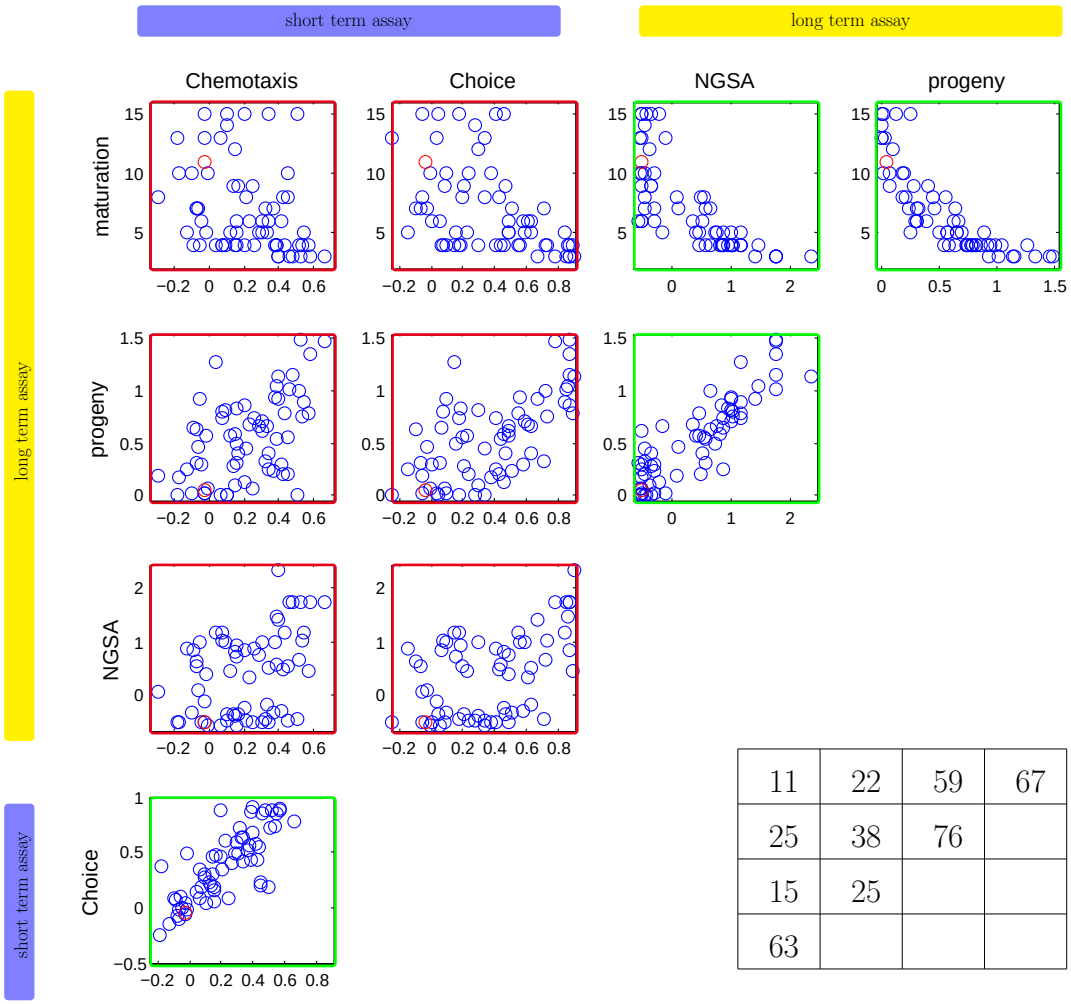

11	22	59	67
25	38	76	
15	25		
63			

Figure 5.4: Long and Short term assays measure different aspects of edibility Each circle represents the mean score for each mutant. The red circle indicates the WT. The different measures of edibility are described in Table 5.1. Red frames indicate values of R^2 below 41 % and green frames indicate values above 57 %.

Inset: the R^2 values for each relationship in a linear regression model.

Chemotaxis: Chemotaxis index observed after 30 min in the FCA. Choice: Choice index observed after 6 h in the FCA. NGSA: The food race score observed in the NGSA is measured in 1/weeks. Progeny: number of progeny observed normalized to the number of progeny produced on *E. coli* OP50. Maturation: time taken from egg to gravid adult in days.

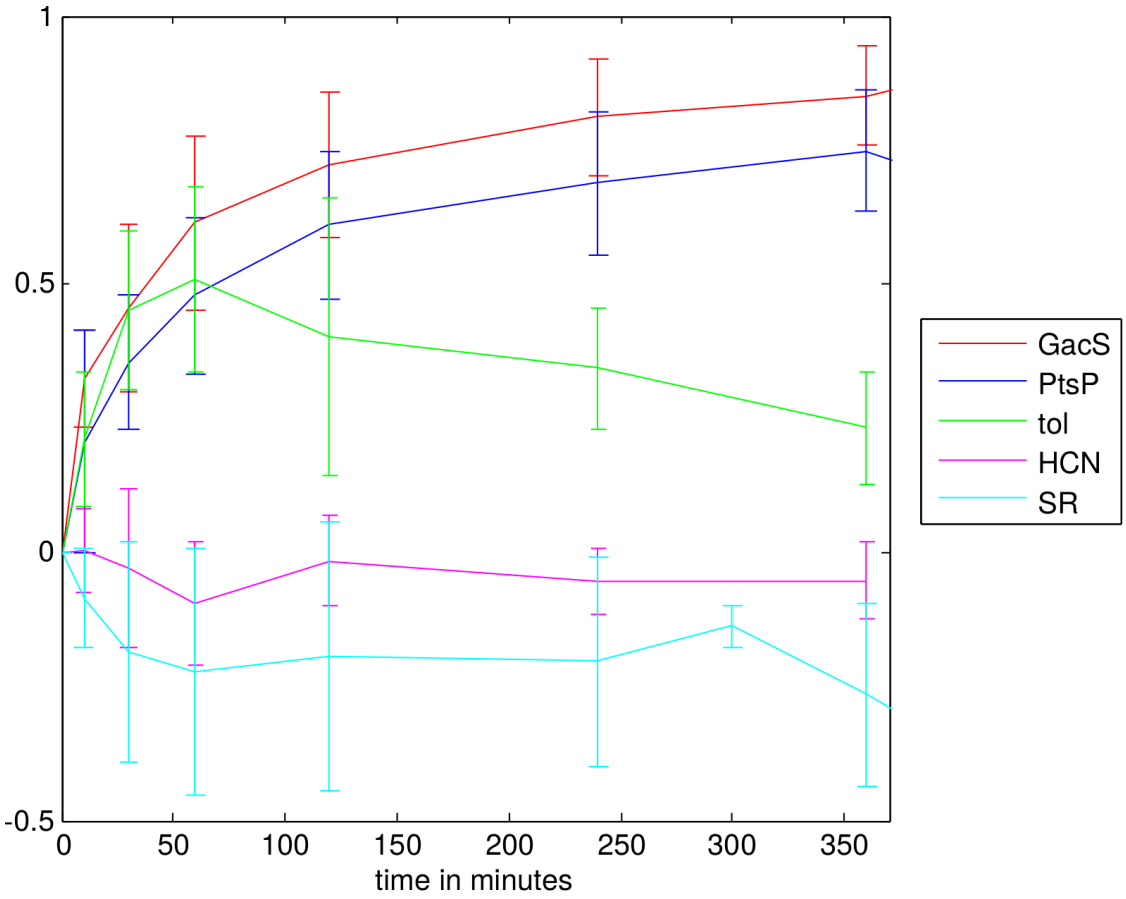

Figure 5.5: Early preference and learning The temporal development of the choice index relative to WT for selected mutants. The inedible but attractive PtsP mutant is as attractive as the GacS mutant during the observational period. The tolaasin mutant is attractive, but nematodes learn to avoid it during the observational period. Repellent mutants, like the HCN mutant are repellent throughout the observational period. The SR mutant (super-repellent, miniTn7 insertion of GFP in WT) is described in Section 5.3.1. Error bars represent standard deviation, each line represents an average of at least three experiments.

large spreads in one of the observed scores and investigate those mutants, which are particularly far from the 'edibility favours choice' hypothesis. For the latter, we will consult the Choice Index at 6 hours and the race score and will pick the top representatives in each corner.

5.3.1 Tagged Strains

Plasmid bearing strains In the previous chapter we identified plasmid bearing strains as being severely growth deficient. The assays conducted in this chapter also show that they are very edible and attractive. This might be a direct result of the growth impairment, as fewer bacteria will secrete less toxins and repellents. As a consequence we will not be able to use plasmid tagged strains to investigate bacterial spreading.

The super-repellent strain In order to investigate bacterial spreading, we attempted to introduce a fluorescent reporter into the bacteria. In Chapter 4 we discovered that plasmids decrease bacterial growth significantly, which, as noted above, significantly increases the edibility of the bacteria. A chromosomal insertion at the att:Tn7 site did not pose the same problems, but, we noticed that this mutant was more repellent towards *C. elegans* than WT. In choice assays we observe a clear avoidance of this strain (see Figures 5.5 and 5.7).

The insertion at the att:Tn7 site next to the GlmS gene in the chromosome could be confirmed by PCR (performed by Caroline Stone). Further analysis of the surrounding genome reveals a gene that has a possible association with a type VI secretion system (see Figure 5.6). The insertion might thus interfere with type VI secretion.

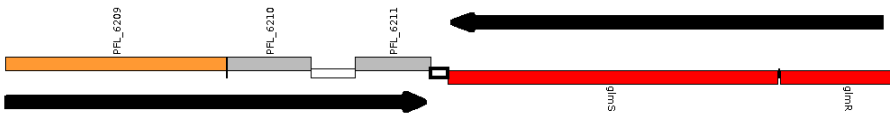

Figure 5.6: Att:Tn7 site in Pf5 From left to right: a PAAR motif containing protein, that could be involved in Type VI secretion (orange). Two unknown hypothetical proteins (grey). The intragenic region containing the Att:Tn7 insertion site (thick line). An operon of two cytoplasmic genes GlmS and GlmR (red). Arrows indicate direction of transcription. Bases 7 051 544 – 7 051 636 are shown.

The increased repellence is noticeable at short timescales (up to 8 hours) particularly through the creation of a more noticeable repellence zone, but also through a negative choice index (see Figures 5.5 and 5.7).

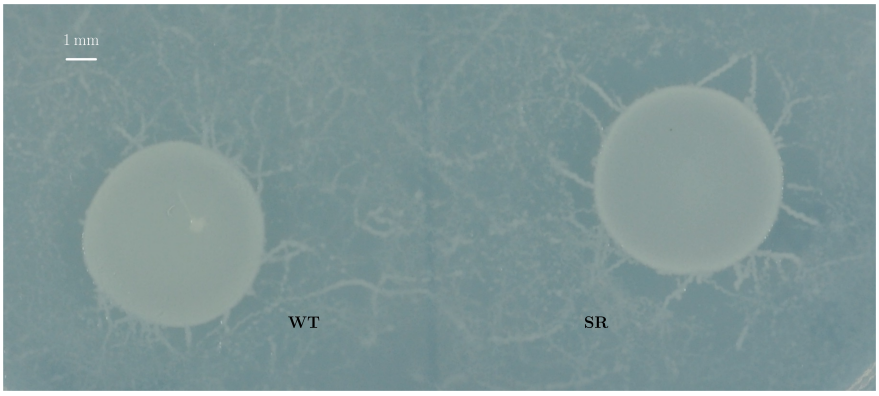

Figure 5.7: Zone of high repellence around super-repellent strain. Wild type (WT) and Tn7:RFP tagged WT (SR) on the same assay plate. The clear zone around the super-repellent strain indicates the area which nematodes avoid. Image taken 24 hours after inoculation with nematode strain N2.

We can also observe long term effects in the food choice assay: on every other one of the plates used for choice index determination the nematodes eradicate all bacterial strains within less than two weeks, first clearing the more edible strain, after which the increased nematode numbers allows the formation of clusters which can fully consume the less edible (usually the WT) strain. However on plates containing

the wild type and the super-repellent strain, only the WT is consumed. Clusters do form on these plates during the first week. After there are no WT bacteria left, these clusters travel towards the super-repellent strain, where the clusters disperse and the nematodes die, leaving the original colonies almost untouched. These effects are not noticeable in any of the other assays measuring edibility. Due to the plate size effect described earlier (page 159) the WT scores are so low that the SR strains cannot score significantly lower.

Thus, an insertion at the previously supposed neutral att:Tn7 site alters the short and long term interactions between NZI7 and *C. elegans*. We have observed this behaviour on strains carrying any of CFP, YFP and RFP instead of the GFP marker. We can be fairly certain that it is not due to the fluorescent marker, as the miniTn5 transposon used also carries a GFP. To verify this further, more insertions at the att:Tn7 site must be made using different transposons with different antibiotic markers.

So far we have not been able to identify the cause of the altered interaction. In a collaboration with Souvik Kusari we have searched for an altered chemical profile using tandem mass spectrometry (MS/MS), but nothing could be identified (data not shown).

An insertion mutant was also created using an EDB mutant. This mutant shows the same short term behaviour as the super-repellent strain described above, but behaves like an EDB mutant in edibility assays. We will describe it further in Section 5.3.4.

The insertion at the att:Tn7 site in a GacS mutant (provided by Michael Bentley) reveals that superrepellence is GacS dependent, as the GacS mutant and the

miniTn7-tagged GacS mutant behave identically in all of the assays (data not shown).

For the rest of this thesis we will refer to the miniTn7 tagged strain as SR - super-repellent, unless otherwise stated it will refer to the WT tagged with GFP, but all other tags yield identical results (data not shown).

5.3.2 Known toxins: tolaasin, HCN and EDB

The scores obtained for the mutants of the three known toxins tolaasin, EDB and HCN as well as double and triple mutants are found in Table 5.2.

Burlinson [91] identified the EDB cluster as a very important factor in influencing bacterial edibility. All of our long term assays confirm that EDB mutants are more edible. However, we only observe a weak attraction to this mutant in behavioural assays. The choice index is not significantly above 0 during the first 6 hours of observation and only a small preference can be observed after 24 hours (data not shown). In particular the chemotaxis index suggests that the colony initially chosen by a nematode is random. This could indicate that the two available strains are identical in their long range chemical profile. Which is further supported by the fact that MS/MS analysis of a WT and EDB mutant strain conducted by Souvik Kusari did not show any difference in chemical profile between the two strains. The large standard deviation observed for the CI suggests that these stochastic effects are very important. The data supports the hypothesis that the colony initially chosen by the nematode influences it in the longer term, as there is a correlation between the chemotaxis index and the choice index in individual experiments (Pearson's coefficient 0.5). EDB is a very important factor in the interaction, as knock out

of EDB allows nematodes to thrive on the bacteria. However the EDB mutant is not very attractive and we have observed that nematodes show some symptoms of sickness. This indicates that other factors are involved in the interaction as well.

Tolaasin is an important factor of mushroom pathogenicity. Tolaasin or tolaasin-like compounds are secreted by many mushroom pathogenic pseudomonads. Due to its action as a surfactant it could also act as a nematode repellent like serrawettin [153]. In grid screens nematodes show an early preference for tolaasin deficient mutants (see Figure 5.10 on page 176). This can also be confirmed in our attraction assays, which indicate an early preference for tolaasin mutants as well as a later aversion, as nematodes learn that the tolaasin mutant is not more edible than WT (see Figure 5.5). The tolaasin mutant does not behave significantly different from WT in edibility assays, and we can thus conclude that tolaasin is not a nematode toxin.

We expected mutants of the cyanide synthesis genes to be at most a little more edible than WT, as the cytotoxin is only weakly expressed in the given conditions. Loss of this pathway might slightly enhance nematode survival in our assays, but could also have no noticeable effect. We did not expect to find mutants less edible or attractive than WT, though a more thorough investigation is necessary to verify the significance of these results. Increased repellence was observed through the behaviour in choice assays as well as in grid screens (see Figure 5.10). A complete lack of surviving offspring in most progeny assays might indicate decreased edibility. We believe that this is due to pleiotropic effects of cyanide synthesis. Cyanide synthesis is costly not just due to the resources required to produce the toxin, but also because of the adverse effects on the producing organism. In Chapter 4 we

Table 5.2: Edibility measures for mutants in known toxins.

Measure [1]	WT	tol	EDB [2]	HCN	1086 [4]	double	triple	GacS [3]
Chemotaxis	-0.03	0.45	0.024	-0.03	-0.08	0.33	0.56	0.52
Choice	-0.05	0.23	0.108	-0.06	0.1	0.63	0.84	0.85
NGSA	-0.5	-0.45	1.245	-0.5	1	-0.16	1.17	1.75
progeny	0.044	0.2	0.853	0.01	0.92	0.66	0.89	1.08
maturation	11	10	4	15	4	5	5	3

[1] Scores are described in the text and in Figure 5.4.
[2] average of mutants EDB1, EDB2, EDB3, EDB4 and the EDB complete deletion
[3] average of GacS insertion and deletion mutants
[4] double mutant of cyanide and EDB

found a significant increase in growth rate in the HCN mutant compared to WT. This might account for more production of other toxins (e.g. EDB or tol) and thus explain the decreased edibility. It is also possible that cyanide itself acts as a negative regulator for other toxins to ensure a constant total amount of toxins which is enough to deter predators without requiring more than the necessary amount of resources. Thus lack of cyanide production could result in an increase in production of other toxins to compensate. A similar effect is observed with the toxins DAPG (2,4-diacetylphloroglucinol) and PLT (pyoluteorin) in CHA0 [103].

The double mutant of cyanide and tolaasin is more attractive than either of the two individual mutants and more edible. This observation combined with the increased repellence observed in the single HCN mutant in the last paragraph, suggests that HCN and tol synthesis may be inversely linked to each other.

The triple mutant of these three toxins can be considered the sum of the double mutant and the EDB mutant (see Figure 5.4). Nematodes raised on the triple mutant as sole food source still show some signs of sickness, indicating that these three toxins are not the only ones involved in nematode–bacteria interactions. We will be able to confirm this by studying the GacS mutant in the next section.

5.3.3 GacS

It appears that all toxic and repellent factors produced by NZI7 are GacS regulated. Nematodes feeding solely on the GacS mutant of *P. fl.* NZI7 show no sign of sickness. This is consistent with observations of GacS mutants in other bacterial strains like DSS73 [47], where the mutant has been described as very edible and accelerating nematode development. We can confirm both of these observations here by the shortened maturation time (3 days compared to 4 days on the standard laboratory food *E. coli* OP50) and the high food race score. While the triple knockout mutant of EDB, tol and HCN is as attractive as the GacS mutant, it is not as edible, indicating that there are other toxins than those known.

5.3.4 Edibility and Attraction are not always linked

PtsP The PtsP mutants (PFL_5899) show the least correlation between attraction and edibility. They are very attractive but barely more edible than the WT. Of the two mutants the one with the identifier 1653 is the more extreme, thus we will use that in our further investigations.

PtsP - Phosphotransferase - encodes the enzyme EI^{Ntr}, which along with EII^{Ntr} and HPr is part of nitrogen regulation in the cell [116,283]. This phosphotransferase system is closely linked with the paralogous system controlling carbon catabolism [283, 284] and is thus important for energy flux in the cell.

The most prominent phenotype of a PtsP defect is an imbalance in carbon and nitrogen metabolism, but a PtsP defect can also influence virulence factors, the ability of the organism to compete with others as well as biofilm formation [285–287].

Notably, in *P. aeruginosa* PtsP defect pleiotropically induces greater production of pyocyanin [288].

The imbalance in carbon and nitrogen metabolism could result in a reduced production of repellent factors, or a production of highly attractive molecules, which are not usually secreted by *P. fl.* NZI7. This would account for an increased attraction without increased edibility. Additionally we noticed in Chapter 4 that the mutant shows slightly enhanced growth, which could lead to a higher production of toxins.

In conclusion, an imbalance in metabolism might account for a decreased production of repellence factors as well as toxins and pathogenicity factors. However, pleiotropic effects and/or the enhanced growth can compensate for this increase in edibility, but apparently not for the increased attraction. A more detailed analysis of the chemical profile of this mutant is necessary to determine the exact mechanism underlying the altered attraction. This could also reveal further repellent factors.

The temporal development of the choice index (see Figure 5.5) highlights the great attraction of the strain, and also shows that even after 6 hours nematodes have not learned to avoid this mutant. However, after 24 hours nematodes are found mainly away from the bacterial colonies, consistent with observations made on other inedible mutants.

Super-repellent EDB After observing the superrepellence effect of WT strains tagged at the Tn7 site, it is clear that the most repellent but edible strain will contain a miniTn7 insertion in an edible mutant. This is exemplified by the EDB mutant with an RFP insertion at the Tn7 site. While this mutant is able to support nematode growth similar to the EDB mutant, it is clearly rejected by nematodes

when given WT as an alternative option, which is less edible, but also less repellent. This remains true even after three days (data not shown), which means that nematodes never learn to prefer the edible mutant in this scenario. The nematode behaviour observed in choice assays including the super-repellent EDB mutant is not accurately described by the model, where we see that edibility will dominate over attraction (as seen for example in Figure 5.14). This indicates that innate aversion and attraction, which can be measured in chemotaxis assays, and learned aversion and attraction, which influence long term behaviour, operate through different pathways, as the same pathway approach used in the model cannot describe this phenomenon accurately.

5.3.5 Stochastic Effects

A large variance in a score indicates a high importance of statistical fluctuations. On rare occasions nematode clusters can form in nematode growth support assays even on the WT bacterial strain. These usually nucleate on impurities in the agar, contaminations or spontaneous Gac mutations. The clusters, if they persist, can travel across the entire plate and consume the whole bacterial population. In Food Choice Assays, some mutants cause an alteration in the time scale over which nematodes learn to avoid the bacteria. If this time scale falls near the time point of observation, we will see a large variance.

A large standard deviation is particularly noticeable in the chemotaxis index ($CI_{30\ min}$), indicating that chemotaxis is not a strong effect. Only the most attractive strains of the ones tested show a score significantly different from 0 in this assay. These include all of the GacS mutants and all of the tolaasin mutants as well as the WT

strains which bear a plasmid.

5.3.6 WT-like mutants

In the next chapter we will wish to make use of the luminescence property of the mutants due to the insertion of a *lux* cassette on the miniTn5 transposon. This will allow us to monitor bacterial spreading. However, as we have failed to neutrally tag the WT with a *lux* cassette, we decided to find mutants carrying a miniTn5 transposon in a neutral site. In the previous chapter we identified several such mutants which show WT like growth. We note here that none of them seem to have any phenotypes in nematode interaction assays.

Using Tail PCR we have obtained sequence information for one of the mutants (2075). The insertion of the miniTn5 transposon appears to be in an intragenic region. In *P. protegens* Pf5 it is located near base 95004 which is found in an intragenic region between PFL_0094 and PFL_0095.

5.4 Volatility Assays

To determine whether the important chemicals are water soluble and diffusing through the agar, or whether they are volatile and sensed through the air, we conducted three different volatility assays. In none of these assays did we find any evidence that volatile compounds secreted by *P. fl.* NZI7 play any role in determining food choice in *C. elegans* (data not shown). This is contrary to many reports which exist on nematodes responding to volatile organic compounds [54, 289]. It might be

possible that volatile substances diffuse too quickly through the air to establish a gradient in the small scale experiments we have conducted, and thus volatile substances do not influence behaviour. This does not exclude the possibility of volatiles affecting nematode health in longer term studies as has been previously observed with cyanide [77]. Similarly pyrrolnitrin secreted by the *Pseudomonas chlororaphis* strain PA23 is suspected to have an effect as a volatile on the long term nematode behaviour [77]. It is probable that the assays we used are not refined enough to detect the effects of volatile compounds on nematode behaviour, but they do suggest that the effects are not very strong. To investigate the effect of volatiles more thoroughly better methods to expose nematodes to the relevant volatiles or absorb them from the system have to be developed, this could be done by using a maze setup [290].

5.5 An Overall Edibility Score

We have used different assays to investigate the edibility of the mutants selected for this study. In each of the assays we have found that the mutants span a large range, which is densely covered. In order to link edibility to any other phenotype and especially spreading efficiency it would be advantageous to generate an overall edibility score for each mutant. The low correlation between the scores obtained by the different assays makes it necessary to include all values in this overall score. However, we do not have any knowledge of how each of them should be weighted, and thus an overall score of edibility cannot be constructed from these results. Nonetheless, we can select some of those strains for further analysis, which show a

correlation in all measures of edibility and can thus be ranked unambiguously. In addition we choose two mutants with a negative correlation between choice index and race score, to determine whether long or short term effects are more important for spreading. The mutants selected are:

- GacS (913) - the most edible strain by any measure,
- the triple mutant of tol, HCN and EDB,
- chorismate mutant (921),
- WT,
- SR - more repellent than WT,
- EDB (917) - is repellent in the short term but edible in the long term,
- double mutant tol and HCN - is attractive in the short term but not edible in the long term,
- PtsP - is very attractive in the short term but not edible in the long term.

All of these mutants are highlighted in Figure 5.8.

5.6 Nematode Variants

In this section we will investigate the mechanisms governing nematode behaviour which are essential in the observed nematode–bacteria interactions. For this purpose we have selected some nematode genotypes which might have phenotypes in the edibility assays (see also Table 2.1:

- diminished olfaction: Hawaiian, *che-3*
- increased pathogen susceptibility: Hawaiian, *daf-16*, *sek-1*
- impaired learning: *daf-22*, octopamine pathway (*tyra-3* and *ser-3*)

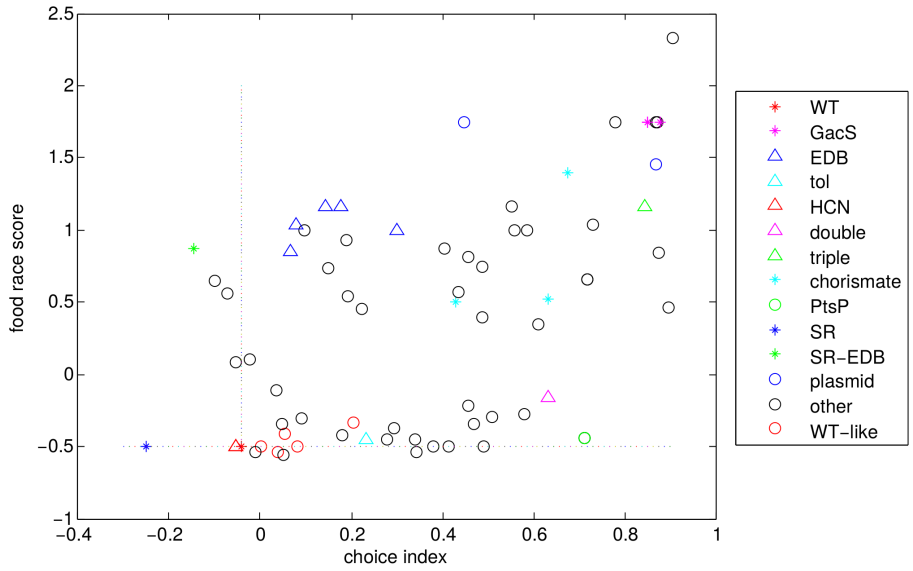

Figure 5.8: Choice versus Edibility The relationship between the ability to support nematode growth (y-axis) and attractiveness (CI on the x-axis). Each symbol represents one bacterial mutant. The choice index is computed after 6 hours as described in Equation (5.1). The food race score is described in Section 2.1.4. Each of the mutants/mutant groups selected for further study is highlighted. SR - super-repellent, plasmid - WT bearing one of the plasmids, WT-like - mutants with no observed phenotype to date (see Section 5.3.6), other - all mutants listed in Table 1.2 which are not highlighted.

WT	mucoid	chorismate	1654	triple	HCN
tol	1086	2076	EDB1	2076	EDB2
mucoid	double	WT	967	chorismate	1086
chorismate	WT	triple	tol	HCN	2076
EDB1	HCN	WT	EDB2	1654	967
1654	tol	1654	mucoid	double	WT
double	967	chorismate	967	tol	EDB1
triple	2076	EDB2	1086	double	HCN

Figure 5.9: Template used in the grid screen for screening nematode variants for altered interaction with the bacterial mutants. Bacteria were inoculated onto a 90 mm NGM plate (see Figure 2.4) and nematodes were released on the left and right side of the grid. 967 is an alternative mutant of chorismate synthase, 1086 is the double mutant of EDB and HCN, 1654 is a severely growth deficient mutant and 2076 is a WT like mutant.

strain	EDB2	double	1015	2076	WT	967	mucA	choris	1086	EDB1	triple	tol	1654
Daf-22	0	0	0	0.03	0	0	0	0.04	0	0.00	0.05	0.06	0.82
Che-3	0	0	0	0.00	0	0	0.00	0.00	0.10	0.46	0	0.00	0.44
Daf-16	0.00	0.00	0.00	0.00	0.04	0.00	0.00	0.00	0.00	0.00	0.12	0.38	0.46
O	0.00	0	0.00	0.00	0.00	0.02	0.03	0.01	0.00	0.00	0.19	0.15	0.60
CB4856	0.00	0.01	0.02	0.00	0.00	0.01	0.01	0.00	0.00	0.00	0.14	0.16	0.66
Sek-1	0.00	0.03	0.00	0.00	0.02	0.04	0.00	0.08	0.05	0.01	0.05	0.09	0.62
N2	0.00	0.00	0.02	0.01	0.01	0.03	0.09	0.02	0.00	0.00	0.18	0.18	0.46

strain	2076	WT	EDB2	HCN	double	967	1086	choris	EDB1	tol	triple	mucA	1654
Sek-1	0.00	0.00	0.00	0.00	0.00	0.00	0.04	0.00	0.22	0.00	0.00	0.00	0.74
Daf-22	0	0	0	0	0	0	0	0	0	0.14	0.00	0.53	0.33
Daf-16	0.00	0.00	0.00	0.01	0.00	0.00	0.00	0.03	0.00	0.05	0.08	0.03	0.81
Che-3	0	0.00	0.01	0.02	0.01	0.01	0.00	0.00	0.00	0.09	0.14	0.02	0.70
CB4856	0.00	0.00	0.01	0.02	0.01	0.02	0.00	0.01	0.00	0.11	0.15	0.13	0.53
O	0.00	0	0.00	0.00	0.00	0.01	0.00	0.02	0.00	0.15	0.23	0.16	0.42
N2	0.01	0.02	0.01	0.01	0.04	0.05	0.07	0.07	0.01	0.15	0.12	0.10	0.35

strain	HCN	2076	1086	WT	EDB2	EDB1	967	double	choris	tol	triple	mucA	1654
Daf-22	0	0	0	0	0	0	0	0	0	0.05	0.19	0.38	0.38
Che-3	0	0	0	0.10	0	0	0.06	0.18	0.12	0	0	0.16	0.37
Daf-16	0.06	0.19	0.09	0.06	0.07	0.05	0.06	0.04	0.05	0.19	0.05	0	0.08
O	0.01	0	0.05	0.01	0.06	0.06	0.05	0.04	0.05	0.12	0.18	0.18	0.19
CB4856	0.02	0.01	0.05	0.01	0.05	0.07	0.03	0.03	0.13	0.04	0.15	0.21	0.21
Sek-1	0.06	0.03	0.02	0.06	0.02	0.04	0.10	0.05	0.11	0.11	0.13	0.07	0.22
N2	0.02	0.02	0.05	0.01	0.08	0.07	0.07	0.05	0.05	0.07	0.17	0.15	0.18

strain	HCN	2076	WT	tol	choris	double	1086	967	EDB2	EDB1	triple	1654	mucA
Daf-16	0.00	0.00	0.00	0.00	0.00	0.00	0.00	0.00	0.00	0.00	0.00	0.27	0.73
Che-3	0	0	0	0.00	0	0	0.00	0.06	0.00	0	0	0.19	0.75
Sek-1	0.00	0.00	0.00	0.00	0.00	0.00	0.00	0.00	0.00	0.00	0.14	0.43	0.43
Daf-22	0	0	0	0	0	0.03	0	0	0	0.00	0.20	0.44	0.33
CB4856	0.00	0.00	0.00	0.02	0.02	0.05	0.06	0.02	0.06	0.07	0.19	0.18	0.34
O	0.00	0	0.02	0.03	0.04	0.03	0.07	0.05	0.12	0.10	0.13	0.12	0.29
N2	0.01	0.01	0.01	0.06	0.07	0.06	0.07	0.08	0.07	0.09	0.15	0.15	0.17

Figure 5.10: Predation scores for different nematode genotypes Scores obtained from the initial nematode screen for each of the first four days of the assay (top to bottom). Scores can range from 0 (red - complete avoidance) to 1 (green - bacteria completely depleted), with larger scores indicating greater preference. Bacterial mutants are sorted by total preference. Nematode variants are sorted by selectivity (see text). choris = chorismate. O represents the pooled scores of two octopamine pathway nematode mutants *tyra-3* and *ser-3*, there is no variation between the two strains (data not shown). 967 is an alternative mutant of chorismate synthase, 1086 is the double mutant of EDB and HCN, 1654 is a severely growth deficient mutant and 2076 is a WT like mutant.

As a preliminary screen we observed all these variants on the same grid (see Figure 5.9). The grid was designed to contain representatives from the list above as well as WT and a growth deficient strain (1654). The GacS mutant was omitted from this screen, as its high attraction of nematodes will obscure any other effects and will increase the chances of false positives in the neighbouring colonies. Each mutant is included several times to exclude effects of the assay geometry. As those colonies closest to the left and right edge will be encountered first by the nematodes, they could mask more edible strains in the interior parts of the plate, therefore we ensure that each strain is represented along this edge.

Students enrolled on the DTC Oxford experimental techniques course inoculated the plates with nematodes and estimated their initial number. Afterwards all plates were photographed daily and each colony was scored for depletion by nematodes. After 2 days the assay plates are completely covered with a bacterial lawn, but the original colonies are still recognizable as they are much more densely populated. Only these original colonies are considered in the scores. Colonies were independently scored for nematode presence by students of the course. For each plate, scores were averaged across the repeats of the bacteria and then divided by the total score obtained for the plate. The latter adjusts for differences due to initial nematode numbers and observational bias between the different people scoring the plates. The predation scores are summarized in Figure 5.10.

The bacterial mutants are sorted from least favoured to most favoured for each day. In the previous assays we had already observed that the HCN mutant appears to be less edible than WT. In this screen, we can again observe that its edibility is below that of the WT strain and the WT-like mutant. The screen also confirms the high

edibility of the growth deficient strain 1654, the mucoid mucA mutant and the triple mutant HCN, EDB and tol.

The *sek-1* mutant did not survive for long on the assay plate, and only consumed the most edible bacterial mutants. All other strains display good population growth. To identify nematode variants with altered behaviour, we will look at the selectivity they display towards the different bacterial mutants offered. For each nematode variant we define selectivity as the difference in the predation scores between the largest and smallest score, divided by the number of non-zero scores. This selectivity score can range from 0 (no selection) to 1 (very selective). Many of the scores we obtain are below 0.1, including the N2 reference strain. The maximum score we see in our data is 0.36 for the *daf-16* strain on day 4. The nematode variants have been sorted from most to least selective for each day. The *daf-22*, *daf-16* and the *che-3* mutants appear to show greater selectivity than the other mutants. None of the variants display reduced selectivity compared to the N2 reference strain. We did not observe any phenotype for the mutants of the octopamine pathway in this assay. As we do not expect to see a phenotype for these mutants in any of the other assays, they will not be included in further studies. All remaining mutants are tested in food choice assays and nematode growth support assays with some selected bacteria.

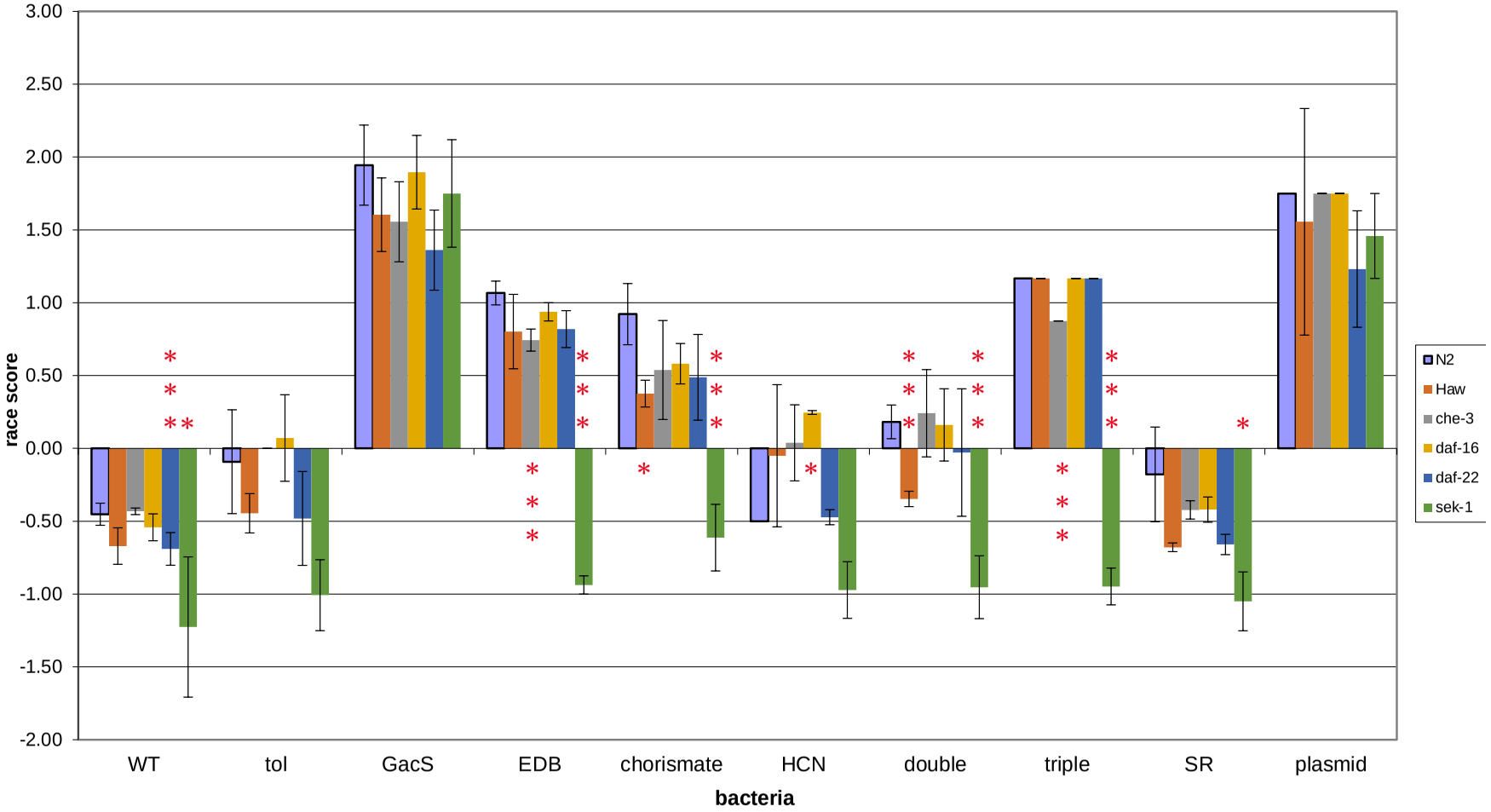

Figure 5.11: Effect of nematode genotype on food race scores Six different nematode genotypes were scored for survival on selected bacterial mutants of *P. fl.* NZI7. The race score is defined in Section 5.1.2. Positive scores indicate good nematode growth, while negative scores indicate that nematodes are killed. SR - WT with miniTn7:GFP insertion, plasmid: WT carrying a *lux* plasmid. Error bars show standard deviation. Scores which are significantly different from WT after application of a Sidak correction are indicated by one to three red * (p= 0.05, p= 0.01, p= 0.005 respectively). Each assay was repeated at least three times.

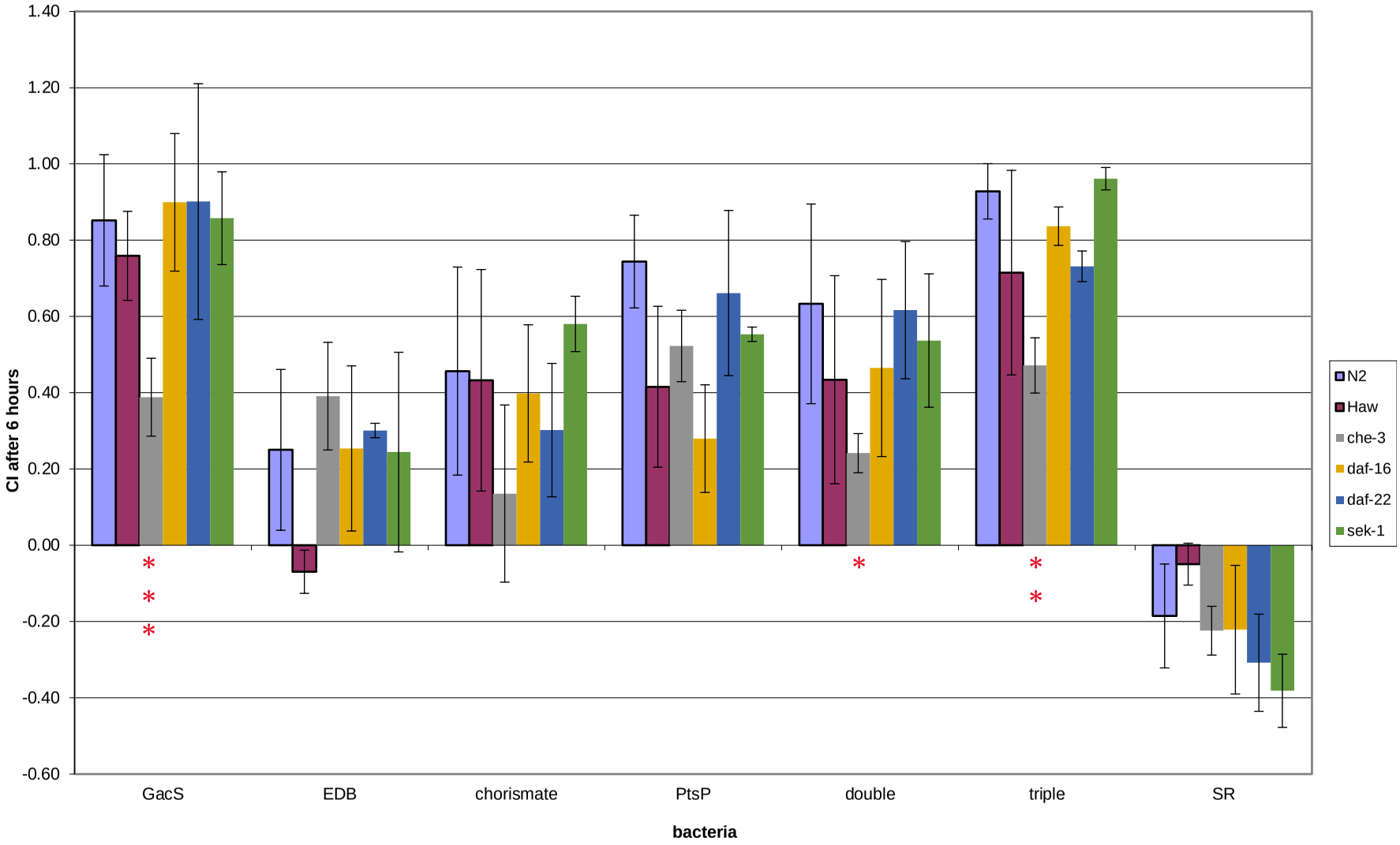

Figure 5.12: Effect of nematode genotype on food choice The behaviour of 6 different nematode genotypes was observed for 6 hours in choice assays with selected bacterial mutants. The choice index is defined in Section 5.1.1. Positive scores indicate a preference for the mutant bacteria over the WT. SR - WT with miniTn7:GFP insertion. Error bars show standard deviation. Scores which are significantly different from WT after application of a Sidak correction are indicated by one to three red * (p= 0.05, p= 0.01, p= 0.005 respectively). Each preference assay was repeated at least three times.

Pathogenicity of *P. fl.* NZI7. *Sek-1* is an important regulator of *C. elegans* innate immunity. Therefore, we can use a *sek-1* mutant to investigate *P. fl.* NZI7 pathogenicity. When *sek-1* mutants feed on *P. fl.* NZI7 we can observe the first dead worms after only 6 hours, which is much earlier than anything reported previously [213]. The hypersensitivity of *sek-1* shows that pathogenic effects might play a role in the interaction and account for some of the symptoms of sickness we observe in the nematodes. However, this does not rule out the possibility that toxins are also important, or even play the dominant role. Thus, *P. fl.* NZI7 is more pathogenic than the slightly pathogenic *E. coli* OP50, on which the mutant nematodes survive well. Even the triple mutant of tolaasin, HCN and EDB is lethal to *sek-1* mutants (see Figure 5.11), indicating that one of the remaining unknown factors is a pathogenicity factor. The increased susceptibility does not appear to influence the behaviour of the nematodes (see Figure 5.12). Greater susceptibility to the pathogenic effects of the mutants does not lead to any significantly altered behaviour.

The Hawaiian strain is more susceptible to *P. fl.* NZI7. The Hawaiian strain CB4856 shows increased susceptibility to *P. fl.* NZI7 and most of the mutants tested (see Figure 5.11). It has previously been reported as being less resistant to pathogens [204, 291]. Reduced fitness of the Hawaiian strain has been attributed to the negative effects of crowding in clusters [204]. However, in our food race assays we do not observe cluster formation on WT bacteria, as nematodes do not reach high enough density. On the contrary, as observed above, when clusters of nematode do form (for example due to impurities in the agar), nematodes can consume even the most toxic bacteria. Another proposed mechanism for increased susceptibility results

from a higher probability of Hawaiian nematodes to occupy a lawn of pathogenic bacteria compared to N2 animals [182, 291]. While we did not investigate this effect specifically, the proportions of non-feeding nematodes found in food choice assays confirm this phenotype (data not shown).

Reduced Fitness To investigate the reduced fitness of the *sek-1* mutant and the Hawaiian strain further, we test them in progeny assays using the EDB and the chorismate mutants, which have intermediate scores when tested with N2. As expected the *sek-1* mutant did not produce any offspring which survived to adulthood. The Hawaiian strain showed reduced scores in both cases, but the same maturation time.

Chemosensation mutants are impaired in their choice The chemosensation mutant *che-3* shows a significantly reduced and/or delayed preference in most of the attraction assays. It is not surprising that the *che-3* mutant shows no preference when the chemotaxis score is considered, as the mutant is entirely deficient in chemotaxis, and thus cannot distinguish the bacterial colonies without having sampled them. Furthermore we had defined the chemotaxis score such that the *che-3* mutant shows no preference. Much more surprising is the fact that the mutant shows any preference at all after some incubation. This indicates that *C. elegans* must have some means, which are independent of chemosensation, of detecting that the bacteria are harmful after just a few hours of exposure. Alternative mechanisms of pathogen avoidance have been proposed in the past [182], but have not yet been studied in the chemosensation mutant.

As expected, the chemosensation deficient mutant shows a particularly reduced choice index for attractive but inedible mutants (i.e. the PtsP mutant and the

Table 5.3: Summary of the behavioural and survival phenotypes observed in different *C. elegans* variants compared to N2.

	FCA	**NGSA**
Hawaiian	no effect	increased susceptibility
che-3	delayed choice	no effect
daf-16	no effect	no effect
daf-22	no effect	delayed development
sek-1	no effect	hypersusceptible

double mutant of HCN and tolaasin). The fact that the *che-3* mutant displays any choice in these cases probably results from the slightly increased edibility in these strains. On the other hand the mutant displays the same behaviour as the N2 WT on the edible but not attractive EDB mutant. This can also be observed in the *tax-2* and *tax-4* mutants (data not shown). These two observations further support our hypothesis that attraction and edibility are not tightly linked. Attraction acts through the chemosensation pathway, while edibility acts through an alternative pathway, which still awaits further description.

The short term choice assay conducted so far is not sufficient to determine whether preference is reduced or just delayed to a point after our observation. We will aim to discover this in the following section.

5.7 Chemotaxis is Not Required for Food Choice

The unusual results obtained with the chemosensation deficient strain *che-3* and similar observations made with *tax-2* and *tax-4* mutants (data not shown) encouraged us to investigate this mutant further, as it will help us to identify what role chemosensation plays in nematode learning.

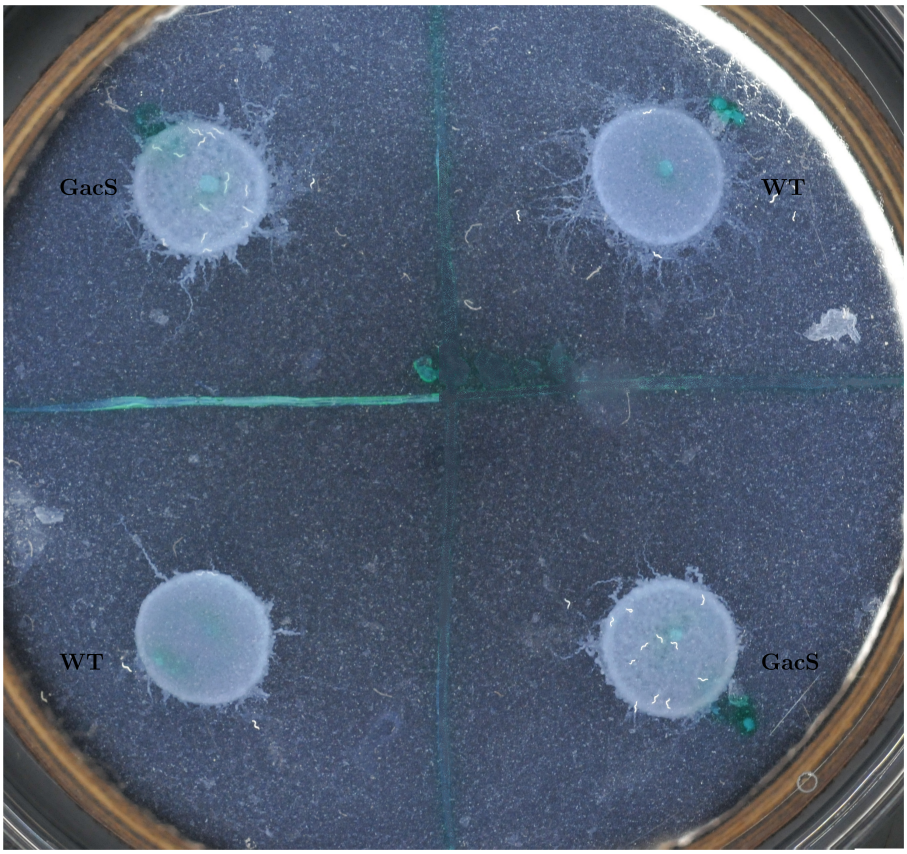

Figure 5.13: Macrophotography allows monitoring nematode behaviour for 24 hour periods. After 20 hours most of the che-3 mutant nematodes on the plate are associated with the GacS colonies and not with the WT. The right half of the image has been manually enhanced to improve contrast between nematodes and background.

5.7.1 Medium term Behaviour of *che-3* Mutants

We will study the behaviour of the chemosensation mutant in the most extreme case of WT bacteria versus the GacS mutant. Macrophotography is used to sample the distribution of nematodes overnight (see Figure 5.13). This setup allows us to estimate choice indices for periods of 24 h. To obtain usable images for analysis, one can use phytagel instead of agar for preparing the plates. However on these plates food choice appears to be less pronounced than on agar plates (data not shown), so that we cannot use this setup for comparison with observations made on agar

plates, but instead must interpret the two different setups separately. Observations using the macrophotography setup as well as observations made on agar plates after 24 hours allow us to draw the following conclusions: While initially randomly distributed, *che-3* mutants gradually prefer the more edible GacS mutant. Most of the nematodes do not alter their choice after 10–14 hours, and stay associated with the same colony afterwards. More mutant nematodes leave the assay plate than N2 WT ones, which results in a lower choice index as we divide by the number of worms placed. Adjusting for this loss of nematodes does not change any of our conclusions. After one day the behaviour of both nematode variants is indistinguishable. Combined these observations suggest that choice of edible bacteria is only delayed in the chemosensation mutants, not reduced.

Shtonda and Avery emphasised the importance of food leaving in making a choice [195]. This would provide a mechanism for food choice which does not require chemosensation, as long as nematodes can use any other sensory system to realize that they are currently feeding on toxic or pathogenic bacteria. This could, for example, happen through the gut lining. We can investigate whether differential food leaving is sufficient to explain food choice by using the model generated in Chapter 3.

5.7.2 Model Without Chemotaxis

The model developed in Chapter 3 can be adapted to run without chemotaxis, by removing those rules which rely on chemosensation. When doing so we can see the same qualitative effects as in experiment (see Figure 5.14), indicating that by itself, aversion due to edibility and thus higher food leaving probabilities could be sufficient

to explain food choice.

5.8 Conclusion

There are several different assays with which we can investigate the edibility of bacteria. These can be divided into short and long term assays which mainly measure bacterial attraction and edibility respectively. Each of the two groups gives very different results, but even within the two groups we cannot establish an unambiguous order. Therefore we cannot define a universal score of edibility. Using just one of the assays may not be enough to characterize bacteria, while combining the measures obtained from multiple assays requires additional information to find the optimal weighting of each score.

We use the edible EDB mutant and the attractive PtsP mutant to show that behaviour of the chemosensation mutant is influenced only by edibility and not attraction. The disparity between long term edibility and short term attraction allows us to identify the different roles of repellents and toxins. Mutants of *P. fl.* NZI7 which are more attractive, without being less lethal indicate that repellents play an important part in the interactions. The mushroom pathogenicity factor tolaasin is one such repellent. On the other hand, mutations which favour long term survival of nematodes highlight the importance of toxins and pathogenicity. We have been able to verify EDB as a very important factor in the nematode–bacteria interactions. It does not have repellent properties, but we were unable to classify whether it is a toxin or a pathogenicity factor. However, we do have evidence that each of these types exist: hydrogen cyanide is a well-known cytotoxin employed by many

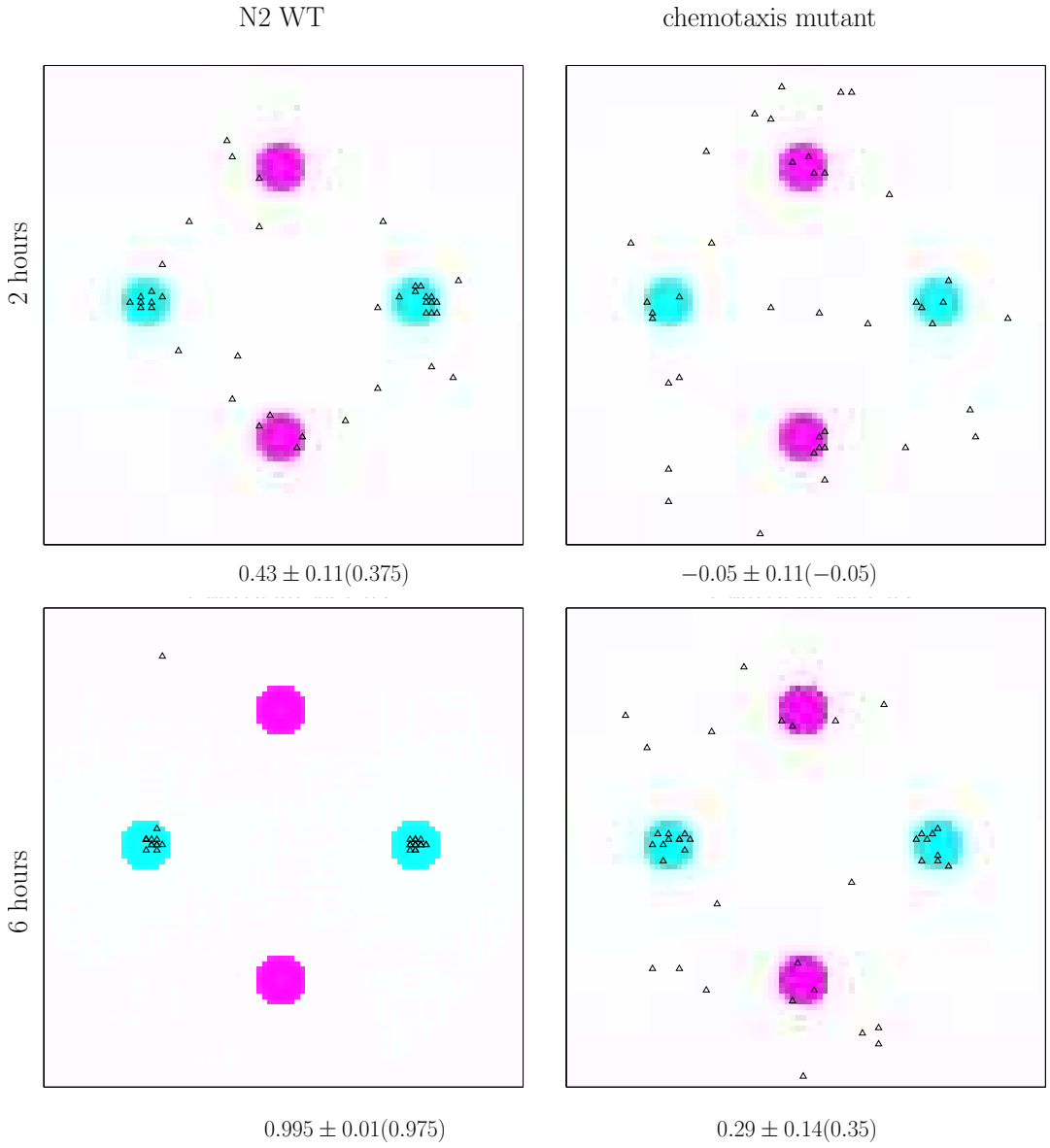

Figure 5.14: Food Choice in the Model Nematode (triangle) distribution after 2 (top) and 6 (bottom) simulated hours. Left: using the settings for N2, Right: using the settings for a chemotaxis mutant. Numbers indicate the choice index computed for simulations as follows: mean ± standard deviation (example in Figure). Fixed parameters are described in Chapter 3. Initial_attraction is 0.0001 for bacteria 1 (pink) and -0.0001 for bacteria 2 (cyan). Edibility is -0.0012 for bacteria 1 and 0.0012 for bacteria 2.

pseudomonads. The high susceptibility of the immunocompromised *sek-1* mutant of *C. elegans* to *P. fl.* NZI7 even when feeding on and the triple mutant (HCN, tol, EDB) indicates that pathogenicity factors also play a role in the interactions. Altogether this highlights the fact that *P. fl.* NZI7 employs a large range of different factors to reduce predation by nematodes.

We have established a list of interesting mutants for further analysis. This list consists of several unambiguously rated strains in terms of edibility and some strains which will allow us to investigate the different impacts of long and short term effects. We have also seen that either tagging technique tried in this study leads to phenotypes in edibility assays. Of particular interest is the superrepellence phenotype which results from chromosomal insertion at the Tn7 site. Using the superrepellence in an edible mutant we can show that nematode behaviour is influenced by bacterial attraction even at long time scales. Unfortunately the phenotype also means that we cannot use tagged bacteria to investigate dispersal of the bacteria by nematodes. Therefore we have defined a set of WT-like mutants, which show no phenotype in any of the screens and assays conducted, but carry a *lux* reporter from the miniTn5 insertion.

We have used different nematode genotypes to investigate the mechanisms employed by *C. elegans* to choose edible food. The chemosensation deficient mutant showed that chemotaxis is an important mechanism for food choice, but it is not the only one. In the model constructed in Chapter 3 we can take out the chemotaxis mechanism. Doing so we found that the alterations in food leaving probability were enough to confer a choice. Nematode mutants deficient in pheromone production showed no phenotype in our assays, indicating that pheromones are not involved in

food choice.

The assays conducted in this chapter can be used to empirically fit some of the parameters in our model. The initial attraction that nematodes show for the GacS mutants helps us to determine the range of the initial_attraction parameter. The length of time taken for nematodes to accept the repellent but edible EDB strain identifies the scale on which the edibility parameter ought to be relative to the initial_attraction. The time scale over which nematodes will return even to the most toxic bacteria lets us parametrize the starvation attraction relative to the initial_attraction and edibility parameters.

Chapter 6

Nematodes Spread Bacteria

Many pathogens employ vectors to aid their dispersal. This is particularly necessary for pathogens of non-mobile hosts like plants and mushrooms. Wind and water are universal vectors found in most systems. There are also many known systems of biotic vectors which can spread pathogens with greater precision, as they move between similar areas [51,64,65,235]. We know from previous observations that bacteria can adhere to the nematode cuticle and are thus spread [34,86,89,91,147]. The efficiency with which this happens may depend on a large variety of factors such as the ability of the bacteria to adhere to the nematode surface. Whether the bacteria can successfully establish themselves in the new environment, or whether they are rapidly consumed by predators will partially depend on their growth parameters. Bacterial spreading might also be influenced by the flagellum as the bacteria's own ability to move can affect self-dispersal, but might also affect bacterial adherence to the nematode surface through biofilm formation or similar traits [292]. In Chapter 5 we found that attraction and edibility do not appear to be influenced by the presence of a flagellum.

Table 6.1: Factors which influence spreading and are investigated in this chapter

Factor influencing spreading	Investigation
Edibility	Bacterial mutants with different edibility
Bacterial growth	Plasmid bearing bacteria
Attachment to cuticle	Mucoid mutant
Nematode behaviour	Different nematode variants

The success of dispersal, and thus the spread of the disease in a mushroom farm, will also depend on the nematode behaviour, which is partly determined by the nematode genetics, but also depends on the edibility and attraction of the bacteria. As we have seen, nematodes are likely to remain in proximity to very edible bacteria (Section 5.3.3), thus reducing the chances of dispersal, while the likelihood of leaving toxic or pathogenic bacteria is quite high, thus facilitating good bacterial spread. In the following sections we will investigate all of these factors summarized in Table 6.1. The main focus will be to link attraction and edibility to spreading.

Successful spreading of bacteria probably requires a balance of repellence, toxicity and attraction. Nematodes must come into contact with the bacterial colony which requires bacteria not be too repellent. Nematodes will remain in the bacterial colony for some time to graze; to keep the number of grazing nematodes low, bacteria have to be repellent enough. In addition, bacteria must not be too toxic, to avoid killing nematodes during this period. Finally, bacteria must be inedible enough, through toxicity or pathogenicity, to cause nematodes to leave the colony and thus disperse bacteria to fresh areas. We thus hypothesise that an ideal strategy will involve contact repellence, which allows the nematodes to come close enough to pick up bacteria, but encourages them to leave, but not die, before they have significantly reduced the bacterial colony. Contact repellence can be achieved either through low

levels of toxicity, mild pathogenicity or repellent factors which do not diffuse.

We can test the importance of edibility and attraction by investigating how edible mutants of *P. fl.* NZI7 are spread (Section 6.2.3. To investigate the effects of rapid nematode death through the action of the bacteria, we will study the immunocompromised *sek-1* nematode mutant, which we know from Chapter 5 to be hypersensitive to *P. fl.* NZI7. In Section 6.3we will also study the effects of foraging behaviour as characterized by the food leaving probability. It has been observed that *che-3* mutants have decreased food leaving probability and *daf-16* mutants as well as the Hawaiian strain have increased food leaving probability [212]. Thus we would expect spreading efficiency to be *che-3* <N2 <*daf-16*, Hawaiian.

6.1 Measuring Spreading

6.1.1 Visual Inspection

A crude measure of the initial spreading can be obtained by estimating the area visibly covered by bacteria in the food race assay. This measure does not take bacterial density into account, but simply applies a threshold such that areas are counted as occupied if bacteria are dense enough to be seen. There is a time delay between bacteria being spread to an area and them having multiplied enough that they can be distinguished by eye. A further inaccuracy is introduced into this measure through the estimation made by the observer. The results from this estimate are presented in Table 6.2. We give the data here without any estimate of error, as the error in measurement will be dominant and cannot be estimated.

The observational bias could be removed through an image analysis approach

using macrophotography. However, even more information on the bacterial distribution is lost in this way, as a thin bacterial lawn cannot be easily detected by a camera. This, as well as the problems observed when using phytagel in the previous chapter, makes an assay using photography unattractive.

6.1.2 Using fluorescence

Fluorescent tagging is popular for estimating bacterial numbers and proportions of populations [293]. Our system would have benefitted from exploiting this technique, as in addition to seeing bacterial distribution, we could have also looked at the bacteria associated with nematodes. Unfortunately the GFP located on the miniTn5 transposon is not expressed enough to be visible, and as noted in the last two chapters, we have been unable to tag bacteria neutrally with a fluorescent marker, so we will be unable to use fluorescence.

6.1.3 The Bioluminescence Assay

A more quantitative way to measure the spread of bacteria exploits the fact that the mini-Tn5 vector used for mutagenesis contains a *lux* cassette. Using a very sensitive camera which can pick up individual photons, this allows us to monitor the spread of bacteria for several days (see Figure 6.1). This assay is very low throughput, so can only be conducted for a very small number of strains, which are indicated in Table 6.2. In addition it is very sensitive to contaminations, and it is often not possible to notice contamination during the assay, causing considerable time loss and possibly even corrupted data. In Chapter 4 we saw that on a plate which is fully covered with bacteria, nutrients are exhausted after 50 hours. In these assays,

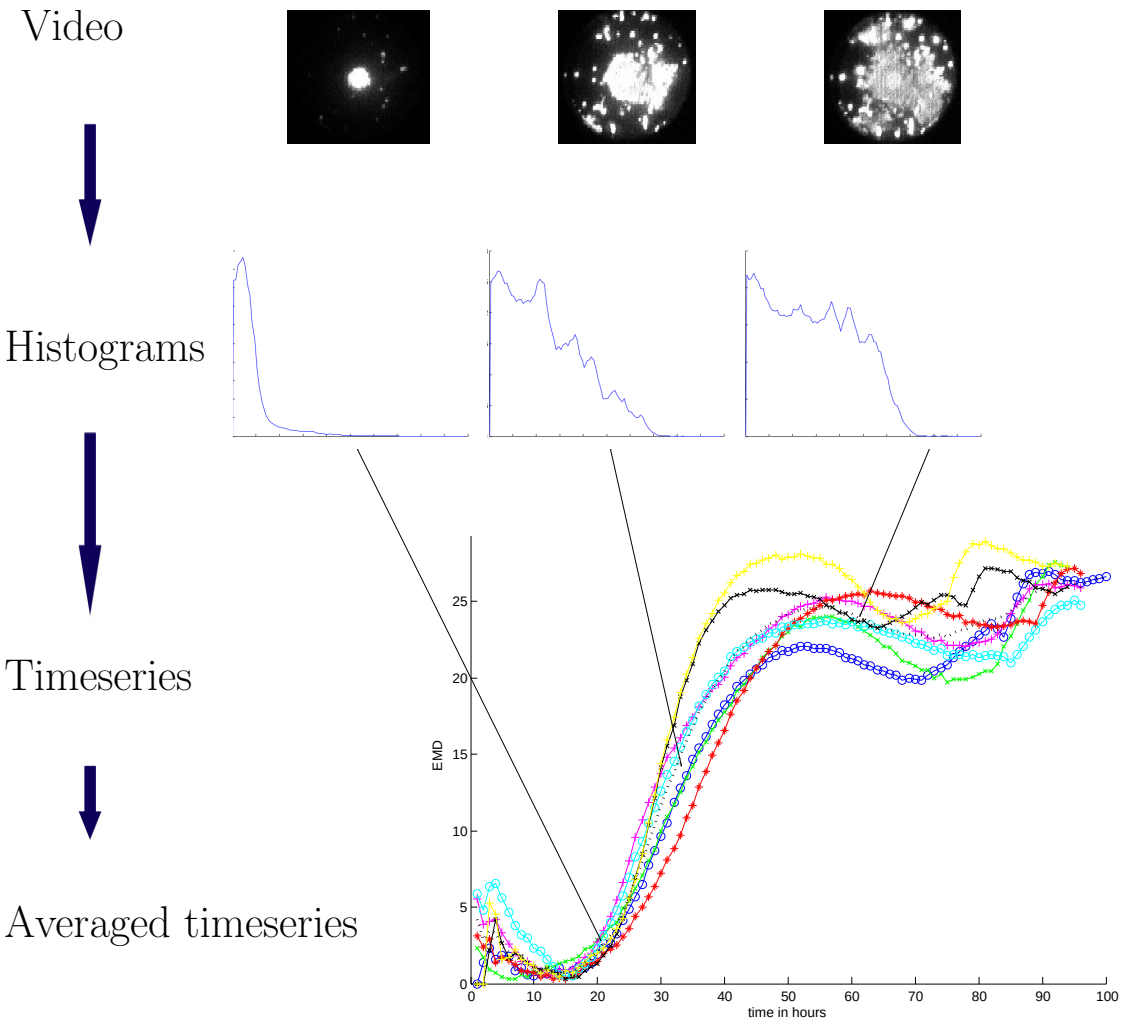

Figure 6.1: Estimating bacterial spreading using the luminescence property of the bacterial mutants Analysis of data gathered using the photon counting technique. Each image taken captures the photons gathered during one hour. The image is converted to a histogram which represents average light intensity as a function of the distance from the centre of the original colony. These histograms can be compared to each other (see Section 6.1.3) to yield a time series of distances which represent spread of the bacterial colony. These are averaged across multiple repeats for further analysis.

where the plates are initially only partly covered, we notice that after 70–90 hours the resources on the agar plate become so depleted that the signal decays.

In each assay we collect photons for over 90 hours. All runs in which the equipment failed before 50 hours are discarded. For each photon collected we know the location it was collected from as well as the time when it was detected. The information is binned into one hour images. We thus have a sequence of at least 50 images for each plate. These are converted to histograms, which represent the average light intensity as a function of the distance from the centre of the original bacterial inoculation. Histograms are normalized such that the area under each curve is unity. Thus histograms represent the distribution of light rather than absolute light intensity values. This is necessary for analysis, but also normalizes for different light expression levels in the different strains. These histograms are analysed and compared to each other using one of several measures (see below), which generates a time series for each plate. These can be averaged over multiple repeats of the same experiment. This outline is represented in Figure 6.1.

Distance Measure

Having generated a series of histograms it will be useful to characterize each histogram by a single number. This can be done by measuring the difference between histograms and using this measure of difference as a measure of spread. Many measures are available to asses the similarity of two histograms. For histograms with cross bin relationships (i.e. where bins have a defined distance from each other) one can use the Earth mover's measure of work or the quadratic Chi distance. The earth mover's distance (EMD) of work, computes the amount of work that would

be required to change one pile of earth in the shape of one histogram into the shape of the other. This is very appealing in our case, as we wish to measure how much nematodes have moved bacteria around. The quadratic Chi distance is closely related but reduces the effects of large bins. This might introduce undesirable bias, but could also be advantageous in reducing the effect of the original colony. The computation of the histogram measures is explained in the appendix.

If we compare each histogram with an equivalent one, generated from a plate on which no spreading has happened, we can use the distance between these histograms as a measure of spreading. The broadest histograms resulting from very spread plates will differ most from the tight ones representing no spread (see Figure 6.1). The question arises, what is a good unspread control? For example we could compare the histogram of the sample plate (i.e. the one inoculated with nematodes) with the histogram generated at the same time from the uninoculated plate. Alternatively, we could compare each histogram of a time series with the very first one. Using either of these two approaches shows large oscillations during the first few hours of the experiment. These originate from the fact that the initial images are very dim, and thus have a low signal to noise ratio. In fact, some of them are so dim that they cannot be analysed at all. Therefore one could alternatively compare each histogram with the one generated after 5 or 10 hours, i.e., just before spreading is visible when inspecting the videos generated by eye.

We are mainly interested in the bacterial distribution away from the original inoculation site. The starting colony will also be the first area of the plate where nutrients become exhausted and thus the signal decays. Therefore it could be advantageous to consider just the areas of the plate, which are outside this initial

inoculation site. Unfortunately this will place further restrictions on the early time point images, as the signal to noise ratio is particularly bad in the very dim areas.

All in all this provides 16 different ways to generate a time series from the histograms computed.

For one strain all of these measures are shown in Figure 6.2. On the measurements obtained by comparing to one of the earlier images we can see that nematodes spread the bacteria compared to the no nematode control.

All measurements yield similar trends, so that for further analysis it does not signify much, which measure we use. However, as comparing to the first image can be unfeasible due to dimness, and comparing to any later image is too arbitrary, we will focus in the following sections on comparisons with the no-nematode control. Similarly we cannot easily justify to cut the histograms at a particular point, as the edge of the colony can be difficult to define (see first histogram in Figure 6.1). The data we obtain when cutting histograms in such a way is not very tight, suggesting that this procedure introduces a large error. This makes the Earth mover's distance or the Quadratic Chi Distance on the unaltered histograms the most preferable. Both show very tight data across repeats and appear to yield very similar results. We will use the earth mover's distance for the rest of this chapter, but analysis performed using the Quadratic Chi Distance yields the same qualitative results.

6.2 Spreading Depends on Bacterial Phenotype

In this section we will investigate the spreading success of different bacterial mutants. This will include an in-depth analysis of several edible mutants as determined

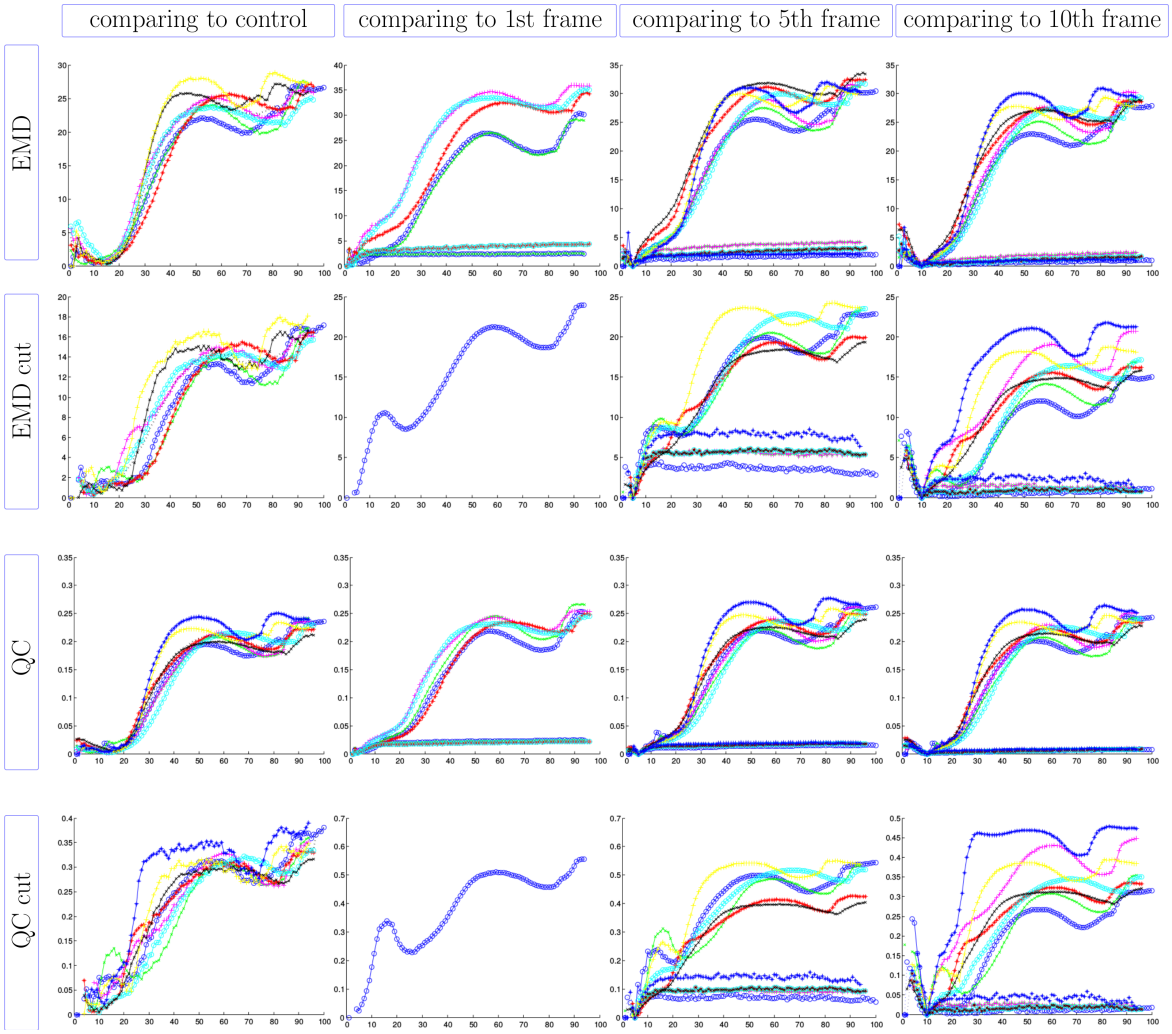

Figure 6.2: 16 different methods for comparing histograms All histograms generated for one bacterial mutant (HCN) and nematode variant (N2) are analysed in the 16 different ways described in the text. Analysis failed in several instances when comparing to the first image gathered, making this option unattractive. EMD - earth mover's distance, QC - Quadratic Chi distance, cut: analysis is done such that the original colony is ignored. All subsequent measures of spreading will use the EMD relative to the control plates, i.e. as shown in the first image.

in Chapter 5 as well as the mucoid mutant (mucA) which might have altered attachment properties. At first we use a semi-quantitative measure of spreading, to allow a measurement of all bacterial mutants. In the second part of this section we will use the luminescence property of the mutants to measure spreading more quantitatively using a photon counting camera.

6.2.1 Overview

For an intial overview of how well nematodes spread the different mutants of NZI7, we will estimate the area of the plate covered after 1 and 2 days of incubation with nematodes in the nematode growth support assay, as described in Section 6.1.1. These estimates are shown in Table 6.2. The table also indicates the mutants we will investigate further using the Bioluminescence assay described above.

Table 6.2: Percentage plate coverage during the first two days after inoculation with nematodes. At the start of the experiment bacteria occupy 5 % of the plate.

Identifier	**Lum** [1]	**1 day**	**2 days**	**Notes** [2]
WT	no	18	91	
tol	no	18	59	
2073	yes	30	85	
2074	yes	10	95	
2075	yes	27	92	
2076	yes	50	90	
2077	yes	20	89	
904	no	38	45	Does not always reach full coverage ***
956	no	10	90	
955	no	10	90	
908	no	6	50	*
912	no	9	15	*
961	no	29	92	**
mucoid (mucA)	yes	9	40	

Continued on next page

[1] Strains which are further investigated using the luminescence property are indicated.
[2] * Symbols indicate growth deficiency as described in Table 4.1

Table 6.2 – continued from previous page				
Identifier	**Lum** [1]	**1 day**	**2 days**	**Notes** [2]
906	no	50	75	*
FliF	no	53	80	***
1638	no	23	85	
959	no	6	95	*
1015	yes	37	88	
970	no	25	95	
1642	no	23	93	
954	no	10	80	**
910	no	50	65	
957	no	50	95	
964	no	10	95	
1046	no	12	39	**
967	no	10	80	
chorismate	yes	11	55	
1644	no	50	93	
GacS	yes	8	20	Never reaches full coverage
963	no	18	92	
1663	no	11	63	Does not always reach full coverage ***
1646	no	50	93	***
1654	no	6	12	Never reaches full coverage ***
1659	no	15	90	
1643	no	8	50	
969	no	23	78	
EDB2	no	19	84	
EDB3	no	31	88	
EDB4	no	20	95	
EDB1	yes	50	87	
916	no	23	90	
985	no	6	48	
1639	no	30	90	***
1657	no	30	93	
958	no	5	50	
1655	no	50	90	
1660	no	20	93	
PtsP	yes	41	88	
918	no	9	40	
965	no	18	55	
1048	no	6	30	
971	no	50	90	
1734	no	10	50	**

Continued on next page

[1] Strains which are further investigated using the luminescence property are indicated.

[2] * Symbols indicate growth deficiency as described in Table 4.1

Table 6.2 – continued from previous page				
Identifier	**Lum** [1]	**1 day**	**2 days**	**Notes** [2]
1652	no	30	95	
1664	no	22	93	
978	no	9	27	Never reaches full coverage
989 (GacS)	no	7	24	
1003 (GacS, EDB)	yes	8	29	Never reaches full coverage
1004 (GacS, EDB)	yes	8	21	Never reaches full coverage
1086	no	65	82	
double	yes	25	88	
triple	yes	20	45	
1900	no	26	77	
2079	no	40	93	
2080	no	30	85	
2082	no	6	60	
2083	yes	5	10	Never reaches full coverage ***
2085	no	6	15	Never reaches full coverage

[1] Strains which are further investigated using the luminescence property are indicated.

[2] * Symbols indicate growth deficiency as described in Table 4.1

In most strains nearly the whole assay plate ($> 90\%$) is covered after 2 days, while a few strains take 3 days, or never reach full coverage. This observation lets us estimate the model parameters for attachment_rate and deposition_rate through a parameter sweep. In more detailed screens we will be particularly interested in the spreading behaviour between 40 and 70 hours. From this initial screen we note that: Most growth deficient strains (904, 908, 1654, 1663, 2083) are spread less successfully. GacS mutants are consumed before the plate is fully covered.

6.2.2 Spreading of *P. fl.* NZI7 WT

Due to the difficulties we have experienced in neutrally tagging the WT strain with a *lux* cassette or fluorescent marker (see Chapters 4 and 5), we have selected some mutants which did not show a phenotype in any screen conducted either previously (see [91]) or during this study (see Chapters 4 and 5). These are the strains 2073–

2077 in our list of mutants. The semi-quantitative spreading screen (see Section 6.2.1) indicates that they also behave similarly to the WT in terms of spreading. We will use these WT like strains to find a control in our spreading assays. All five strains show very similar behaviour in our assay (see Figure 6.3). This gives us reason to hope that they are indeed very close to WT in terms of spreading behaviour. In future comparisons with mutants, we will use an average of these five strains as a WT spreading control. Figure 6.3 also highlights again that the growth deficient plasmid bearing strain is not spread well by nematodes. The figure also shows that the large relative error during the first 30 hours mean that no conclusions can be made about the spreading behaviour during this period.

6.2.3 Edibility Affects Spreading

In Section 5.5 we determined a list of mutants which could be unambiguously ordered in terms of edibility. This allows us to estimate the effect edibility has on spreading. In Table 6.2 we can already see that the most edible mutants (GacS) are spread much less than all others. This is confirmed using the photon counting technique. In Figure 6.4 we notice a large spike in the trace for the GacS mutant. At this point the bacteria are nearly completely eradicated, as can be seen in the representative images displayed below the graph. This results in a spike in the data, as an almost empty plate is very different from one with a central bacterial colony. The multiple spikes occur only in the average, as the timing of the spike is slightly different in the separate repeats. The inset in Figure 6.4 shows a representative sequence of luminescence during such a spike. As bacterial food becomes limiting, the active nematode population declines. The reduced predation pressure allows the surviving

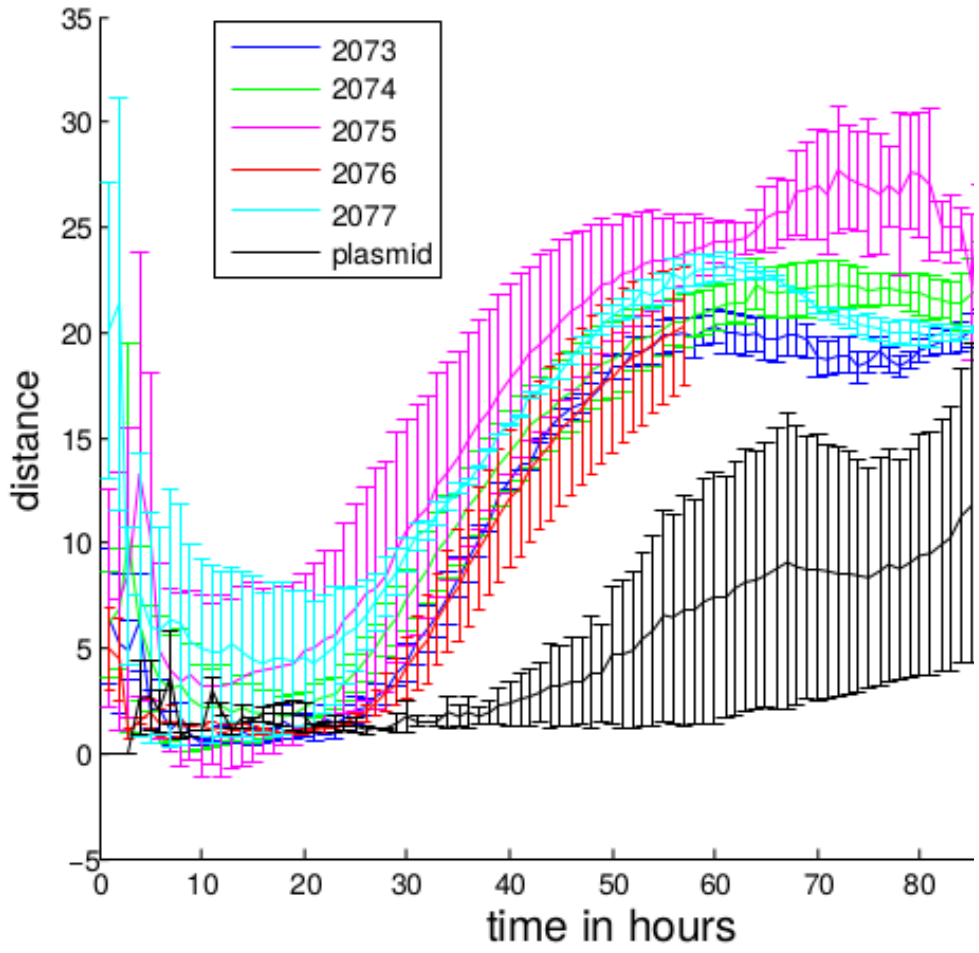

Figure 6.3: Spreading of WT-like mutants of *P. fl.* NZI7 WT spreading cannot be measured directly using luminescence, as the WT is not luminescent and cannot be tagged neutrally (the *lux* plasmid bearing strain (black) is spread much less efficiently). We use miniTn5 insertion mutants with no known phenotype (growth, nematode interaction or production in exoproducts) as a proxy to estimate WT spreading dynamics. Details of how the measure is calculated can be found in Section 6.1.3. Each line represents the average of at least 4 measurements carried out. Error bars show standard deviation.

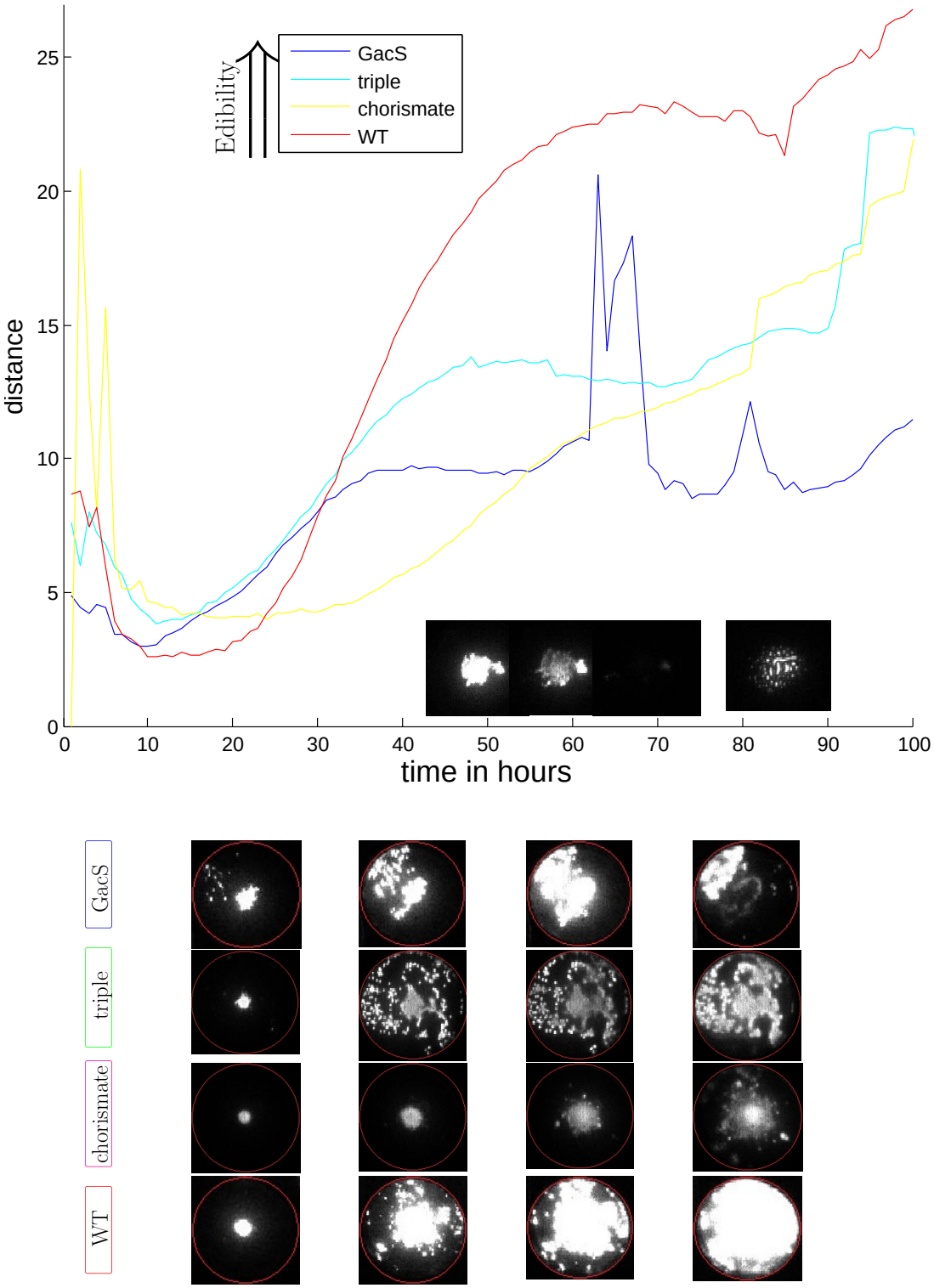

Figure 6.4: Edibility decreases spreading success Spreading success appears to be inversely proportional to edibility. The spike observed in the GacS data is characteristic of near complete bacterial extinction (as can be seen in the representative frames underneath). The granulated appearance of bacterial patches at a later time point indicates the development of bacterial phase change (see Section 6.4). Traces represent averaged EMD for at least four series of luminescence images.

bacteria to multiply and form bacterial clumps (phase change) at the site of the original colony.

To compare spreading efficiency we will have to choose an adequate time point for this we will have to take into account the following: During the first thirty hours the signal to noise ratio is too low to draw conclusions. After 90 hours the nutrients on the plate become exhausted. Many of our time series do not go past 80 hours, so we will have insufficient replication for later time points. The spike in the GacS trace represents a time, when our measure fails to represent spreading. Therefore we will look at spreading efficiency after 48 and 72 hours.

In Figure 6.5 we can clearly see that the increased edibility of any of the selected mutants leads to reduced spreading during the assay. To verify the inverse relationship which is suggested in Figure 6.4 the uncertainty in the measurements must be reduced. This can probably be achieved through greater replication in the experiments, as the error in the WT measurements, where we have 19 time series is much smaller than in the mutants, where we have at most 8.

6.2.4 Attraction versus Edibility

We saw in the last section that edibility is a major determinant of spreading success. Thus we will investigate which of the aspects identified in Chapter 5 is most important for spreading success. For this purpose we have selected a mutant which behaves like WT in the short term, but can be identified as edible in long term experiments. This is true of the EDB mutants. All EDB mutants show the same trends (data not shown). We also have two mutants (PtsP and the double mutant HCN and tolaasin) which are very attractive in the short term, but show low edi-

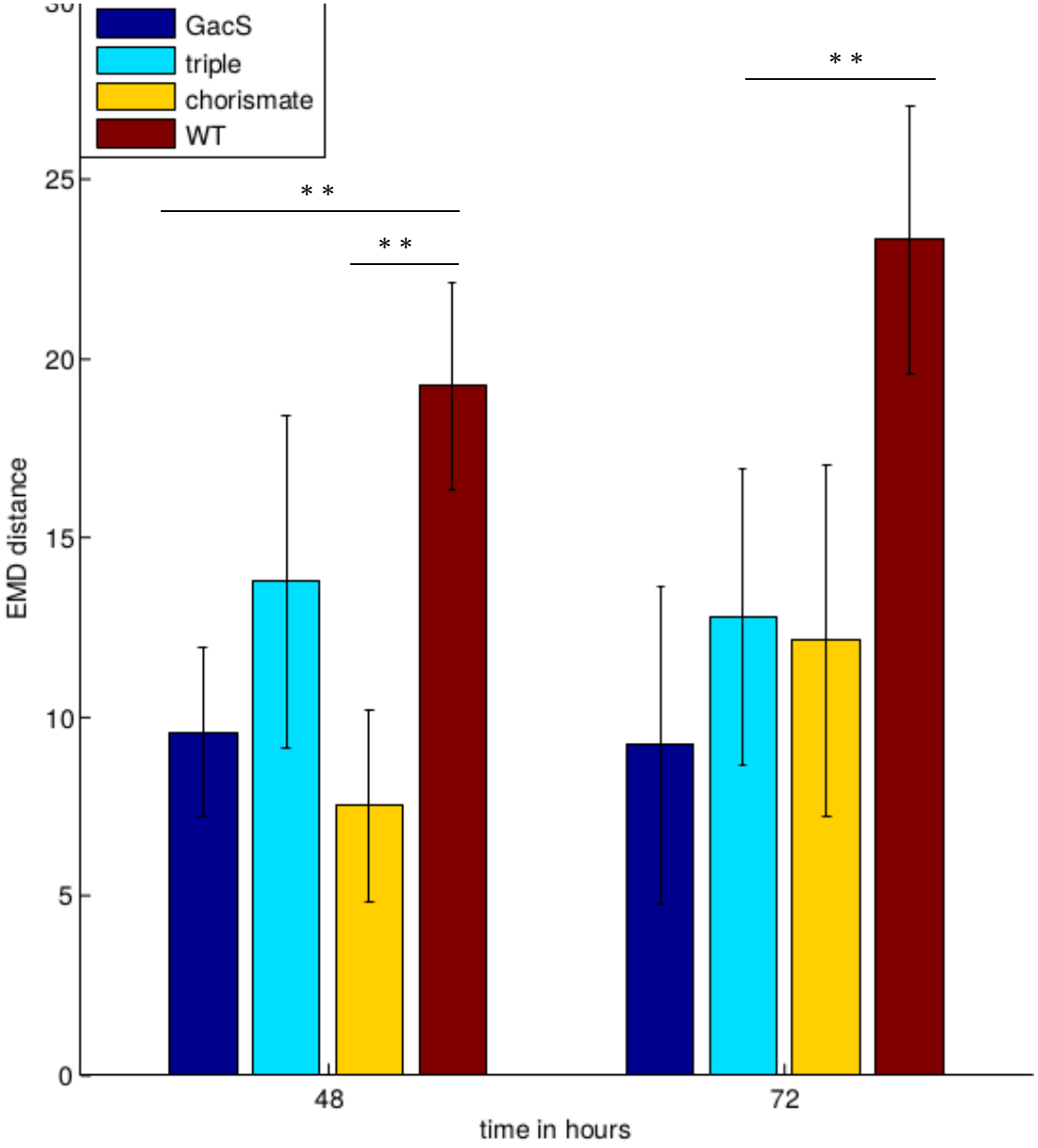

Figure 6.5: Edibility reduces spreadability The WT strain is spread much more efficiently than the more edible mutants. Asterices highlight significant differences after Sidak correction with $p = 0.005$.

bility in longer term assays. We see little difference in either of these mutants from WT during the course of these experiments (see Figure 6.6). However the less edible strains eventually kill their predator, while *C. elegans* dominates on long term edible bacteria (EDB) and consumes all the bacteria it can find within one week. On the inset in Figure 6.6 we can see large bright areas. These correspond to nematode clusters which are moving inwards to consume the bacteria. The high light level seen here probably originates from a high expression of the interrupted EDB gene, as bacteria are trying to repel their predator. The phase change observed in the bacteria means that bacteria will survive nonetheless in the end. This will be explored further in Section 6.4.

6.2.5 Bacterial Attachment

The mucoid mutant might have an altered interaction with nematodes due to the different consistency of the colony. This could influence bacterial adherence to the cuticle, but could also alter nematode movement, as they struggle to leave the almost liquid phase of the colony. The mucA mutant is between the chorismate mutant and the triple mutant in terms of edibility, but is better spread than either of these two mutants (see Figure 6.7). This disproves the hypothesis that nematodes get stuck in the liquid extracellular matrix and cannot leave the bacterial colonies, and raises the question, whether the mucoid mutant has different adherence properties to the nematode cuticle and can thus be spread better.

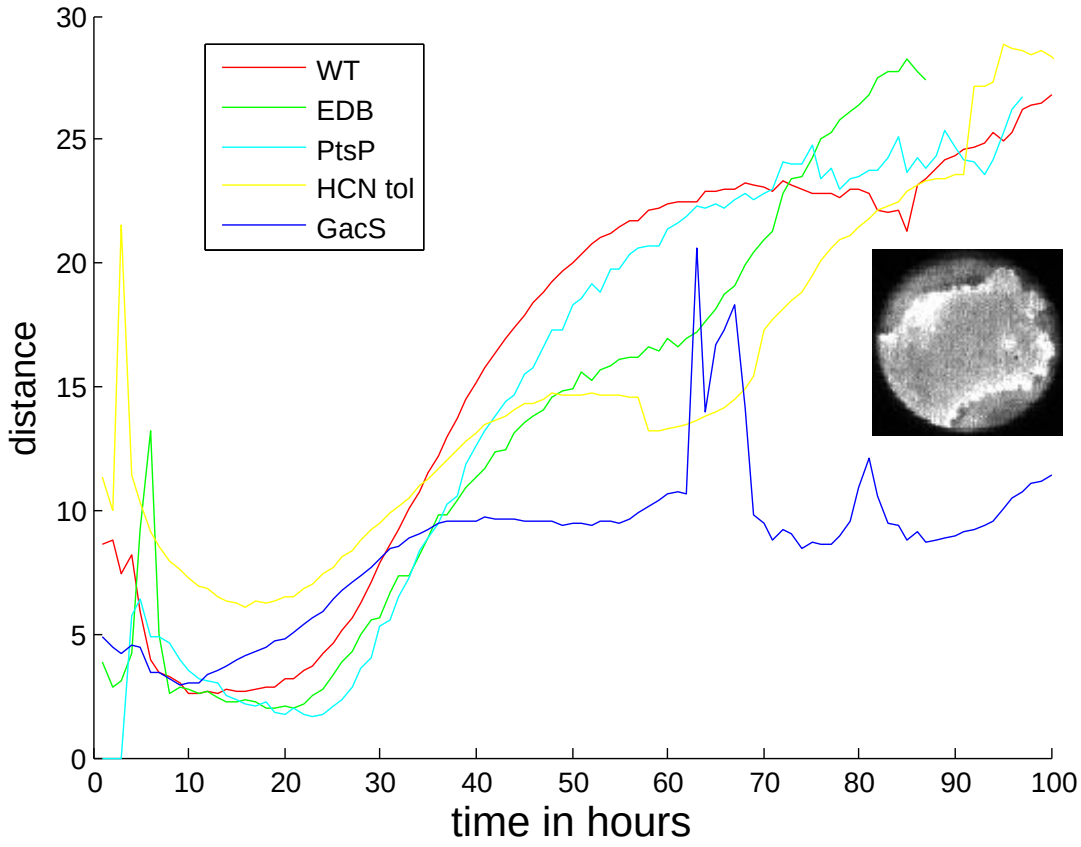

Figure 6.6: Attraction versus Edibility Neither increased attraction (PtsP, HCN tol) nor edibility (EDB) on their own decrease spreading efficiency over the period of the experiment. The inset shows the luminescence of an EDB mutant after 100 hours incubation with nematodes. Traces represent averaged EMD for at least four series of luminescence images.

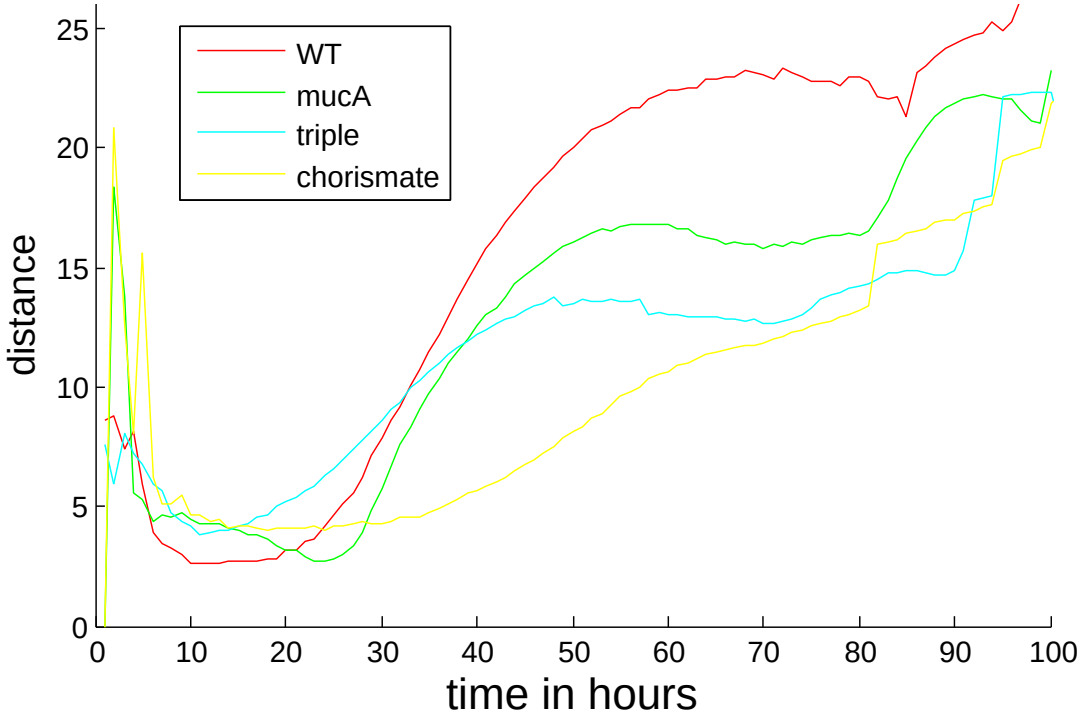

Figure 6.7: Factors other than edibility influence spreading The mucoid mutant (mucA) is close to the chorismate and the triple mutant in terms of edibility, but we find that it is spread more efficiently than either of them. Each line represents the average of 4 replicates.

6.2.6 Spreading in the Model

We have used the time scale of spreading observed through inspection of plates by eye to determine the attachment parameters. The model is quite sensitive to these parameters. An increase in attachment rate means that more bacteria are spread, while a decrease in deposition rate causes bacteria to be spread further.

Running the model in the setting with just one bacterial strain (see Section 3.6) we can recreate the experimental setup. In Figure 6.8 we see that the model also predicts better spread of the less edible strain, while the more edible strain supports good nematode growth, resulting in rapid depletion of bacteria at later time points. All simulations start with an initial bacterial population of around 16 bac, where bac is the arbitrary measure of bacterial numbers we have defined in Chapter 3. Spreading by nematodes combined with growth at the newly populated sites results in an increase in total bacterial numbers on the simulated assay plate. We have simulated four runs for each of the different parameter settings to compute an average and standard deviation. Repellant bacteria (see Figure 6.8 for details) increase to 113 ± 2 bac after 30 hours, while attractive bacteria reach the significantly ($p = 0.0007$) smaller bacterial population of 83 ± 6. At the same time the nematode population is significantly higher ($p = 2^{-8}$) on the more edible strain with 669 versus 149 individuals.

While investigating the spreading behaviour in the model we particularly notice the importance of starvation attraction. Without this mechanism nematodes would not touch repellent bacteria often enough for spreading to happen.

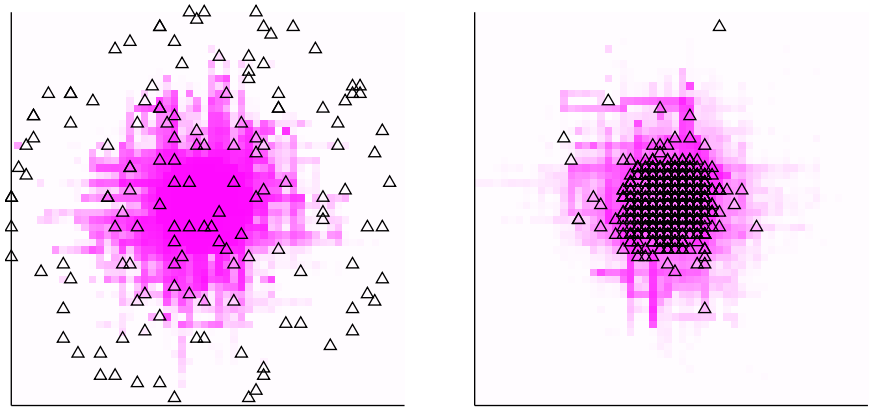

Figure 6.8: Model corroborates that repellence favours spreading Left: a repellent strain is spread very efficiently. Right: a more edible strain is spread less and supports better nematode reproduction. Images are taken after 30 simulated hours. Black triangles represent sites occupied by nematodes and pink represents the bacterial distribution. Parameters are described as in Chapter 3, with variable parameters as follows left: initial_attraction= -0.5, edibility= -0.5; right: initial_attraction= 0.5, edibility= 0.5.

6.3 Spreading Depends on Nematode Strain

The success of bacterial spreading through predators also depends on the behaviour of the predator. Due to their longer ranged movement, flies have often been identified as the main vector for pathogens in mushroom farms [18, 43, 62]. We have previously investigated variants of *C. elegans* which might show different behaviour or survival when challenged with *P. fl.* NZI7. Here we will investigate how the differences observed in the last chapter will impact on spreading. In addition, some of the mutants have phenotypes which might directly influence their ability to spread bacteria.

In the following we will present data gathered on the spreading of one of the WT-like mutants (2075). However, the same trends can be observed using an EDB mutant (data not shown).

6.3.1 Pathogenicity

The hypersusceptibility of the *sek-1* mutant to the bacteria might cause these nematodes to die or leave the plate before they have fully explored it. This would result in less spread over longer timescales, but, the mutant might also display a greater food leaving probability due to the high pathogenicity of the food. This nematode mutant could demonstrate that there is a disadvantage to the bacteria if they kill their predator too quickly. The time delay between infection and nematode death might not be large enough to optimize spreading. This is noticeable in the NGSA, where we see that plates are not fully covered with bacteria at the end of the assay. However, when the bioluminescence setup is used this lack of spreading does not become apparent. It seems instead that bacteria are spread more efficiently (see Figure 6.9).

This could be due to an underestimation of the covered area in NGSA. While it initially appears that the *sek-1* mutant dies before the whole plate is covered with bacteria when observing NGSA, one must bear in mind that there is a time delay between the bacteria being spread and the spreading becoming visible to the observer. However, we can see evidence of clear patches left on the plate when inspecting the videos which use the *sek-1* mutant. These might not be evident after the analysis, due to compensating growth effects. When small areas of agar are left unpopulated by bacteria, the neighbouring bacterial patches can grow better, as more nutrients are available to them. Thus we see a pattern of very bright and very dark areas. During the analysis this is averaged, and the pattern will not leave a distinguishable trace in the data. Finally, we cannot disregard the possibility that

sek-1 mutant nematodes might have a higher food leaving probability on pathogenic bacteria than N2 WT. This has not been measured to date.

6.3.2 Food-Leaving Probability

The *daf-16* mutant senses constant satiation and thus, like the wild type strain CB4856 is known to have a higher food leaving probability [212]. The chemosensation mutant on the other hand is associated with lower food leaving probabilities [212]. Observing plate coverage in the NGSA it appears as if the Hawaiian strain is more efficient than N2 nematodes at spreading bacteria, and the che-3 mutant less so. In all assays conducted, bacteria were spread fastest by the Hawaiian strain (see Figure 6.9). We could also observe that spreading by the chemosensation deficient strain was not as effective as spreading by N2. We could not, however find a significant increase in spreading by the *daf-16* mutant, which might be because the food leaving probability is only slightly increased in this mutant.

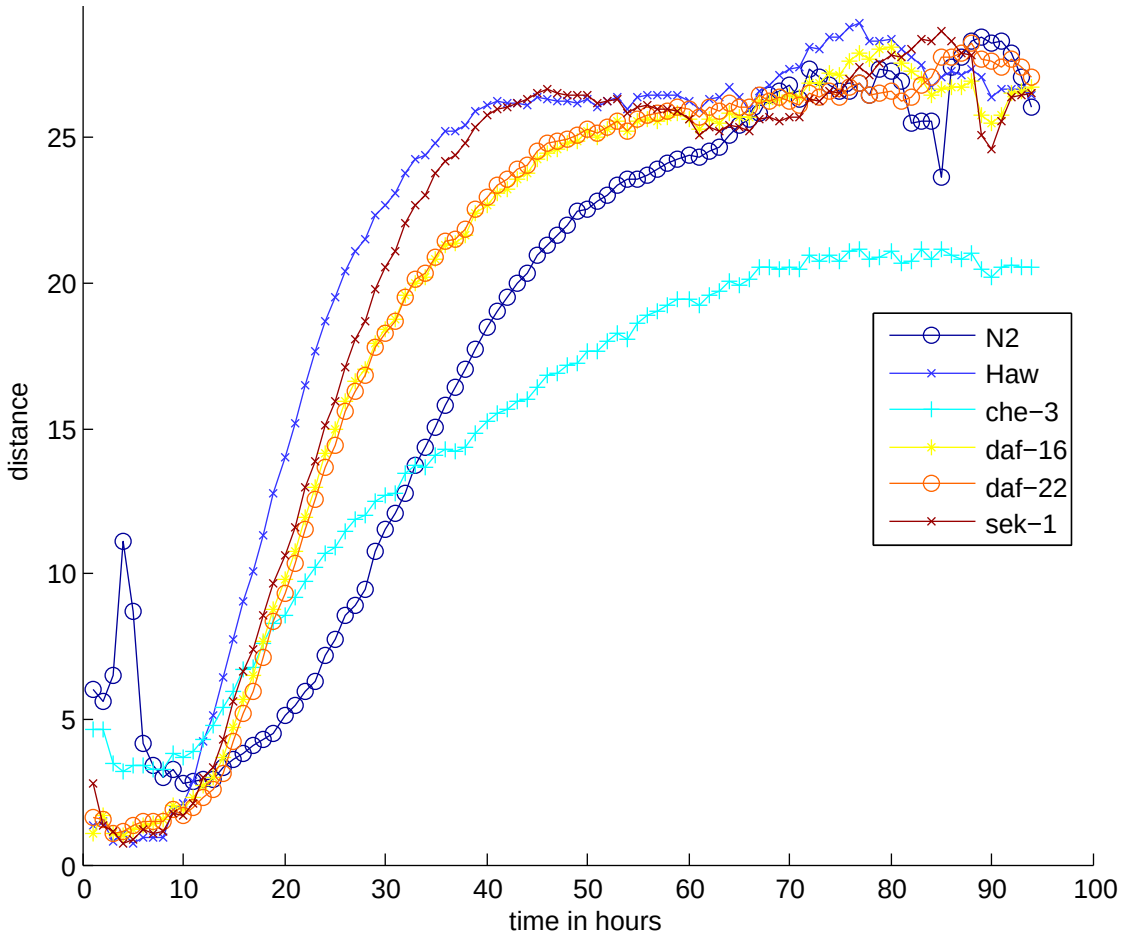

Figure 6.9: Food leaving probability influences spreading Nematode strains with high food leaving probability (Hawaiian) are more efficient at spreading bacteria, while those with reduced food leaving probability (*che-3*) are less efficient. Each line represents the average earth movers distance for at least four replicates.

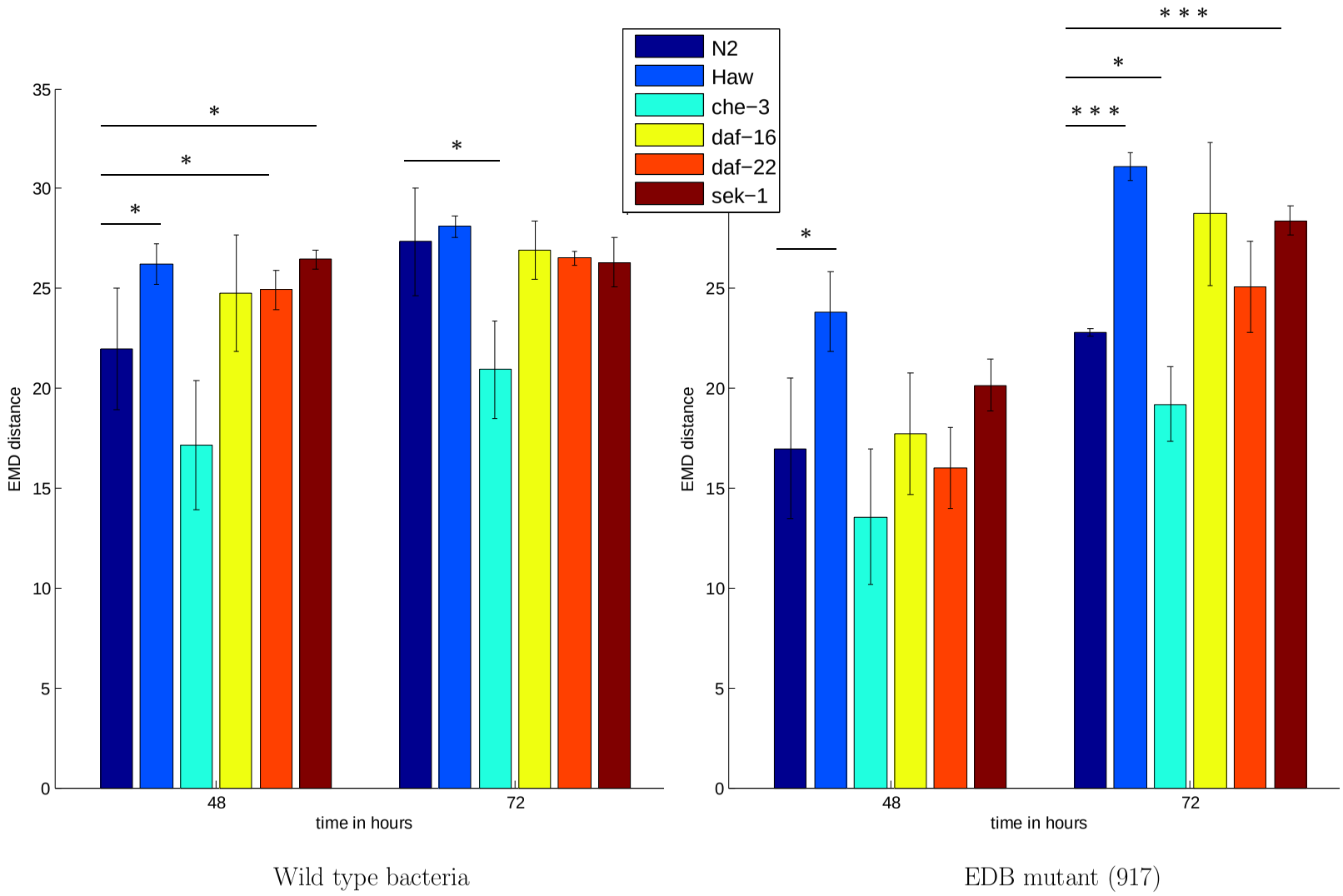

Figure 6.10: Food leaving probability influences spreading 48 and 72 hour time points of the curves represented in Figure 6.9 (left) and a similar experiment using the EDB mutant bacteria (917) (right) with standard deviation (error bars). Asterix indicate significant difference at p= 0.05 (*) and p= 0.005 (***) after Sidak correction for 5 comparisons. Time points are chosen such that nutrients are not limiting.

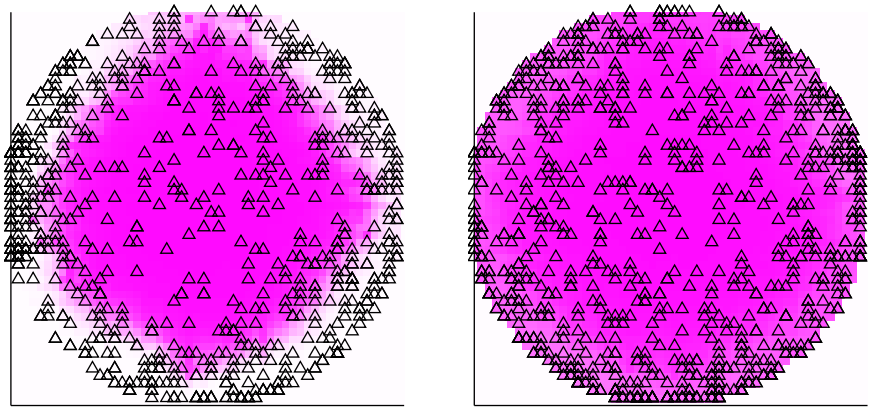

Figure 6.11: The model predicts efficient spreading by Hawaiian nematodes. Bacteria (pink) and nematode (triangles) distribution in the model after 54 simulated hours. Fixed parameters are as described in Chapter 3. Variable parameters are as follows: initial_attraction = -0.5, edibility = -0.5. Left: the N2 WT strain, right: the Hawaiian WT strain

6.3.3 Spreading in the Model

The model easily allows for the representation of the Hawaiian strain, by removing the slowing response on food (see Section 3.4). We have previously used the model to represent the chemosensation deficient strain. This involves removing the response to chemical stimuli (see Section 3.4). However, this is not sufficient to generate the reduced food leaving probability observed in this strain, so we do not expect our model to succeed in reproducing the reduced spreading observed in this strain.

In our model the Hawaiian strain is characterized by an increased on-food speed. During simulations of bacterial spreading (see Figure 6.11) it appears that this is sufficient to explain the higher efficiency of the Hawaiian WT at spreading bacteria. After 54 simulated hours the N2 strain has spread the bacteria to increase their population from 16 to 332 ± 6 bac, while the increase in simulations using the Hawaiian strain is up to 467 ± 9 bac ($p = 10^{-6}$).

6.4 Bacterial Clumping

We observed that under heavy nematode predation bacteria change phase. Unpredated bacterial colonies also showed signs of phase change especially at the edge of the colony (see Figure 6.12). These were laid bare through the action of nematodes. However, most phase changes developed after bacteria had been spread to fresh areas of the plate and during strong nematode predation. This clumping usually takes between 8 and 60 hours to develop, and is thus difficult to observe in strains which are rapidly consumed. This new phase consists of dense clumps of bacteria, which are resistant to nematode predation (see Figure 6.13). The bacterial clumps do not dissociate in liquid, unless vortexed heavily (>1̃ min). Bacterial clumps are luminescent (see Figure 6.4), so we can deduce that they are metabolically active. Transferring the clumps to a nematode free plate we observe that a normal bacterial lawn regrows from the clumps, confirming that they are viable, and also indicating that the phase change is not permanent.

All *P. fl.* NZI7 mutants tested clump under heavy nematode predation. In addition to the mutants described in Table 1.2, we tested a set of mutants with defects in DNA repair (recJ, recBCD, LexA), starvation stress response (ppGpp) and cell division (minC). A random screen of mutants conducted by students enrolled on the DTC experimental techniques course in 2014 and 2015 also did not yield any mutants defective in phase change. The ability to change phase was also tested in other pseudomonads (see Table 2.2) and was observed in all strains tested which were not consumed within the first 60 hours, including *Pseudomonas aeruginosa* PAO1 and representatives from both of the fluorescent complexes. The ability to undergo



Figure 6.12: Phase change development Clusters of nematodes (*) move along the colony edge to deplete bacteria which have not changed phase ($). In doing so they excavate those bacteria in the colony, which have changed phase (#).

such a phase change has also been observed in stressed budding yeast [294] and marine pseudomonads [225], and could thus be a widely conserved stress response.

6.5 Conclusion

It is difficult to measure spreading. The visual estimate of the area covered cannot reliably incorporate information on bacterial density. Instead a threshold is necessarily applied between 'not enough to be visible' and 'detectable by eye'. Any attempts to use fluorescent tagging have so far been unsuccessful due to the alteration in edibility (see Section 5.3.1) or growth parameters (see Chapter 4) these cause. Thus, in this chapter we have used the luminescence of the mutants gen-

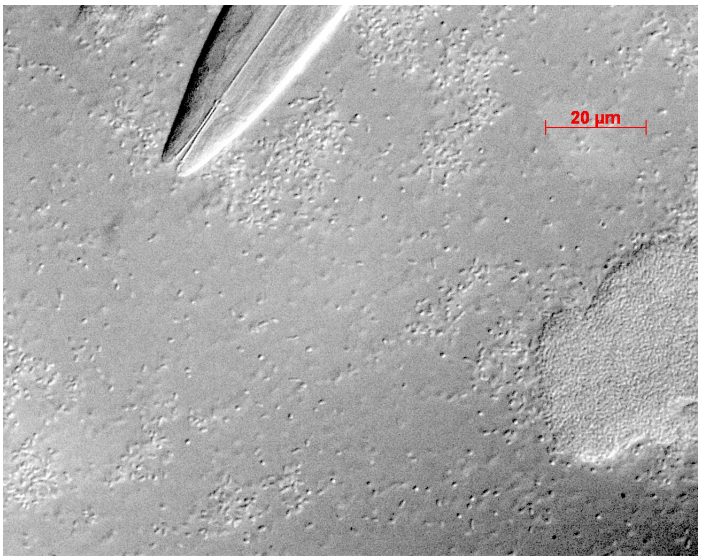

Figure 6.13: Clumping protects bacteria from predation by nematodes. During bacterial phase change bacteria form large clumps (bottom right), which cannot be taken up by the nematode through the comparatively narrow pharynx (top left).

erated. Using a photon counting camera, we can generate informative images of the bacterial distribution. Mathematical measures which allow the comparison of histograms can capture some, but not all, of the observations made when inspecting the images by eye. All the different methods of investigation clearly show that very edible bacteria are spread less efficiently. This can also be recreated using the model developed in Chapter 3. The model also recreates the higher nematode density on edible bacteria, indicating that low numbers could be a result of poor nutrition due to spending time away from the bacterial colony. When investigating the Hawaiian strain and the *che-3* mutant, we could also confirm that food leaving probability plays an important role in spreading, with spreading efficiency being proportional to food leaving probability.

Under heavy nematode predation, bacteria change phase to form inedible clumps. These can persist until the predation pressure has subsided, after which bacteria

resume normal growth. Even in the least favourable conditions the disease is thus spread by *C. elegans*.

Chapter 7

Conclusion

In this study we wanted to investigate how bacteria can be spread by their predators. We used the mushroom pathogen *P. fl.* NZI7 and the model organism *C. elegans* to investigate this phenomenon. Both species can be found on mushroom farms in Britain.

Our main focus was to determine which impact bacterial edibility has on nematode behaviour and how this in turn influences the efficiency with which nematodes spread the bacteria. While characterizing bacteria in terms of their edibility we found it necessary to investigate their growth through liquid culture growth assays (Chapter 4), as this can be a major factor for both nematode–bacteria interactions and spreading efficiency. To investigate bacterial edibility we used a range of different assays, which measured nematode attraction, fertility and survival (Chapter 5). We made use of the luminescence property of our bacterial mutants to explore bacterial spreading (Chapter6).

7.1 *P. fl.* NZI7 Reduces Predation by *C. elegans*

To study the interactions of *P. fl.* NZI7 with *C. elegans*, we investigated a range of mutants which had been identified as more edible in previous studies [91]. Our study suggests that *P. fl.* NZI7 secretes many different secondary metabolites, which reduce grazing by *C. elegans* through a variety of mechanisms: toxins are known to poison nematodes independent of bacterial presence, pathogenicity factors aid in gut colonisation and repellents cause nematodes to avoid bacteria, even though they are not harmful.

All of these factors appear to be regulated by the GacS/A system. Consistent with a knockout of all adverse factors the GacS mutants accelerate nematode growth and increase brood size. We could not observe any adverse effects on nematodes that were raised on the GacS mutant.

The individual factors are often unknown and difficult to classify into one of the three groups described above. *P. fl.* NZI7 secretes the known nematocide HCN. However this is produced at sub lethal levels in the conditions used in this study. Tolaasin is a known factor of mushroom pathogenicity, but we could also identify it as a nematode repellent.

The chemically unknown EDB is either a toxin or a pathogenicity factor. EDB appears to be the single most important determinant for nematode survival and thus also for bacterial survival.

We know that there must be at least one more pathogenicity factor in *P. fl.* NZI7, as the immunocompromised nematode mutant *sek-1* does not survive on the EDB mutant or even the triple mutant of all three factors mentioned above.

7.2 Attractive and Edible Bacteria

Many studies have reported that *C. elegans* can identify and select less toxic/pathogenic bacteria [142, 143, 195]. On the other hand studies on serrawettin mutants of serratia have also shown that strong attraction does not necessarily mirror high edibility [172].

Here we look at nematode learning in a setting involving its natural food. We found evidence for both, high attraction to inedible bacteria and long term learning despite no initial attraction, suggesting that repellence and inedibility are governed by different factors. Work by Maria Ordovas-Montanes (King/Preston lab), as well as studies on a super-repellent EDB mutant show that nematodes will prefer more attractive bacteria over more edible ones. We can conclude that attractive mutants are not necessarily edible and vice versa.

As nematode mutants deficient in chemosensation (*che-3*) or pheromone production (*daf-22*) can identify edible mutants, we know that neither chemotaxis nor pheromones are necessary for edibility dependent choice. However, the ability to sense chemical gradients and thus recognize bacterial colonies accelerates the decision process by an order of magnitude.

We thus conclude that nematodes can learn to prefer mutants of toxicity and pathogenicity factors over longer timescales through sampling all available food patches. Learning by nematodes could be explained through differential food leaving probabilities. The acceleration of decision making observed in strains which can use chemotaxis suggests that there is some association of food quality with the metabolites secreted by bacteria.

7.3 Edibility Determines how Bacteria are Spread by Nematodes

Bacteria can adhere to the nematode cuticle and thus disperse. They gain a clear advantage through the presence of their predator over short timescales (1–2 days).

Over longer timescales (3–5 days) the edibility of the bacteria becomes important, as edible bacteria are consumed (esp. the GacS mutant) while less edible bacteria are spread further.

The least edible of the bacterial mutants tested can kill the nematode population after they have colonised all available space. Thus the nematodes promote their own death, by surrounding themselves with bacterial toxins. On more edible bacteria on the other hand nematodes will proliferate and eventually consume all available bacteria. In this case nematodes gain an advantage through bacterial farming [51]. As less spread is observed for very edible mutants, we can assume that bacterial farming is not done intentionally.

Bacteria can survive extensive nematode predation in a phase changed state, from which they can regrow a continuous lawn. Therefore even the most edible bacteria gain an advantage from their predator at long timescales.

We predict that in a natural setting one would observe the short term effects. However effects observed after 2 days are mainly dictated by the fact that nematodes are trapped in the petri dish, while given more space and choice they would explore other areas and find more edible food sources. In the natural environment, as well as on a petri dish, repellence, toxicity and pathogenicity do not just help *P. fl.* NZI7 to survive by reducing predation, but also allow it to be spread efficiently by *C. elegans*.

7.4 Food Leaving Probability is an Important Factor in Bacterial Dispersal

The effect of nematode foraging strategies on bacterial spread can be explained using the food leaving probability. The Hawaiian WT has increased food leaving probability compared to the laboratory domesticated N2 strain, thus they spend more time dispersing bacteria, which they have just picked up from a colony. This is noticeable on the larger scale as they spread bacteria quicker. Likewise the reduced food leaving probability of the *che-3* mutant can be detected by looking at the reduced speed of bacterial spread.

7.5 A Model of the Interaction

We have constructed a computational model of the nematode–bacteria interactions to go alongside the assays conducted in this study. We have been able to reproduce many of the qualitative observations from the experiments (like spreading and food choice), thus it is reasonable to assume that the model covers most of the fundamental aspects of the nematode–bacteria interactions relevant over short timescales ($\sim$ 3 days). The model does not perform well over longer timescales, as it does not capture the adverse effects of toxic or pathogenic bacteria on nematodes.

Many parameters (like bacterial attachment to nematodes) have been estimated by fitting observations to those made in experiments. We have not yet been able to test the model on settings with larger spatial scales, which would help us to make better estimates of these parameters.

Many mechanisms in the model are based on assumptions, as our knowledge gained from experiments is not sufficient for a complete description. This is particularly evident in the learning process, where we have shown that the model does not capture all aspects.

We have also made many simplifications, in order to make the model comprehensible and computationally less expensive. While these simplifications can be justified for representing the system over short time and length scales, more detailed descriptions will be necessary when extending the model. These include in particular bacterial phase change, which has so far not been incorporated, nematode reproduction, which is currently based on a very simplified picture ignoring nematode development and health and a distinction between the two different modes of dissemination: externally or by passage through the gut.

Using the model we verified that increased aversion from inedible bacteria is sufficient to explain learning, confirming that pheromones and chemotaxis are not necessary for making food choices, but also highlighted the importance of chemosensation to facilitate quick learning. We could also reproduce increased spreading by the Hawaiian strain through including the higher on-food speed. When reproducing the spreading of inedible bacteria we noticed that it is important to model nematode starvation response, to make *C. elegans* return to food patches. Therefore, we have identified the following mechanisms as essential for representing the nematode–bacteria interactions:

- nematode motion speed is increased on aversive bacteria,
- nematodes update their perception of bacterial edibility when on food,

- nematodes off food are increasingly attracted to bacteria.

Additionally chemosensation must be taken into account when attempting to obtain quantitatively accurate results, as indicated by the altered timescales on which nematodes choose bacterial food when they cannot use chemotaxis.
We have not been able to satisfactorily reproduce the distinction between attractive and edible bacteria. The clear separation between these two properties in experiments indicates that we need to describe them separately in the model as well.

7.6 Future Work

This work suggests a range of further investigation into the bacterial and nematode aspects of the interaction. In particular, the following can be identified as the most important avenues for future work:

- Investigate the super-repellence induced by miniTn7 insertion noted in Chapter 5. To date, mass spectrometric analysis has not yielded any differences in the excretome between WT and tagged WT. The next step will be to try a range of different culture conditions prior to extraction of extracellular factors and employ techniques which focus on different classes of molecules. Exploiting this method further might also yield further insight into the chemical nature of EDB.
- A mutant screen of *P. fl.* NZI7 in the HCN/tol/EDB triple mutant background using the *sek-1* nematode mutant might identify a further pathogenicity factor.
- To identify the learning mechanisms used by *C. elegans* a more comprehensive mutant screen through the *C. elegans* library is necessary, possibly in the *che-3* background. This could be further supplemented by laser ablation of neurons. Together these two techniques would allow to identify the role of different genes and neurons in the learning process.
- Nematode tracking will allow better characterization of nematode movement parameters on pathogenic bacteria. It can also be used as an indicator of health [295].

- Explore bacterial adhesion to the nematode surface cuticle, through the use of bacterial mutants and surface mutants of *C. elegans*
- Spreading might also be facilitated by passage through the gut. This could be investigated alongside gut colonisation experiments.
- To find the ideal biocontrol agent for mushroom farms, we will need a predator that does not spread bacteria. This could be found by screening surface mutants of *C. elegans* to find one which bacteria cannot adhere to.
- Explore spreading in a more complex natural setting providing more space and food options
- Testing the model alongside all of the future nematode–bacteria interaction studies will help us to elaborate on its description and confirm those parameters which were empirically determined. In particular studying nematode learning will improve our description of this process.
- Extend the possible simulation length of the model by incorporating long term effects like nematode death and bacterial clumping.

Bibliography

[1] D. C. Griffith, L. A. Kelly-Hope, and M. A. Miller. Review of reported cholera outbreaks worldwide, 1995–2005. *The American Journal of Tropical Medicine and Hygiene*, 75:973–977, 2006.

[2] J. Holmgren and A.-M. Svennerholm. Mechanisms of disease and immunity in cholera: a review. *Journal of Infectious Diseases*, 136:S105–S112, 1977.

[3] S. C. McCombie. Treatment seeking for malaria: a review of recent research. *Social Science & Medicine*, 43:933–945, 1996.

[4] M. Ettling, D. A. McFarland, L. J. Schultz, and L. Chitsulo. Economic impact of malaria in Malawian households. *Tropical Medicine and Parasitology: Official Organ of Deutsche Tropenmedizinische Gesellschaft and of Deutsche Gesellschaft fur Technische Zusammenarbeit (GTZ)*, 45:74–79, 1994.

[5] A. H. Purcell. Insect vector relationships with procaryotic plant pathogens. *Annual Review of Phytopathology*, 20:397–417, 1982.

[6] G. F. Killeen, U. Fillinger, and B. G. J. Knols. Advantages of larval control for African malaria vectors: low mobility and behavioural responsiveness of immature mosquito stages allow high effective coverage. *Malaria Journal*, 1:1, 2002.

[7] D. D. Mara. Water, sanitation and hygiene for the health of developing nations. *Public Health*, 117:452–456, 2003.

[8] S. Cairncross, C. Hunt, S. Boisson, K. Bostoen, V. Curtis, I. CH Fung, and W-P Schmidt. Water, sanitation and hygiene for the prevention of diarrhoea. *International Journal of Epidemiology*, 39:i193–i205, 2010.

[9] L. J. Dowley and E. O'Sullivan. *Late Blight & the Potato in Ireland*. Teagasc, 1995.

[10] B. J. Nielsen, S. G. Schmidt, L. Bødker, R. Kjøller, and S. Rosendahl. Population genetics of *Phytophthora infestans* in Denmark reveals dominantly clonal populations and specific alleles linked to Metalaxyl-M resistance. *Plant Pathology*, 65:744–753, 2015.

[11] R. J. Mitchell, J. K. Beaton, P. E. Bellamy, A. Broome, J. Chetcuti, S. Eaton, C. J. Ellis, A. Gimona, R. Harmer, A. J. Hester, N. G. Hodgetts, Iason G. R., G. Kerr, M. A. Littlewood, S. Newey, J. M. Potts, G. Pozsgai, D. Ray,

D. A. Sim, J. A. Stockan, A.F.S Taylor, and S. Woodward. Ash dieback in the UK: A. review of the ecological and conservation implications and potential management options. *Biological Conservation*, 175:95–109, 2014.

[12] R. N. Strange and P. R. Scott. Plant disease: a threat to global food security. *Phytopathology*, 43:83–116, 2005.

[13] F. N. Lee and M. C. Rush. Rice sheath blight: A. major rice disease. *Plant Disease*, 67:829–833, 1983.

[14] R. J. Hillocks and D. L. Jennings. Cassava brown streak disease: a review of present knowledge and research needs. *International Journal of Pest Management*, 49:225–234, 2003.

[15] H. M. Grogan. Challenges facing mushroom disease control in the 21st century. In *Mushroom biology and mushroom products. Proceedings of the Sixth International Conference on Mushroom Biology and Mushroom Products, Bonn, Germany, 29 September-3 October, 2008*, pages 120–127. GAMU GmbH, Institut für Pilzforschung, 2008.

[16] T. Y. James, F. Kauff, C. L. Schoch, P. B. Matheny, V. Hofstetter, C. J. Cox, G. Celio, C. Gueidan, E. Fraker, J. Miadlikowska, H. T. Lumbsch, A. Rauhut, V. Reeb, A. E. Arnold, A. Amtoft, J. E. Stajich, K. Hosaka, G-H Sung, D. Johnson, B. O'Rourke, M. Crockett, M. Binder, J. M. Curtis, J. C. Slot, Z. Wang, A. W. Wilson, A. Schussler, J. E. Loncore, K. O'Donnell, S. Mozley-Standridge, D. Porter, P. M. Letcher, M. J. Powell, J. W. Taylor, M. M. White, G. W. Griffith, D. R. Davies, R. A. Humber, J. B. Morton, J. Sugiyama, A. Y. Rossman, J. D. Rogers, D. H. Pfister, D. Hewitt, K. Hansen, S. Hambleton, R. A. Shoemaker, J. Kohlmayer, B. Volmann-Kohlmeyer, R. A. Spotts, M. Serdani, P. W. Crous, K. W. Hughes, K. Matuura, E. Langer, G. Langer, W. A. Untereiner, R. Luecking, B. Buedel, D. M. Geiser, A. Aptroot, P. Diederich, I. Schmitt, M. Schultz, R. Yahr, D. S. Hibbett, F. Lutzoni, D. J. McLaughlin, J. W. Spatafora, and R. Vilgalys. Reconstructing the early evolution of fungi using a six-gene phylogeny. *Nature*, 443:818–822, 2006.

[17] FAO, http://faostat3.fao.org/home/E, 2013. accessed on 7th July 2016.

[18] A. A. Richards. *Modern mushroom cultivation.* London : Collingridge ; New York : Transatlantic Arts, 1954.

[19] M. L. Largeteau and J.-M. Savoie. Microbially induced diseases of *Agaricus bisporus*: biochemical mechanisms and impact on commercial mushroom production. *Applied Microbiology and Biotechnology*, 86:63–73, 2010.

[20] J. T. Fletcher. Bacteria and mushrooms. *Mushroom Journal (UK)*, 84, 1979.

[21] W. C. Wong, J. T. Fletcher, B. A. Unsworth, and T. F. Preece. A note on ginger blotch, a new bacterial disease of the cultivated mushroom, *Agaricus bisporus*. *Journal of Applied Bacteriology*, 52:43–48, 1982.

[22] P. Singh, H.-C. Langowski, A. A. Wani, and S. Saengerlaub. Recent advances in extending the shelf life of fresh *Agaricus* mushrooms: a review. *Journal of the Science of Food and Agriculture*, 90:1393–1402, 2010.

[23] C. Soler-Rivas, N. Arpin, J. M. Olivier, and H. J. Wichers. WLIP, a lipodepsipeptide of *pseudomonas reactans*, as inhibitor of the symptoms of the brown blotch disease of *agaricus bisporus*. *Journal of Applied Microbiology*, 86:635–641, 1999.

[24] J. F. Smith. The mushroom industry. In *Exploitation of Microorganisms*, pages 249–271. Springer, 1993.

[25] T. R. Fermor, M. B. Henry, J. S. Fenlon, M. J. Glenister, S. P. Lincoln, and J. M Lynch. Development and application of a biocontrol system for bacterial blotch of the cultivated mushroom. *Crop Protection*, 10:271–278, 1991.

[26] S. A. C. Godfrey, J. W. Marshall, and J. D. Klena. Genetic characterization of Pseudomonas NZI7–a novel pathogen that results in a brown blotch disease of *Agaricus bisporus*. *Journal of Applied Microbiology*, 91:412–420, 2001.

[27] P. Munsch, T. Alatossava, N. Marttinen, J-M Meyer, R. Christen, and L. Gardan. *Pseudomonas costantinii sp. nov.*, another causal agent of brown blotch disease, isolated from cultivated mushroom sporophores in Finland. *International Journal of Systematic and Evolutionary Microbiology*, 52:1973–1983, 2002.

[28] P. Munsch, V. A. Geoffroy, T. Alatossava, and J.-M. Meyer. Application of siderotyping for characterization of *Pseudomonas tolaasii* and *Pseudomonas reactans* isolates associated with brown blotch disease of cultivated mushrooms. *Applied and Environmental Microbiology*, 66:4834–4841, 2000.

[29] P. A. Zarkower, P. J. Wuest, D. J. Royse, and B. Myers. Phenotypic traits of fluorescent pseudomonads causing bacterial blotch of *Agaricus bisporus* mushrooms and other mushroom-derived fluorescent pseudomonads. *Canadian Journal of Microbiology*, 30:360–367, 1984.

[30] H.-S. Han, C.-S. Jhune, J.-C. Cheong, J.-A. Oh, W.-S. Kong, J.-S. Cha, and C.-J. Lee. Occurrence of black rot of cultivated mushrooms (*Flammulina velutipes*) caused by *Pseudomonas tolaasii* in Korea. *European Journal of Plant Pathology*, 133:527–535, 2012.

[31] G. Thorn and A. Tsuneda. Molecular genetic characterization of bacterial isolates causing brown blotch on cultivated mushrooms in Japan. *Mycoscience*, 37:409–416, 1996.

[32] T. Tsukamoto, A. Shirata, and H. Murata. Isolation of a gram-positive bacterium effective in suppression of brown blotch disease of cultivated mushrooms, *Pleurotus ostreatus* and *Agaricus bisporus*, caused by *Pseudomonas tolaasii*. *Mycoscience*, 39:273–278, 1998.

[33] A. R. Estrada and D. J. Royse. Determination of *Pseudomonas tolaasii* threshold concentrations required to produce symptoms of bacterial blotch disease in *Pleurotus eryngii*. *Fifth International Conference on Mushroom Products*.

[34] P. Burlinson, D. Studholme, J. Cambray-Young, D. Heavens, J. Rathjen, J. Hodgkin, and G. M. Preston. *Pseudomonas fluorescens* NZI7 repels grazing by *C. elegans*, a natural predator. *The ISME Journal*, 7:1–13, 2013.

[35] P. S. Grewal and P. N. Richardson. Effects of *Caenorhabditis elegans* (Nematoda: Rhabditidae) on yield and quality of the cultivated mushroom *Agaricus bisporus*. *Annals of Applied Biology*, 118:381–394, 1991.

[36] D. B. Kearns, J. Robinson, and L. J. Shimkets. *Pseudomonas aeruginosa* exhibits directed twitching motility up phosphatidylethanolamine gradients. *Journal of Bacteriology*, 183:763–767, 2001.

[37] Y. Iino and K. Yoshida. Parallel use of two behavioural mechanisms for chemotaxis in *C. elegans*. *Journal of Neuroscience*, 29:5370–5380, 2009.

[38] M. De Bono and C. I. Bargmann. Natural variation in a neuropeptide Y receptor homolog modifies social behavior and food response in *C. elegans*. *Cell*, 94:679–689, 1998.

[39] P. Boisier, M. Rasolomaharo, G. Ranaivoson, B. Rasoamanana, L. Rakoto, Z. Andrianirina, B. Andriamahefazafy, and S. Chanteau. Urban epidemic of bubonic plague in Majunga, Madagascar: epidemiological aspects. *Tropical Medicine and International Health*, 2:422–427, 1997.

[40] H. Lee, M-k Choi, D. Lee, H-s Kim, H. Hwang, H. Kim, S. Park, Y-k Paik, and J. Lee. Nictation, a dispersal behavior of the nematode Caenorhabditis elegans, is regulated by IL2 neurons. *Nature Neuroscience*, 15:107–112, 2012.

[41] J. F. Campbell and R. Gaugler. Nictation behaviour and its ecological implications in the host search strategies of entomopathogenic nematodes (heterorhabditidae and steinernematidae). *Behaviour*, 126:155–169, 1993.

[42] M.-A. Félix and C. Braendle. The natural history of *Caenorhabditis elegans*. *Current Biology*, 20:R965–R969, 2010.

[43] J. J. Hesling. role of eelworms (nematodes) in the culture of mushrooms in the United Kingdom. *Mushroom Journal*, 84, 1979.

[44] L. Frézal and M.-A. Félix. *C. elegans* outside the petri dish. *Elife*, 4:e05849, 2015.

[45] E. Karanastasi, N. Vassilakos, I. M. Roberts, S. A. MacFarlane, and D. J. F. Brown. Immunogold localization of tobacco rattle virus particles within *Paratrichodorus anemones*. *Journal of Nematology*, 32:5–12, 2000.

[46] D. S. Gibbs, G. L. Anderson, L. R. Beuchat, L. K. Carta, and P. L. Williams. Potential role of *Diploscapter sp.* strain LKC25, a bacterivorous nematode from soil, as a vector of food-borne pathogenic bacteria to preharvest fruits and vegetables. *Applied and Environmental Microbiology*, 71:2433–2437, 2005.

[47] L. Bjørnlund, R. Rønn, M. Péchy-Tarr, M. Maurhofer, C. Keel, and O. Nybroe. Functional GacS in Pseudomonas DSS73 prevents digestion by *Caenorhabditis elegans* and protects the nematode from killer flagellates. *The ISME Journal*, 3:770–779, 2009.

[48] M W. Khan and K. N. Pathak. Nematodes as vectors of bacterial and fungal plant pathogens. In *Nematode Interactions*, pages 251–272. Springer, 1993.

[49] J.-Y. Hsiao, C.-Y. Chen, M.-J. Yang, and H.-C. Ho. Live and dead GFP-tagged bacteria showed indistinguishable fluorescence in *Caenorhabditis elegans* gut. *Journal of Microbiology*, 51:367–372, 2013.

[50] C. E. Taylor. Nematode interactions with other pathogens. *Annals of Applied Biology*, 116:405–416, 1990.

[51] T. A. Ciche and J. C. Ensign. For the insect pathogen *Photorhabdus luminescens*, which end of a nematode is out? *Applied and Environmental Microbiology*, 69:1890–1897, 2003.

[52] E. M. Jorgensen and S. E. Mango. The art and design of genetic screens: *Caenorhabditis elegans*. *Nature Reviews Genetics*, 3:356–369, 2002.

[53] I. A. Hope. *C. elegans: A. Practical Approach*. Oxford University Press, 1999.

[54] E. L. Ardiel and C. H. Rankin. An elegant mind: Learning and memory in *Caenorhabditis elegans*. *Learning and Memory*, 17:191–201, 2010.

[55] M.-W. Tan, L. G. Rahme, J. A. Sternberg, R. G. Tompkins, and F. M. Ausubel. *Pseudomonas aeruginosa* killing of *Caenorhabditis elegans* used to identify *P. aeruginosa* virulence factors. *Proceedings of the National Academy of Sciences*, 96:2408–2413, 1999.

[56] C. Couillault and J. J. Ewbank. Diverse bacteria are pathogens of *Caenorhabditis elegans*. *Infection and Immunity*, 70:4705–4707, 2002.

[57] D. C. Altieri. Validating survivin as a cancer therapeutic target. *Nature Reviews Cancer*, 3:46–54, 2003.

[58] S. Kotak and P. Gönczy. Mechanisms of spindle positioning: cortical force generators in the limelight. *Current Opinion in Cell Biology*, 25:741–748, 2013.

[59] Hubert Hilbi, Stefan S Weber, Curdin Ragaz, Yves Nyfeler, and Simon Urwyler. Environmental predators as models for bacterial pathogenesis. *Environmental microbiology*, 9(3):563–575, 2007.

[60] J. Hodgkin and T. Doniach. Natural variation and copulatory plug formation in *Caenorhabditis elegans*. *Genetics*, 146:149–164, 1997.

[61] M.-A. Félix and F. Duveau. Population dynamics and habitat sharing of natural populations of *Caenorhabditis elegans* and *C. briggsae*. *BMC Biology*, 10:1–18, 2012.

[62] W. C. Wong and T. F. Preece. *Pseudomonas tolaasi* in mushroom crops: a note on primary and secondary sources of the bacterium on a commercial farm in england. *Journal of Applied Bacteriology*, 49:305–314, 1980.

[63] P. S. Grewal. Influence of bacteria and temperature on the reproduction of *Caenorhabditis Elegans* (nematoda: Rhabditidae) infesting mushrooms (agaricus bispor us). *Nematologica*, 37:72–82, 1991.

[64] D. Shrestha, H. J. McAuslane, S. T. Adkins, H. A. Smith, N. Dufault, and S. E. Webb. Transmission of squash vein yellowing virus to and from cucurbit weeds and effects on sweetpotato whitefly (hemiptera: Aleyrodidae) behavior. *Environmental Entomology*, 45:967–973, 2016.

[65] G. N. Oldfield and G. Proeseler. 1.4. 9 Eriophyoid mites as vectors of plant pathogens. *World Crop Pests*, 6:259–275, 1996.

[66] S. T. Chang and W.A. Hayes, editors. *The Biology and cultivation of edible mushrooms*. Academic Press, 1978.

[67] A. S. Daba, S. S. Kabeil, W. A. Botros, and M. A. El-Saadani. Production of mushroom (pleurotus ostreatus) in Egypt as a source of nutritional and medicinal food. *World Journal of Agricultural Sciences*, 4:630–634, 2008.

[68] C. Sánchez. Modern aspects of mushroom culture technology. *Applied Microbiology and Biotechnology*, 64:756–762, 2004.

[69] T. Uyeda. *Mushroom culture including the possibilities of new substitutes for manure as a culture medium*. PhD thesis, University of British Columbia, 1934.

[70] J. Thirsk. *Alternative Agriculture: a history: from the Black Death to the present day*. OUP Oxford, 1997.

[71] R. Noble, A. Dobrovin-Pennington, P. J. Hobbs, J. Pederby, and A. Rodger. Volatile C8 compounds and pseudomonads influence primordium formation of *Agaricus bisporus*. *Mycologia*, 101:583–591, 2009.

[72] N. Chikthimmah. *Microbial ecology of mushroom casing soils and preharvest strategies to enhance safety and quality of fresh mushrooms*. ProQuest, 2006.

[73] W. C. Wong and T. F. Preece. Sources of *Verticillium fungicola* on a commercial mushroom farm in england. *Plant Pathology*, 36:577–582, 1987.

[74] J. R. Govan and V. Deretic. Microbial pathogenesis in cystic fibrosis: mucoid *Pseudomonas aeruginosa* and *Burkholderia cepacia*. *Microbiological Reviews*, 60:539–574, 1996.

[75] S. S. Hirano and C. D. Upper. Population biology and epidemiology of *Pseudomonas syringae*. *Annual Review of Phytopathology*, 28:155–177, 1990.

[76] J. T. de Souza, M. de Boer, P. de Waard, T. A. van Beek, and J. M. Raaijmakers. Biochemical, genetic, and zoosporicidal properties of cyclic lipopeptide surfactants produced by *Pseudomonas fluorescens*. *Applied and Environmental Microbiology*, 69:7161–7172, 2003.

[77] M. Nandi, C. Selin, A. K. C. Brassinga, M. F. Belmonte, WG D. Fernando, P. C. Loewen, and T. R. De Kievit. Pyrrolnitrin and hydrogen cyanide production by *Pseudomonas chlororaphis* strain PA23 exhibits nematicidal and repellent activity against *Caenorhabditis elegans*. *PloS one*, 10, 2015.

[78] D. N. Dowling and F. O'Gara. Metabolites of Pseudomonas involved in the biocontrol of plant disease. *Trends in Biotechnology*, 12:133–141, 1994.

[79] G. Defago, C. H. Berling, U. Burger, D. Haas, G. Kahr, C. Keel, C. Voisard, P. H. Wirthner, B. Wüthrich, and D. Hornby. Suppression of black root rot of tobacco and other root diseases by strains of *Pseudomonas fluorescens*: potential applications and mechanisms. In *Biological control of soil-borne plant pathogens.*, pages 93–108. CAB International, 1990.

[80] P. Wirthner, D. Haas, and G. Dfago. Suppression of root diseases by *Pseudomonas fluorescens* CHA0: importance of the bacterial secondary metabolite 2, 4-diacetylphloroglucinol. *Molecular Plant-Microbe Interactions Journal*, 5:4–13, 1992.

[81] D. M. Weller. Pseudomonas biocontrol agents of soilborne pathogens: looking back over 30 years. *Phytopathology*, 97:250–256, 2007.

[82] B. Schippers, A. W. Bakker, and P. A. H. M. Bakker. Interactions of deleterious and beneficial rhizosphere microorganisms and the effect of cropping practices. *Annual Review of Phytopathology*, 25:339–358, 1987.

[83] A. G. Tolaas. A bacterial disease of cultivated mushrooms. *Phytopathology*, 5, 1915.

[84] S. A. C. Godfrey, S. A. Harrow, J. W. Marshall, and J. D. Klena. Characterization by 16S rRNA sequence analysis of pseudomonads causing blotch disease of cultivated *Agaricus bisporus*. *Applied and Environmental Microbiology*, 67:4316–4323, 2001.

[85] M. Alexander. Why microbial predators and parasites do not eliminate their prey and hosts. *Annual Reviews in Microbiology*, 35:113–133, 1981.

[86] J. Hodgkin, M-A Félix, L. C. Clark, D. Stroud, and M. J. Gravato-Nobre. Two *Leucobacter* strains exert complementary virulence on *Caenorhabditis* including death by worm-star formation. *Current Biology*, 2013.

[87] L. A. Gallagher and C. Manoil. *Pseudomonas aeruginosa* PAO1 kills *Caenorhabditis elegans* by cyanide poisoning. *Journal of Bacteriology*, 183:6207–6214, 2001.

[88] A. Jousset, L. Rochat, M. Péchy-Tarr, C. Keel, S. Scheu, and M. Bonkowski. Predators promote defence of rhizosphere bacterial populations by selective feeding on non-toxic cheaters. *The ISME journal*, 3:666–674, 2009.

[89] P. S. Grewal. Effects of *Caenorhabditis elegans* (nematoda: Rhabditidae) on the spread of the bacterium *Pseudomonas tolaasii* in mushrooms (*Agaricus bisporus*). *Annals of Applied Biology*, 118:47–55, 1991.

[90] G. L. Anderson, S. J. Kenney, P. D. Millner, L. R. Beuchat, and P. L. Williams. Shedding of foodborne pathogens by *Caenorhabditis elegans* in compost-amended and unamended soil. *Food Microbiology*, 23:146–153, 2006.

[91] P. Burlinson. *Characterization and regulation of anti-eukaryote factors in Pseudomonas fluorescens NZI7*. PhD thesis, University of Oxford, 2008.

[92] A. R. Hauser. The type III secretion system of *Pseudomonas aeruginosa*: infection by injection. *Nature Reviews Microbiology*, 7:654–665, 2009.

[93] R. D Hood, P. Singh, F.S. Hsu, T. Güvener, M. A Carl, R. R. S. Trinidad, J. M. Silverman, B. B. Ohlson, K. G Hicks, R. L. Plemel, m. Li, S. Schwarz, W. Y. Wang, A. J. Merz, D. R Goodlett, and J. D. Mougous. A type VI secretion system of *Pseudomonas aeruginosa* targets a toxin to bacteria. *Cell host & microbe*, 7:25–37, 2010.

[94] S. Bleves, V. Viarre, R. Salacha, G. P. F. Michel, A. Filloux, and R. Voulhoux. Protein secretion systems in *Pseudomonas aeruginosa*: a wealth of pathogenic weapons. *International Journal of Medical Microbiology*, 300:534–543, 2010.

[95] I. T. Paulsen, C. M. Press, J. Ravel, D. Y. Kobayashi, G. SA Myers, D. V. Mavrodi, R. T. DeBoy, R. Seshadri, Q. Ren, R. Madupu, R. J. Dodson, A. S. Durkin, L.M Brinkac, S. C. Daugherty, S. A. Sullivan, M. J. Rosovitz, M. L. Gwinn, L. Zhou, D. J. Schneider, S. W. Cartinhour, W. C. Nelson, J. Weidman, K. Watkins, K. Tran, H. Khouri, E. A. Pierson, L. S. Pierson, L. S. Thomashow, and J. E. Loper. Complete genome sequence of the plant commensal *Pseudomonas fluorescens* Pf-5. *Nature Biotechnology*, 23:873–878, 2005.

[96] G. M. Preston, N. Bertrand, and P. B. Rainey. Type III secretion in plant growth-promoting *Pseudomonas fluorescens* SBW25. *Molecular microbiology*, 41:999–1014, 2001.

[97] M. Svercel, B. Duffy, and G. Défago. PCR amplification of hydrogen cyanide biosynthetic locus hcnAB in pseudomonas spp. *Journal of Microbiological Methods*, 70:209–213, 2007.

[98] P. B. Rainey, C. L. Brodey, and K. Johnstone. Biological properties and spectrum of activity of tolaasin, a lipodepsipeptide toxin produced by the mushroom pathogen *Pseudomonas tolaasii*. *Physiological and Molecular Plant Pathology*, 39:57–70, 1991.

[99] T. H. Nielsen, D. Sørensen, C. Tobiasen, J. B. Andersen, C. Christophersen, M. Givskov, and J. Sørensen. Antibiotic and biosurfactant properties of cyclic lipopeptides produced by fluorescent *Pseudomonas spp.* from the sugar beet rhizosphere. *Applied and Environmental Microbiology*, 68:3416–3423, 2002.

[100] A. H. A. Parret and R. De Mot. Bacteria killing their own kind: novel bacteriocins of *Pseudomonas* and other γ-proteobacteria. *Trends in Microbiology*, 10:107–112, 2002.

[101] A Jousset, S Scheu, and M Bonkowski. Secondary metabolite production facilitates establishment of rhizobacteria by reducing both protozoan predation and the competitive effects of indigenous bacteria. *Functional Ecology*, 22:714–719, 2008.

[102] I. Ali Siddiqui, D. Haas, and S. Heeb. Extracellular protease of *Pseudomonas fluorescens* CHA0, a biocontrol factor with activity against the root-knot nematode *Meloidogyne incognita*. *Applied and Environmental Microbiology*, 71:5646–5649, 2005.

[103] N. Neidig, R. J. Paul, S. Scheu, and A. Jousset. Secondary metabolites of *Pseudomonas fluorescens* CHA0 drive complex non-trophic interactions with bacterivorous nematodes. *Microbial Ecology*, 61:853–859, 2011.

[104] Y. Zhang, J. M. Foster, L. S. Nelson, D. Ma, and C. K. S. Carlow. The chitin synthase genes chs-1 and chs-2 are essential for *C. elegans* development and responsible for chitin deposition in the eggshell and pharynx, respectively. *Developmental Biology*, 285:330–339, 2005.

[105] J. M. Raaijmakers, I. de Bruijn, and M. J. D. de Kock. Cyclic lipopeptide production by plant-associated *Pseudomonas spp.*: diversity, activity, biosynthesis, and regulation. *Molecular Plant-Microbe Interactions*, 19:699–710, 2006.

[106] J. D'aes, N. P. Kieu, V. Léclère, C. Tokarski, F. Eyiwumi Olorunleke, K. De Maeyer, P. Jacques, M. Höfte, and M. Ongena. To settle or to move? the interplay between two classes of cyclic lipopeptides in the biocontrol strain *Pseudomonas* CMR12a. *Environmental Microbiology*, 2014.

[107] I. De Bruijn, M. J. D. De Kock, P. De Waard, T. A. Van Beek, and J. M. Raaijmakers. Massetolide A biosynthesis in *Pseudomonas fluorescens*. *Journal of Bacteriology*, 190:2777–2789, 2008.

[108] M. Sharma and S. K. Anand. Swarming: a coordinated bacterial activity. *Current Science-Bangalore-*, 83:707–714, 2002.

[109] B. Koch, T. H. Nielsen, D. Sørensen, J. B. Andersen, C. Christophersen, S. Molin, M. Givskov, J. Sørensen, and O. Nybroe. Lipopeptide production in *Pseudomonas sp.* strain DSS73 is regulated by components of sugar beet seed exudate via the Gac two-component regulatory system. *Applied and Environmental Microbiology*, 68:4509–4516, 2002.

[110] C. L. Brodey, P. B. Rainey, M. Tester, and K. Johnstone. Bacterial blotch disease of the cultivated mushroom is caused by an ion channel forming lipodepsipeptide toxin. *Molacular Plant-Microbe Interaction*, 4:407–411, 1991.

[111] A.-S. Blier, J. Vieillard, E. Gerault, A. Dagorn, T. Varacavoudin, F. Le Derf, N. Orange, M. Feuilloley, and O. Lesouhaitier. Quantification of *Pseudomonas aeruginosa* hydrogen cyanide production by a polarographic approach. *Journal of Microbiological Methods*, 90:20–24, 2012.

[112] B. J. Clawson and C. C. Young. Preliminary report on the production of hydrocyanic acid by bacteria. *Journal of Biological Chemistry*, 15:419–422, 1913.

[113] C. Blumer and D. Haas. Mechanism, regulation, and ecological role of bacterial cyanide biosynthesis. *Archives of Microbiology*, 173:170–177, 2000.

[114] P. A. Castric. Hydrogen cyanide, a secondary metabolite of *Pseudomonas aeruginosa*. *Canadian Journal of Microbiology*, 21:613–618, 1975.

[115] W. B. Goldfarb and H. Margraf. Cyanide production by *Pseudomonas aeruginosa*. *Annals of Surgery*, 165:104, 1967.

[116] Kegg: Kyoto Encyclopedia of Genes and Genomes.

[117] C. Reimmann, C. Valverde, E. Kay, and D. Haas. Posttranscriptional repression of GacS/GacA-controlled genes by the RNA-binding protein RsmE acting together with RsmA in the biocontrol strain *Pseudomonas fluorescens* CHA0. *Journal of Bacteriology*, 187:276–285, 2005.

[118] C. Blumer, S. Heeb, G. Pessi, and D. Haas. Global GacA-steered control of cyanide and exoprotease production in *Pseudomonas fluorescens* involves specific ribosome binding sites. *Proceedings of the National Academy of Sciences*, 96:14073–14078, 1999.

[119] S. Heeb and D. Haas. Regulatory roles of the GacS/GacA two-component system in plant-associated and other gram-negative bacteria. *Molecular Plant-Microbe Interactions*, 14:1351–1363, 2001.

[120] P. Munsch and T. Alatossava. Several pseudomonads, associated with the cultivated mushrooms *Agaricus bisporus* or *Pleurotus sp.*, are hemolytic. *Microbiological Research*, 157:311–315, 2002.

[121] K. A. Hassan, A. Johnson, B. T. Shaffer, Q. Ren, T. A. Kidarsa, L. DH Elbourne, S. Hartney, R. Duboy, N. C. Goebel, T. M. Zabriskie, I. T. Paulsen, and J. E. Loper. Inactivation of the GacA response regulator in *Pseudomonas*

fluorescens Pf-5 has far-reaching transcriptomic consequences. *Environmental Microbiology*, 12:899–915, 2010.

[122] M. Frederix, A. Edwards, A. Swiderska, A. Stanger, R. Karunakaran, A. Williams, P. Abbruscato, M. Sanchez-Contreras, P. S. Poole, and J. A. Downie. Mutation of praR in rhizobium leguminosarum enhances root biofilms, improving nodulation competitiveness by increased expression of attachment proteins. *Molecular Microbiology*, 93:464–478, 2014.

[123] M. V. Brennerova and D. E. Crowley. Direct detection of rhizosphere-colonizing *Pseudomonas sp.* using an *Escherichia coli* rRNA promoter in a Tn7-lux system. *FEMS Microbiology Ecology*, 14:319–330, 1994.

[124] B. Koch, L. E. Jensen, and O. Nybroe. A panel of Tn7-based vectors for insertion of the GFP marker gene or for delivery of cloned DNA into gram-negative bacteria at a neutral chromosomal site. *Journal of Microbiological Methods*, 45:187–195, 2001.

[125] W.-K. Huh, J. V. Falvo, L. C. Gerke, A. S. Carroll, R. W. Howson, J. S. Weissman, and E. K. O'Shea. Global analysis of protein localization in budding yeast. *Nature*, 425:686–691, 2003.

[126] J. Davison. Genetic tools for pseudomonads, rhizobia, and other gram-negative bacteria. *BioTechniques*, 32:386–401, 2002.

[127] L. K. Arciszewska, D. Drake, and N. L. Craig. Transposon Tn7: cis-acting sequences in transposition and transposition immunity. *Journal of Molecular Biology*, 207:35–52, 1989.

[128] N. L. Craig. Tn7: a target site-specific transposon. *Molecular Microbiology*, 5:2569–2573, 1991.

[129] M. Klausen, A. Heydorn, P. Ragas, L. Lambertsen, A. Aaes-Jørgensen, S. Molin, and T. Tolker-Nielsen. Biofilm formation by *Pseudomonas aeruginosa* wild type, flagella and type IV pili mutants. *Molecular Microbiology*, 48:1511–1524, 2003.

[130] M.A Matilla, M. Espinosa-Urgel, J. J. Rodríguez-Herva, J. L. Ramos, and M. I. Ramos-González. Genomic analysis reveals the major driving forces of bacterial life in the rhizosphere. *Genome Biology*, 8:R179, 2007.

[131] K.-H. Choi, J. B. Gaynor, K. G. White, C. Lopez, C. M. Bosio, R. A. R. Karkhoff-Schweizer, and H. P. Schweizer. A Tn7-based broad-range bacterial cloning and expression system. *Nature Methods*, 2:443–448, 2005.

[132] M. de Bono and A. Villu Maricq. Neuronal substrates of complex behaviors in *C. elegans*. *Annual Review of Neuroscience*, 28:451–501, 2005.

[133] K. Yook, T. W. Harris, T. Bieri, A. Cabunoc, J. Chan, W. J. Chen, P. Davis, N. De La Cruz, A. Duong, R. Fang, U. Canesan, C. Grove, K. Howe, K. Snehalata, R. Kishore, R. Lee, Y. Li, H-M. Muller, C. Nakamura, B. Nash,

P. Ozersky, M. Paulini, D. Raciti, A. Rangarajan, G. Schindelman, X. Shi, E. M. Schwarz, M. A. Tuli, K. Van Auken, D. Wnag, X. Wang, G. Williams, J. Hodgkin, M. Berriman, R. Durbin, P. Kersey, J. Spieth, L. Stein, and P. W. Sternberg. WormBase 2012: more genomes, more data, new website. *Nucleic Acids Research*, page gkr954, 2011.

[134] CGC *Caenorhabditis* Genetics Centre, http://cbs.umn.edu/cgc/home.

[135] M. M. Broadway, E. A. Rogers, C. Chang, I.-H. Huang, P. Dwivedi, S. Yildirim, M. P. Schmitt, A. Das, and H. Ton-That. Pilus gene pool variation and the virulence of *Corynebacterium diphtheriae* clinical isolates during infection of a nematode. *Journal of Bacteriology*, 195:3774–3783, 2013.

[136] D. A. Garsin, C. D. Sifri, E. Mylonakis, X. Qin, K. V. Singh, B. E. Murray, S. B. Calderwood, and F. M. Ausubel. A simple model host for identifying gram-positive virulence factors. *Proceedings of the National Academy of Sciences*, 98:10892–10897, 2001.

[137] N. A. Bishop and L. Guarente. Two neurons mediate diet-restriction-induced longevity in *C. elegans*. *Nature*, 447:545–549, 2007.

[138] S. H. Chung, D. A. Clark, C. V. Gabel, E. Mazur, and A. D. T. Samuel. The role of the AFD neuron in *C. elegans* thermotaxis analyzed using femtosecond laser ablation. *BMC Neuroscience*, 7:1, 2006.

[139] C. I. Bargmann, E. Hartwieg, and H. R. Horvitz. Odorant-selective genes and neurons mediate olfaction in *C. elegans*. *Cell*, 74:515–527, 1993.

[140] A. H. Ludewig and F. C. Schroeder. Ascaroside signaling in *C. elegans*. *WormBook: The Online Review of C. elegans Biology*, page 1, 2013.

[141] L. Luo, Q. Wen, J. Ren, M. Hendricks, M. Gershow, Y. Qin, J. Greenwood, E. R. Soucy, M. Klein, H. K. Smith-Parker, A. C. Calvo, D. A. Coln-Ramos, A. D. Samuel, and Y. Zhang. Dynamic encoding of perception, memory, and movement in a *C. elegans* chemotaxis circuit. *Neuron*, 82:1115–1128, 2014.

[142] Y. Zhang, H. Lu, and C. I. Bargmann. Pathogenic bacteria induce aversive olfactory learning in *Caenorhabditis elegans*. *Nature*, 438:179–184, 2005.

[143] H. Sasakura and I. Mori. Behavioral plasticity, learning, and memory in *C. elegans*. *Current Opinion in Neurobiology*, 23:92–99, 2013.

[144] K. Yamada, T. Hirotsu, M. Matsuki, R. A. Butcher, M. Tomioka, T. Ishihara, J. Clardy, H. Kunitomo, and Y. Iino. Olfactory plasticity is regulated by pheromonal signaling in *Caenorhabditis elegans*. *Science*, 329.

[145] J. T. Pierce-Shimomura, T. M. Morse, and S. R. Lockery. The fundamental role of pirouettes in *Caenorhabditis elegans* chemotaxis. *The Journal of Neuroscience*, 19:9557–9569, 1999.

[146] P. S. Grewal and P. Hand. Effects of bacteria isolated from a saprophagous rhabditid nematode *Caenorhabditis elegans* on the mycelial growth of *Agaricus bisporus*. *Journal of Applied Bacteriology*, 72:173–179, 1992.

[147] J. A. Hodgkin, P. E. Kuwabara, and B. Corneliussen. A novel bacterial pathogen, *Microbacterium nematophilum*, induces morphological change in the nematode *C. elegans*. *Current Biology*, 10:1615–1618, 2000.

[148] C. Darby, J. W. Hsu, N. Ghori, and S. Falkow. *Caenorhabditis elegans*: plague bacteria biofilm blocks food intake. *Nature*, 417:243–244, 2002.

[149] A. Aballay and F. M. Ausubel. *Caenorhabditis elegans* as a host for the study of host–pathogen interactions. *Current Opinion in Microbiology*, 5:97–101, 2002.

[150] D. A. Garsin, J. M. Villanueva, J. Begun, D. H. Kim, C. D. Sifri, S. B. Calderwood, G. Ruvkun, and F. M. Ausubel. Long-lived *C. elegans* daf-2 mutants are resistant to bacterial pathogens. *Science*, 300:1921–1921, 2003.

[151] C. D. Sifri, J. Begun, and F. M. Ausubel. The worm has turned–microbial virulence modeled in *Caenorhabditis elegans*. *Trends in Microbiology*, 13:119–127, 2005.

[152] J. E. Irazoqui, E. R. Troemel, R. L. Feinbaum, L. G. Luhachack, B. O. Cezairliyan, and F. M. Ausubel. Distinct pathogenesis and host responses during infection of *C. elegans* by *P. aeruginosa* and *S. aureus*. *PLoS Pathogens*, 6:e1000982, 2010.

[153] G. V. Mallo, C. L. Kurz, C. Couillault, N. Pujol, S. Granjeaud, Y. Kohara, and J. J. Ewbank. Inducible antibacterial defense system in *C. elegans*. *Current Biology*, 12:1209–1214, 2002.

[154] L. Ott, A. McKenzie, M. T. Baltazar, S. Britting, A. Bischof, A. Burkovski, and P. A. Hoskisson. Evaluation of invertebrate infection models for pathogenic corynebacteria. *FEMS Immunology & Medical Microbiology*, 65:413–421, 2012.

[155] T. I. Moy, A. R. Ball, Z. Anklesaria, G. Casadei, K. Lewis, and F. M. Ausubel. Identification of novel antimicrobials using a live-animal infection model. *Proceedings of the National Academy of Sciences*, 103:10414–10419, 2006.

[156] H. R. Nicholas and J. A. Hodgkin. The ERK MAP kinase cascade mediates tail swelling and a protective response to rectal infection in *c. elegans*. *Current Biology*, 14:1256–1261, 2004.

[157] M. C. Jud, M. J. Czerwinski, M. P. Wood, R. A. Young, C. M. Gallo, J. S. Bickel, E. L. Petty, J. M. Mason, B. A. Little, P. A. Padilla, and J. A. Schisa. Large P body-like RNPs form in *C. elegans* oocytes in response to arrested ovulation, heat shock, osmotic stress, and anoxia and are regulated by the major sperm protein pathway. *Developmental Biology*, 318:38–51, 2008.

[158] F. K. Nelson and D. L. Riddle. Functional study of the *Caenorhabditis elegans* secretory-excretory system using laser microsurgery. *Journal of Experimental Zoology*, 231:45–56, 1984.

[159] S. T. Lamitina, R. Morrison, G. W. Moeckel, and K. Strange. Adaptation of the nematode *Caenorhabditis elegans* to extreme osmotic stress. *American Journal of Physiology-Cell Physiology*, 286:C785–C791, 2004.

[160] C. I. Bergmann. Chemosensation in *C. elegans*. *WormBook: The Online Review of C. elegans Biology*.

[161] J. T. Pierce-Shimomura, M. Dores, and S. R. Lockery. Analysis of the effects of turning bias on chemotaxis in *C. elegans*. *Journal of Experimental Biology*, 208:4727–4733, 2005.

[162] J. M. Gray, J. J. Hill, and C. I. Bargmann. A circuit for navigation in *Caenorhabditis elegans*. *Proceedings of the National Academy of Sciences*, 102:3184–3191, 2005.

[163] A. Ward, J. Liu, Z. Feng, and X. Z. S. Xu. Light-sensitive neurons and channels mediate phototaxis in *C. elegans*. *Nature Neuroscience*, 11:916–922, 2008.

[164] L. Avery and Y-J You. *C. elegans* feeding. *WormBook: the online review of C. elegans biology*, pages 1–23, 2012.

[165] K. Milward, K. E. Busch, R. J. Murphy, M. de Bono, and B. Olofsson. Neuronal and molecular substrates for optimal foraging in *Caenorhabditis elegans*. *Proceedings of the National Academy of Sciences*, 108:20672–20677, 2011.

[166] M. A. Hilliard, C. I. Bargmann, and P. Bazzicalupo. *C. elegans* responds to chemical repellents by integrating sensory inputs from the head and the tail. *Current Biology*, 12:730–734, 2002.

[167] C. I. Bargmann and H. R. Horvitz. Chemosensory neurons with overlapping functions direct chemotaxis to multiple chemicals in *C. elegans*. *Neuron*, 7:729–742, 1991.

[168] D. Ramot, B. L. MacInnis, and M. B. Goodman. Bidirectional temperature-sensing by a single thermosensory neuron in *C. elegans*. *Nature Neuroscience*, 11:908–915, 2008.

[169] A. Kuhara, M. Okumura, T. Kimata, Y. Tanizawa, R. Takano, K. D. Kimura, H. Inada, K. Matsumoto, and I. Mori. Temperature sensing by an olfactory neuron in a circuit controlling behavior of *C. elegans*. *Science*, 320:803–807, 2008.

[170] A. Vidal-Gadea, K. Ward, C. Beron, N. Ghorashian, S. Gokce, J. Russell, N. Truong, A. Parikh, O. Gadea, and J. Ben-Yakar, A. Pierce-Shimomura. Magnetosensitive neurons mediate geomagnetic orientation in *Caenorhabditis elegans*. *Elife*, 4:e07493, 2015.

[171] S. Ward, N. Thomson, J. G. White, and S Brenner. Electron microscopical reconstruction of the anterior sensory anatomy of the nematode *caenorhabditis elegans*. *Journal of Comparative Neurology*, 160:313–337, 1975.

[172] E. Pradel, Y. Zhang, N. Pujol, T. Matsuyama, C. I. Bargmann, and J. J. Ewbank. Detection and avoidance of a natural product from the pathogenic bacterium *Serratia marcescens* by *Caenorhabditis elegans*. *Proceedings of the National Academy of Sciences*, 104:2295–2300, 2007.

[173] K. Yoshida, T. Hirotsu, T. Tagawa, S. Oda, T. Wakabayashi, Y. Iino, and T. Ishihara. Odour concentration-dependent olfactory preference change in *C. elegans*. *Nature Communications*, 3:739, 2012.

[174] C. M. Coburn and C. I. Bargmann. A putative cyclic nucleotide–gated channel is required for sensory development and function in *C. elegans*. *Neuron*, 17:695–706, 1996.

[175] H. Komatsu, I. Mori, J. Rhee, N. Akaike, and Y. Ohshima. Mutations in a cyclic nucleotide–gated channel lead to abnormal thermosensation and chemosensation in *C. elegans*. *Neuron*, 17:707–718, 1996.

[176] J. M. Gray, D. S. Karow, H. Lu, A. J. Chang, J. S. Chang, R. E. Ellis, M. A. Marletta, and C. I. Bargmann. Oxygen sensation and social feeding mediated by a *C. elegans* guanylate cyclase homologue. *Nature*, 430:317–322, 2004.

[177] D. L. Noelle, C. M. Coburn, J. Eastham, A. Kistler, G.a Gallegos, and C. I. Bargmann. The cyclic GMP-dependent protein kinase EGL-4 regulates olfactory adaptation in *C. elegans*. *Neuron*, 36:1079–1089, 2002.

[178] T. J. Maures, L. N. Booth, B. A. Benayoun, Y. Izrayelit, F. C. Schroeder, and A. Brunet. Males shorten the life span of *C. elegans* hermaphrodites via secreted compounds. *Science*, 343:541–544, 2014.

[179] M. Fujiwara, P. Sengupta, and S. L. McIntire. Regulation of body size and behavioral state of *C. elegans* by sensory perception and the EGL-4 cGMP-dependent protein kinase. *Neuron*, 36:1091–1102, 2002.

[180] L. A. Perkins, E. M. Hedgecock, J. N. Thomson, and J. G. Culotti. Mutant sensory cilia in the nematode *Caenorhabditis elegans*. *Developmental Biology*, 117:456–487, 1986.

[181] E. E. Glater, M. V. Rockman, and C. I. Bargmann. Multigenic natural variation underlies *Caenorhabditis elegans* olfactory preference for the bacterial pathogen *Serratia marcescens*. *G3: Genes— Genomes— Genetics*, 4:265–276, 2014.

[182] H. C. Chang, J. Paek, and D. H. Kim. Natural polymorphisms in *C. elegans* HECW-1 E3 ligase affect pathogen avoidance behaviour. *Nature*, 480:525–529, 2011.

[183] J. G. White, E. Southgate, J. N. Thomson, and S. Brenner. The structure of the nervous system of the nematode *Caenorhabditis elegans* (the mind of a worm). *Philosophical Transactions of the Royal Society B*, 314:1–340, 1986.

[184] S. R. Wicks, C. J. de Vries, H. G. A. M. van Luenen, and R. H. A. Plasterk. CHE-3, a cytosolic dynein heavy chain, is required for sensory cilia structure and function in *Caenorhabditis elegans*. *Developmental Biology*, 221:295–307, 2000.

[185] E. R. Sawin, R. Ranganathan, and H. R. Horvitz. *C. elegans* locomotory rate is modulated by the environment through a dopaminergic pathway and by experience through a serotonergic pathway. *Neuron*, 26:619–631, 2000.

[186] W. S. Schackwitz, T. Inoue, and J. H. Thomas. Chemosensory neurons function in parallel to mediate a pheromone response in *C. elegans*. *Neuron*, 17:719–728, 1996.

[187] M. de Bono, D. M. Tobin, M. W. Davis, L. Avery, and C. I. Bargmann. Social feeding in *Caenorhabditis elegans* is induced by neurons that detect aversive stimuli. *Nature*, 419:899–903, 2002.

[188] C. E. Cho, C. Brueggemann, D. L. Noelle, and C. I. Bargmann. Parallel encoding of sensory history and behavioral preference during caenorhabditis elegans olfactory learning. *eLife*, 5:e14000, 2016.

[189] E. Z. Macosko, N. Pokala, E. H. Feinberg, S. H. Chalasani, R. A. Butcher, J. Clardy, and C. I. Bargmann. A hub-and-spoke circuit drives pheromone attraction and social behaviour in *C. elegans*. *Nature*, 458:1171–1175, 2009.

[190] A. Kocabas, C-H Shen, Z. V. Guo, and S. Ramanathan. Controlling interneuron activity in *Caenorhabditis elegans* to evoke chemotactic behaviour. *Nature*, 490:273–277, 2012.

[191] P. N Inglis, G. Ou, M. R Leroux, and J. M Scholey. The sensory cilia of *Caenorhabditis elegans*. 2005.

[192] H. A. Colbert, T. L. Smith, and C. I. Bargmann. OSM-9, a novel protein with structural similarity to channels, is required for olfaction, mechanosensation, and olfactory adaptation in *Caenorhabditis elegans*. *The Journal of Neuroscience*, 17:8259–8269, 1997.

[193] D. B. Dusenbery. Analysis of chemotaxis in the nematode *Caenorhabditis elegans* by countercurrent separation. *Journal of Experimental Zoology*, 188:41–47, 1974.

[194] H. A. Colbert and C. I. Bargmann. Odorant-specific adaptation pathways generate olfactory plasticity in *C. elegans*. *Neuron*, 14:803–812, 1995.

[195] B. B. Shtonda and L. Avery. Dietary choice behavior in *Caenorhabditis elegans*. *Journal of Experimental Biology*, 209:89–102, 2006.

[196] P. Sengupta. The belly rules the nose: feeding state-dependent modulation of peripheral chemosensory responses. *Current Opinion in Neurobiology*, 23:68–75, 2013.

[197] T. Hills, P. J. Brockie, and A. V. Maricq. Dopamine and glutamate control area-restricted search behavior in *Caenorhabditis elegans*. *The Journal of Neuroscience*, 24:1217–1225, 2004.

[198] M. Peliti, J. S. Chuang, and S. Shaham. Directional locomotion of *C. elegans* in the absence of external stimuli. *PloS One*, 8:e78535, 2013.

[199] L. R. Baugh and P. W. Sternberg. DAF-16/FOXO regulates transcription of cki-1/Cip/Kip and repression of lin-4 during *C. elegans* L1 arrest. *Current Biology*, 16:780–785, 2006.

[200] R. A. Butcher, J. R. Ragains, W. Li, G. Ruvkun, J. Clardy, and H. Y. Mak. Biosynthesis of the *Caenorhabditis elegans* dauer pheromone. *Proceedings of the National Academy of Sciences*, 106:1875–1879, 2009.

[201] S. H. von Reuss, N. Bose, J. Srinivasan, J. J. Yim, J. C. Judkins, P. W. Sternberg, and F. C. Schroeder. Comparative metabolomics reveals biogenesis of ascarosides, a modular library of small-molecule signals in *C. elegans*. *Journal of the American Chemical Society*, 134:1817–1824, 2012.

[202] J. Srinivasan, F. Kaplan, R. Ajredini, C. Zachariah, H. T. Alborn, P. EA Teal, R. U. Malik, A. S. Edison, P. W. Sternberg, and F. C. Schroeder. A blend of small molecules regulates both mating and development in *Caenorhabditis elegans*. *Nature*, 454:1115–1118, 2008.

[203] J. W. Golden and D. L. Riddle. A gene affecting production of the *Caenorhabditis elegans* dauer-inducing pheromone. *Molecular and General Genetics MGG*, 198:534–536, 1985.

[204] E. C. Andersen, J. S. Bloom, J. P. Gerke, and L. Kruglyak. A variant in the neuropeptide receptor npr-1 is a major determinant of *Caenorhabditis elegans* growth and physiology. *PLoS Genetics*, 10:e1004156, 2014.

[205] R. A. Butcher, J. R. Ragains, and J. Clardy. An indole-containing dauer pheromone component with unusual dauer inhibitory activity at higher concentrations. *Organic Letters*, 11:3100–3103, 2009.

[206] C. Rogers, A. Persson, B. Cheung, and M. de Bono. Behavioral motifs and neural pathways coordinating O_2 responses and aggregation in *C. elegans*. *Current Biology*, 16:649–659, 2006.

[207] Juliet C Coates and Mario de Bono. Antagonistic pathways in neurons exposed to body fluid regulate social feeding in caenorhabditis elegans. *Nature*, 419(6910):925–929, 2002.

[208] S. Gart, D. Vella, and S. Jung. The collective motion of nematodes in a thin liquid layer. *Soft Matter*, 7:2444–2448, 2011.

[209] C. T. Murphy. The search for DAF-16/FOXO transcriptional targets: approaches and discoveries. *Experimental gerontology*, 41:910–921, 2006.

[210] S. Ogg, S. Paradis, S. Gottlieb, G. I. Patterson, L. Lee, H. A. Tissenbaum, and G. Ruvkun. The fork head transcription factor DAF-16 transduces insulin-like metabolic and longevity signals in *C. elegans*. *Nature*, 389:994–999, 1997.

[211] M. Wolf, F. Nunes, A. Henkel, A. Heinick, and R. J. Paul. The map kinase jnk-1 of caenorhabditis elegans: Location, activation, and influences over temperature-dependent insulin-like signaling, stress responses, and fitness. *Journal of Cellular Physiology*, 214:721–729, 2008.

[212] K. E. Busch and B. Olofsson. Should I stay or should I go? volume 1, pages 182–186. Taylor & Francis, 2012.

[213] D. H. Kim, R. Feinbaum, G. Alloing, F. E. Emerson, D. A. Garsin, H. Inoue, M. Tanaka-Hino, N. Hisamoto, K. Matsumoto, M-W Tan, and F. M. Ausubel. A conserved p38 MAP kinase pathway in *Caenorhabditis elegans* innate immunity. *Science*, 297:623–626, 2002.

[214] C. L. Kurz and J. J. Ewbank. *Caenorhabditis elegans*: an emerging genetic model for the study of innate immunity. *Nature Reviews Genetics*, 4:380–390, 2003.

[215] C. Huffaker. Experimental studies on predation: dispersion factors and predator-prey oscillations. *California Agriculture*, 27:343–383, 1958.

[216] R. M May. Limit cycles in predator-prey communities. *Science*, 177:900–902, 1972.

[217] J. D. Murray. *Mathematical Biology*. Springer-Verlag, 1989.

[218] Gregory Stephanopoulos and AG Fredrickson. Extinction probabilities in microbial predation: a birth and death approach. *Bulletin of Mathematical Biology*, 43(2):165–181, 1981.

[219] P. A Abrams. The evolution of predator-prey interactions: theory and evidence. *Annual Review of Ecology and Systematics*, 31:79–105, 2000.

[220] G. J Vermeij. The evolutionary interaction among species: selection, escalation, and coevolution. *Annual Review of Ecology and Systematics*, 25:219–236, 1994.

[221] P Kareiva. Habitat fragmentation and the stability of predator–prey interactions. *Nature*, 326:388–390, 1987.

[222] Y. Liu, B. S. Samuel, P. C. Breen, and G. Ruvkun. *Caenorhabditis elegans* pathways that surveil and defend mitochondria. *Nature*, 508:406–410, 2014.

[223] A Andersson, U Larsson, and Å Hagström. Size-selective grazing by a microflagellate on pelagic bacteria. *Marine Ecology Progress Series*, pages 51–57, 1986.

[224] K. Jürgens and C. Matz. Predation as a shaping force for the phenotypic and genotypic composition of planktonic bacteria. *Antonie van Leeuwenhoek*, 81:413–434, 2002.

[225] M. W. Hahn, E. R. B. Moore, and M. G. Höfle. Role of microcolony formation in the protistan grazing defense of the aquatic bacterium *Pseudomonas* sp. MWH1. *Microbial Ecology*, 39, 2000.

[226] C. Matz and S. Kjelleberg. Off the hook–how bacteria survive protozoan grazing. *Trends in microbiology*, 13:302–307, 2005.

[227] K. Vaitkevicius, B. Lindmark, G. Ou, T. Song, C. Toma, M. Iwanaga, J. Zhu, A. Andersson, M.-L. Hammarström, S. Tuck, and S. N. Wai. A *Vibrio cholerae* protease needed for killing of *Caenorhabditis elegans* has a role in protection from natural predator grazing. *Proceedings of the National Academy of Sciences*, 103:9280–9285, 2006.

[228] M.-W. Tan, S. Mahajan-Miklos, and F. M. Ausubel. Killing of *Caenorhabditis elegans* by *Pseudomonas aeruginosa* used to model mammalian bacterial pathogenesis. *Proceedings of the National Academy of Sciences*, 96:715–720, 1999.

[229] Kerry F Harris and Karl Maramorosch. *Vectors of plant pathogens*. Academic Press, 2013.

[230] A. Shamshad, A.D. Clift, and S. Mansfield. The effect of tibia morphology on vector competency of mushroom sciarid flies. *Journal of Applied Entomology*, 133:484–490, 2009.

[231] Ulrich G Mueller, Nicole M Gerardo, Duur K Aanen, Diana L Six, and Ted R Schultz. The evolution of agriculture in insects. *Annu. Rev. Ecol. Evol. Syst.*, 36:563–595, 2005.

[232] Jacobus J Boomsma. Evolutionary biology: farming writ small. *Nature*, 469(7330):308–309, 2011.

[233] C. Xia, L. Wang, S. Sun, and J. Wang. An SIR model with infection delay and propagation vector in complex networks. *Nonlinear Dynamics*, 69:927–934, 2012.

[234] S. Ruan and D. Xiao. Stability of steady states and existence of travelling waves in a vector-disease model. *Proceedings of the Royal Society of Edinburgh: Section A. Mathematics*, 134:991–1011, 2004.

[235] A. Yoshimura, K. Kawasaki, F. Takasu, K. Togashi, K. Futai, and N. Shigesada. Modeling the spread of pine wilt disease caused by nematodes with pine sawyers as vector. *Ecology*, 80:1691–1702, 1999.

[236] D. Balcan, B. Gonçalves, H. Hu, J. J. Ramasco, V. Colizza, and A. Vespignani. Modeling the spatial spread of infectious diseases: The GLobal Epidemic and Mobility computational model. *Journal of Computational Science*, 1:132–145, 2010.

[237] S. Turner, J. A. Sherratt, K. J. Painter, and N. J. Savill. From a discrete to a continuous model of biological cell movement. *Physical Review E*, 69:021910, 2004.

[238] F. Farina and A. Dennunzio. A predator-prey cellular automaton with parasitic interactions and environmental effects. *Fundamenta Informaticae*, 83:337–353, 2008.

[239] G. B. Ermentrout and L. Edelstein-Keshet. Cellular automata approaches to biological modeling. *Journal of Theoretical Biology*, 160:97–133, 1993.

[240] R. M. Z. dos Santos and S. Coutinho. Dynamics of HIV infection: A. cellular automata approach. *Physical Review letters*, 87:168102, 2001.

[241] A. R. A. Anderson and M. A. J. Chaplain. Continuous and discrete mathematical models of tumor-induced angiogenesis. *Bulletin of Mathematical Biology*, 60:857–899, 1998.

[242] S. Brenner. The genetics of *Caenorhabditis elegans*. *Genetics*, 77:71–94, 1974.

[243] J. W. Golden and D. L. Riddle. A gene affecting production of the caenorhabditis elegans dauer-inducing pheromone. *Molecular and General Genetics MGG*, 198:534–536, 1985.

[244] K. Lin, J. B. Dorman, A. Rodan, and C. Kenyon. daf-16: An HNF-3/forkhead family member that can function to double the life-span of *Caenorhabditis elegans*. *Science*, 278:1319–1322, 1997.

[245] J. A. Lewis and J. A. Hodgkin. Specific neuroanatomical changes in chemosensory mutants of the nematode caenorhabditis elegans. *Journal of Comparative Neurology*, 172:489–510, 1977.

[246] R. T. Wragg, V. Hapiak, S. B. Miller, G. P. Harris, J. Gray, P. R. Komuniecki, and R. W. Komuniecki. Tyramine and octopamine independently inhibit serotonin-stimulated aversive behaviors in *Caenorhabditis elegans* through two novel amine receptors. *The Journal of Neuroscience*, 27:13402–13412, 2007.

[247] S. Suo, Y. Kimura, and H. HM Van Tol. Starvation induces cAMP response element-binding protein-dependent gene expression through octopamine–Gq signaling in *Caenorhabditis elegans*. *Journal of Neuroscience*, 26:10082–10090, 2006.

[248] C. R. Buell, V. Joardar, M. Lindeberg, J. Selengut, I. T. Paulsen, M. L. Gwinn, R. J. Dodson, R. T. Deboy, A. S. Durkin, J. F. Kolonay, R. Madupu, S. Daugherty, L. Brinkac, M. Beanan, D. Haft, W. Nelson, T. Davidsen, N. Zafar, L. Zhou, J. Liu, Q. Yuan, H. Khouri, N. Fedorova, B. Tran, D. Russell, K. Berry, T. Utterback, S. Van Aken, T. Feldblyum, M. D'Ascenzo, W. Deng, A. Ramos, J. Alfano, S. Cartinhour, A. Chatterjee, T. Delaney, S. Lazarowitz, G. Martin, D. Schneider, X. Tang, C. Bender, O. White, C. Fraser, and A. Collmer. The complete genome sequence of the arabidopsis and tomato

pathogen *Pseudomonas syringae* pv. tomato DC3000. *Proceedings of the National Academy of Sciences*, 100:10181–10186, 2003.

[249] A.-M. Collignon and J. Dexheimer. Parietal interactions between *Pseudomonas fluorescens* strain BBc6 and the ectomycorrhizal fungus *Laccaria laccata* S238. *Journal of Trace and Microprobe Techniques*, 12:201–208, 1994.

[250] C. K. Stover, X. Q. Pham, A. L. Erwin, S. D. Mizoguchi, P. Warrener, M. J. Hickey, F. S. L. Brinkman, W. O. Hufnagle, D. J. Kowalik, M. Lagrou, R. Garber, L. Goltry, E. Tolentino, S. Westbrock-Wadman, Y. Yuan, L. Brody, S. Coulter, K. Folger, A. Kas, K. Larbig, R. Lim, K. Smith, D. Spencer, G. Wong, Z. Wu, I. Paulsen, J. Reizer, M. Saier, R. Hancock, S. Lory, and M. Olson. Complete genome sequence of *Pseudomonas aeruginosa* PAO1, an opportunistic pathogen. *Nature*, 406:959–964, 2000.

[251] J. A. Kimbrel, S. A. Givan, A. B. Halgren, A. L. Creason, D. I. Mills, G. M. Banowetz, D. J. Armstrong, and J. H. Chang. An improved, high-quality draft genome sequence of the germination-arrest factor-producing *Pseudomonas fluorescens* WH6. *BMC Genomics*, 11:1, 2010.

[252] K-H Choi and H. P. Schweizer. mini-Tn7 insertion in bacteria with single attTn7 sites: example *Pseudomonas aeruginosa*. *Nature Protocols*, 1:153–161, 2006.

[253] O. Pele and M. Werman. The quadratic-chi histogram distance family. In *Computer Vision–ECCV 2010*, pages 749–762. Springer, 2010.

[254] W. P. Gardiner. *Statistics for the Biosciences*. Prentice Hall Europe, 1997.

[255] N. Roussel, C. A. Morton, F. P. Finger, and B. Roysam. A computational model for *C. elegans* locomotory behavior: application to multiworm tracking. *IEEE Transactions on Biomedical Engineering*, 54:1786–1797, 2007.

[256] J. Karbowski, G. Schindelman, C. J. Cronin, A. Seah, and P. W. Sternberg. Systems level circuit model of *C. elegans* undulatory locomotion: mathematical modeling and molecular genetics. *Journal of Computational Neuroscience*, 24:253–276, 2008.

[257] J.-X. Xu and X. Deng. Biological modeling of complex chemotaxis behaviors for *C. elegans* under speed regulationa dynamic neural networks approach. *Journal of Computational Neuroscience*, 35:19–37, 2013.

[258] W. M. Roberts, S. B. Augustine, K. J. Lawton, T. H. Lindsay, T. R. Thiele, E. J. Izquierdo, S. Faumont, R. A. Lindsay, M. C. Britton, N. Pokala, C. I. Bargmann, and S. R. Lockery. A stochastic neuronal model predicts random search behaviors at multiple spatial scales in *C. elegans*. *eLife*, 5:e12572, 2016.

[259] K. D. Farnsworth and J. A. Beecham. How do grazers achieve their distribution? a. continuum of models from random diffusion to the ideal free distribution using biased random walks. *The American Naturalist*, 153:509–526, 1999.

[260] H. Othmer. Notes on space-and velocity-jump models of biological movement. *Theoretical Biology*, 10:913–917, 2010.

[261] H. Fujikawa and S. Morozumi. Modeling surface growth of *Escherichia coli* on agar plates. *Applied and Environmental Microbiology*, 71:7920–7926, 2005.

[262] H. Fujikawa, A. Kai, and S. Morozumi. A new logistic model for bacterial growth. *Shokuhin Eiseigaku Zasshi. Journal of the Food Hygienic Society of Japan*, 44:155–160, 2003.

[263] M. A. Kacena, G. A. Merrell, B. Manfredi, E. E. Smith, D. M. Klaus, and P. Todd. Bacterial growth in space flight: logistic growth curve parameters for escherichia coli and bacillus subtilis. *Applied Microbiology and Biotechnology*, 51:229–234, 1999.

[264] W. H. Press, B. P. Flannery, S. A. Teukolsky, and W. T. Vetterling. *Numerical Recipes The art of Scientific Computing*. Cambridge University Press, 1990.

[265] K. Samprovalaki, P. T. Robbins, and P. J. Fryer. Investigation of the diffusion of dyes in agar gels. *Journal of Food Engineering*, 111:537–545, 2012.

[266] M. D. Egbert, X. E. Barandiaran, and E. A. Di Paolo. A minimal model of metabolism-based chemotaxis. *PLoS Computational Biology*, 6:e1001004, 2010.

[267] L. Byerly, R. C. Cassada, and R. L. Russell. The life cycle of the nematode *Caenorhabditis elegans*: I. wild-type growth and reproduction. *Developmental biology*, 51:23–33, 1976.

[268] M. Gomez, E. De Castro, E. Guarin, H. Sasakura, A. Kuhara, I. Mori, T. Bartfai, C. I Bargmann, and P. Nef. Ca 2+ signaling via the neuronal calcium sensor-1 regulates associative learning and memory in *C. elegans*. *Neuron*, 30:241–248, 2001.

[269] M. H. Zwietering, I. Jongenburger, F. M. Rombouts, and K. Van't Riet. Modeling of the bacterial growth curve. *Applied and Environmental Microbiology*, 56:1875–1881, 1990.

[270] B. C. Crump, C. S. Hopkinson, M. L. Sogin, and J. E. Hobbie. Microbial biogeography along an estuarine salinity gradient: combined influences of bacterial growth and residence time. *Applied and Environmental Microbiology*, 70:1494–1505, 2004.

[271] E. Bååth and K. Arnebrant. Growth rate and response of bacterial communities to ph in limed and ash treated forest soils. *Soil Biology and Biochemistry*, 26:995–1001, 1994.

[272] R. Kolter, D. A. Siegele, and A. Tormo. The stationary phase of the bacterial life cycle. *Annual Reviews in Microbiology*, 47:855–874, 1993.

[273] K. M. Pruitt and D. N. Kamau. Mathematical models of bacterial growth, inhibition and death under combined stress conditions. *Journal of Industrial Microbiology*, 12:221–231, 1993.

[274] J. R. Lobry, J. P. Flandrois, G. Carret, and A. Pave. Monod's bacterial growth model revisited. *Bulletin of Mathematical Biology*, 54:117–122, 1992.

[275] D. van den Broek, T. FC Chin-A-Woeng, G. V. Bloemberg, and B. J. J. Lugtenberg. Molecular nature of spontaneous modifications in gacS which cause colony phase variation in *Pseudomonas* sp. strain pcl1171. *Journal of Bacteriology*, 187:593–600, 2005.

[276] A. Narang and S. S. Pilyugin. Bacterial gene regulation in diauxic and non-diauxic growth. *Journal of Theoretical Biology*, 244:326–348, 2007.

[277] D. S. Kompala, D. Ramkrishna, N. B. Jansen, and G. T. Tsao. Investigation of bacterial growth on mixed substrates: experimental evaluation of cybernetic models. *Biotechnology and Bioengineering*, 28:1044–1055, 1986.

[278] A. Narang, A. Konopka, and D. Ramkrishna. *Escherichia coli* K12. *Biotechnology and Bioengineering*, 55:747–757, 1997.

[279] *BD Bionutrient Technical Manual*. 2016.

[280] B. M. O'Leary, H. C. Neale, R. W. Geilfus, C.-M.and Jackson, D. L. Arnold, and G. M. Preston. Early changes in apoplast composition associated with defence and disease in interactions between *Phaseolus vulgaris* and the halo blight pathogen *Pseudomonas syringae* pv. phaseolicola. *Plant, Cell & Environment*, 2016.

[281] W. Harder and L. Dijkhuizen. Physiological responses to nutrient limitation. *Annual Reviews in Microbiology*, 37:1–23, 1983.

[282] S-J Lee, A. B. Hwang, and C. Kenyon. Inhibition of respiration extends *C. elegans* life span via reactive oxygen species that increase HIF-1 activity. *Current Biology*, 20:2131–2136, 2010.

[283] K. Pflüger-Grau and B. Görke. Regulatory roles of the bacterial nitrogen-related phosphotransferase system. *Trends in Microbiology*, 18:205–214, 2010.

[284] M. Chavarría, R. J. Kleijn, U. Sauer, K. Pflüger-Grau, and V. de Lorenzo. Regulatory tasks of the phosphoenolpyruvate-phosphotransferase system of *Pseudomonas putida* in central carbon metabolism. *MBio*, 3:e00028–12, 2012.

[285] F. Velázquez, K. Pflüger, I. Cases, L. I. De Eugenio, and V. de Lorenzo. The phosphotransferase system formed by PtsP, PtsO, and PtsN proteins controls production of polyhydroxyalkanoates in *Pseudomonas putida*. *Journal of Bacteriology*, 189:4529–4533, 2007.

[286] O. V. Mavrodi, D. V. Mavrodi, D. M. Weller, and L. S. Thomashow. Role of ptsP, orfT, and sss recombinase genes in root colonization by *Pseudomonas fluorescens* Q8r1-96. *Applied and Environmental Microbiology*, 72:7111–7122, 2006.

[287] A. Godino, A. Príncipe, and S. Fischer. A ptsP deficiency in PGPR *Pseudomonas fluorescens* SF39a affects bacteriocin production and bacterial fitness in the wheat rhizosphere. *Research in Microbiology*, 167:178–189, 2016.

[288] H. Xu, W. Lin, H. Xia, S. Xu, Y. Li, H. Yao, F. Bai, X. Zhang, Y. Bai, P. Saris, and M. Qiao. Influence of ptsP gene on pyocyanin production in *Pseudomonas aeruginosa*. *FEMS Microbiology Letters*, 253:103–109, 2005.

[289] Q. Niu, X. Huang, L. Zhang, J. Xu, D. Yang, K. Wei, X. Niu, Z. An, J. W. Bennett, C. Zou, J. Yang, and K.-Q. Zhang. A trojan horse mechanism of bacterial pathogenesis against nematodes. *Proceedings of the National Academy of Sciences*, 107:16631–16636, 2010.

[290] J. Qin and A. R Wheeler. Maze exploration and learning in *C. elegans*. *Lab on a Chip*, 7:186–192, 2007.

[291] K. C. Reddy, E. C. Andersen, L. Kruglyak, and D. H. Kim. A polymorphism in npr-1 is a behavioral determinant of pathogen susceptibility in *C. elegans*. *Science*, 323:382–384, 2009.

[292] G. A. O'Toole and R. Kolter. Flagellar and twitching motility are necessary for *Pseudomonas aeruginosa* biofilm development. *Molecular Microbiology*, 30:295–304, 1998.

[293] S. Mitri, E. Clarke, and K. R. Foster. Resource limitation drives spatial organization in microbial groups. *The ISME Journal*, 10:1471–1482, 2016.

[294] S. Smukalla, M. Caldara, N. Pochet, A. Beauvais, S. Guadagnini, C. Yan, M. D. Vinces, A. Jansen, M. C. Prevost, J-P Latgé, G. R. Fink, K. R. Foster, and K. J Verstrepen. FLO1 is a variable green beard gene that drives biofilm-like cooperation in budding yeast. *Cell*, 135:726–737, 2008.

[295] R. F. Schwarz, R. Branicky, L. J. Grundy, W. R. Schafer, and A. E. X. Brown. Changes in postural syntax characterize sensory modulation and natural variation of *C. elegans* locomotion. *PLoS Computational Biology*, 11:e1004322, 2015.

[296] J. Hafner, H. S. Sawhney, W. Equitz, M. Flickner, and W. Niblack. Efficient color histogram indexing for quadratic form distance functions. *IEEE Transactions on Pattern Analysis and Machine Intelligence*, 17:729–736, 1995.

Appendix

A1. ANOVA Theory

ANOVA theory was used to compute the variance of the normalized growth parameters in Chapter 4. The formuli for grand mean and variance are also used to combine the datasets for the WT-like mutants in the bioluminescence assays. In the following we describe the analysis for K; an analogous analysis is performed on r:

Let K_i be the mean of the parameters K obtained for a given strain during the ith experiment, with a standard deviation of $\sigma(K_i)$.
Let K_i^W be the mean of the parameters K obtained for the WT strain during experiment i with standard deviation $\sigma(K_i^W)$.
Then the normalized value K_i^n of K_i is given by:

$$K_i^n = \frac{K_i}{K_i^W}. \tag{7.1}$$

Let n_i be the number of replicates in experiment i, and N the number of experiments performed.
The standard deviation of K_i^n is denoted $\sigma(K_i^n)$ and is computed as:

$$\sigma^2(K_i^n) = \frac{\sigma^2(K_i)}{(K_i^W)^2} + \frac{(K_i^n)^2 \times \sigma^2(K_i^W)}{(K_i^W)^4}. \tag{7.2}$$

Let $\bar{K}$ be the grand mean, i.e.

$$\bar{K} = \frac{1}{\Sigma_{i=1}^N n_i} \Sigma_{i=1}^N n_i K_i, \tag{7.3}$$

then we can compute the grand variance $\sigma^2(K)$ as

$$\sigma^2(K) = \frac{\text{SST}}{\Sigma_i^N(n_i) - 1}, \tag{7.4}$$

where the Total Sum of Squares of the difference from the grand mean (SST) can be calculated as the sum of the contributions from the Means (SSM) and the individual Errors (SSE), which are given as:

$$\text{SSM} = \Sigma_{i=1}^N n_i \times (K_i^n - \bar{K})^2 = \Sigma_{i=1}^N n_i \times (K_i^n)^2 - \Sigma_{i=1}^N n_i \times (\bar{K})^2, \tag{7.5}$$

and

$$\mathrm{SSE} = \Sigma_{i=1}^{N}(n_i - 1) \times \sigma^2(K_i^n). \tag{7.6}$$

A2. Probability of random cluster

Consider the site i, one of the N sites in the model. We can describe the random distribution of n worms over all sites, as conducting n individual experiments (place a worm) with the probability of success (lands on site i) $p = \frac{1}{N}$. The probability of having exactly k worms on site i is given by the binomial distribution as:

$$P(K_i = k) = \binom{n}{k} p^k (1-p)^{n-k} \tag{7.7}$$

For n large and p small we can assume that all of the sites are independent, so that a random distribution of worms across the sites can be viewed as N repetitions of the experiment described above. Therefore we would expect to see

$$N * \binom{n}{k} p^k (1-p)^{n-k} \tag{7.8}$$

sites on which we have exactly k nematodes.

A3. Distance measures for histograms

The earth mover's distance (EMD) is computed as follows:

$$\mathrm{EMD} = \Sigma|\mathrm{EMD}_i|, \tag{7.9}$$

where

$$\begin{aligned} \mathrm{EMD}_0 &= 0, & (7.10)\\ \mathrm{EMD}_{i+1} &= (A_i + \mathrm{EMD}_i) - B_i, & (7.11) \end{aligned}$$

where A_i and B_i are the ith bins of the two histograms.

The quadratic Chi (QC) Distance on the other hand is computed as:

$$\begin{aligned} Z &= (P+Q) \times A & (7.12)\\ Z(Z == 0) &= 1 & (7.13)\\ X &= Z \times Z & (7.14)\\ D_{ij} &= (P_{ij} - Q_{ij})/Z_{ij} & (7.15)\\ QC &= \sqrt{D \times A \times D^t}, & (7.16) \end{aligned}$$

where P and Q represent the two histograms and A is the similarity matrix according to Haffner [296].